Human regulatory T cell physiology -

Lessons learnt from newborns and adults

By

Mingjing HU, MBBS, MD

Faculty of Medicine

University of Sydney

A thesis submitted in fulfilment of the requirements for the

degree of Doctor of Philosophy

June 2018

DISCLAIMER

The work presented in this thesis is original. Professor Ralph Nanan provided the ideas and helped me with the conceptualization of this thesis. I certify that I performed the majority of the work, including experimental design, laboratory work, data analyses, writing and revision of the thesis. This thesis contains material published in section 3.3.3 (1) and section 3.3.4 (2). I did some of the in vitro experiments and flow cytometric analyses, and contributed to the manuscript preparation (list of detailed contributions is provided at the beginning of section 3.3). For the work that I did not complete myself, I would like to acknowledge:

Dr Brigitte Nanan, who performed all the cell sorting in this thesis, most of the in vitro experiments in section 3.3.3, and *in vitro* suppression assays presented in section 4.3.3 and section 5.3.3.

Collaborators from Monash University, Dr Eliana Marino Moreno, who performed the animal experiments, Dr Fiona Collier and Professor Peter Vuilleman from Deakin University who performed the acetate quantification presented in section 3.3.1.

Dr Thomas Watkins, Professor John Miles from James Cook University, who performed the TCR sequencing in section 3.3.2.

Dr Peter Hsu and Catherine Lai from The Children's Hospital at Westmead, who performed some of the flow cytometric stains presented in section 3.3.4.

Dr Hani Harb, Professor Harald Renz and Dr Daniel P. Potaczek, our collaborators from Philipps University Marburg, Germany, who performed the ChIP-qPCR presented in section 4.3.4.

ACKNOWLEDGMENTS

I would like to show my gratitude to Professor Michael Peek for offering me this great opportunity to study at the University of Sydney and all the supports during this period. Much appreciation to Professor Ralph Nanan for his guidance and instructions throughout the PhD period. I am very grateful to Dr Brigitte Santner-Nanan, who taught me all the required laboratory techniques with patience and professionalism. She helped design experiment protocols and perform all the *in vitro* suppression assays. Additionally, she also acted like a family member to me.

Special thanks to the Department of Education and Training, Australian Government for providing me with the 2014 Prime Minister's Australia Asia Scholarship.

Catherine Lai, I really appreciate her accompany for the past three years. She is a supportive friend and a caring sister, who helped greatly not only in the lab, but in everyday life as well.

I would also like to thank all the lovely staff (Kristy, Sue, Vicky, Mani, Gayya, Karen, Sally, Khairunnessa) and other PhD candidates (Sandra, Abudullar) on Level 5, Nepean Clinical School. Though I was far away from the main campus and the city centre, you made my stay in Australia enjoyable.

Finally, my sincere gratitude to my parents (ZhangZhen HU & YuanFang ZHANG) and my husband (JianWei CHEN). Thanks to their understanding and encouragement, I am able to complete my study here in Australia!

PUBLICATIONS ARISING FROM THESIS

1. Hsu P, Santner-Nanan B, **Hu Mingjing**, Skarratt K, Lee CH, Stormon M, et al. IL-10 Potentiates Differentiation of Human Induced Regulatory T Cells via STAT3 and Foxo1. Journal of Immunology. 2015;195(8):3665-74. *Attached in Appendix*.

2. Hsu P, Lai C, **Hu Mingjing**, et al. Interleukin 2 enhances gut homing potential of human naïve regulatory T cells early in life. Journal of Immunology. 2018. doi:10.4049/jimmunol.1701533. *Attached in Appendix*.

3. **Hu Mingjing**[*], Eviston David[*], Hsu Peter[*], et al. Fetal thymic and regulatory T cell development is impaired in preeclampsia. Currently reviewed by *Nature Communications*. (**These authors contributed equally to this work*)

4. Thomas S. Watkins, Helen M. McGuire, **Mingjing Hu**, et al. Distinctive cellular immunity resides at the human fetomaternal interface. *Reviewed and currently revised by Immunity*.

5. **Hu Mingjing**, Santner-Nanan Brigitte, HARB Hani, et al. SCFAs potentiate the differentiation and suppressive capacity of induced regulatory T cells via Histone Acetylation inhibition. *Manuscript in preparation for submission to Journal of Allergy and Clinical Immunology*.

Other publication:

Li Q, Lee CH, Peters LA, et al. Variants in TRIM22 that affect NOD2 signalling are associated with Very-early-onset inflammatory bowel disease. Gastroenterology. 2016;150(5):1196-207. *Attached in Appendix*

Table of Contents

ABSTRACT

Human Regulatory T (Treg) cells play a critical role in the immune system. They can suppress the activation, proliferation and cytokine production of various immune cells including T cells, B cells, Dendritic Cells (DCs), natural killer (NK) cells and macrophages. This special suppressive capacity to control immune responses makes Treg cells indispensable for self-tolerance and the prevention of over-reactivity to maintain immune homeostasis. Deficiency and dysfunction of Treg cells lead to severe autoimmune disease like immune dysregulation, polyendocrinopathy, enteropathy, X-linked syndrome (IPEX), allergy and asthma, inflammatory bowel disease, graft versus host disease (GVHD), as well as fetal-maternal intolerance during pregnancy. Hence, understanding Treg cell physiology is of vital importance.

In humans, Treg cell differentiation starts from 8.2 gestational weeks *in utero* under the influence of the maternal immune environment. The increase in the fetal Treg cell compartment compared to adults proves that the fetal immune system is prone to differentiate into Tregs in order to maintain a tolerogenic status. Whilst there is abundant indirect evidence from clinical observations for transplacental Treg cell programming, there is a paucity of direct mechanistic data. It is known that various soluble immunomodulatory factors, including anti-inflammatory cytokine IL-10 and microbiota metabolites, short chain fatty acids (SCFAs), contribute to the transplacental immune programming by shaping the fetal immune system, specifically Treg cells. Therefore, this thesis aims to provide further evidence for the Treg cell transplacental programming, and to explain how IL-10 and SCFAs contribute to this process.

SCFAs are organic fatty acids with fewer than 6 carbon atoms. They are the major bacterial fermentation products in the human intestine. SCFAs have been shown to have profound influences on both the innate and adaptive immune systems, particularly Treg cells. Upon production in the GI tract, they are absorbed into the gut epithelium cells and then circulated to other organs to exert immune regulatory effects through the portal vein. In the animal models, it has already been proven that they contribute greatly to the pTreg induction *in vivo*, as well as iTreg induction *in vitro*. In addition, SCFAs also suppress the expression of pro-inflammatory cytokines by murine DCs, skewing murine colonic macrophages and DCs towards a tolerogenic phenotype, thus promoting Treg induction. Although their effects have been consistently proven in different animal models, their efficacy in modulating immune cells in humans still remains unclear. Therefore, I aim to explore thoroughly the effects of SCFAs on different types of immune cells, especially Treg cells *in vitro*; and to investigate how SCFAs alter the histone acetylation of genes involved in immune tolerance.

To study Treg cell transplacental programming, various types of experiments were conducted, such as animal experiments, serum acetate level detection, TCR sequencing and flow cytometric analyses. To explore thoroughly the effects of SCFAs on different types of immune cells, especially Treg cells *in vitro*, mononuclear cells from cord blood and adult peripheral blood were isolated. After *in vitro* culture with SCFAs, cells were examined phenotypically using multi-colour flow cytometry and functionally by *in vitro* suppression assay.

Our collaborators were able to demonstrate how the maternal microbial composition influences fetal thymus and Treg cell development. The absence of maternal gut microbiota caused significantly reduced fetal thymus size and fewer thymic $Foxp3^+$ Treg

cell numbers. Supplementation of acetate could rescue all these reductions in thymus size and thymic output. Moreover, the fetal-maternal correlation of serum acetate levels we found in human pregnancy implied that maternal acetate likely crossed the placenta. TCR sequencing data also suggested that fetal antigen receptor immunity was not inherited, but rather driven by local immunomodulatory factors. Taken together, it can be concluded that maternally acquired metabolites (acetate) play an important role in shaping fetal thymic development and output, hence exerting their influences on fetal immunity.

In addition to the context of pregnancy, this thesis extends the knowledge of the regulatory effects of SCFAs on both neonate and adult immune cells *in vitro*. The most essential finding is that we are the first to demonstrate the effectiveness of SCFAs in Treg cell differentiation via histone acetylation inhibition *in vitro* in humans. The addition of butyrate and propionate, but not acetate, enhanced histone 3 and histone 4 acetylation of various immune tolerance related gene loci, thus potentiating the expression of these phenotypic markers. The suppressive capacity of induced human Treg cells was therefore augmented. Compared to Cord Blood Mononuclear Cells (CBMCs), adult PBMCs had a completely different induction pattern with a reduced level of activation. We postulated that this differential induction patterns of adult iTregs accounted for the inconsistent effectiveness of human iTregs as well as the concealment of SCFAs' effects, considering the higher proportion of non-activated iTregs in adults. ChIP analysis also provided additional evidence for the observed differential induction patterns in adults. The epigenetic histone acetylation due to SCFAs treatment initiated much later in adult cells compared to cord blood cells. Additionally, we also proved the tolerogenic effects of SCFAs on other immune cells in humans, including MoDCs and different T cell subsets. We showed that both butyrate and propionate, but not acetate, could inhibit the

differentiation and maturation of MoDCs, skewing them towards immature or tolerogenic status. When cocultured with naive $CD4^+$ T cells, these tolerogenic MoDCs upregulated the immune tolerance related phenotypic markers and increased the suppressive capacity of cultured $CD4^+$ T cells. These tolerogenic effects of SCFAs also applied to different T cell subsets regardless of their Foxp3 expression *in vitro*. These results highlight the important role of SCFAs in immune tolerance, particularly in Treg cell physiology.

In conclusion, maternally derived SCFAs play a pivotal role in the Treg cell transplacental programming *in utero* and during early life. Additionally, SCFAs can potentiate the expression of immune tolerance related phenotypic markers via histone acetylation inhibition, thus promoting the differentiation of tolerogenic human iTregs and MoDCs *in vitro*. These results provide theoretical evidence for a new non-pharmaceutical approach as immune therapeutic manipulation, not only feasible during pregnancy, but also in infancy and adulthood. Since diet is closely interlinked with the composition of gut microbiota and SCFAs production, dietary interventions or direct SCFAs supplementation, may alleviate or treat various non-communicable diseases, or even prevent the development of autoimmune diseases via modulating Treg cells. Most importantly, this non-pharmaceutical immune therapy is cost-effective, side-effects free, and beneficial for all generations.

LIST of TABLES

LIST OF FIGURES

ABBREVIATIONS

acetyl-CoA	Acetyl Coenzyme A
APCs	Antigen Presenting Cells
AIRE	Autoimmune Regulator
BCR	B Cell Receptor
CFSE	CarboxyFluorescein Succinimidyl Ester
ChIP	Chromatin ImmunoPrecipitation
cDCs	Classical/Myeloid Dendritic Cells
Tconv	Conventional T cells
CLA	Cutaneous Lymphocyte Antigen
CTLA-4, CD152	Cytotoxic T Lymphocyte Associated protein 4
DCs	Dendritic Cells
DOHaD	Developmental Origins of Health and Disease
DN	Double Negative
DP	Double Positive
ERK	Extracellular signal-Regulated Kinase
EVT	Extravillous Trophoblast
FCS	Fetal Calf Serum
Foxp3	Forkhead box P3
GPR	G Protein-coupled Receptors
GI	Gastrointestinal
GITR	Glucocorticoid-Induced TNF-Related protein
GVHD	Graft Versus Host Disease

GM-CSF	Granulocyte Macrophage - Colony Stimulating Factor
HSCs	Hematopoietic Stem Cells
HDACs	Histone Deacetylases
HKG	HouseKeeping Gene
HLA-DR	Human Leukocyte Antigen – antigen D Related
IPEX	Immune Dysregulation, Polyendocrinopathy, Enteropathy, X-linked syndrome
iTregs	In vitro Induced Treg Cells
IDO	Indoleamine 2,3-DiOxygenase
ICOS, CD278	Inducible T-cell CoStimulator
IBD	Inflammatory Bowel Disease
ILCs	Innate Lymphoid Cells
IFN-γ	Interferon-γ
IL-10	Interleukin-10
LPS	lipopolysaccharide
LAG-3, CD223	Lymphocyte Activation Gene 3
MDP	Macrophage-DC Progenitor
MHC	Major Histocompatibility Complex
MAPK	Mitogen-Activated Protein Kinase
MoDCs	Monocyte-derived DCs
NK	Natural Killer
NF-kB	NF-kappaB
CNS	Non-Coding Sequences
NIMAs	Non-Inherited Maternal Alloantigens

NOD	Non-Obese Diabetic
PRRs	Pattern-Recognition Receptors
PBMCs	Peripheral Blood Mononuclear Cells
pTregs	Peripheral-Derived Treg Cells
pDCs	Plasmacytoid Dendritic Cells
PD-L1, CD274	Programmed Cell Death – Ligand 1
PD-1, CD279	Programmed Cell Death protein 1
PD-L1	Programmed Cell Death-Ligand 1
PD-L2	Programmed Cell Death-Ligand 2
RTEs	Recent Thymic Emigrants
RAG	Recombination Activating Gene
Bregs	Regulatory B cells
Treg	Regulatory T
RAR	Retinoic Acid Receptor
RT	Room Temperature
SCFAs	Short Chain Fatty Acids
SP	Single Positive
TCR	T Cell Receptor
Teff	T effector
Th	T helper
tTregs	Thymus-Derived Treg Cells or Natural Treg Cells
TRA	Tissue–Restricted Antigens
TLRs	Toll-Like Receptors
TGF-β	Transforming Growth Factor-β

TSDR	Treg cell Specific Demethylated Region
Treg-Me	Treg cell Specific DNA hypoMethylation
TNF	Tumour Necrosis Factor

Chapter 1 – Introduction

1.1 Immune system

The immune system, involving multiple organs and cells, is a holistic and complicated defence system, which helps to protect the body from a variety of potential threats. To function properly, the immune system requires tight regulatory processes to maintain a fine balance. A hyper or hypoactive immune system can lead to different types of diseases. Reduced or absent responses to foreign antigens, can cause recurrent or life-threatening infections, while over-active responses, including those against self-antigens, can result in autoimmune diseases.

1.1.1 Innate immune system

The immune system can be divided into innate and adaptive immune systems. The innate immune system provides first-line protection against pathogens infiltrating the body (3). A broad, non-specific inflammatory response is initiated immediately. Foreign substances are identified and removed by specialised phagocytes. Then immune cells migrate to the site of infection guided by cytokines and chemokines. In addition, the complement cascade is activated by pathogens directly or indirectly via antibodies. This is followed by a transition that activates the adaptive immune system (4), initiated by antigen presentation to orchestrate a more targeted immune response and combat the foreign pathogen.

There are several types of immune cells involved in innate immune responses, including granulocytes, NK cells, monocytes, macrophages, and DCs. Granulocytes generally arrive first at the site of infection, where they identify and remove the foreign substances in a similar manner to macrophages. Rather than directly attacking the invading

pathogens, NK cells eliminate cells with decreased levels of major histocompatibility complex (MHC) I, which is known as "missing self-recognition" (5). The majority of cancer cells also exhibit down regulation of MHC I expression (6), thus can be recognised and cleared by NK cells. Monocytes are the progenitors of macrophages and DCs. Macrophages are the most competent phagocytes to engulf and destroy pathogens. Other immune cells can be recruited by macrophages to the site of infection (7). Finally, DCs are professional antigen presenting cells (APCs), which play a pivotal role in regulating the adaptive immune system (8, 9).

1.1.2 Adaptive immune system and antigen presentation

Unlike the innate immune system, the adaptive immune system is highly antigen specific. B lymphocytes can directly recognise antigens in their native forms via the B cell receptor (BCR). However, T lymphocyte activation requires antigen presentation by APCs. The T cell receptor (TCR) can only recognise antigens that have been processed into peptides presented on MHC molecules (10). MHC molecules consist of MHC-I and MHC-II, which are recognised by $CD8^+$ and $CD4^+$ T cells, respectively. MHC-I molecules are displayed on the surface of all nucleated cells. *De novo* generated antigens are processed into peptides intracellularly by the proteosome and loaded onto MHC-I (11). They are recognised by naïve $CD8^+$ T cells, which then differentiate into cytotoxic T lymphocytes.

MHC-II molecules are mainly expressed on the surface of professional APCs, such as dendritic cells, macrophages and B cells. Extracellular antigens are internalised through endocytosis, processed into peptides, and then bound to MHC-II (12). This complex is subsequently recognised by naïve $CD4^+$ T cells, which differentiate into effector and memory T helper cells.

1.1.3 T lymphocytes differentiation

The differentiation of T lymphocytes from hematopoietic stem cells (HSCs) involves multiple stages, and it mainly takes place in the thymus. Figure 1.1 summarises T cell development (adapted from (13)).

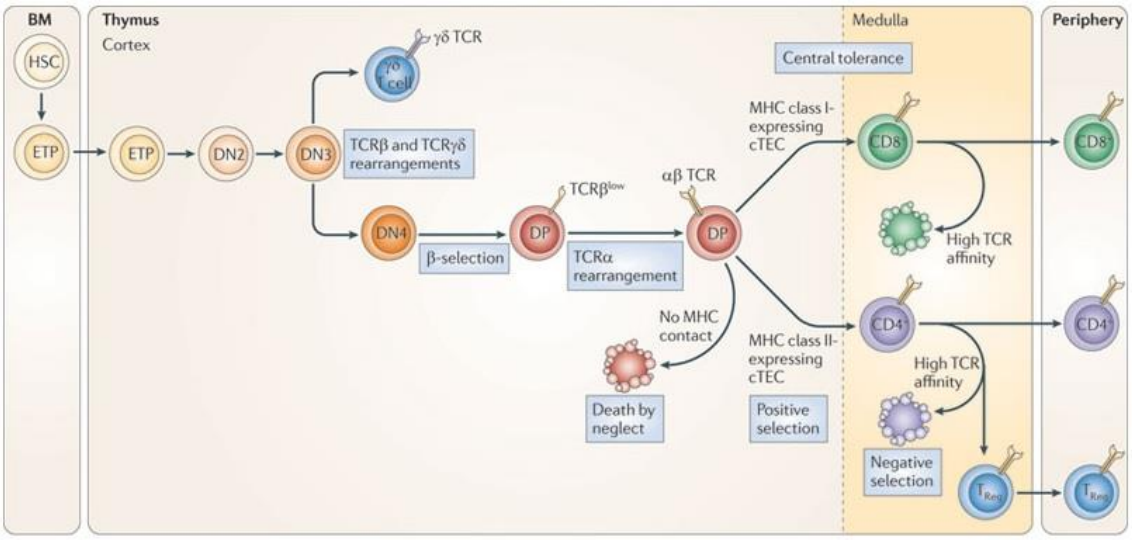

Figure 1.1 T lymphocyte differentiation in the thymus.

Early thymic progenitors, originating from HSCs in the bone marrow, become double negative (DN) cells after losing the potential to differentiate into B cells and dendritic cells (14). DN cells do not express either the TCR or the co-receptors CD4 and CD8. During this stage in the thymic cortex, the essential rearrangement of TCR genes occur. Double positive (DP) cells are generated after TCRβ gene selection (refer to β selection in Figure 1.1) and they express the CD4 and CD8 co-receptors. After this selection, the TCR α-chain locus rearranges to complete the αβ TCR (15). T cells which fail to acquire contact with MHC molecules die by neglect. DP cells develop into either CD4 or CD8 single positive (SP) cells, which is known as positive selection (16). Then in the medulla region of the thymus, the strength of TCR self-reactivity determines the destiny of T cell

differentiation. SP cells with high avidity to MHC–peptide ligands undergo negative selection, whereas SP cells with low avidity eventually develop into naive T cells and migrate out to the periphery where they undergo further selection (17).

Regulatory T (Treg) cells, a special type of suppressive cells, originate in this late stage of thymic development. The transcription factor Forkhead box P3 (Foxp3) is upregulated when a small proportion of self-reactive $CD4^+$ thymocytes with an intermediate avidity for MHC class II molecules escape negative selection (18). Then with an appropriate duration of TCR stimulation, these $Foxp3^+$ cells eventually develop into Treg cells (19).

1.2 Immune tolerance

Antigens recognised by T cells can be divided into "self" antigens, which are synthesised by the organism's own cells and "non-self" or foreign antigens, which do not derive from cells of the organism. The ability to discriminate "self" and "non-self" antigens to avoid attacking own cells in the body is of vital importance. The immune system needs to trigger sufficient immune responses to basically all foreign antigens, meanwhile avoids harmful immunity to self by distinguishing between self from non-self and maintaining a proper grade of immune responses (20). The process of "Self" and "Non-self" discrimination is referred to as immune tolerance, which was first proposed in the 1950s by Sir F. Macfarlane Burnet theoretically and Medawar experimentally (21, 22).

Immune tolerance first takes place in the thymus. Currently, it is widely accepted that during T cell development, thymocytes undergo multiple selection stages, among which negative selection occurred in the medulla of the thymus is the most important one to eliminate self-reactive TCR repertoires (17). Medullary epithelial cells provide the source

of “self” antigens by expressing tissue restricted antigens (TRAs) ectopically induced by Autoimmune Regulator (AIRE) (23). The expression of TRAs initiates after AIRE expression, and they are positively correlated in a dose-dependent manner (24). T cells with receptors that strongly recognise these TRAs are eliminated by negative selection (25). This process is called central tolerance, a variety of autoimmune diseases can occur if this process is jeopardised (26).

Self and non-self discrimination also takes place in the extrathymic environment, and this process is referred to as peripheral tolerance. T cells with intermediate avidity to self-antigen can escape the negative thymic selection and migrate into the periphery (27). These cells pose a threat to cause pathogenic autoimmune diseases. Several mechanisms are proposed as to how these self-reactive cells are eliminated. DCs play a role in the peripheral tolerance via T cell anergy. When DCs fail to present costimulatory factors, T cells could not proliferate upon stimulation of self-antigen alone (28). T cell depletion caused by activation-induced cell death through CD95 (Fas) signalling is another mechanism (29). Moreover, these self-reactive T cells are selectively downregulated by Qa-1-restricted $CD8^+$ T cells (30). Regulatory B cells (Bregs) (31, 32) and innate lymphoid cells (ILCs) (33, 34) also contribute to the peripheral immune tolerance. However, the most intriguing cell type involved is Treg cells. Thymus-derived Treg cells are produced to suppress self-reactive cells that have escaped thymic negative selection in the periphery (35).

1.2.1 Regulatory T Cells

1.2.1.1 History

In 1970, a thymus-derived suppressive lymphocyte population was first discovered in mice by Gershon and Kondo (36). The existence of these suppressor T cells was confirmed in animal models by different groups (37-40). They performed thymectomy on rodents at around day 3 after birth, resulting in severe autoimmune diseases, which showed that these suppressor T cells were crucial for maintaining immune tolerance.

Suppressor T cells were later renamed Treg cells. They are naturally present in the immune system (41). In healthy human peripheral blood mononuclear cells (PBMCs), the percentage of $CD4^+$ Tregs within $CD4^+$ T cells is around 6.7-9.9%. In comparison, the percentage of $CD8^+$ Tregs within $CD8^+$ T cells is more variable and much lower (0.1–1%) (42). Generally, three main subsets of Treg cells have been described, thymus-derived Treg cells or natural Treg cells (tTregs), peripheral-derived Treg cells (pTregs) and *in vitro* induced Treg cells (iTregs) (43).

1.2.1.2 Phenotypic Markers

The first specific marker CD25 (IL-2 receptor α-chain) was not defined until 1995 in mice. T cells prepared from BALB/c mice lymph nodes and spleens were depleted of $CD4^+CD25^+$ cells. Subsequently, these $CD4^+CD25^+$ depleted T cells were adoptively transferred to BALB/c athymic nude mice. All BALB/c athymic mice subsequently developed evident autoimmune diseases spontaneously (44). In mice, this $CD4^+CD25^+$ population was distinct; however, in humans $CD4^+CD25^+$ consisted of both $CD4^+CD25^{low}$ and $CD4^+CD25^{high}$ populations. The $CD4^+CD25^{low}$ cells could not suppress the proliferation of co-cultured $CD4^+CD25^-$ responder T cells, whereas the

$CD4^+CD25^{high}$ cells cultured alone could strongly inhibit the proliferation of responder cells (45). Therefore, CD25 alone was insufficient to define Treg cells in humans and more surrogate markers were needed.

This later resulted in the use of Foxp3, a member of the forkhead/winged-helix family of transcription factors, as an appropriate marker for tTregs. However, the associations between FoxP3 and Treg cells were confirmed much later than its initial discovery. Foxp3 was first discovered in the Scurfy mouse in 1949 (46). Scurfy is an X-linked recessive, fatal lymphoproliferative disorder (47-50). In 2001, DNA sequencing revealed that IPEX was the human equivalent of mouse scurfy (51). It was confirmed that mutations of the human *Foxp3* gene, the ortholog of the gene mutated in Scurfy mice, led to impaired Treg cell development and function, subsequently causing IPEX (41, 52).

As for the *Foxp3* gene locus, there is one promoter as well as three conserved non-coding sequences (CNS), which are the main targeted regions for epigenetic modifications and transcriptional factor modulations (53, 54). The promoter region containing a TATA box, a GC box and a CAAT box, is cell-specific and induced following TCR engagement (55). It is completely demethylated (1.4%±0.95% methylated) in human $CD4^+CD25^{high}$ Treg cells, while $CD4^+CD25^{low}$ T cells had a 27.9%±7.1% methylated promoter region (56). Although stimulated $CD4^+CD25^{low}$ T cells remained partially demethylated, they could only transiently express Foxp3. Thus, the promoter demethylation status might regulate the stable Foxp3 expression and Treg commitment (56). CNS-1, containing binding motifs for Smad3, NFAT, AP-1 and retinoic acid receptor (RAR), is a transforming growth factor-β (TGF-β) sensitive enhancer region, hence crucial for the peripheral induction of Foxp3 in gut-associated lymphoid tissues but not in the thymus (57). In contrast, the pioneer element CNS-3, binding c-Rel and p65, is indispensable for potently

initiating Foxp3 induction in the thymus as well as the periphery (54, 58). CNS-2, also known as Treg cell specific demethylated region (TSDR), is rich in CpG motifs (details refer to section 1.3.3.1). Although expendable for Foxp3 induction, CNS-2 is more important in promoting the stabilization of Foxp3 expression in Treg cells (57, 59).

1.2.1.3 Regulatory T Cell Differentiation

As stated in Section 1.1.3, Treg cell differentiation occurs quite late during T cell development and starts with an upregulation of the Foxp3 expression. Despite the significance of the Foxp3 expression in Treg cell development, various experiments proved that the expression of this transcriptional factor alone is insufficient to establish the Treg cell lineage. Growing evidence has suggested that in humans, a small subset of $CD4^+$ and $CD8^+$ T cells transiently up-regulate Foxp3 expression at a low level upon *in vitro* stimulation without acquiring Treg cell suppressive activity (60, 61). Thus, the expression of Foxp3 is normal following T cell activation, thus not a specific marker for iTregs in humans. Furthermore, in $Foxp3^{gfp}$ mice, where Foxp3 expression has been disrupted by the insertion of the GFP gene, thymocytes could still develop into T cells sharing the same Treg characteristics (62). These features include similar thymic development, the exclusive expression of αβTCRs, and cell surface phenotype (62).

Therefore, Treg cell development appears to involve multiple processes, and other independent processes may also be obligatory for Treg cell development (63). For example, epigenetic modifications such as Treg-cell-specific DNA hypomethylation (64, 65).

1.2.1.3.1 Epigenetic Modifications

Epigenetics is defined by the regulation of gene expression without changing nucleotide sequences in the genome (66, 67). There are various types of epigenetic modifications, such as histone modifications, DNA methylation, and chromosome conformational changes (68). In particular, DNA methylation and histone modifications are involved greatly in the cell-lineage determination and maintenance because they are inheritable through cell divisions (69), which have already been documented at the *Foxp3* locus (64, 69).

Complete demethylation of CpG motifs (Treg cell specific DNA hypomethylation, Treg-Me) and histone modifications within the conserved region was shown by Bisulfite sequencing and chromatin immunoprecipitation (ChIP) assays in *ex vivo* $CD4^+CD25^+Foxp3^+$ Tregs (70). CpG hypomethylation of Foxp3 TSDR is exclusively imprinted in tTreg cells compared with other T cell subpopulations including retroviral Foxp3-overexpressing conventional T cells (Tconv) and iTregs (64). This indicates that the establishment of Treg-Me is independent of the Foxp3 expression over the course of tTreg cell development from the thymus to the periphery (64). Foxp3-expressing thymocytes without the Treg-Me pattern lost the Foxp3 expression and failed to differentiate into Treg cells (19).

1.2.1.3.2 Role of TCR Signalling

Several animal studies have revealed the significance of TCR signalling in Treg cell development, which is also confirmed by direct sequence analysis of the TCR repertoires between Treg and non-Treg cells. TCR transgenic mice, but not recombination activating gene (RAG) deficient αβTCR transgenic mice, developed $CD4^+CD25^+$ T cells that

predominantly expressed TCRs with endogenous α-chains (71). There are also considerably reduced numbers of Foxp3$^+$ Treg cells in αβTCR and βTCR transgenic mice, suggesting that gene rearrangement at the TCR α-chain locus is required in Treg cell development in the thymus (72, 73). Direct sequence analysis of the TCR repertoires expressing a fixed transgenic TCR-β chain showed the diversity of TCR-α sequences in Treg cells and they only partially overlapped with non-Treg cells (74, 75). Wolf et al. also found that there were only a limited number of TCR sequences shared between Tconv and Tregs (76).

TCR signalling plays a pivotal role in the induction of Foxp3 expression as well as Treg-Me to support Treg cell development. However, the quality of TCR stimulation required for the Foxp3 induction or Treg-Me seems to be different (19). The intensity of TCR stimulation mainly determines Foxp3 induction (73), whereas the acquisition of Treg-Me chiefly depends on the duration of TCR stimulation (64).

1.2.1.3.3 Co-stimulatory Factors and Cytokines

CD28 is expressed on T cells. After binding to its ligands CD80 (B7.1) and CD86 (B7.2), CD28 serves as costimulatory signals for T cell activation or inhibition in addition to TCR signals (77). In the B7$^{-/-}$ non-obese diabetic (NOD) mice, a significant reduction of CD4$^+$CD25$^+$ T cells was observed, suggesting that the CD28/B7 costimulatory pathway contribute greatly to Treg cell development and homeostasis (78, 79). Tai et al. proved that CD28 co-stimulation independently promoted the expression of Foxp3 in TCR-signalled, double positive thymocytes hence initiating tTreg differentiation (80).

Cytotoxic T lymphocyte associated protein 4 (CTLA-4, CD152) and CD28 are homologs, both binding to B7 and have opposing functions (81). Zheng et al. found that TGF-β was

unable to induce Foxp3 expression in CTLA-$4^{-/-}$ mice and the addition of anti-CTLA-4 to $CD4^{+}CD25^{-}$ cells *in vitro* eliminated TGF-β induce iTregs completely in a mouse model (82). Wing et al. generated BALB/c mice with an impaired CTLA-4 gene expression, and found that CTLA-4 deficiency led to the spontaneous development of fatal T cell-mediated autoimmune disease (83). This exhibited the same pathological condition seen with the Foxp3 deficiency in both humans (51) and mice (52), demonstrating that both CTLA-4 and CD28 play significant roles in the Treg differentiation.

$Foxp3^{+}$ Treg cells were found to be generated from peripheral $CD4^{+}$ T cells in 2003 when Chen et al. used TCR stimulation and TGF-β to induce Foxp3 expression and convert naïve peripheral murine $CD4^{+}CD25^{-}Foxp3^{-}$ T cells into $Foxp3^{+}$ pTreg cells (84). The role of TGF-β in Treg development was confirmed later in humans both *in vitro* (85, 86) and *in vivo* (87). Whilst TGF-β contributes greatly to the differentiation of pTreg and iTreg cells, there is also increasing evidence pointing to its critical role in the generation of tTreg cells (88-90).

IL-2 is essential for T cell growth *in vitro* and plays a critical role in the maintenance of the Foxp3 expression and T cell tolerance *in vivo* (91, 92). IL-2 alone is inadequate to induce the Foxp3 expression, but it is indispensable for TGF-β-mediated Foxp3 induction in naïve $CD4^{+}$ cells (93).

1.2.1.4 Treg Cell Subsets

Though tTregs, pTregs and iTregs are of different origin, all three subsets share common features, including expression of phenotypical markers Foxp3, CD25 and CTLA-4 (65,

94). The differences will be discussed in terms of Treg-Me, TCR repertoire, the stability of the Foxp3 expression and suppressive function.

Treg-Me, especially at the Foxp3 CNS2 domain (TSDR), is similar between tTreg cells and pTreg cells (95) but is different from iTreg cells. *In vitro* TGF-β treatment failed to induce complete DNA hypomethylation characteristic of tTregs (64). However, it should be noted that the timing of TSDR hypomethylation detection for different types of Treg cells varied significantly in these studies. Timing might be critical since TSDR demethylation in $CD4^+Foxp3^+$ tTreg cells is not yet complete in the thymus (70).

According to their cell origin, pTregs and iTregs inherit TCR repertoires from naïve conventional T cells (96). In contrast, tTregs which recognise self-antigens have different TCR repertoires from pTregs and iTregs.

Since stable Foxp3 expression relies on the status of TSDR methylation (70, 95), epigenetic differences at the Foxp3 TSDR locus leads to a difference in the Foxp3 expression stability between tTregs, pTregs and iTregs. iTregs rapidly lose their Foxp3 expression either *in vitro* (70, 97) or following adoptive transfer *in vivo* (97-99). Moreover, the instability of the Foxp3 expression in iTreg correlates with the strength of TCR signals *in vivo* (97), and it can be stabilised by modulating TSDR hypomethylation.

Distinct functional differences have not been conclusively demonstrated between tTregs and pTregs. tTregs play an important role in preventing autoimmune diseases, whereas pTregs are mostly involved in the mucosal tolerance and inflammatory reactions towards foreign antigens (65, 100). As for iTregs, the results are controversial. iTregs have been shown to effectively prevent the development of inflammation in Scurfy mice (101) and several animal disease models including Myasthenia Gravis (102), type 1 Diabetes (103),

Experimental Autoimmune Encephalomyelitis (98), and Autoimmune Gastritis (104). In humans, Treg cells have already been tested for treating various medical conditions especially GVHD since 2009 (105, 106). However, all the candidate cells used in immunotherapy for autoimmune diseases till now are *ex vivo* expanded Tregs due to their stable Foxp3 TSDR demethylation (107), rather than iTregs. Various studies showed that unlike in mice, human iTregs were neither anergic nor suppressive and produced pro-inflammatory cytokines upon stimulation even with stable Foxp3 expression (86, 108).

1.2.1.5 Mechanisms of Treg cell-mediated immune tolerance

Treg cells are naturally present in the immune system (41). They can suppress the activation, proliferation and cytokine productions of various immune cells including T cells, B cells, DCs, NK cells and macrophages (109). This particular suppressive capacity to control immune responses makes Treg cells indispensable for self-tolerance and the prevention of over-reactivity to maintain immune homeostasis (109). Deficiency and dysfunction of $Foxp3^+$ Treg cells lead to severe autoimmune disease such as IPEX (41, 52), allergy and asthma (110), inflammatory bowel disease (IBD) (41, 111), GVHD (112), as well as fetal-maternal intolerance during pregnancy (109, 113, 114).

There are several mechanisms by which Tregs contribute to immune tolerance as summarised in Figure 1.2 (115-118). Tregs can act directly by cell-contact dependent suppression or by the secretion of immunosuppressive cytokines. They can also indirectly act through modifications of APCs.

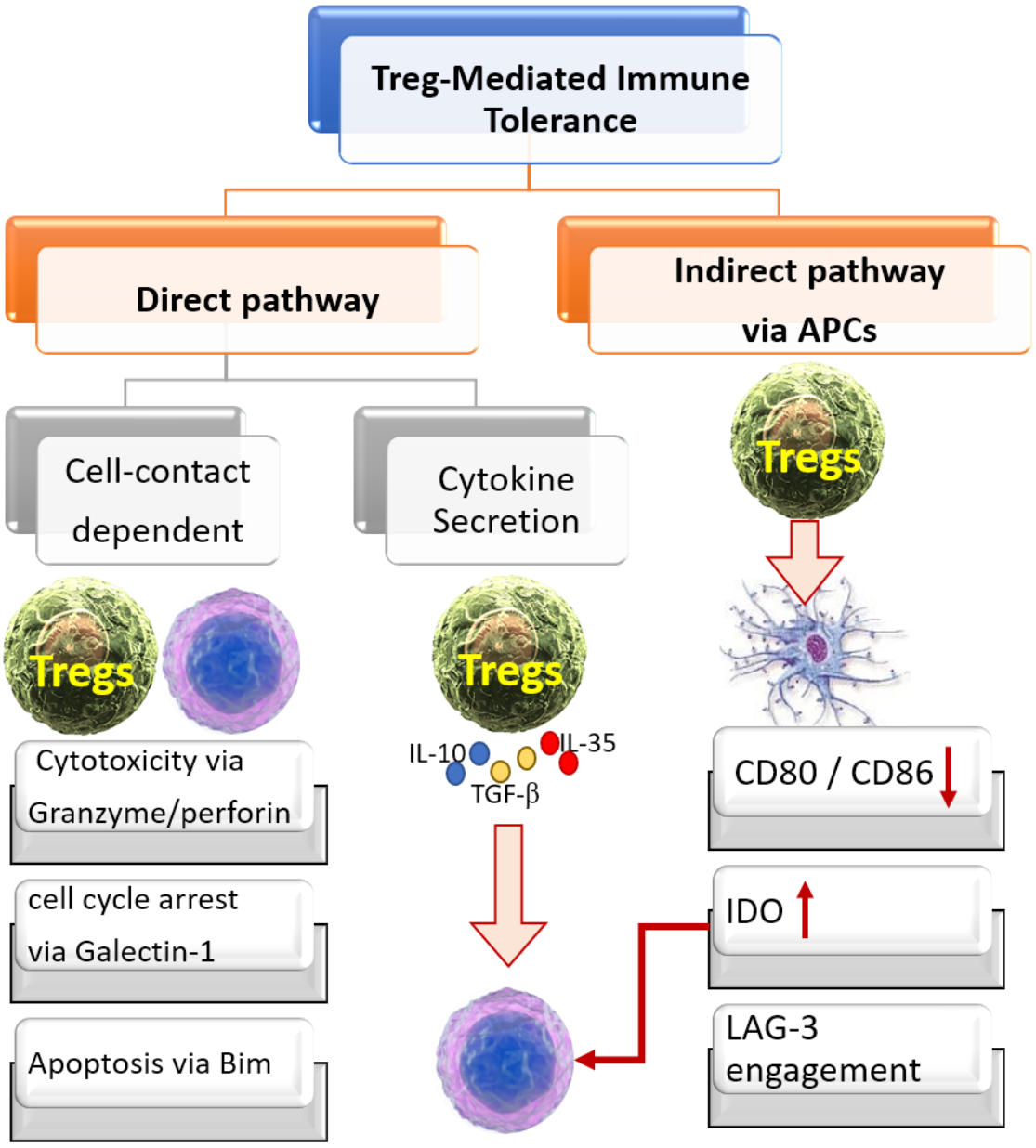

Figure 1.2 Mechanisms involved in the SCFA-medicated immune tolerance.

The mechanism of cell-contact-dependent suppression first came from *in vitro* studies. In order to evaluate the suppressive capacity of Treg cells, they were cocultured with responder cells and stimulated with a specific antigen or a polyclonal TCR stimulator in the presence or absence of APCs *in vitro* (119, 120). Tregs failed to suppress the proliferation of responder T cells when they were separated by a semi-permeable

membrane (119, 120), suggesting a cell-contact-dependent mechanism. After direct cell contact, Tregs may exert cytotoxicity on APCs and responder T cells through either granzyme A/B and perforin (121-123), or induce cell cycle arrest via Galectin-1 expression (118, 124). By competing for IL-2, Tregs could also inhibit the proliferation of responder cells, causing Bim-mediated apoptosis (125).

Different from the direct cell-contact mechanism discovered in the *in vitro* suppression, *in vivo* experiments and disease models mentioned above indicated that secretion of immunosuppressive cytokines worked as another mechanism (109, 126). Interleukin (IL)-10 and TGF-β are proposed as the main negative immunoregulators secreted by Tregs (115-118). Despite mounting evidence showing the importance of IL-10 and TGF-β in Treg-mediated suppression, there are some controversial results. Autoimmune gastritis in BALB/c mice was successfully prevented by IL-10-deficient T cells (127). Blockage of IL-10 exerted no effect on the suppressive capacity of Tregs in the *in vitro* proliferation assay (119, 120). In addition, the suppression mediated by tTregs isolated from neonatal TGF-β knockout mice were intact *in vitro* (128). These tTregs could also prevent IBD *in vivo* (129). Another cytokine investigated was IL-35. IL-35-deficient Tregs had no therapeutic effect on IBD *in vivo* and recombinant IL-35 could suppress T effector (Teff) cells *in vitro* (130). Bardel et al. investigated the expression of IL-35 in Treg cells isolated from multiple human organs (131). Unlike their murine counterpart, IL-35 expression of Treg cells was not detected.

Furthermore, Tregs could also functionally modify APCs via three pathways: (a) downregulating or preventing upregulation of CD80 and CD86 (132); (b) upregulating the expression a potent regulatory molecule, indoleamine 2,3-dioxygenase (IDO) on DCs to suppress Teff cell activation (133); and (c) Lymphocyte activation gene 3 (LAG-3,

CD223) engagement with MHC II inhibiting DC activation (134, 135); hence maintaining the tolerogenic status of APCs.

Interestingly, pathways (a) and (b) mentioned above appear to be CTLA-4 dependent (132, 133). Wing et al. generated BALB/c mice with flawed CTLA-4 gene expression and found that CTLA-4 deficiency in Tregs could lead to the spontaneous development of fatal T cell-mediated autoimmune disease (83). CTLA-4-deficient Tregs could still develop and survive without altering thymic selection, only affecting Treg suppressive capacity in the periphery as well as *in vitro*. This is probably due to CTLA-4 dependent mechanisms dampening the potency of APCs described above (132, 133).

1.2.1.6 Other Genes Related to Treg-mediated Immune Tolerance

Apart from *Foxp3* and *CTLA-4*, there are also various other genes contributing to immune tolerance mediated by Treg cells.

1.2.1.6.1 Glucocorticoid-Induced TNFR-related protein (GITR)

Glucocorticoid-induced TNF-related protein (GITR) is also known as tumour necrosis factor receptor superfamily member 18 (TNFRSF18). GITR is predominantly expressed on Treg cells. GITR contributes to the maturation and expansion of tTregs in both humans and mice (136). Moreover, GITR plays a crucial role in Treg cell function and is involved in various diseases (136). Antibodies against GITR reverse the suppressive capacity of $CD4^+CD25^+$ T cells (137), thus producing autoimmune disease in mice (138). Removal of GITR-expressing T cells can also result in autoimmunity (138).

1.2.1.6.2 CD39

CD39 is nucleoside triphosphate diphosphohydrolase-1 (NTPDase 1), an ectoenzyme that degrades ATP to AMP. CD39 is expressed primarily by Treg cells in both humans and mice (139). In mice, it is present on nearly all $CD4^+CD25^+$ cells; while in humans, only around 60% of Tregs are $CD39^+$ (139). $Foxp3^+CD39^+$ Treg cells display a demethylated TSDR and higher suppressive capacity. The secretion of the pro-inflammatory cytokines interferon-γ (IFN-γ) and tumour necrosis factor-α (TNF-α) are also diminished in $CD39^+$ Tregs after *in vitro* stimulation (140). The suppressive capacity of Treg cells isolated from CD39-deficient mice are diminished *in vitro*, and these cells were unable to block allograft rejection *in vivo* (141). CD39 contributes to the suppressive effects through catalytic inactivation and conversion of extracellular pro-inflammatory ATP (139).

1.2.1.6.3 Inducible T-cell CoStimulator (ICOS, CD278)

Inducible T-cell costimulator (ICOS, CD278) belongs to CD28-superfamily (142). It is expressed at low levels on resting naïve T cells. Upon TCR recognition and CD28 costimulation, it is upregulated and highly expressed on activated T cells (143). In gene knockout $ICOS^{-/-}$ mice, the early expansion of Treg cells was jeopardised and the percentage of $CD4^+Foxp3^+$ Treg cells was significantly lower (144). The addition of ICOS-blocking antibody could lead to the impaired Treg differentiation and function in humans as well (145). In addition, IL-10 production was significantly reduced by $CD4^+Foxp3^+$ Treg cells in the $ICOS^{-/-}$ mice (143, 144). In fact, IL-10 production was found to be significantly correlated to the levels of ICOS expression on $CD4^+$ T cells (146). In ICOS-deficient patients, there was also extensive T cell dysfunction, including

imbalance between effector and regulatory cells (147). Collectively, ICOS is pivotal for the expansion, maintenance and IL-10 production of Treg cells.

1.2.1.6.4 Programmed Cell Death Protein 1 (PD-1, CD279) and Programmed Cell Death-Ligand 1 (PD-L1, CD274)

Programmed cell death protein 1 (PD-1, CD279) is another B7 family member and a CD28 homologue. It is a cell surface receptor mainly expressed on T cells, B cells, and NK cells (148). PD-1 is not expressed on naive T cells, but it can be upregulated in response to T cell activation (149). It binds to its ligands Programmed cell death-ligand 1 (PD-L1, CD274) and Programmed cell death-ligand 2 (PD-L2). While the expression of PD-L2 is restricted, PD-L1 is widely expressed on different immune cells (including T cells, B cells, DCs and macrophages), as well as various organs and solid tumour cells (150). Apart from PD-1, PD-L1 also binds to B7-1 to inhibit T cell responses, and this interaction is specifically restricted to PD-L1 but not PD-L2 (151).

The pathway involving the interactions between PD-1 and PD-L1 (PD-1: PD-L1) contributes greatly to the maintenance of self-tolerance by exerting inhibitory signals to prevent autoimmunity (152, 153). A deficiency of PD-1 in mice led to various types of autoimmune diseases, such as Type 1 diabetes and experimental autoimmune encephalomyelitis (154, 155). The generation of $CD4^{+}Foxp3^{+}$ Tregs was greatly increased by PD-L1, and $PD\text{-}L1^{-/-}$ APCs were unable to induce Tregs, indicating the important role of PD-L1 in Treg cell induction (156, 157). In addition to its essential role in autoimmunity, PD-1: PD-L1 has been demonstrated to successfully reduce tumour growth and suppress metastasis, providing a ground-breaking therapeutic intervention for cancer treatment (150).

1.2.1.6.5 CD127

Interleukin-7 receptor subunit alpha (IL7R-α) is also known as CD127. In humans, CD127 is downregulated on all T cells upon T cell activation, then re-expression occurs on most of the effector and memory T cells (158, 159). However, CD127 expression remains low for $Foxp3^+$ Treg cells (160). Unlike CD25, which has no correlation with Foxp3 in $CD4^+$ cells, CD127 expression was inversely associated with not only Foxp3 expression, but also the suppressive function of Treg cells in both humans and mice (160). These results indicate that low CD127 expression is also a typical feature of Treg cells, compared to conventional T cells.

1.2.1.6.6 Human Leukocyte Antigen – antigen D Related (HLA-DR)

Human leukocyte antigen – antigen D related (HLA-DR) belongs to MHC-II class, encoded by the HLA complex on chromosome 6 (161). Interestingly, the expression HLA-DR is restricted to human Tregs only, since murine Tregs cannot transcribe CIITA required for MHC-II expression (162). Compared to $HLA\text{-}DR^-$ Tregs, *in vitro* generated $HLA\text{-}DR^+$ Tregs have higher Foxp3 expression and exhibit better suppressive capacity (163). Moreover, the suppressive capacity of *ex vivo* isolated HLA- DR^+ Tregs is also more effective (163). Hence, HLA-DR expression identifies a highly functional subset of Tregs.

1.2.2 Antigen Presenting Cells

Professional APCs are a group of specialised cells which present antigens via MHC-II at the cell surface and express costimulatory signals recognised by TCRs and costimulatory receptors respectively on T cells. They include DCs, macrophages and B cells. The main

role of APCs is to process and present antigens to initiate the adaptive immune responses conferred by T cells. Apart from their contributions to immunity, there is growing research indicating that APCs also play a significant role in immune tolerance.

APCs, particularly DCs, regulate immune responses towards either immunity or tolerance, depending on the context of antigen exposure and different environmental stimuli. Several signals are required for DCs to activate T cell responses, involving the MHC-II complex, the expression of costimulatory molecules and secretion of soluble factors (164). All three types of signals are integral components for the initiation of T cell differentiation.

1.2.2.1 Dendritic Cells

DCs are present in various tissues, such as the skin, the inner layer of the respiratory tract and gastrointestinal tract, which have straight contact with the outer environment. Once activated by antigens, DCs migrate to the draining lymph nodes and interact with mainly T cells to trigger the adaptive immune responses. As implied in their name, they grow branched projections (dendrites) during certain developmental stages. The term "Dendritic Cells" was first introduced by Ralph Steinman in 1973 (165). He was awarded the Nobel Prize in Physiology/Medicine in 2011 for his breakthrough discovery of dendritic cells and their role in orchestrating the adaptive immune response (8, 9).

The DC lineage is perhaps the most complicated hematopoietic pathway yet to be explained (166). The observation of Flt3 expression led to the identification of a common precursor for monocytes, macrophages, and classical DCs in the bone marrow, known as macrophage-DC progenitor (MDP) (167). It has been confirmed that MDPs can differentiate into monocytes, macrophages and classical DCs depending on different

cytokine milieus both *in vivo* (168) and *in vitro* (169). Common-DC progenitor (CDP), identified downstream of MDPs, are a DC-restricted progenitor producing classical/myeloid dendritic cells (cDCs) and plasmacytoid dendritic cells (pDCs) (168). The split in monocyte, macrophages and DC lineage begins between the MDP and CDP stages (170). In humans, research into DC differentiation is restricted to *in vitro* studies, which utilised monocytes and $CD34^+$ hematopoietic precursor cells (8, 171, 172) to generate human DCs. The exact contribution that lymphoid precursors, myeloid precursors and monocytes make to the human DC pool *in vivo* is, however, unclear.

The definition and classification of human DCs are somewhat ambiguous, due to their heterogeneity. Typically, a set of inclusion and exclusion criteria is used to define DCs. Firstly, cells expressing leukocyte lineage markers (such as CD3, CD19, CD14, CD16 and CD56) need to be excluded. Then MHC II (such as HLA-DR) and CD11c (a leukocyte integrin surface marker for all DCs in mouse) expressions are used as inclusion criteria (173, 174). Depending on their tissue-specific presence, DCs exhibit phenotypic differences (175). For example, CD1a is used in Langerhans cells in the skin (176). In human peripheral blood, blood dendritic cell antigens (BDCAs) can identify distinct subsets (173). In various other tissues, CD83 has been used as a specific marker of mature DCs (177).

DCs are normally divided into cDCs and pDCs (178). Compared to cDCs, pDCs express high levels of CD123 and low levels of MHC-II, whereas CD11c is expressed equally in both types. PDCs accumulate mainly in the lymphoid tissues and blood. Upon recognition of viruses, they produce high amounts of interferon-α and acquire the capacity to present foreign antigens (179). cDCs refer to all DCs other than pDCs. They are usually located

in the spleen marginal zone and nonlymphoid tissues, where they constantly acquire tissue antigens (175).

DCs are versatile in their function in accordance with their activation status. Under steady state conditions, DCs are referred to as immature DCs (iDCs) with a weak T cell stimulating property due to the low expression of MHC-II molecules and costimulatory molecules, including CD80/CD86, PD-L1 as well as CD40 (180). These iDCs located in the blood and lymph nodes, favour the differentiation of pTreg cells. Taken together, iDCs contribute greatly to peripheral tolerance (8, 9). Under pathogenic or inflammatory conditions, iDCs become activated or matured (referred to as mDCs) after capturing, processing and presenting foreign antigens in MHC-II complexes. After activation, they migrate from various tissues into spleen and lymph nodes, where they can activate antigen-specific T cells, produce pro-inflammatory cytokines, hence inducing immunity (8, 9). Thus, it is the maturation status that distinguishes between tolerogenic and immunogenic DCs (181).

1.2.2.2 Monocyte-Derived Dendritic Cells

Monocyte-derived DCs (MoDCs) are a special type of DCs differentiated *in vitro*, sharing similar dendritic morphology and antigen presenting ability as DCs *in vivo*. They are differentiated from monocytes when cocultured with granulocyte macrophage - colony stimulating factor (GM-CSF) and IL-4 *in vitro* (172). These immature MoDCs can further differentiate into mature MoDCs when presented with various stimuli (172, 182), such as lipopolysaccharide (LPS). Monocytes are the most commonly used cells for DC generation *in vitro*.

1.2.3 Regulatory B cells

Breg cells are a collection of B cells with suppressive capacity. They were first discovered in guinea pigs in the mid-1970s. Upon the adoptive transfer of sensitised splenocytes, B cells were able to suppress delayed-type hypersensitivity (183). The suppressive nature of B cells was confirmed later in mice, where B-cell-deficient mice failed to recover from experimental autoimmune encephalitis (184). The term Bregs was introduced only in 2002 by Bhan, who showed that IL-10 producing B cells featured by CD1d upregulation appeared in chronic intestinal inflammatory conditions (185). Bregs were not discovered in humans until 2007, and these cells also produce IL-10 (186).

Several disease models demonstrate that Bregs are heavily involved in autoimmune diseases, allergies, tumour immunity, infection, and transplantations (32). Breg cells can inhibit the differentiation of pro-inflammatory T cells, especially T helper (Th) 1 and Th17 cells, through the production of IL-10, TGF-β, and IL-35. In contrast, the differentiation of anti-inflammatory T cells, such as $Foxp3^+$ T cells and T regulatory 1 (Tr1) cells, can be induced by Bregs (31). However, most data are only focused on the interaction between Bregs and T cells, but not on other immune cells.

1.2.4 Innate lymphoid cells

ILCs are a special type of innate immune cells discovered in 2009 (187). Later, researchers found that there was a variety of cells sharing the same features. These cells are defined by the absence of antigen-specific BCRs or TCRs, and they do not express myeloid or dendritic cell markers. ILCs belong to the lymphoid lineage and are defined as cell lineage marker-negative cells (188, 189). The ILC family contains cytotoxic ILCs (NK cells) and non-cytotoxic ILCs. The latter normally divides into three distinct groups

according to the differential expression of cell surface markers, transcription factors and functional criteria: group 1 ILCs (ILC1s), group 2 ILCs (ILC2s) and group 3 ILCs (ILC3s) including lymphoid tissue inducer (LTi) cells(189). ILC1s are involved in immunity to intracellular pathogens due to their capability of producing IFN-γ and TNF-α. On the other hand, ILC2s secrete Th2 cell-associated cytokines (IL-4, IL-5, IL-9 and IL-13), hence take part in defence against parasite infections, allergens, and epithelial injuries. Finally, ILC3s contribute to combating bacterial and fungal infection, since they produce the Th17 cell-associated cytokines IL-17 and IL-22 (33, 34). IL-22 is part of the IL-10 family and contributes to innate and nonspecific immunity in tissues (190).

ILCs, despite lacking antigen presentation capability, are functionally similar to their adaptive immune system counterparts in the T helper cell population (33). ILCs react promptly to signals from infected or injured tissues and release a wide range of cytokines to initiate innate responses or regulate the adaptive immune system via the expression of MHC II molecules or through the regulation of DCs. Dysregulated ILC responses result in chronic inflammatory diseases, autoimmune diseases, metabolic disorders and cancers (33, 34).

1.3 Immune Tolerance and Programming during Pregnancy

1.3.1 Medawar's hypotheses

One of the foremost enigmas of reproductive biology is that a healthy woman with a normal functioning immune system can carry a semi-allogeneic fetus successfully to full term without apparent immune rejection. The maternal immune system undergoes relevant immunological changes for the semi-allogeneic fetus so that it can be tolerated (191). This phenomenon proves the involvement of immune tolerance during a normal

pregnancy. In humans, the semi-allogeneic fetus has to be successfully tolerated throughout pregnancy, which is typically 40 weeks.

Fetal alloantigens encoded by polymorphic genes inherited from biological father should theoretically trigger a maternal immune rejection, which does not normally occur (192). The remarkable nature of this immunological paradox was recognised by Sir Peter Medawar in 1953, who worked on skin graft rejection in genetically different individuals. He hypothesized that the recognition of fetal alloantigens by maternal immune cells is dampened by the placenta, which works as a physiological barrier that strictly separates the fetus from maternal tissues (193). At the time, he proposed three mechanisms in pregnancies which contribute to the prevention of maternal rejection of the fetal allograft: an anatomical separation between the mother and the fetus, the reduced number of antigens possessed by the fetus (194), and the rendered inertness of the maternal immune system (195).

Undoubtedly, Medawar pioneered the research relating to immunological tolerance during pregnancy and his hypotheses were proven to a certain extent. It is now known that the placenta, extravillous trophoblast (EVT) cells per se, separates most of the fetal antigens from the maternal immune system. EVTs have poor antigen presentation property due to the lack of classical MHC-I (except HLA-C) and MHC-II molecules (194). It would seem plausible that the maternal immune system is compromised by non-recognition of fetal antigens in favour of a successful pregnancy. However, as there is accumulated evidence indicating the existence of anti-fetal HLA antibodies in maternal serum (196, 197), the maternal immune system has continuously been activated by fetal cells (195).

1.3.2 Immune Tolerance during pregnancy

During pregnancy, immune adaptations happen locally in the fetal-maternal interface, the decidua, as well as systemically. Immediately after implantation, fetal trophoblast cells infiltrate in the endometrium and gradually develop into the decidua. This trophoblast invasion needs proper immunological regulation to maintain the survival of fetal trophoblast cells while limiting their invasion (198). Local immune cells, such as NK cells, macrophages, DCs and Treg cells, are present *in situ* before implantation. They are subject to certain adaptations (for example, increased cell numbers) immediately following implantation (199). After the final establishment of the placenta circulation in the first trimester (before 12 weeks of gestation), the fetal syncytiotrophoblasts begin to come in close contact with maternal peripheral blood (200), hence inducing systemic immune responses. For the purpose of this thesis, special attention will be focused on the decidua and regulatory T cells.

1.3.2.1 The Fetal-Maternal Interface: Decidua

The decidua is the interface between the fetus and the maternal uterine endometrium during pregnancy. The decidua consists of decidua basalis, decidua capsularis, and decidua parietalis based on their anatomical location. At the fetal-maternal interface, the decidua participates in exchanges of nutrients, gases, and waste. Most importantly, it plays an essential role in immune tolerance during pregnancy. There are mainly three types of cells in the decidua: fetal EVTs, decidua stromal cells, and maternal immune cells (which accounts for nearly 50% of cells) such as uterine NK cells (201). There is a bidirectional passage of cells across the fetal-maternal interface, proved by the presence of microchimerism in both the mother and the fetus (202, 203). Microchimerism refers to

the existence of low numbers of cells originated from another individual and genetically distinct from the host cells (204).

1.3.2.2 Regulatory T cells in Human Pregnancy

It is now evident that there is a systemic increase in maternal Treg cells during normal pregnancy (205, 206). In contrast, deficits in Treg cell number and function result in unexplained infertility (207), miscarriage (208) and pre-eclampsia (206). In addition, there was a specific and significant correlation of Treg cells in the paired maternal-fetal (dyads) samples, while this correlation didn't exist between the father and the fetus (209). This indicated that transplacental immune regulation was through a soluble immune modulatory factor(s), which can cross the placenta. Since fetal T cells, including Treg cells, are of different origins from adults (210), it is less likely that maternal Treg cells migrate into the fetal Treg cell compartment.

1.3.3 Transplacental Immune Programming

During pregnancy, the maternal immune system undergoes changes to adjust to the semi-allogeneic fetus while the fetus also develops its own immune system. Though separated by the placenta, there is crosstalk between the mother and the fetus. For example, maternal IgG antibodies can cross the placenta to either pass on temporary protective passive immunity to the offspring (211), or cause neonatal hyperthyroidism by the presence of maternal TSH receptor antibodies (212). Also, the presence of fetal microchimerism was found in the peripheral blood of the mother (203).

1.3.3.1 Developmental Origins of Health and Disease

This transplacental immune programming is part of the theory of Developmental Origins of Health and Disease (DOHaD). It was originally postulated by Barker and Osmond in 1984 (213). Together with other observational studies, Barker formulated his developmental programming hypothesis, stating that nutrition in prenatal and early life periods is essential for noncommunicable diseases (for example, ischemic heart disease) later in life. Since then, numerous investigations proved that fetal organ systems during this sensitive period of development experience programmed structural or functional changes depending on the intrauterine environment. These changes lead to various diseases later in adulthood (214).

Numerous human studies support the DOHaD theory in the context of inflammatory and immune diseases (215-217). The mechanism for immune programming is not yet well defined, but evidence suggests that both fetal innate and adaptive immune systems are involved (209, 216, 218-222).

1.3.3.2 The development of the fetal immune system

In human fetuses, hematopoietic stem cells migrate to the thymus as early as 8.2 gestational weeks, then T cell differentiation starts (223). In the fetal thymus, T cell differentiation is similar to the adult, achieved through positive selection in the cortex and negative selection in the medulla. However, Treg cell development is somewhat different. A population of thymocytes already initiates the expression of CD25, during the transition from DP $CD27^-$ cells to DP $CD27^+$ cells (224). From 10 weeks of gestation, T cells migrate from the thymus to peripheral lymphoid organs (223). Unlike newborns and adults, the frequency of fetal Treg cells is significantly higher, around 15-20% of total

$CD4^+$ T cells (225). This increase in the Treg cell compartment proves that the fetal immune system is prone to differentiate into Tregs upon stimulation in order to maintain a tolerogenic status.

1.3.3.3 The influence of maternal immune environment on the fetal immune system

In response to stimulation with maternal alloantigens, fetal T cells differentiate into Tregs and those specific for non-inherited maternal alloantigens (NIMAs) are maintained for a long time until adulthood (226). It can also be proved in a study focus on the effects of tolerance to NIMAs on the survival of kidney transplantation from haploidentical siblings. The 10-year graft survival rate from sibling donors expressing NIMAs was similar to that from HLA-identical siblings, indicating the maternal modulation of the fetal immune system induced a long-lasting form of tolerance (227).

There is also other evidence for transplacental immune regulation during pregnancy. In BALB/c mouse model, maternal Th1 and regulatory immune responses to schistosome infection could protect the offspring from the onset of allergic airway inflammation. Associated schistosome-specific cytokine and gene expression changes were also seen within the fetal-maternal interface (228). In addition, the offspring of tolerised mice were completely protected against asthma due to the transplacental transfer of allergen-specific IgG (218). Additionally, in both humans and mice, microbial stimulation of the pregnant mother could lead to decreased levels of atopic sensitisation and asthma in the offspring (229-231).

The mechanisms for immune programming are still not well understood. The transplacental transport of allergen-specific IgG contributes to the protection of asthma via the fetal innate immune system (218). Moreover, the expression of Toll-like receptors

(TLRs; pattern recognition receptors that recognise bacterial components) is elevated upon maternal contact with farm animals and cats (219), which contributes to the prevention of allergy pathogenesis (220). As for the fetal adaptive immune system, the frequency and function of Treg cells are increased and associated with lower Th2 cytokine secretion after maternal farm exposure (216), possibly via soluble factors such as IL-10 (209) or bacterial metabolites (221). Collectively, these findings provide evidence that appropriate stimulation of the maternal immune system *in utero* may educate and shape the fetal immune system.

1.4 Gut Microbiota, Immune Homeostasis and Dietary Manipulation

1.4.1 Gut Microbiota

The mammalian gastrointestinal (GI) tract is home to a massive number of microorganisms (approximately 100 trillion) (232), and a majority of them are commensal bacteria. This gut microbial community (referred to as microbiota) has evolved together with its host. Various factors, including age, genetics, environment, antibiotics and diet, play an essential role in the composition of gut microbiota (232, 233).

Depending on the mode of delivery (vaginal birth or through Caesarean Section), infants have different compositions of gut microbiota at birth, due to the different maternal colonization *in situ*. The gut microbiota develops quickly during the first year of life based on the feeding habits (breastfeeding or formula) (234, 235), and reaches maturation eventually at around 2-3 years old, having a similar composition compared to adults (236). Antibiotic exposure, which is commonly seen during early life, also has significant effects on the gut microbiota and later onset of allergies (237). The overall diversity is compromised and there are more *Proteobacteria* and less *Actinobacteria* populations

(238). Despite harbouring trillions of microbes, adult gut microbiota is mainly dominated by three types of bacterial phyla, *Firmicutes*, *Bacteroidetes*, and *Actinobacteria* (232, 239).

1.4.2 Diet Influence the Gut Microbiota

Various global cross-sectional studies showed that the diet significantly influences the diversity of the intestinal microbiota, and subsequently its metabolites production (240). The effect of long-term diet on the composition of the gut microbiota has been well demonstrated (232, 241, 242). Interestingly, it has been shown that even short-term change in diet could influence the gut microbiota (243, 244). The relative abundance of each bacteria changed rapidly within hours of a diet switch in gnotobiotic mice (243), which are colonised by known strains of bacteria and other microorganisms. It was also confirmed in humans that gut microbiota could be altered rapidly and reproducibly (244). Only specific categories of bacterial species are stimulated according to the major macronutrient in a particular type of diet (245). For example, high fibre diet is always associated with increased *Bacteroidetes* production (221, 246).

1.4.3 Gut Microbiota and immune homeostasis

It is well accepted that the composition and metabolic products of the gut microbiota have profound and critical effects on immune homeostasis. A germ-free (GF) animal model is established by raising animals in a sterile environment so they have never been exposed to any microorganisms. This GF model unveils the significance of the gut microbiota in modulating both innate and adaptive immunity (247). Aberration in the gut microbiota and thus its impact on immune homeostasis will result in various diseases, including IBD,

multiple sclerosis, rheumatic arthritis, type 1 diabetes and metabolic syndrome (248, 249).

1.4.3.1 Gut Microbiota and innate immunity

Gut microbiota and its crosstalk with the innate immune system are important for the immune homeostasis locally as well as systemically. Pattern-recognition receptors (PRRs) are heavily involved in these interactions, since they can sense microorganisms through conserved molecular structures, hence acting as the monitoring system for the gut microbiota (250). TLRs and nucleotide-binding oligomerization NOD-like receptors (NLRs) are two typical PRRs (251).

1.4.3.1.1 APCs

There is direct evidence about the critical role gut microbiota plays in the development of local APCs in GF animal models. There was no DCs in the diffuse lymphoid tissue of the jejunum in GF animals (252). As for macrophages, the results are not conclusive. However, they were devoid of any co-expression of MHC class II, thus their role may be restricted to mainly phagocytic (252, 253).

The distinct character of intestinal APCs is to maintain immune homeostasis towards the normal resident gut microbiota, while at the same time protecting the body from infection. DCs isolated from Peyer's patches are able to produce IL-10 in large amounts, and prime T cells to secrete much less IFN-γ, compared to DCs isolated from the spleen (254). Apart from DCs, intestinal macrophages also have much less production of the pro-inflammatory cytokines, even after bacteria phagocytosis (255). This inflammatory "anergy" feature is due to NF-kappaB (NF-kB) inactivation (256). Though derived from

peripheral blood monocytes, the phenotypic expression and cytokine production of intestinal macrophages are completely downregulated even with high phagocytic and bacteriocidal activity (257). These macrophages also have impaired or no expression of innate response receptors, growth factor receptors, and the integrin LFA-1. In addition, production of pro-inflammatory cytokines, such as IL-1, IL-6, and TNF-α, is also abolished (257).

1.4.3.1.2 Innate Lymphoid Cells

The development of ILCs is independent of the gut microbiota (258). However, gut colonization does contribute significantly to the maturation and proper function of ILCs (259, 260). ILCs contribute to the local anatomical containment of the gut microbiota via IL-22 production (261), since IL-22 receptor is mainly expressed in the epithelial cells of the intestine (190). In addition, they also regulate commensal microbiota-specific $CD4^+$ T cell responses for immune tolerance (262), specifically ILC3 cells (263).

1.4.3.2 Gut Microbiota and adaptive immunity

Apart from their unique function in shaping the innate immune system, the gut microbiota also induces B cell differentiation. Most gut-associated B cells are plasma cells and they produce large amounts of IgA (264). The number of plasma cells and IgA level were significantly reduced in the intestine of GF animal models (265), which could be reversed by microbial colonization (266).

However, the effects of gut microbiota on the differentiation of $CD4^+$ T cells attract most attention. In GF mice, the number of $CD4^+$ cells was reduced markedly in the gut (267) as well as in the spleen and mesenteric lymph node, together with an imbalance between

Th1 and Th2 cells (268). Growing evidence reveals the correlations of specific bacterial species with the development of different T cell subsets.

1.4.3.2.1 Th17 cells

Th17 cells are a lineage of $CD4^+$ T helper cells expressing RAR-related orphan receptor (ROR)γt (269). They are mostly found in the lamina propria of the intestine. The microbiota is pivotal for Th17 cell differentiation as demonstrated by GF animal models, where the number of Th17 cells is diminished in the lamina propria of the intestine (270). Th17 cells control various bacterial and fungal infections at mucosal cells through their signature cytokine production, including IL-17A, IL-17F, and IL-22 (271). However, they also show significant pathogenic features. Upon stimulation with IL-1β, IL-23, and certain types of fatty acids, Th17 cells result in autoimmune diseases through the cross-reactivity between microbial peptides and self-antigens, or alternatively, microbiota-specific Th17 cells lowering the activation threshold of auto-reactive T cells after migrating into the targeted organs (272).

1.4.3.2.2 Regulatory T cells

Among all the above-mentioned cells, Treg cells are the most important cell type for gut homeostasis due to their IL-10 production and contribution to the suppression of the abnormal activation of other effector cells. The intestine contains thymus-derived tTreg cells, peripherally differentiated $ROR\gamma t^-$ and $ROR\gamma t^+$ pTreg cells (272). The gut microbiota is indispensable for the development of $ROR\gamma t^+$ pTreg cells in the colon, especially several species of *Bacteroides* (273, 274). These cells do not exist in GF animal models. On the other hand, $ROR\gamma t^-$ pTreg cells are induced by dietary antigens in the small intestine (275).

Short chain fatty acids (SCFAs), which are the end metabolic products from fermentation by the gut microbiota, mainly *Bacteroidetes*, can also promote *de novo* generation of pTreg cells in mice (276-278).

1.5 Short chain fatty acids

1.5.1 Production and Absorption

SCFAs are organic fatty acids with fewer than 6 carbon atoms. They are the major bacterial fermentation products in the human intestine (279). They are derived from polysaccharide, oligosaccharide, protein, and glycoprotein precursors. However, carbohydrates are the most important source for SCFAs production (280, 281). The principal SCFAs are acetate (C2), propionate (C3) and butyrate (C4). Other types of SCFAs including formate, valerate, caproate, the branched chain fatty acids isobutyrate, 2 methyl butyrate and isovalerate are produced in lesser amounts (280). The production of SCFAs is highly affected by the host internal environment and gut microbiota. Among all the bacterial phylum, *Bacteroidetes* plays an essential role in the production of SCFAs (221, 246). Oligosaccharide prebiotics can also produce acetate, butyrate and propionate after digestion resistance in the small intestine and microbial fermentation in the colon (279). Since gut microbiota is closely interlinked with diet and its composition can be rapidly changed even after a short-term diet shift (refer to section 1.4.2 for detail), the production of SCFAs is not steady and the concentration varies significantly.

SCFAs are water soluble and thereby easily absorbed or transported via carriers (cell surface receptors or transporters) into cells, because there are relatively shorter hydrophobic chains as well as the hydrophilic carboxyl group in the molecular structure (282). The SCFAs are predominantly absorbed by simple passive diffusion, since there is

linear absorption under various concentrations and no competition or enhancement of absorption when multiple SCFAs were present (283). SCFAs are either be utilized in the colon as fuel for epithelial cells or circulated to other organs through the portal vein. Changes in the molar ratios of the three principal SCFAs (% of total acetate+propionate+butyrate) moving from the colon to portal blood, then to the hepatic vein indicated the differential uptake patterns. Butyrate is mainly (70–90%) absorbed by the colonic epithelium, whereas propionate is mostly taken up by the liver (279). The ratio of the three principle SCFAs (butyrate: propionate: acetate) metabolised by the colonocytes is 9:3:5 (284), hence making butyrate the most essential SCFA in colonocyte metabolism.

Total SCFAs concentration was high in the colon, ranging from 131±9 mMol/Kg in the caecum to 80±11mMol/Kg in the descending colon, whereas portal vein concentration was as high as 375±70 μM/L (279). However, total SCFAs in the peripheral blood dropped significantly to 79±22 μM/L. Among the types of SCFAs detected, acetate was the principal anion, and it was consistent in all studies that acetate was the main SCFA in peripheral blood. Meanwhile, propionate and butyrate concentrations (1–13 and 1-12 μM, respectively) were much lower (279). Despite the extremely low concentration already observed, Wolever *et al.* detected propionate and butyrate at a concentration of 4.5–6.6 μM and 2.0–3.9 μM, respectively (285). Corresponding values recorded by Muir *et al.* were slightly higher at 17.8–32.8 μM and 36.3–65.5 μM in peripheral blood (286). This extremely wide range of serum concentrations of butyrate and propionate is mostly due to the non-standard collection protocols used across the different studies. In addition, the serum levels of SCFAs varied significantly during the day, with a tendency to decrease after breakfast and increase transiently after lunch and dinner (285, 286).

1.5.2 Receptors and Transporters of SCFAs

Although SCFAs are predominantly absorbed by simple passive diffusion, they can enter cells via Na^+/glucose coupled transporter SLC5a8 or by activating the G protein-coupled receptors (GPR) on the cell surface to exert their effects (287).

1.5.2.1 G Protein-Coupled Receptor 41 and 43

GPR41 and GPR43 belong to a homologous family of orphan G-protein–coupled receptors, which are encoded by a single chromosomal locus in both humans and mice (288). GPR41 shares 52% similarity and 43% identity with GPR43, and can be activated by similar ligands with short chain carboxylic acid anions in a dose-dependent and dose-specific manner (288). The three principal SCFAs have different affinities towards GPR41 and GPR43. The rank order of the agonist activity potency on GPR43 is propionate > acetate = butyrate, while for human GPR41, the rank order of potency shows notable differences as propionate > butyrate >> acetate (289).

GPR41 and GPR43 expressions are characterised by a high specificity using TaqMan quantitative reverse transcriptase (RT)-PCR. GPR41 mRNA levels were highest in human adipose tissue. Much lower expression levels were detected across all other normal human tissues, and there was no detection in lymphocytes, monocytes or dendritic cells (288, 289). Compared to GPR41, GPR43 expression appeared less widespread and at relatively high levels. Polymorphonuclear cells (PMNs), PBMCs, as well as purified monocytes, had relatively more GPR43 mRNA (50-fold greater than that of the whole spleen). However, no signals were detected for both GPR41 and GPR43 in lymphocytes (288, 289). Furthermore, GPR41 and GPR43 were not expressed at functional levels in

bone marrow-derived dendritic cells and cultured $CD4^+$ T cells regardless of SCFAs (290).

GPR41-knockout and GPR43-knockout mice showed slower and reduced immune responses against pathogen, indicating the critical role of GPR41 and GPR43 on the modulation of host immune responses (291). Various intracellular signalling cascades are coupled to these two receptors, including intracellular Ca^{2+} release, inhibition of cAMP accumulation, extracellular signal-regulated kinase (ERK) 1/2 activation and p38 mitogen-activated protein kinase (MAPK) activation (289). Upon activation, these signalling pathways can induce the production of chemokines and cytokines to regulate appetite, electrolyte and fluid secretion, and inflammatory responses (287).

1.5.2.2 G Protein-Coupled Receptor 109a

GPR109a (encoded by *Niacr1*), also known as hydroxycarboxylic acid receptor 2 or HCA2, is another G-protein–coupled receptor for nicotinate (292). It also recognises butyrate with low affinity, since a high concentration of butyrate (millimolar level) is required for the activation of GPR109a (293). GPR109a is expressed on the apical membrane of intestinal epithelial cells, white and brown adipose tissue as well as immune cells, including monocytes, neutrophils, macrophages, dendritic cells and epidermal Langerhans cells (293, 294).

GPR109a signalling favours macrophages and dendritic cells to promote the differentiation of Treg cells and IL-10-producing cells, skewing colonic macrophages and dendritic cells towards an anti-inflammatory phenotype. Furthermore, GPR109a signalling also plays an essential role in IL-18 production in colonic epithelium to

suppress inflammation. Therefore, mice with GPR109a deficiency tend to suffer from lethal colitis and colonic inflammation (295).

1.5.2.3 SLC5A8

Apart from binding to GPRs, SCFAs can also enter the cells directly with the assistance of transporters. The *Slc5a8* gene encodes for a Na^+/glucose coupled transporter for SCFAs. Exposure of this transporter to SCFAs induces inward currents under voltage-clamp conditions in a Na(+)-dependent manner (296). SLC5a8 is expressed on the lumen-facing apical membrane of epithelial cells in both small intestine and colon (297). It is expressed in T cells as well, albeit at low levels (298).

SLC5A8 was originally discovered as a tumour suppressor silenced in colon cancer (299). A study of $Slc5a8^{-/-}$ mice revealed its effect on immune cells. Although there was no difference in the Treg cell compartment in the colon between $SLC5a8^{-/-}$ mice and WT mice, butyrate/SLC5a8 could robustly facilitate DCs to suppress the generation of IFN-γ^+ T-cells from naïve T cells (300). The differentiation of DCs was also blocked by butyrate/SLC5a8 signalling *in vitro* (301).

1.5.3 SCFAs as Histone Deacetylase Inhibitor

1.5.3.1 Histone Deacetylase

Two duplicates of each histone protein (H2A, H2B, H3, and H4) form an octamer, wrapped with 145–147 base pairs of DNA to form a nucleosome core (302). Histone deacetylases (HDACs) are a class of enzymes that remove acetyl moiety of acetyl coenzyme A (acetyl-CoA) from a ε-N-acetyl lysine amino acid on the core histones, so that the histones can wrap the DNA more tightly. Allfrey *et al.* discovered this histone

modification in the 1960s (303). HDACs are now also called lysine deacetylases (KDAC), because it has become clear that they target various protein complexes in addition to histones (304).

In humans, HDACs are classified into four classes according to their structure: class I (including HDAC1, HDAC2, HDAC3, HDAC8), class IIa (including HDAC4, HDAC5, HDAC7, HDAC9), class IIb (including HDAC6, HDAC10), class III (including SIRT1 to SIRT7) and class IV (HDAC11) (305). These HDAC classes have similarities to different yeast transcriptional repressors. Class I is homologous to yeast *Rpd3* and both class II HDACs are more similar to yeast *Hda1*, whereas HDAC11 shows comparable homology to both *Rpd3* and *Hda1*, thus defined as a different group (class IV) (305). Analysis of the silent information regulator (SIR) protein in yeast and its homologues in higher eukaryotes (SirT 1–7) has unravelled a nicotinamide adenine dinucleotide (NAD^+) dependent HDAC activity (306), referred to as class III HDACs.

1.5.3.2 SCFAs as pan-HDAC Inhibitor

SCFAs, particular butyrate, were proved to inhibit histone deacetylation in the 1970s. The addition of millimolar concentration of butyrate can cause hyperacetylation of H3 and H4 in various vertebrate cell lines (307, 308). Other SCFAs including acetate, isobutyrate, and propionate, also have inhibitory effects of deacetylases *in vitro*, albeit at different efficiencies with butyrate being highest (80%) (309). With the exception of H2A, other core histones H2B, H3 and H4 are acetylated at four or five sites; thus a nucleosome has potentially 28 or more sites of acetylation (310). Apart from the increased histone acetylation, SCFAs can also decrease repressive histone trimethylation, for example, H3K9Me3 and H3K27Me3 (311).

The inhibitory effects of SCFAs on the histone deacetylation mainly target class I and class II HDACs, but class III SirT1 is also involved (311). Activated $CD4^+$ T cells have higher HDAC activity, and SCFAs (C2, C3 and C4) can effectively suppress the HDAC activity in T cells in a dose-dependent manner (290).

1.5.4 The Mechanisms of SCFAs-mediated Immune Tolerance

SCFAs have been shown to have profound influences on both the innate and adaptive immune systems. Upon production in the GI tract, they are absorbed into the gut epithelium cells and exert immune regulatory effects. Figure 1.3 summarises the mechanisms involved in the regulation of SCFA-medicated immune tolerance. SCFAs exert their regulatory effects via three major ways: GPRs-mediated signalling pathways, energy metabolism, and HDAC inhibition.

1.5.4.1 GPRs-mediated signalling pathway

After SCFAs bind to the GPR41 and GPR43 on the surface of the gut epithelial cells, several intracellular signalling cascades are initiated, including intracellular Ca^{2+} release, inhibition of cAMP accumulation, ERK1/2 activation, and p38 MAPK activation (289). Subsequently, downstream transcriptional factors are activated, such as activating transcription factor 2 (ATF2) (312). Activation of these intracellular cascades can result in the production of inflammatory regulators and chemokines, which play a pivotal role in leukocyte recruitment and T cell activation in response to inflammatory stimuli (291). IL-18 induction is also increased through butyrate-GPR109a activation, and IL-18 contributes to the suppression of colonic inflammation and inflammation-associated cancers (295). When GPR41 and GPR43 on enteroendocrine cells are activated, the induction of glucagon-like peptides (GLP-1 and PYY) is promoted, and these peptides

take part in the gut barrier function locally and in the energy metabolism of other organs, including adipose tissue, liver and pancreas (313).

SCFAs can also regulate immune cells via GPRs activation. Neutrophils undergo chemotaxis (289, 314) and degranulation (315) in a GPR43-dependent manner. GPR109a signalling skews colonic macrophages and dendritic cells towards a tolerogenic phenotype to promote the differentiation of Treg cells and IL-10 producing cells (295). As for lymphocytes, RT-PCR was unable to detect signals at functional levels for all the three types of GPRs (288, 289, 294). Moreover, no significant differences were observed in the percentages of IL-10^+ T cells, Th17 and Th1 cells in several different organs of GPR41-deficient and GPR43-deficient mice (290). Therefore, the role of the GPR-mediated signalling pathway is dispensable for the SCFA effect on T cells.

1.5.4.2 Energy Metabolism Regulation

SCFAs act as the core energy source for the gut epithelial cells, once entering the cells via simple diffusion or the Na^+/glucose coupled transporter SLC5a8. SCFAs are converted to Acetyl-CoA (316), which plays a vital role in energy metabolism. Its main function is to facilitate energy production and increase cellular ATP levels by conveying the carbon atoms within the acetyl group to the Krebs cycle for oxidization (317).

In addition to the energy production, SCFAs regulate the differentiation between Teff and Treg cell lineage commitment by activating the mTOR pathway (318). Since mTOR is influenced by the intracellular concentration of ATP and mTOR is an ATP sensor itself (319), SCFAs also increase both the local IgA and systemic IgG production of B cells via energy metabolism regulation. Cellular metabolism (including acetyl-CoA level, lipid

droplets and ATP/ADP ratio) is elevated in B cells to boost mTOR activation and promote plasma B cell differentiation and antibody responses (320).

1.5.4.3 HDAC Inhibition

HDAC inhibition increases the acetylation of core histones to unwrap DNA and facilitate DNA transcription. The acetylation of protein is modified by HDAC inhibition as well to prevent proteasome degradation (321). Therefore, SCFAs can influence a variety of genes and proteins in different cells. Whether the SCFA receptors are involved in the process of HDAC inhibition is controversial and is dependent on the cell type. SCFAs can enter cells directly without binding to the surface receptors of neutrophils to exert their inhibitory activity (322). However, in GF mouse models, SCFAs can only restore and promote the colonic Treg compartment and function via enhanced histone acetylation-dependent on the GPR43 expression (277).

The major mechanism proposed for the regulatory effect of SCFAs on T cells is HDAC inhibition, especially considering the lack of significant levels of GPRs on the T cell surface. SCFAs act as a pan-HDAC inhibitor to various intracellular pathways. For example, NF-kB, ERK, p70 S6 kinase (S6K, downstream of mTOR pathway) are hyper-acetylated and initiate downstream effector protein expression (290). It has been confirmed both *in vivo* and *in vitro* that SCFAs promote the generation of pTregs by enhancing histone H3 acetylation at both promoter and CNS3 regions of the *Foxp3* gene locus and Foxp3 protein via HDAC inhibition (276, 278). In addition, the expressions of IL-10, IFN-γ and IL-17 are also elevated in T cells (290). Collectively, these results suggest that the HDAC inhibition activity alone is enough to facilitate the SCFAs' effect

on T cells. Apart from Tregs, effector T cells could also be regulated by SCFAs under different cytokine milieus (290).

SCFAs also exert their regulatory effects on macrophages and DCs via HDAC inhibition. SCFAs act as HDAC inhibitors to suppress the expression of pro-inflammatory cytokines of DCs, thus promoting Treg induction (276). The reduction of NF-kβ transcriptional factor contributes to the SCFAs effect on macrophages and DCs (323-325).

The mechanisms of SCFAs-mediated immune tolerance are summarised in Figure 1.3.

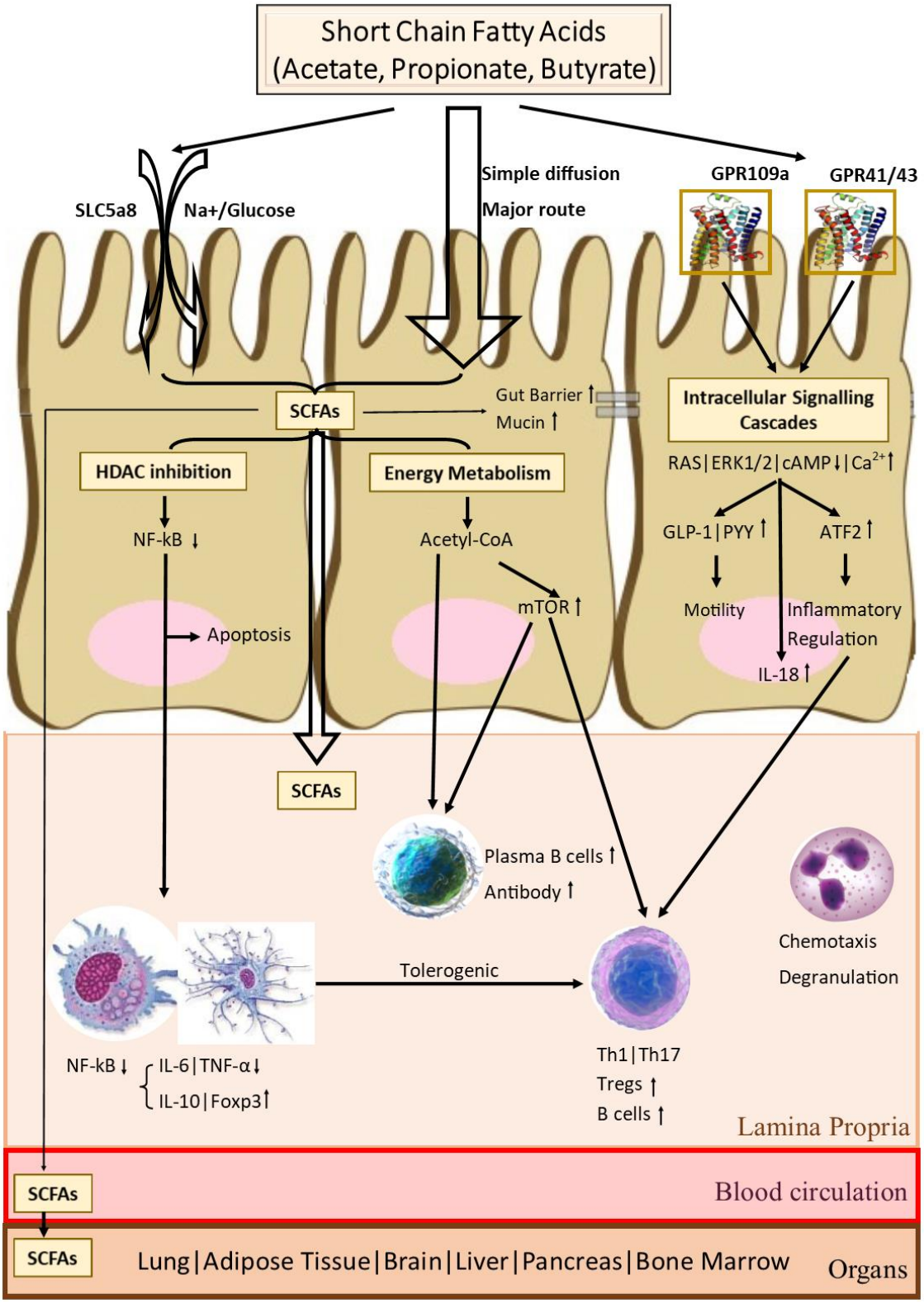

Figure 1.3 Summary of mechanisms involved in the regulation of SCFA-medicated immune tolerance.

1.5.4.4 Butyrate Induced Apoptosis

Compared to other types of SCFAs, butyrate has a unique growth suppression function and apoptotic character (293, 298, 322, 326, 327). Butyrate exhibited much lower EC_{50} value in the resazurin reduction assay, which is a cell viability assay. This effect of butyrate on cell proliferation is dose-dependent and HDAC mRNAs are downregulated (327). In comparison, the EC_{50} values were unable to be determined for acetate and propionate due to their low cytotoxicity (326).

In T cells, the apoptosis induced by butyrate is via HDAC inhibition and is Fas-mediated, since Fas promoter hyperacetylation and Fas upregulation were induced by butyrate mediated HDAC1 inhibition (298). Butyrate-induced apoptosis of neutrophils is also likely related to the HDAC inhibition activity irrespective of GPRs (322). In colon cancer cells, butyrate triggers re-expression of GPR109a and induce apoptosis. However, the inhibition of histone deacetylation does not take part in this apoptosis via GPR109a activation in colon cancer cells (293). It is the downregulation of Bcl-2, Bcl-xL, and cyclin D1 and the upregulation of the death receptor pathway involved in the primary changes in this apoptotic process.

1.6 Aims and Hypotheses

1.6.1 Aims

The aims of this PhD thesis are to address in detail the human Treg cell physiology, from *in utero* stages to adult life, and investigate the exact role of SCFAs in human Treg cell differentiation.

a) To provide evidence on Treg cell transplacental programming, and how IL-10 and SCFAs contribute to this process;

b) To test whether SCFAs could skew different human T lymphocyte subsets, especially Treg cells, towards tolerogenic phenotypes *in vitro*;

c) To investigate how SCFAs alter the histone acetylation of genes involved in immune tolerance applying ChIP-qPCR;

d) To investigate the effects of SCFAs on the tolerogenic potential of MoDCs *in vitro.*

1.6.2 Hypotheses

1.6.2.1 Treg cell programming *in utero* and during early life

a) Microbiota metabolites (acetate), rather than genetics, are pivotal in the transplacental programming for fetal thymus and T cell development *in utero*

b) Treg cell ontogeny early in life: IL-2 enhances gut homing potential of human naïve Treg cells during early life

c) Soluble immunomodulatory IL-10 contributes to transplacental Treg cell programming via potentiating Treg cell induction

1.6.2.2 Short chain fatty acids exert a tolerogenic effect on human lymphocytes *in vitro* by histone acetylation of genes associated with immune tolerance

a) There are differential induction patterns in the generation of human Tregs between cord blood and adult peripheral blood cells *in vitro* via SCFAs

b) Butyrate and propionate, but not acetate, potentiate the expression of phenotypic markers of human TGF-β–induced Tregs *in vitro*

c) Butyrate and propionate, but not acetate, enhance the suppressive capacity of human TGF-β–induced Tregs *in vitro*

d) Butyrate and propionate augment iTreg cell phenotype and function through Histone deacetylation inhibition

e) SCFAs also have tolerogenic effects on other T cell subsets

1.6.2.3 Short chain fatty acids induce human tolerogenic MoDCs *in vitro*

a) SCFAs skew human monocyte-derived dendritic cells towards tolerogenic phenotype *in vitro*

b) The proliferation of naïve $CD4^+$ T cells was influenced by SCFA-treated monocyte-derived dendritic cells

c) $CD4^+$ T cells cocultured with SCFA-treated monocyte-derived dendritic cells had enhanced suppressive capacity

Chapter 2 – Materials and Methods

2.1 Materials

2.1.1 Patients and subjects

All research was conducted according to ethically approved protocols. Research conducted at Nepean Hospital was reviewed and approved by the Human Research Ethics Committee (HREC) of Nepean Blue Mountains Local Health District according to the Declaration of Helsinki. Various cohorts of donors were recruited on a volunteer basis. All volunteers were informed of the study and signed a written consent prior to donating blood.

For IL-10 potentiates differentiation of human induced regulatory T cells: peripheral blood was obtained from healthy volunteers (n=20).

For *in vitro* Treg induction, a total of 23 samples, including 13 healthy adults and 10 cord blood samples from healthy pregnancies, were recruited from 09/2015 to 07/2016.

For MoDC phenotyping and functional assay, a total of 14 peripheral blood samples were collected from healthy adults from 08/2016 to 08/2017.

For PBMC culture, a total of 7 peripheral blood samples were collected from healthy adults from 11/2016 to 02/2017.

All subjects with a history of atopy, autoimmunity or concurrent infections were excluded. Indications for all pregnant women undergoing Caesarean Sections (C.S.) include repeated C.S., malpresentation or other non-medical issues. Women with gestational diabetes, chorioamnionitis, placenta praevia, chronic villitis or twin

pregnancies were excluded. Detailed characteristics of adult participants and newborns are summarised in Table 2-1 and 2-2 separately.

Table 2-1 Characteristics of Adult Participants.

Study	Numbers of Participants	Gender (N)	Age (Mean±SD)
***in vitro* Treg induction**	13	Male (9)	27.1±6.6
		Female (4)	34.3±4.8
MoDC phenotyping	8	Male (3)	23.7±0.6
		Female (5)	29.6±5.8
MoDC functional assay	6	Male (2)	24.0±1.4
		Female (4)	37.0±9.3
PBMC culture	7	Male (2)	27.7±11.6
		Female (4)	30.5±11.4

Table 2-2 Characteristics of Newborns

Numbers of Participants	Newborn Gender (N)	Maternal Age (Mean±SD)	Gestational Week (Mean±SD)	Parity (Mean±SD)	Birth Weight (g) (Mean±SD)
12	Male (8)	28.1±5.7	38.6±1.3	2.4±0.9	3665.0±514.6
	Female (4)	32.3±4.5	39.3±0.1	2.3±0.5	3398.8±363.6

2.1.2 Blood collection and PBMC isolation

- ❖ Lithium heparinised vacuum tubes (BD Biosciences, USA)
- ❖ Ficoll-Paque Plus (GE Healthcare, Sweden)
- ❖ Phosphate buffered saline (PBS; pH 7.4; Sigma-Aldrich, USA)
- ❖ Trypan blue (0.4% stock; Life Technologies, USA)

2.1.3 Cell culture media

- ❖ RPMI 1640 medium (Life Technologies, USA) supplemented with:
  - o 2mM Glutamax (Sigma-Aldrich, USA)
  - o 100U/mL Penicillin (Sigma-Aldrich, USA)
  - o 100ug/mL Streptomycin (Sigma-Aldrich, USA)
- ❖ 10% Fetal Calf Serum (FCS) (Life Technologies, USA)
- ❖ 1% HEPES (Life Technologies, USA)

2.1.4 Other reagents for cell culture and functional assay

Table 2-3 Reagents used for cell culture

Products	Concentration (for culture)	Manu-facturer	Catalogue Number	Application
CD14 MicroBeads, human		Miltenyi	130-050-201	Cell Isolation
$CD4^+CD25^+$ Regulatory T Cell Isolation Kit, human		Miltenyi	130-091-301	Cell Isolation

Products	Concentration (for culture)	Manu-facturer	Catalogue Number	Application
Treg Suppression Inspector, human		Miltenyi	130-092-909	Functional Assay
LEAF™ Purified anti-human CD3, OKT3	10 ug/ml	Bio-Legend	317304	Stimulation
LEAF™ Purified anti-human CD28, CD28.2	2 ug/ml	Bio-Legend	302914	Co-stimulation
Human GM-CSF, premium grade	50 ng/ml	Miltenyi	130-093-865	Cell Culture
Human IL-4, premium grade	50 ng/ml	Miltenyi	130-093-921	Cell Culture
Lipopolysaccharides	100 ng/ml	Sigma-Aldrich	62326	Cell Culture
Human IL-2 IS, premium grade	50 U/ml	Miltenyi	130-097-745	Cell Culture
Recombinant Human TGF-β1	5 ng/ml	Pepro-Tech	100-21	Cell Culture
Sodium Acetate*	1000 uMol	Sigma-Aldrich	S5636-250G	Cell Culture
Sodium Butyrate*	500 uMol	Sigma-Aldrich	B5887-250MG	Cell Culture
Sodium Propionate*	1000 uMol	Sigma-Aldrich	P5436-100G	Cell Culture

* Purchased in powder, then dissolved in sterile PBS according to the final concentration.

2.1.5 Antibodies for flow cytometry

The flow cytometer used was BD FACSverse. A maximum of 8 different fluorochromes was used at any one time. The fluorochromes used include: FITC or equivalent (Alexa Fluor 488), PE, PerCP-Cy5.5 or equivalent (PerCP efluor710/PerCP Vio700), PE-Cy7 or equivalent (PE-Vio770), APC, APC-Cy7 or equivalent (APC-H7), V450 or equivalent (Pacific Blue / eFluor450), and V500 or equivalent (BV510 / Fixable Aqua Dead Cell Stain). The antibodies used in this thesis are listed in Table 2.

Table 2-4 Antibodies (against human antigens) and proteins used for flow cytometry.

Abs	Fluoro-chrome	Clone	Isotype	Manufacturer	Catalo-gue No.	Appli-cation
CD1a	eFluor® 450	HI149	Ms IgG1, k	eBio-science	48-0019-42	FC
CD3	APC-H7	SK7	Ms IgG1, κ	BD	560176	FC
CD4	BV510	SK3	Ms IgG1, κ	BD	562970	FC
CD4	PerCP-Vio700	REA623	recombinant human IgG1	Miltenyi	130-109-455	FC
CD8	BV510	SK1	Ms IgG1, κ	BD	563919	FC
CD11c	PE-Cy7	3.9	Ms IgG1, k	eBio-science	25-0116-42	FC
CD14	APC-H7	MφP9	Ms IgG2b, κ	BD	560180	FC

Abs	Fluoro-chrome	Clone	Isotype	Manufacturer	Catalo-gue No.	Appli-cation
CD14	FITC	REA599	recombinant human IgG1	Miltenyi	130-110-518	FC
CD25	APC	2A3	Ms IgG1, κ	BD	340939	FC
CD39	APC	MZ18-23C8	Ms IgG1, κ	Miltenyi	130-093-504	FC
CD45RO	PerCP-Vio700	UCHL1	Ms IgG2a, κ	Miltenyi	130-097-590	FC
CD80 (B7-1)	PerCP-eFluor™ 710	2D10.4	Ms IgG1, k	eBio-science	46-0809-42	FC
CD83	PE	HB15e	Ms IgG1, κ	Bio-legend	305308	FC
CD86	APC	2331	Ms IgG1, κ	BD	555660	FC
CD127	FITC	HIL-7R-M21	Ms IgG1, κ	BD	560549	FC
CD127 (IL-7Rα)	PE	A019D5	Ms IgG1, κ	Bio-legend	351304	FC
CD152 (CTLA-4)	APC	L3D10	Ms IgG1, κ	Bio-legend	349908	ICFC
CD197 (CCR7)	PerCP-eFluor™ 710	3D12	Rat IgG2a, k	eBio-science	46-1979-42	ICFC
CD209 (DC-Sign)	FITC	DCN46	Ms IgG2b, κ	BD	551264	FC

Abs	Fluoro-chrome	Clone	Isotype	Manufacturer	Catalo-gue No.	Appli-cation
CD274 (PD-L1 / B7-H1)	PE/Cy7	29E.2A3	Ms IgG2b, κ	Bio-legend	329718	FC
CD278 (ICOS)	VioBlue	REA192	Recombinant human IgG1	Miltenyi	130-100-737	FC
CD279 (PD-1)	APC/Cy7	EH12.2H7	Ms IgG1, κ	Bio-legend	329922	FC
CD284 (TLR-4)	APC	HTA125	Ms / IgG2a, k	eBio-science	17-9917-42	FC
CD357 (GITR)	PE	DT5D3	Ms IgG1, κ	Miltenyi	130-092-895	FC
CXCL-9 (MIG)	PE	J1015E10	Ms IgG2a, κ	Bio-legend	357904	ICFC
Foxp3	Alexa Fluor® 488	259D	Ms IgG1, κ	Bio-legend	320212	ICFC
HLA-DR	Pacific Blue™	L243	Ms IgG2a, κ	Bio-legend	307633	FC
IFN gamma	PE	4S.B3	Ms IgG1, k	eBio-science	12-7319-82	ICFC
IL-10	eFluor® 450	JES3-9D7	Rat IgG1, k	eBio-science	48-7108-42	ICFC

Abs	Fluoro-chrome	Clone	Isotype	Manufacturer	Catalo-gue No.	Appli-cation
IL-12 (p35/p70)	PE-Vio770	REA121	recombinant human IgG1	Miltenyi	130-103-677	ICFC
IL-12/IL-23 p40	Alexa Fluor® 488	C11.5	Ms IgG1, κ	Bio-legend	501816	ICFC
IL-4	APC	8D4-8	Ms IgG1, κ	Bio-Legend	500714	ICFC
IL-6	PE/Cy7	MQ2-13A5	Rat IgG1, κ	Bio-legend	501120	ICFC
LAP (TGF-β1)	APC	TW4-2F8	Ms IgG1, κ	Bio-legend	349608	FC
TNF-α	PerCP/Cy5.5	MAb11	Ms IgG1, κ	Bio-legend	502926	ICFC
LIVE/DEAD™ Fixable Aqua Dead Cell Stain Kit				Invitrogen	L34966	FC

2.1.6 Buffers and reagents used for flow cytometry

FACS buffer:

- PBS (pH 7.4; Sigma-Aldrich, USA)
- 0.1% FCS (Life Technologies, USA)
- 0.02% Sodium azide (Sigma-Aldrich, USA)

4% p-formaldehyde buffer

- 4 g p-Formaldehyde (Sigma-Aldrich, USA)

- 100 mL PBS (pH 7.4; Sigma-Aldrich, USA)

0.15% Saponin-PBS buffer

- PBS (pH 7.4; Sigma-Aldrich, USA)
- 0.5% FCS (Life Technologies, USA)
- 0.02% Sodium azide (Sigma-Aldrich, USA)
- Saponin (5% w/v stock, Sigma-Aldrich, USA)

Table 2-5 Other reagents used for flow cytometry.

Buffers/Reagents	Manufacturer	Catalogue No.	Application
BD GolgiStop™	BD	554724	Protein Transport Inhibitor
BD™ CompBeads (Anti-Mouse Ig, κ)	BD	552843	FC
True-Nuclear™ Transcription Factor Buffer Set	BioLegend	424401	ICFC

2.2 Methods

2.2.1 Mononuclear Cell Isolation

Blood samples from recruited women were drawn via venepuncture. For pregnant women, blood samples were drawn within 4 hours prior to caesarean section. Cord blood was collected via sterile aspiration of umbilical vein from the delivered placenta of recruited healthy pregnant women. All blood samples were processed within 2 hours of collection. Plasma was separated from the 1.5ml of collected blood via centrifugation, then stored at -80^0C.

Human mononuclear cells were isolated from peripheral blood by Ficoll-Paque density gradient centrifugation. Blood collected in heparinised vacuum tubes was diluted in a 1:1 ratio with sterile PBS. This mixture was carefully layered over Ficoll-Paque Plus in a 2:1 ratio before centrifugation at 1700rpm for 30 minutes, without brake. The layer containing mononuclear cells was carefully aspirated and washed twice in PBS with 0.5% FCS at 1300rpm for 8 minutes. The mononuclear cells were then resuspended in PBS containing 0.5% FCS. Cells were stained using Trypan blue for counting. Cells were either used immediately for cell culture or processed for cell sorting.

Protocols were summarized in Figure 2.4.

2.2.2 Enrichment of Specific Cell Populations

2.2.2.1 Cell Enrichment by Magnetic Beads

Three different magnetic bead selections were performed for various purposes:

a) Enrichment of $CD4^+$ T prior to cell sorting: $CD4^+$ T cell Isolation Kit (Miltenyi)
b) Generation of MoDCs: CD14 MicroBeads (Miltenyi)
c) Preparing responder cells for suppression assay: $CD4^+CD25^+$ Regulatory T Cell Isolation Kit (Miltenyi)
d) Enrichment of $CD25^{high}$ induced Treg cells for suppression assay: CD25 MicroBeads from the $CD4^+CD25^+$ Regulatory T Cell Isolation Kit (Miltenyi)

The brief steps for the magnetic bead selection are as follows:

a) Determine cell numbers and resuspend cells in 90 µL buffer per 10^7 total cells
b) Add 10µL $CD4^+$ T Cell Biotin-Antibody Cocktail (labelling non-$CD4^+$ cells) per 10^7 total cells, and incubate for 15 minutes in the fridge
c) Add 20µL anti-Biotin MicroBeads per 10^7 cells, and incubate for an additional 10 minutes in the fridge
d) Place LS Column in the magnetic field of a suitable MACS Separator and rinse with 3 ml buffer
e) Apply cell suspension onto the column and wash three times. Collect flow-through containing unlabelled $CD4^+$ cells (negative selection for $CD4^+$ cells).
f) For monocytes, $CD14^+$ cells are labelled for positive selection. Apply cell suspension onto the column and wash three times. Then the column needs to be removed from the separator and placed on a suitable collection tube. Pipette buffer onto the column, then immediately flush out the magnetically labelled cells by

firmly pushing the plunger into the column. To increase the purity of monocytes (≥90%), the eluted fraction is enriched over a second column.

g) For responder cell preparation, repeat the labelling and magnetic separation process for CD25 Microbeads. Collect flow-through containing unlabelled $CD4^{+}CD25^{-}$ cells.

h) For enrichment of $CD25^{high}$ induced Treg cells, CD25 Microbeads are used and it is also a positive selection (refer to CD14 selection for detail). To increase the purity (≥95%), the eluted fraction is enriched over a second column.

An example of purity of $CD14^{+}$ and $CD25^{+}$ bead-selected cells is shown below.

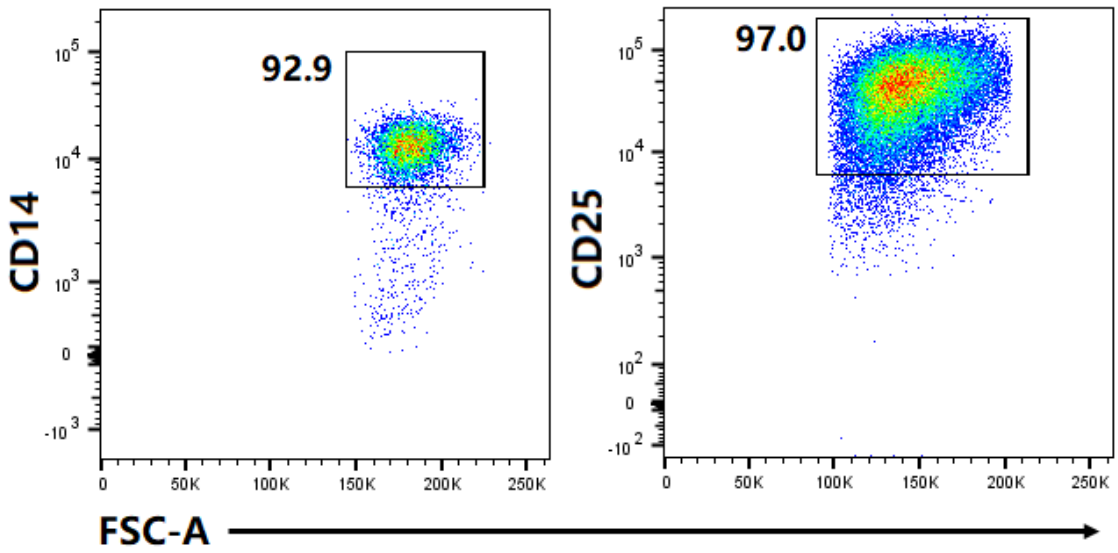

Figure 2.1 Flow cytometry pseudocolour plots showing CD14 (left) and CD25 (right) purity after bead selection.

2.2.2.2 Cell Enrichment by FACS Sorting

Dr Brigitte Nanan and I performed the flow cytometric sorting of lymphocytes. Freshly isolated cells were surface stained with the appropriate fluorochrome-conjugated antibody, including FITC-anti-CD127, PerCp-eFluor710-anti-CD45RO, BDV500-anti-CD4, and APC-anti-CD25. Cells were sorted on a BD FACSAria^{TM} cell sorter (Westmead Millennium Institute) using the appropriate gating strategy. The pre-enriched $CD4^+$ T cells are further sorted for either $CD4^+CD45RO^-CD25^-CD127^{hi}$ for Treg induction, or $CD4^+CD45RO^-$ cells for coculturing with MoDCs. Sorted cell populations had purities of ≥ 97.5%. An example of purity of sorted cells is shown in Figure 2.2.

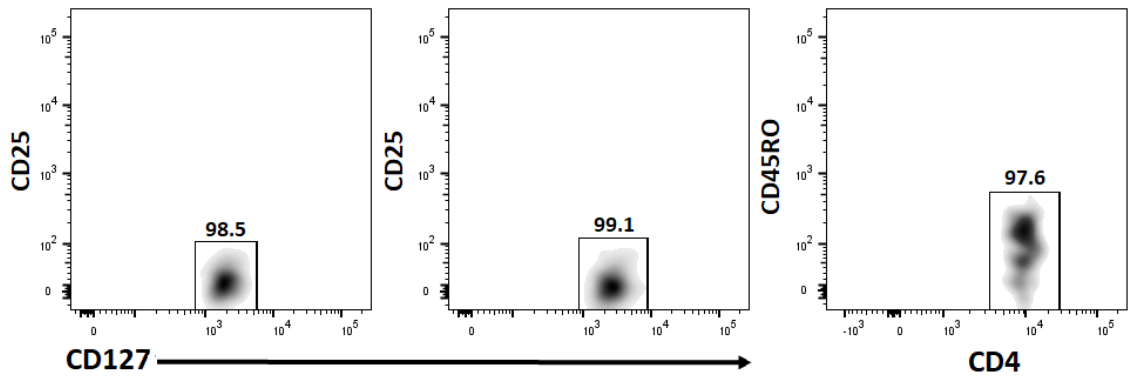

Figure 2.2 Flow cytometry density plots showing the purity of FACS sorted cells.

Flow cytometry density plots showing the purity of FACS sorted non-Treg cells from adult PBMCs (left), non-Treg cells from Cord Blood (middle), and naive CD4+ cells from adult PBMCs (right). Gating for non-Treg cells is based on the surface stain combination of CD25 and CD127, since intracellular stain with Foxp3 would render cells nonviable, preventing any further in vitro experiments.

2.2.3 *In vitro* Cultures

2.2.3.1 *In vitro* Human Regulatory T Cell Induction Protocol

FACS sorted naïve non-Treg cells of both adult and cord blood origins ($CD4^+CD45RO^-CD25^-CD127^{hi}$, >99% purity) were cultured in cell culture medium (RPMI-1640 containing 2mM L-Glutamine, 100U/ml penicillin, 100µg/ml streptomycin plus 10% FCS) in 48 well plates, with immobilised anti-CD3 (OKT3, 10µg/ml, coated overnight in PBS at 4°C) and mobilised anti-CD28 (2µg/ml). Cells were cultured at a concentration of 3.5-5 x 10^5/48 well at 37°C for 5 days under standard culture condition (37°C with pH 7.4 at a CO_2 concentration of 5% and humidity 85-95%). Recombinant human IL-2 (50U/ml), TGF-β (5ng/ml) and in selected cultures, sodium acetate (1000µMol), sodium butyrate (500µMol) or sodium propionate (1000µMol) were added on day 0 and day 3. On day 5, cells were harvested for phenotypic or further functional studies. The concentration of SCFAs was chosen based on the immune cell viability.

For ChIP study: $CD4^+$ cells generated from adult naive non-Tregs were harvest on day 3, while $CD4^+$ cells generated from cord blood were harvest on day 1 and day 3 respectively. Cells were frozen and kept in the liquid nitrogen for later ChIP analysis.

Restimulation for flow cytometric analysis: For certain gene expressions (such as CD39, GITR, and ICOS), iTreg cells needed to be restimulated with anti-CD3 (OKT3, 4µg/ml) for 3.5 hours at 37°C. Afterwards, cells were harvested and stained for flow cytometry as described in section 2.2.4.

Protocols were summarized in Figure 2.5 and Figure 2.6.

2.2.3.2 Suppression Assay

Carboxyfluorescein succinimidyl ester (CFSE) is a membrane permeable, fluorescent small molecule binding covalently to intracellular molecules (328). The concentration of CFSE is diluted in each subsequent cell division, therefore it can be used to trace cell proliferation. Responder cells were washed (1300rpm, 8mins) three times in RPMI-1640 in the absence of FCS at room temperature (RT). T cells were then incubated with 0.5μM CFSE at 37^{o}C for 7 minutes in the dark. The addition of 200μL of FCS could terminate the reaction. Afterwards, cells were washed 3 times with RPMI-1640 with FCS. Non-CFSE labelled induced T cells and CFSE-labelled allogeneic responder cells were cultured at a ratio of between 1:1 to 1:16 and stimulated with Treg Suppression Inspector (cell: bead ratio is 1:1, Miltenyi) in 96 U-bottom plates. Cells were cultured in medium for 3 days under standard culture condition and subsequently harvested for flow cytometry. The percentage of suppression was determined as the difference in the proliferation between negative control and the test sample, expressed as a percentage of the former. An example of suppression assay with negative control is shown in Figure 2.3.

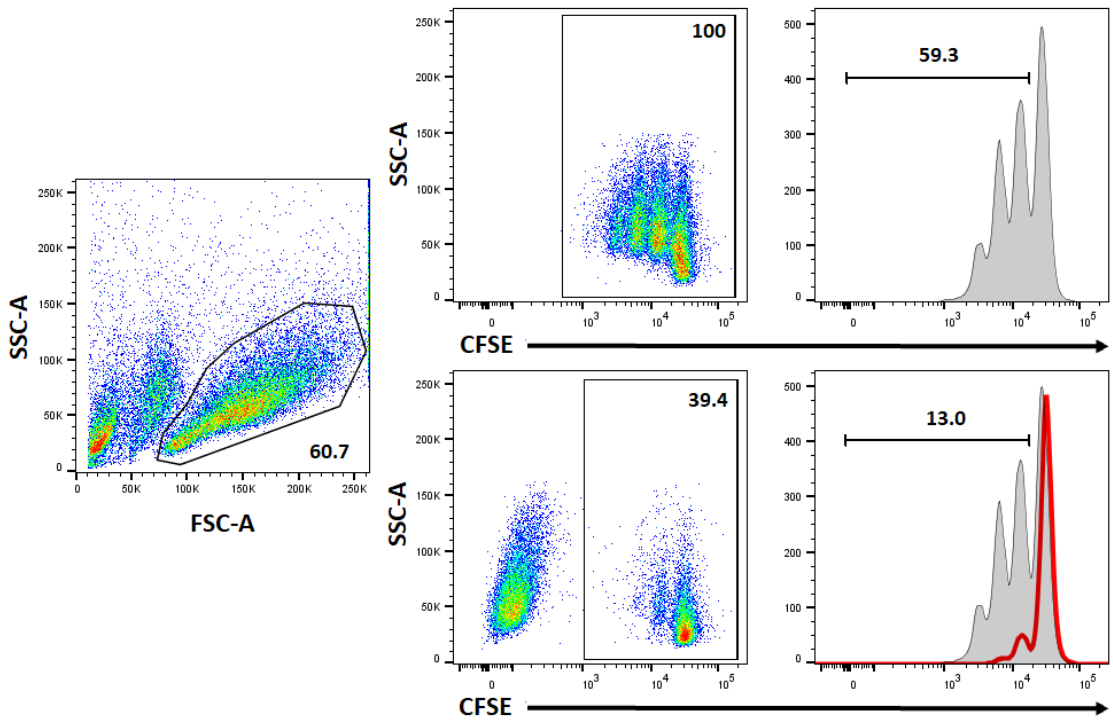

Figure 2.3 Representative flow cytometry analysis for suppression assay.

Lymphocytes (left) were selected and CFSE-labelled responder cells (middle) were gated separately from non-labelled cells (induced T cells). Histogram (lower panel) shows reduced proliferation of suppressed responder cells by induced T cells, compared to histogram (upper panel) showing the normal proliferation of responder cell alone.

2.2.3.3 Monocyte-Derived Dendritic Dell Induction

$CD14^+$ monocytes were isolated from the PBMCs of healthy donors using CD14 MicroBeads (Miltenyi), and purity of > 90% was routinely achieved by additional column selection. 5 x 10^5 monocytes were plated in each well of a 48 well plate with cell culture medium under standard culture conditions. GM-CSF (50ng/ml), IL-4 (50ng/ml), and in selected cultures, sodium acetate (1000µMol), sodium butyrate (500µMol) or sodium propionate (1000µMol) were added to the culture medium on day 0, 3 and 5. 50% of the culture medium plus additives was also replaced on day 3 and 5. On day 6, LPS (100ng/ml, Sigma-Aldrich) was added to selected cultures to induce maturation of MoDCs 24 hours prior to harvesting. On day 7, cultured cells were harvested and washed for flow cytometric analysis or later used for coculture experiments. Immature MoDCs without adding LPS were adherent. Therefore, they were harvested vigorously three times with PBS. Protocols were summarized in Figure 2.7.

2.2.3.4 Naïve $CD4^+$ T cells Proliferation via MoDCs

After being harvested on day 7, MoDCs were pulsed with anti-CD3 (OKT3, 2µg/ml) at 37°C for 3 hours. Then MoDCs were washed extensively with PBS three times to remove any excessive anti-CD3. Afterwards, MoDCs were added to the FACS sorted autologous naïve $CD4^+$ cells ($CD4^+CD45RO^-$, >99% purity) in 48 well plates at a ratio of 1:4-5 (MoDCs: naïve $CD4^+$ cells). Naive $CD4^+$ cells (4-5x10^5/well), together with autologous MoDCs (1x10^5/well) were cocultured for 5 days under standard culture condition supplemented with recombinant human IL-2 (50U/ml). On day 5, cells were harvested for flow cytometry or further functional studies. Protocols were summarized in Figure 2.8.

2.2.3.5 PBMC culture with SCFAs

Freshly isolated PBMCs at a concentration of 1 x 10^6/48 well were cultured in RPMI-1640 plus 10% FCS under standard culture condition for 5 days, in the presence of immobilised anti-CD3 (OKT3, 2µg/ml, coated overnight in PBS at 4°C). Recombinant human IL-2 (100U/ml), and in selected cultures, sodium acetate (1000µMol), sodium butyrate (500µMol) or sodium propionate (1000µMol) were added on day 0 and day 3. On day 5, cells were harvested for flow cytometry analyses. Protocols were summarized in Figure 2.9.

2.2.3.6 PBMC culture with IL-2

Thawed adult PBMCs or CBMCs at a concentration of 1 x 10^6/48 well were cultured in RPMI-1640 plus 10% FCS under standard culture condition for 72 hours in the presence or absence of recombinant human IL-2 (100U/ml, eBioscience). On day 3, cells were harvested for flow cytometry analyses.

2.2.4 Flow Cytometry

Flow cytometric analyses using BD FACSVerse were applied to all the cultured cells, including iTregs, MoDCs and proliferated $CD4^+$ cells.

2.2.4.1 Dead Cell Stain

LIVE/DEAD™ Fixable Aqua Dead Cell Stain Kit was used to determine the viability of all the cultured cells prior to the fixation and permeabilization required for intracellular antibody staining. The brief steps for the stain are as follows:

a) Cultured cells were harvested into polystyrene round-bottom 12x75mm BD Falcon tubes.
b) Cells were washed (centrifugation at 1600rpm, 4mins) twice with PBS and the cell concentration was adjusted to $1x10^6$ cells/ml with PBS.
c) 1µl/ml of the reconstituted fluorescent dye was added to the cell suspension, which was then incubated at RT for 30 min (protected from light).
d) Cells were washed again in PBS before proceeding with surface staining as described in section 2.2.4.2.

2.2.4.2 Surface Stain (FC)

The brief steps for surface stain are as follows:

a) Cells were washed and resuspended in 50µl FACS buffer.
b) A cocktail of the titrated concentration of fluorochrome-conjugated antibodies was then added to the cell suspension.
c) After mixing, cells were incubated for 20 min at 4°C in the dark.

d) Cells were washed once with FACS buffer after incubation, then proceeded to intracellular stain.
e) If no intracellular stain was needed, cells were fixed with 4% p-Formaldehyde for 20 minutes at RT in the dark, washed once with FACS buffer and resuspended in 200µl cold FACS buffer. Cells were kept on ice or at 4°C in the dark until acquisition for the flow cytometer.

2.2.4.3 Intracellular Stain (ICFC)

Two types of fixation and permeabilization buffer, thus different staining protocols were used for intracellular staining.

For intracellular staining of Foxp3 and CTLA-4 staining for iTregs and proliferated $CD4^+$ cells: True-Nuclear™ Transcription Factor Buffer Set was used. The brief steps are as follows:

a) 1mL of the True-Nuclear™ 1X Fix Concentrate was added to each tube, and cell mixture was incubated at RT in the dark for 50 minutes.
b) 2mL of the True-Nuclear™ 1X Perm Buffer was added to each tube for washing.
c) Repeated the washing once with 2mL of the True-Nuclear™ 1X Perm Buffer.
d) The cell pellet was resuspended in 50µL of the True-Nuclear™ 1X Perm Buffer after discarding the supernatant.
e) A cocktail of the titrated concentration of fluorochrome-conjugated antibodies was added into cell suspension (Dilution was made in True-Nuclear™ 1X Perm Buffer), which was then incubated for 30 min at RT in the dark.
f) After incubation, cells were washed once with 2mL of the True-Nuclear™ 1X Perm Buffer, and once with FACS buffer.

g) Cells were finally resuspended in 200µl cold FACS buffer and kept on ice or at 4°C in the dark until acquisition in the flow cytometer.

Intracellular cytokine labelling for MoDCs: 0.67µl/ml protein transport inhibitor (monesin, BD GolgiStop™) was added no longer than 12 hours before flow cytometric analyses. 4% p-Formaldehyde buffer and 0.15% Saponin-PBS buffer were used instead of the True-Nuclear™ Transcription Factor Buffer Set. Otherwise, the protocol was the same.

2.2.4.4 Multicolour flow cytometry panel design

The panel design is important in multicolour flow cytometry to minimize spectral overlap. Compensation was achieved on the BD FACSVerse using pre-designed matrixes. A compensation matrix was constructed using the corresponding combination of antibody labelled Compensation Beads (BD™ CompBeads). An isotype control was included to account for non-specific staining. The panels used in this thesis are listed in the following tables.

Table 2-6 Staining panel for Treg ontogeny

	FITC	PE	PE-Cy7	PerCp-Cy5.5	APC	APC-Cy7	V450	V500
Phenotype-1	Foxp3	β7		CD45RA	CLA	CD3	CD127	CD4

*Used for Section 3.3.4

Table 2-7 Staining panel for iTregs and proliferated $CD4^+$ cells

	FITC	PE	PE-Cy7	PerCp-Cy5.5	APC	APC-Cy7	V450	V500
Phenotype-1	Foxp3	CD127	PD-L1	CD4	CTLA-4	PD-1	HLA-DR	Live/ Dead
Phenotype-2 (after restimulation)	Foxp3	GITR		CD4	CD39		ICOS	Live/ Dead

*Used for Section 4.3.2 and Section 5.3.2

Table 2-8 Staining panel for MoDCs

	FITC	PE	PE-Cy7	PerCp-Cy5.5	APC	APC-Cy7	V450	V500
Phenotype-1	DCsign	CD83	CD11c	CD80	CD86	CD14	HLA-DR	Live/ Dead
Phenotype-2	CD14		PD-L1	CCR7	TLR4	PD-1	CD1a	Live/ Dead
Cytokine-1	IL-12/ IL-23	CXCL9	IL-12	TNF-α	TGF-b	CD14	IL-10	Live/ Dead
Cytokine-2			IL-6			CD14		Live/ Dead

*Used for Section 5.3.1

Table 2-9 Staining panels for PBMCs

	FITC	PE	PE-Cy7	PerCp-Cy5.5	APC	APC-Cy7	V450	V500
Phenotype-1	Foxp3	CD8	PD-L1	CD4	CTLA-4	PD-1	CD127	Live/ Dead
Phenotype-2 (after restimulation)	Foxp3	GITR	CD8	CD4	CD39	CD14	ICOS	Live/ Dead

*Used for Section 6.3

2.2.4.5 Analysis of Flow Cytometry Results

Acquired samples (FCS files) were analysed on FlowJo Version10 (Treestar, San Carlos, CA). Consistent gating strategies were used for all samples in the same set of experiments. An isotype control was included to help with the gating. Mean Fluorescence Intensity (MFI) was calculated using the geometric mean on FlowJo.

2.2.5 Summary of the protocols

The protocols used in this thesis are summarised in flow charts.

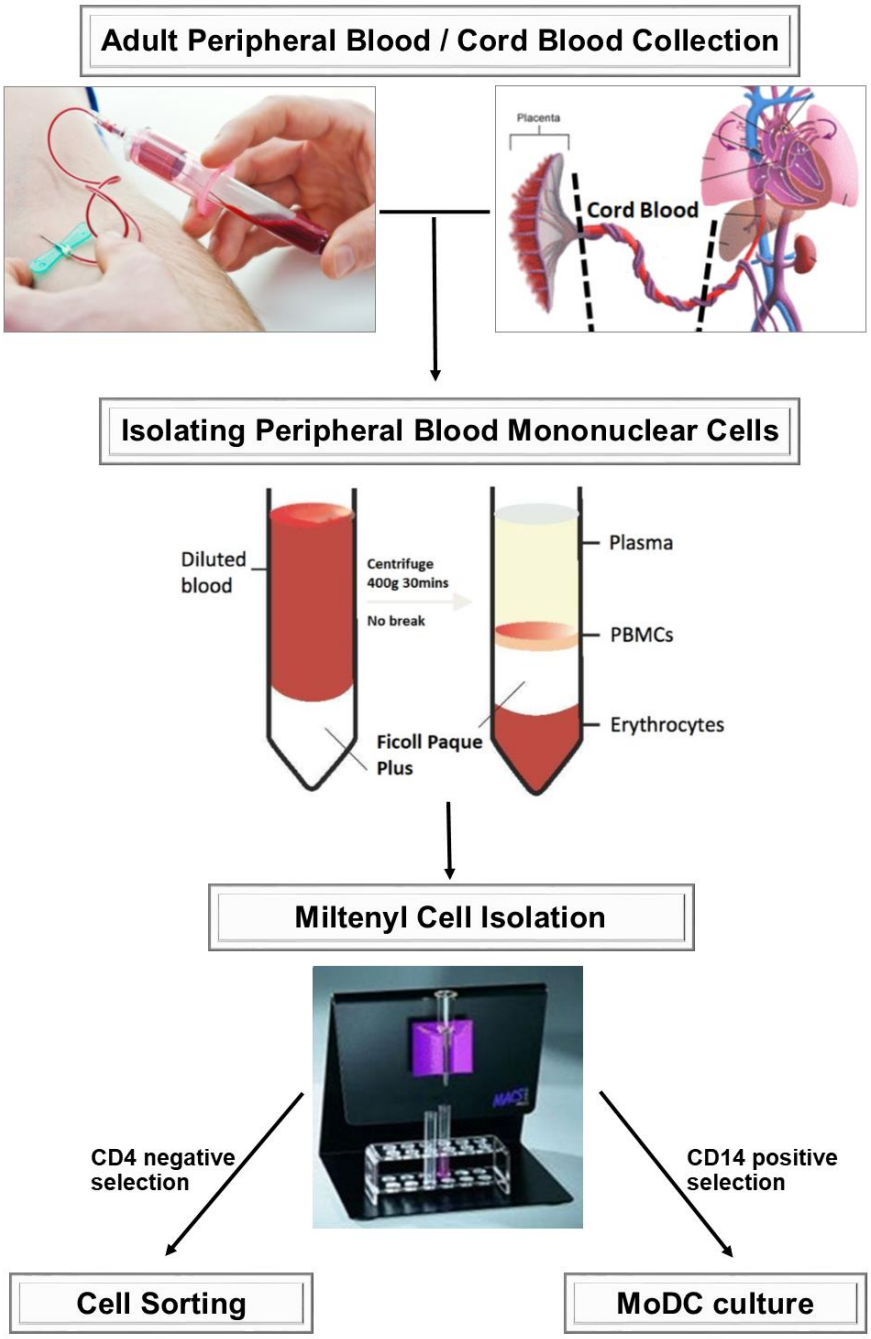

Figure 2.4 Flow chart for cell preparation.

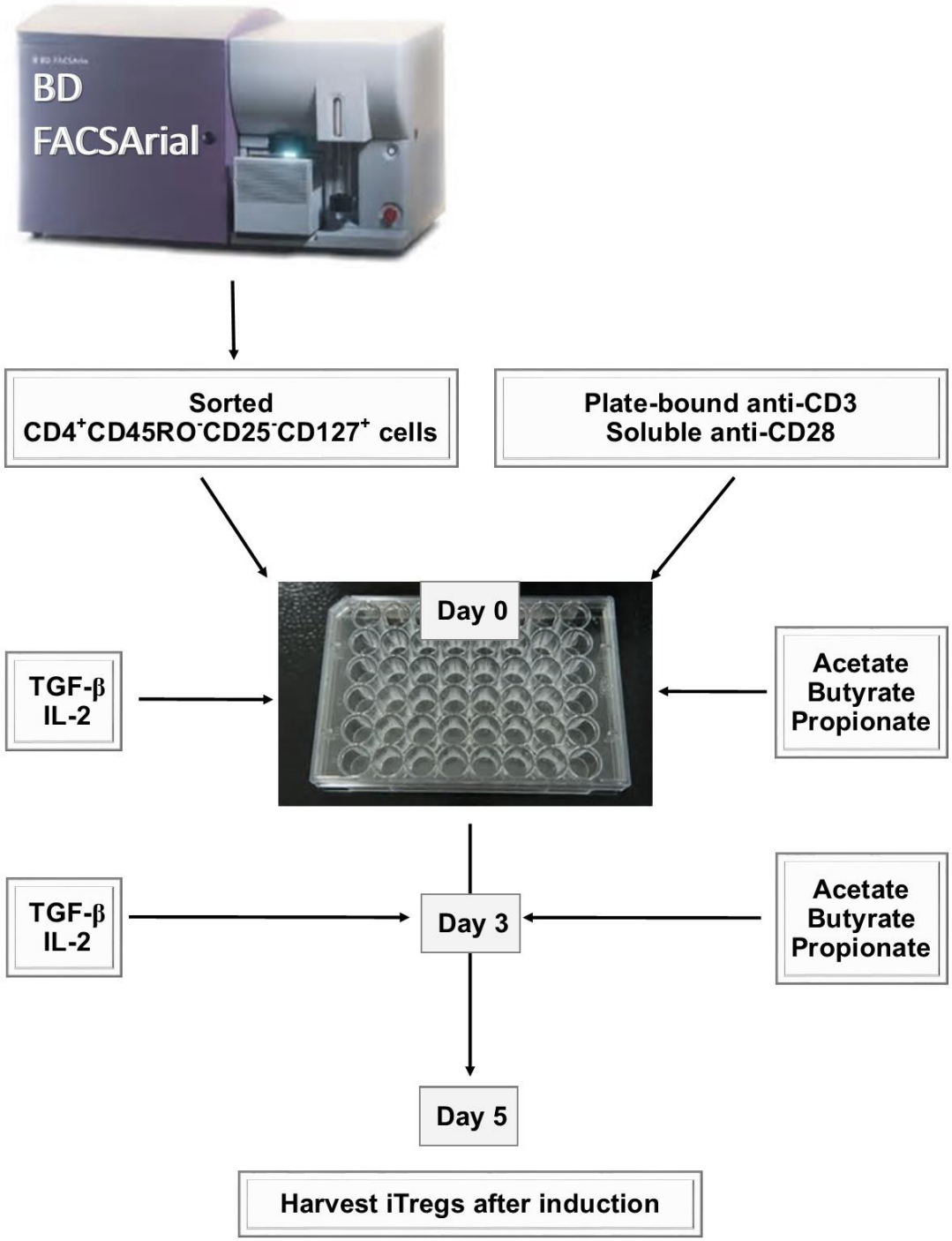

Figure 2.5 *In vitro* Human Treg cell induction protocol

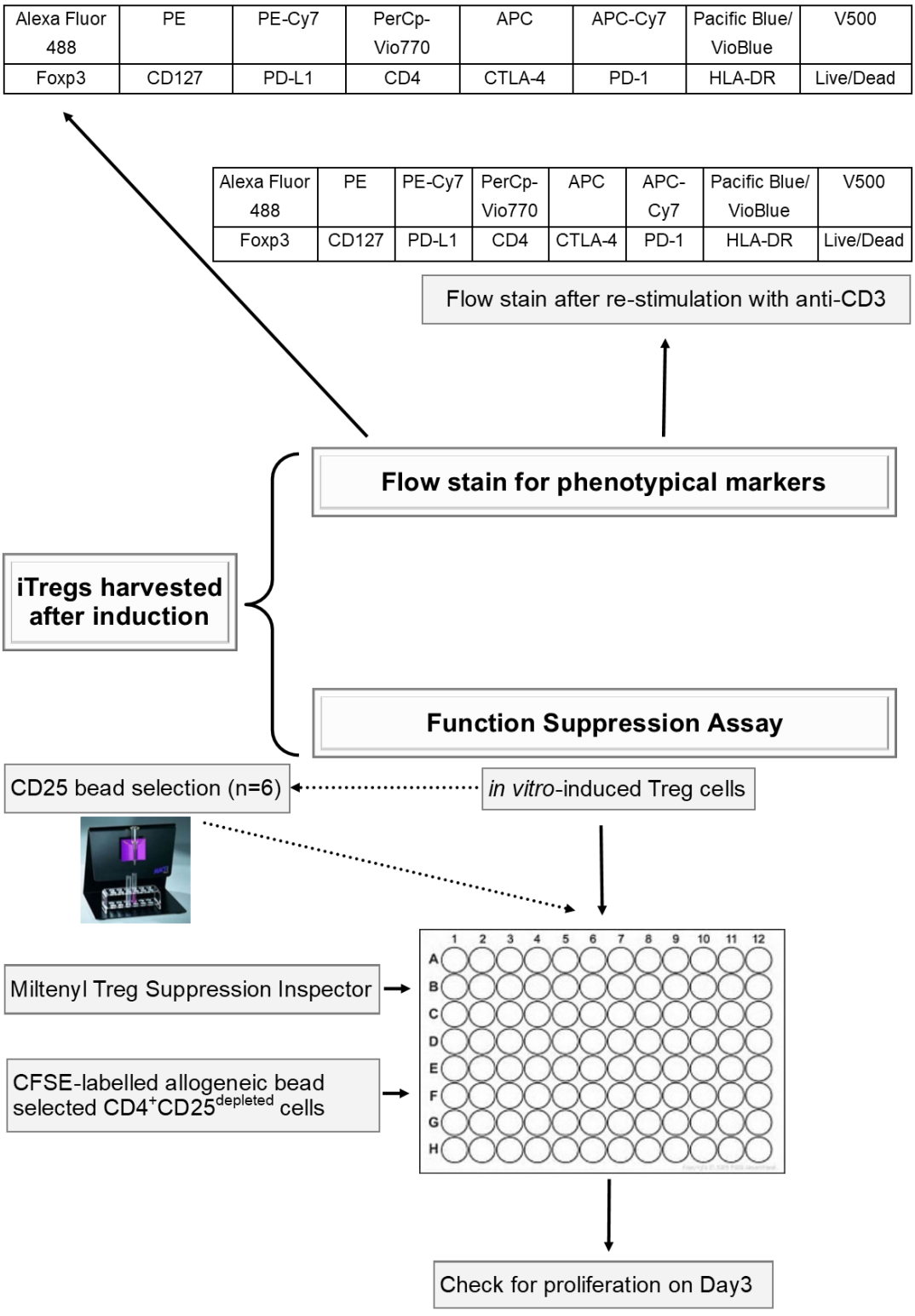

Figure 2.6 Summary of analyses for iTregs after induction

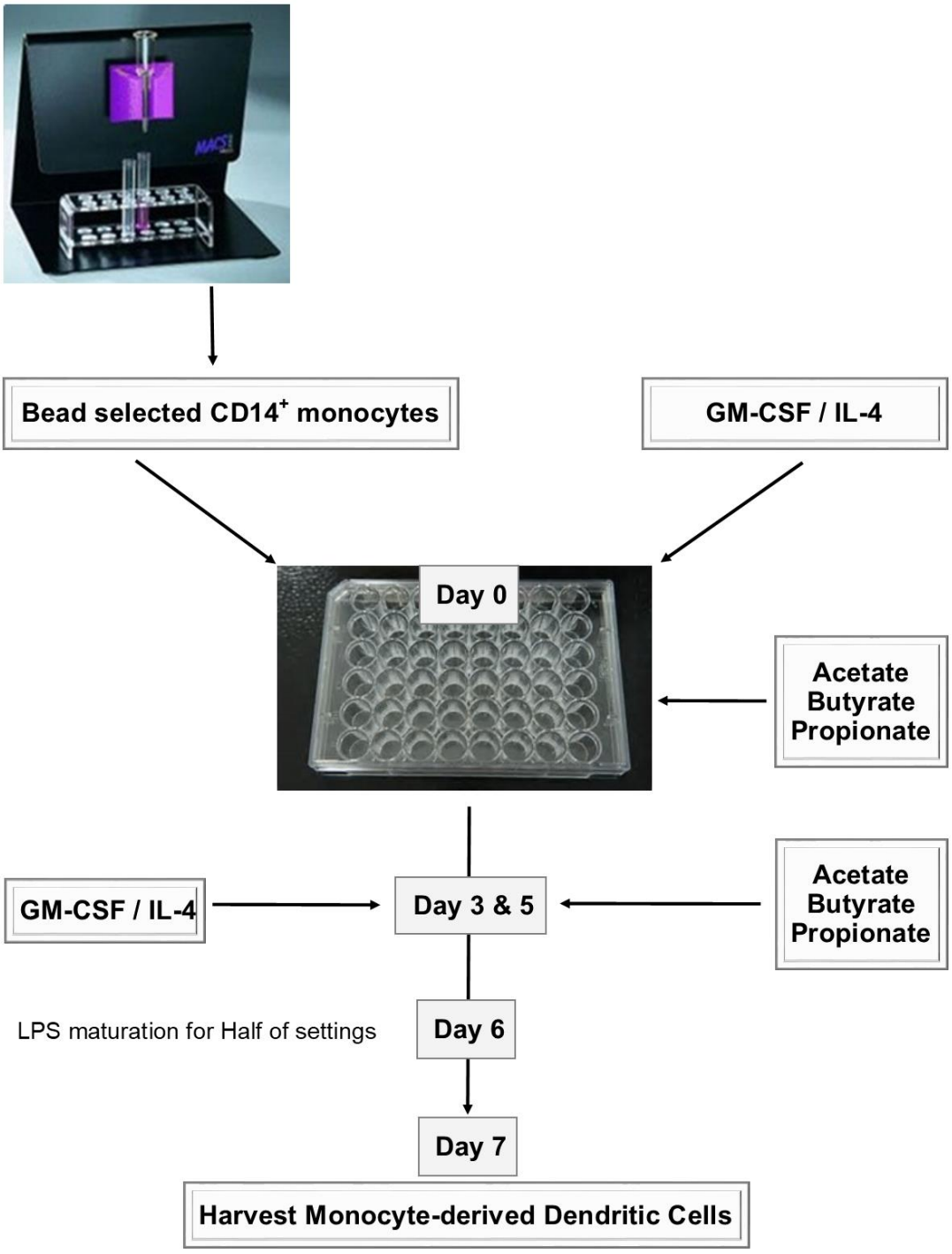

Figure 2.7 *In vitro* Human MoDCs induction protocol

	FITC	PE	PE-Cy7	PerCp-Cy5.5	APC	APC-Cy7	V450/ Pacific Blue	V500
Phenotype-1	DCsign	CD83	CD11c	CD80	CD86	CD14	HLA-DR	Live/ Dead
Phenotype-2	CD14		PD-L1	CCR7	TLR4		CD1a	Live/ Dead
Cytokine	IL-12/IL-23	CXCL9	IL-12	TNF-a	TGF-b	CD14		Live/ Dead

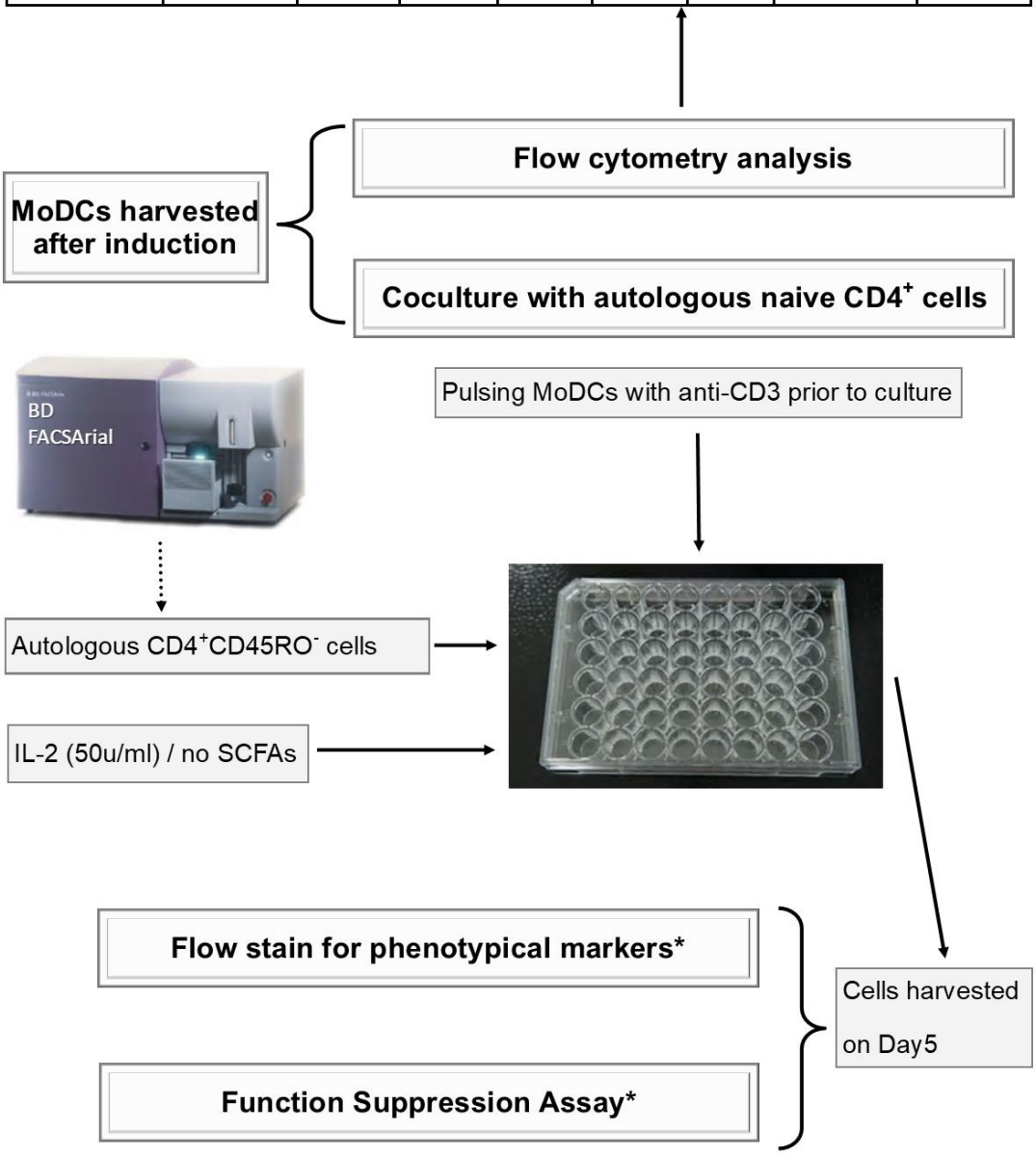

*:same protocol described after iTreg induction.

Figure 2.8 Summary of analyses for MoDCs after induction

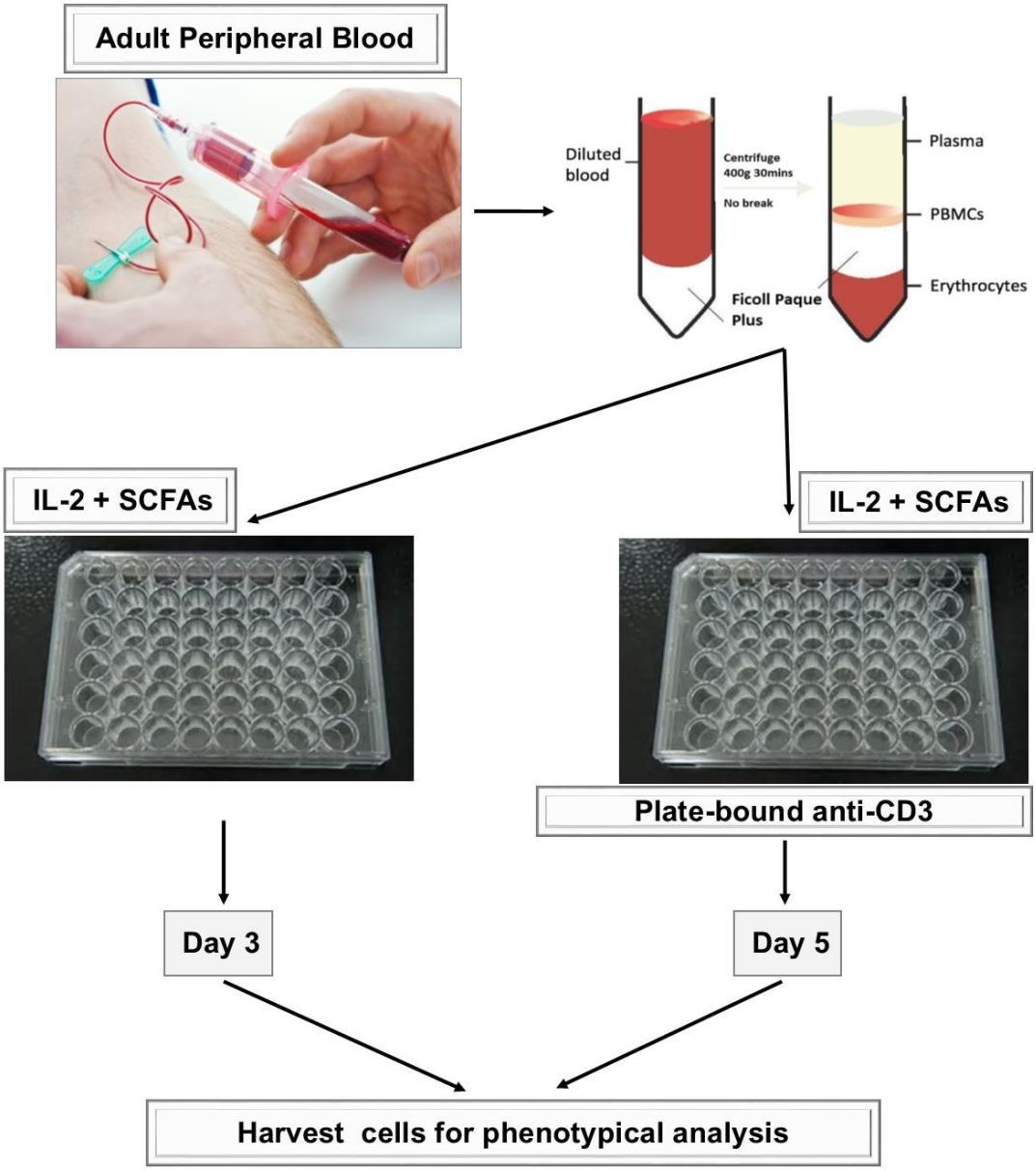

	FITC	PE	PE-Cy7	PerCp-Cy5.5	APC	APC-Cy7	V450/ Pacific Blue	V500
Phenotype	Foxp3	CD8	PD-L1	CD4	CTLA-4	PD-1	CD127	Live/Dead
Phenotype-restimulation	Foxp3	GITR	CD8	CD4	CD39	CD14	ICOS	Live/Dead

Figure 2.9 Protocol for PBMCs culture and analyses

2.2.6 ChIP Study

T-cell chromatin isolation, ChIP, and quantitative assessment of H3 or H4 histone acetylation by polymerase chain reaction (PCR) were conducted as established and thoroughly validated before (329). PCR primers used in the present study are given in Table S-1. Intra- and inter-assay coefficients of variation calculated for percent enrichment should not exceed 10% (329). All samples were processed according to the same standardized protocol and analysed blinded and in a randomized order.

The enrichment was calculated using the following formula: % enrichment = $100 \times 2^{[(CT\ input - 3.3) - CT\ sample]}$. The percent enrichment of the negative control (IgG) was subtracted from this value and then normalized to the *RPL32* housekeeping gene (HKG). The advantage of the application of an HKG measurement method is that the same ChIP samples are used to analyse both sequences of interest and control sequences, eliminating variation caused by sample handling. The normalization was done according to the following formula: normalized enrichment to desired gene = % enrichment to desired gene/% enrichment to HKG.

2.2.7 Statistical Analyses

Statistical analyses were performed on GraphPad, Prism 7 (La Jolla, CA, USA) or IBM SPSS v26 (USA). All the data were not normally distributed due to the small sample size. Therefore, for comparisons among two or more groups, Mann-Whitney test or Friedman test with Dunn's multiple comparison test (*post hoc*) were used to determine statistical significance. For the suppression assay with multiple variables, two-way ANOVA with Tukey's multiple comparison test (*post hoc*) was used. Spearman's correlation coefficient was used for correlation studies. For all analyses, a *p* value of less than 0.05 was deemed statistically significant. Consultations were made with a statistician at all stages of the thesis.

Chapter 3 – Treg Cell Programming during Early Life

3.1 Introduction

The theory of Developmental Origins of Health and Disease (DOHaD) was originally postulated by Barker and Osmond in 1984 (213). Since then, numerous investigations proved that fetal organs and systems during this sensitive period of development experience programmed structural or functional changes according to the intrauterine environment alterations, leading to various diseases later in adulthood (214).

There are growing numbers of studies in human suggesting that the DOHaD theory also applies to the inflammatory and immune diseases (215-217). Collectively, these findings provide evidence that appropriate stimulation to the maternal immune system *in utero* may educate and shape the fetal immune system (209, 216, 218-222). For the purpose of this thesis, special attention will be focused on T cells, especially Treg cell programming.

Fetal and adult T cells are differentiated from different HSCs (210). Upon stimulation with maternal alloantigens, fetal T cells differentiate into Tregs in the fetal thymus, and these Tregs are specific for NIMAs (226). They migrate from the thymus to peripheral lymphoid organs from the 10^{th} gestational week (223, 224). There is an increased proportion of Treg cells in the fetus during mid-gestation (210), around 15-20% of total $CD4^+$ T cells (225), significantly higher than in newborns and adults. At the fetal-maternal interface, $Foxp3^+$ Treg cell percentage is also higher compared to peripheral blood, and half of them are generated locally in the decidua, and are not of thymic origin (330). These changes in Treg cell compartment prove that fetal immune system is prone to differentiate into either tTregs or pTregs in response to stimulation to maintain a tolerogenic status.

Our group previously made a surprising discovery (209) that there was a specific and significant correlation of Treg cells (but not Th1, Th2 or Th17 cells) between maternal-fetal dyads (pairs). The possibility of maternal Treg cells migrating to the fetus could be excluded by HLA typing of the fetal Treg cell population. However, this correlation didn't exist in the paternal fetal dyads, indicating that transplacental factors rather than the genetics cause this alignment. Gene microarray analysis suggested that IL-10 pathway may play a role and it was confirmed by the specific alignment of serum IL-10 at the protein level. The mechanism of how IL-10 contributes to the Treg generation will be explained in detail later (refer to section 3.3.3).

In addition to anti-inflammatory cytokine IL-10, various other environmental factors, such as pregnancy-related hormones or microbiota metabolites, also contribute to the transplacental programming of Treg cells (331). The offspring of C57BL/6 pregnant mice fed with high fibre diet had increased levels of serum SCFAs until day 22 after birth, and these offspring also had a higher percentage of Treg cells accordingly (332). Moreover, the concentration of SCFAs was much lower or undetectable, and there were no *Bacteroidetes* (essential for the SCFAs production (246)) in the gut contents of offspring at day 1 after birth, thus indicating SCFAs derived from the maternal gut were transferred to the fetus throughout pregnancy.

Apart from *in utero* stage, the programming or ontogeny of Treg cells happens after birth as well (333). Early exposure to environmental factors could increase the prevalence of allergies and IBD (334-336) via the modulation of Treg cells. The skin homing marker Cutaneous Lymphocyte Antigen (CLA) is expressed on the majority of adult Treg cells (337), whereas in cord blood there is a higher proportion of gut-homing $\alpha 4\beta 7$ integrin

(made of α4 and β7 subunits) expressing Treg cells (338); thus suggesting age-related differences in Treg cell homing molecule expression.

Therefore, three aspects are explored in detail in this chapter: a) Thymus and Treg cell programming *in utero*, b) postnatal Treg cell ontogeny, and c) how IL-10 contributes to the generation of iTregs.

This chapter is a summary of collaborative works about T cell (especially Treg cell) programming during pregnancy and infancy. Some of these results are unpublished except for section 3.3.3 (1) and section 3.3.4 (2). A detailed list of contributions made by myself and our collaborators will be provided at the beginning of each section.

3.2 Subjects

3.2.1 Fetal Thymus and Treg Cell Development

GF and SPF C57BL/6 mice were used for this section. Some of the pregnant GF mice were fed at libitum with sodium acetate (200 mM) provided in the drinking water. Mouse thymic analyses were performed from two to three separated cohorts of pups to obtain reproducibility.

For serum acetate levels, forty-six maternal peripheral blood samples were collected, and cord blood samples were collected within 4 hours following maternal blood sampling. All babies were born by caesarean section at term.

3.2.2 Unique TCR Repertoires in Cord Blood

Five term healthy pregnant women from Nepean Hospital (Sydney, NSW, Australia) were included in this study with a mean age of 31.1±10.1 years. All babies were born by

caesarean section at a gestational age of 39.0±6 days with a mean weight of 3,546±189 grams. Paired paternal partners were also included with a mean age of 35.8±3.77. Patients with diabetes, infectious conditions, chromosomal abnormalities, and/or morphological anomalies were excluded.

3.2.3 IL-10 Potentiates Differentiation of Human Induced Regulatory T Cells

Peripheral blood was obtained from healthy volunteers (n=20).

3.2.4 Treg cell ontogeny during early life

Peripheral blood was obtained from healthy infants and children aged 0-16 years (n=50) undergoing general anaesthetic for elective surgery. Blood samples were collected at the time of cannulation prior to surgical procedures.

3.3 Results

3.3.1 Fetal Thymus and Treg Cell Development

Table 3-1 List of contributions for Section 3.3.1

	Affiliation	Sample Collection and Processing	Serum Acetate Quantification	Animal Experiment	Data Analysis	Manuscript Preparation
Eliana Marino Moreno	Monash University			√	√	√
Fiona Collier, Peter Vuilleman	Deakin University		√			√
Myself	University of Sydney	√			√	√

It has been proven that bacterial metabolites influence T cells, particularly Treg cell development. Additionally, maternal supplementation of acetate protected offspring against the development of food allergy through modulation of Treg and dendritic cells (339). Animal experiments by our collaborators showed that maternal bacterial load could affect fetal thymic development and Treg cell differentiation (unpublished data).

The fetal thymic weights of fetuses born to GF or SPF mice were measured at 3 weeks. The fetal thymic weight in GF mice was significantly lower (around half) compared to SPF mice (Figure 3.1A). Most importantly, the reduction of fetal thymic weight could be completely rescued by supplementing acetate in drinking water to maternal GF mice, and

the final thymic weight became comparable to SPF mice. In addition, there was also a significant reduction in the total thymic $CD4^+$ T cells numbers (Figure 3.1B), total thymic $Foxp3^+$ Treg cell numbers (Figure 3.1C) and the Foxp3 protein expression per cell in Treg cells (Figure 3.1D) in GF mice. Interesting, they could also be rescued by acetate supplementation until comparable levels of SPF mice, though the increase in the total Treg cell numbers of GF ADW group was not significant. Lastly, in a separate cohort of paired maternal and fetal serum (collected no longer than 4 hours apart), we noticed a significant correlation (Spearman's test, $r=0.4158$ and $p=0.004$) between cord blood and maternal blood acetate levels (Figure 3.2), consistent with transplacental acetate transfer. Collectively these results indicate that metabolites, such as acetate, is pivotal in the transplacental programming for fetal thymus and Treg cell development.

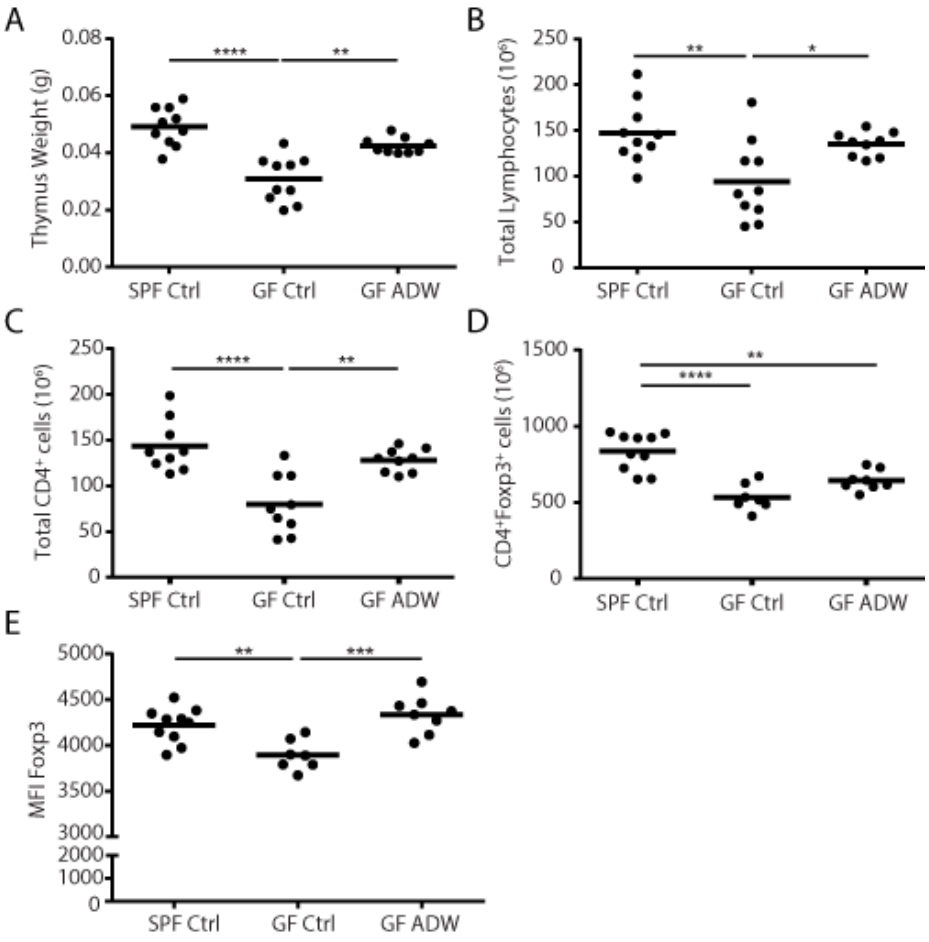

Figure 3.1 Impaired Thymus and Treg Cell Development in GF Mice can be Rescued by Maternal Acetate Consumption.

Cumulative data showing thymus's analyses from pooled female and male C57/Bl6 mice at 3 weeks-old born from SPF mothers and GF mothers treated with normal drinking water (Ctrl) or acetate (ADW) as indicated (n=7-11 per group). Summary dot plot showing (**A**) the thymus weight, (**B**) total thymic lymphocytes, (**C**) total thymic $CD4^+$ T cell number, (**D**) total $Foxp3^+$ Treg cell numbers, and (**E**) MFI of Foxp3 expression per cell on a per-cell basis in thymic $CD4^+Foxp3^+$ T cells. Data were analysed by one-way ANOVA with Bonferroni's multiple comparisons test. Each data set represents two to three independent experiments. *p<0.05, **p<0.01, ***p<0.001, ****p<0.0001. (Figure adapted from our manuscript.)

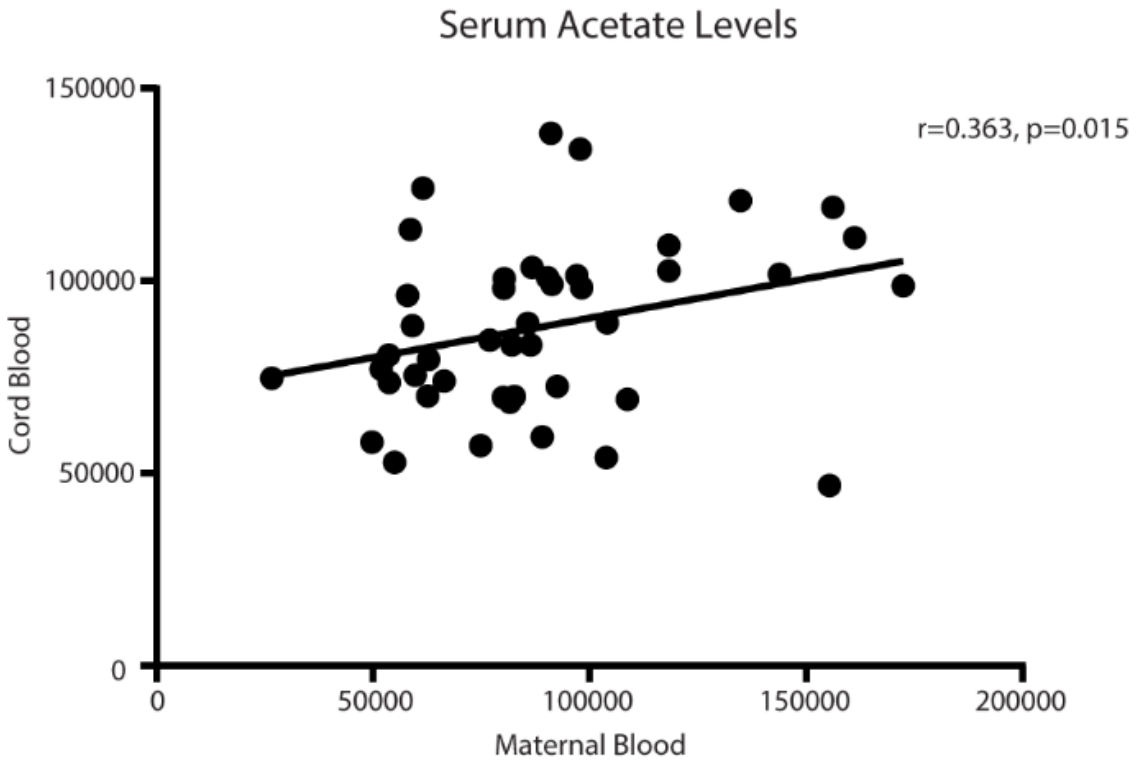

Figure 3.2 Correlation of serum acetate levels between paired maternal peripheral blood and cord blood.

Scattered dot plot showing the relative serum acetate levels in paired term maternal peripheral blood and cord blood (n=44). The acetate levels were based on peak heights from the NMR spectra normalized to the total intensity. Spearman's rank correlation was used. Coefficient *r* and *p* values as indicated. (Figure adapted from our manuscript.)

3.3.2 Unique TCR Repertoires in Cord Blood

Table 3-2 List of contributions for Section 3.3.2

	Affiliation	Sample Collection and Processing	TCR repertoire sequencing	Data Analysis	Manuscript Preparation
Thomas Watkins, John Miles	James Cook University		√	√	√
Myself	University of Sydney	√			√

Together with our collaborators from James Cook University, we also examined the TCR repertoire in family sets (maternal blood-MB, paternal blood-PB, and cord blood-CB) to investigate about TCR repertoire inheritance (unpublished data).

In general, TCR sharing between patients and offspring and between anatomical sites were infrequent and of low abundance, typically <0.5% of the repertoire. Strikingly, it was apparent that the highest degree of TCR repertoire sharing across all T cell subsets was between genetically unrelated newborns rather than between parent-newborn dyads (Figure 3.3). The TCR sharing between MB and CB was very low, and the frequency was similar between CB and PB for all T cell subsets, including memory $CD8^+$ T cells (Figure 3.3A), memory $CD4^+$ T cells (Figure 3.3B), naïve $CD8^+$ T cells (Figure 3.3C), and naïve $CD4^+$ T cells (Figure 3.3D). In contrast, sharing between unrelated CBs was significantly higher in all T cell subsets, especially for memory $CD4^+$ T cells (Figure 3.3B) and naïve

$CD8^+$ T cells (Figure 3.3C). To confirm this unusual observation of the high degree of sharing (>10% within the top 50 clonotypes) in the memory $CD4^+$ T cells of CB, we analysed three unrelated CB sets (Figure 3.3E). Across sets, we observed similar patterns with an average of 10.3% ± 1.2% sharing within the top 50 clonotypes. The antigen specificity and function of this high frequency shared memory clonotypes in neonates are unknown.

We next determined the transcriptional profiles of T cell subsets across MB, PB and CB. Transcriptomic comparisons of both naïve $CD8^+$ T cells (Figure 3.4A) and $CD4^+$ T cells (Figure 3.4B) showed the least degree of variation compared to memory $CD8^+$ T cells (Figure 3.4C) and $CD4^+$ T cells (Figure 3.4D). The CB genes were almost uniformly downregulated when compared to MB except for a few genes, including the chemokine receptor CCR4 and the transcription factor IRF4.

Collectively, the TCR sharing and transcriptomic data showed that neonates are born with TCR repertoire and T cell phenotype that resemble more closely to unrelated neonates compared with parents, indicating again that the environmental cues rather than genetics play a role in the transplacental T cell programming.

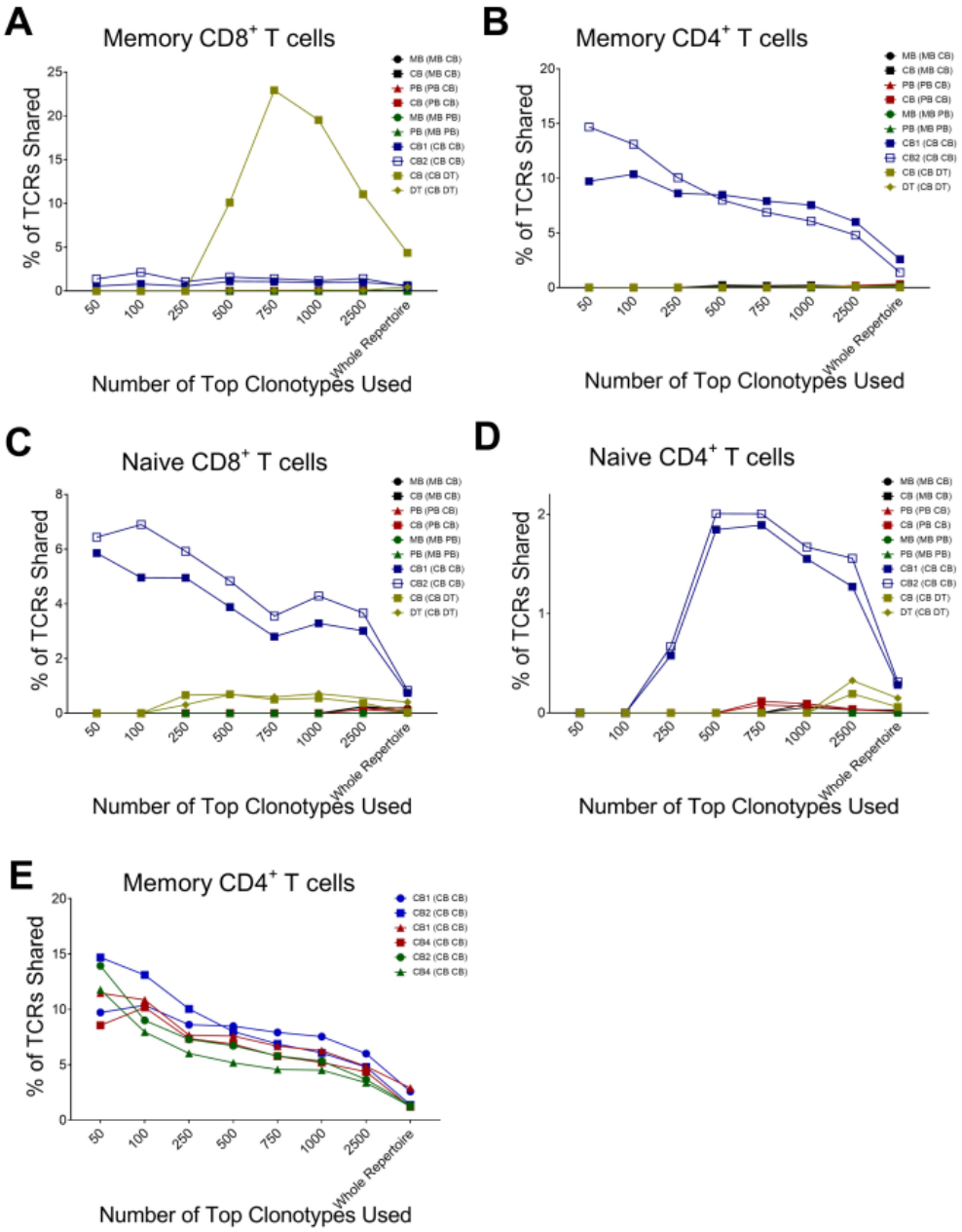

Figure 3.3 TCR repertoires sharing across T cell subsets.

Percentage overlap of memory $CD8^+$ T cells (**A**), memory $CD4^+$ T cells (**B**), naïve $CD8^+$ T cells (**C**) and naïve $CD4^+$ T cells (**D**) by descending clonotype abundance across paired MB, PB and DT samples and unrelated CB sample. (**E**) Percentage overlap in memory $CD4^+$ T cells between unrelated CB samples by descending clonotype abundance. (Figure adapted from our manuscript.)

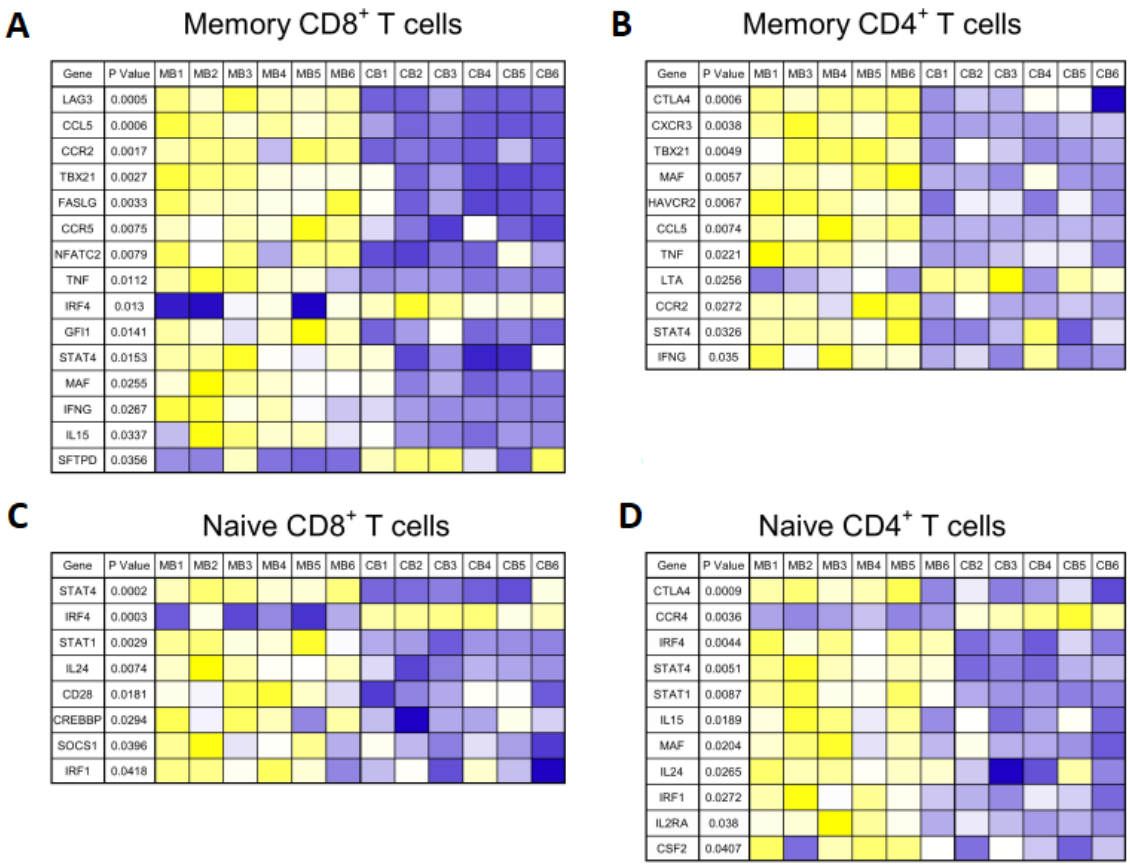

Figure 3.4 Heatmap of differentially expressed genes between MB and CB.

Heatmap of differentially expressed genes between MB and CB memory $CD8^+$ T cells (**A**), memory $CD4^+$ T cells (**B**), naïve $CD8^+$ T cells (**C**) and naïve $CD4^+$ T cells (**D**) with a paired t-test p value less than 0.05. Row normalization ((expression value - mean) / SD) was performed out for each gene. Colour gradient spans highest (yellow) to lowest (blue) gene expression. (Figure adapted from our manuscript.)

3.3.3 IL-10 potentiates differentiation of human induced regulatory T cells

Table 3-3 List of contributions for Section 3.3.3

	Affiliation	Sample Collection and Processing	*In vitro* Experiment	Flow Cytometry	Data Analysis	Manuscript Preparation
Brigitte Nanan	Sydney Medical School Nepean	√	√	√	√	√
Peter Hsu	The Children's Hospital at Westmead	√			√	√
Myself	University of Sydney		√	√		√

To examine the role of IL-10 and IL-6 in human iTreg cell induction, we stimulated FACS sorted naïve $CD4^+CD45RO^-CD25^-CD127^{hi}$ T cells (>97% purity) with anti-CD3/anti-CD28 in the presence of IL-2 and TGF-β with or without IL-10 for 5 days then rested the cells in the presence of IL-2 for 2 days. There was a modest but significant increase in the percentage of $Foxp3^+$ T cells in cultures treated with IL-10 (Figure 3.5A, B), associated with significantly enhanced Foxp3 (Figure 3.5C) and CTLA-4 (Figure 3.5D) expression, as assessed by mean fluorescence intensity. This was also confirmed on the mRNA level. We further show that IL-10 (and to a lesser extent IL-6) treated $Foxp3^+$ T cells secreted significantly less IFNγ corresponding to reduced IFNγ on the mRNA level (Figure 3.5 E&F). These results indicate that IL-10 enhances the phenotype of iTreg cells.

We next tested the suppressive function of cultured cells *in vitro*. IL-10 treated iTreg cells suppressed the *in vitro* proliferation of autologous $CD4^+CD25^-$ cells significantly more than non-IL-10 treated iTreg cells. This was true at all suppressor: responder cell ratios (Figure 3.6A, B) and was highly statistically significant (Figure 3.6C). The suppressive capability of those IL-10 treated iTreg cells was comparable to that of FACS sorted $CD4^+CD25^+CD127^{lo}$ natural Treg cells isolated from the same donor and stimulated/rested *in vitro* for the same period (Figure 3.6B). In stark contrast, IL-6 significantly reduced the suppressive function of TGF-β-induced iTreg cells (Figure 3.6). Overall, these results demonstrate that in contrast to IL-6, IL-10 present at the time of iTreg cell induction, augments the suppressive function of iTreg cells.

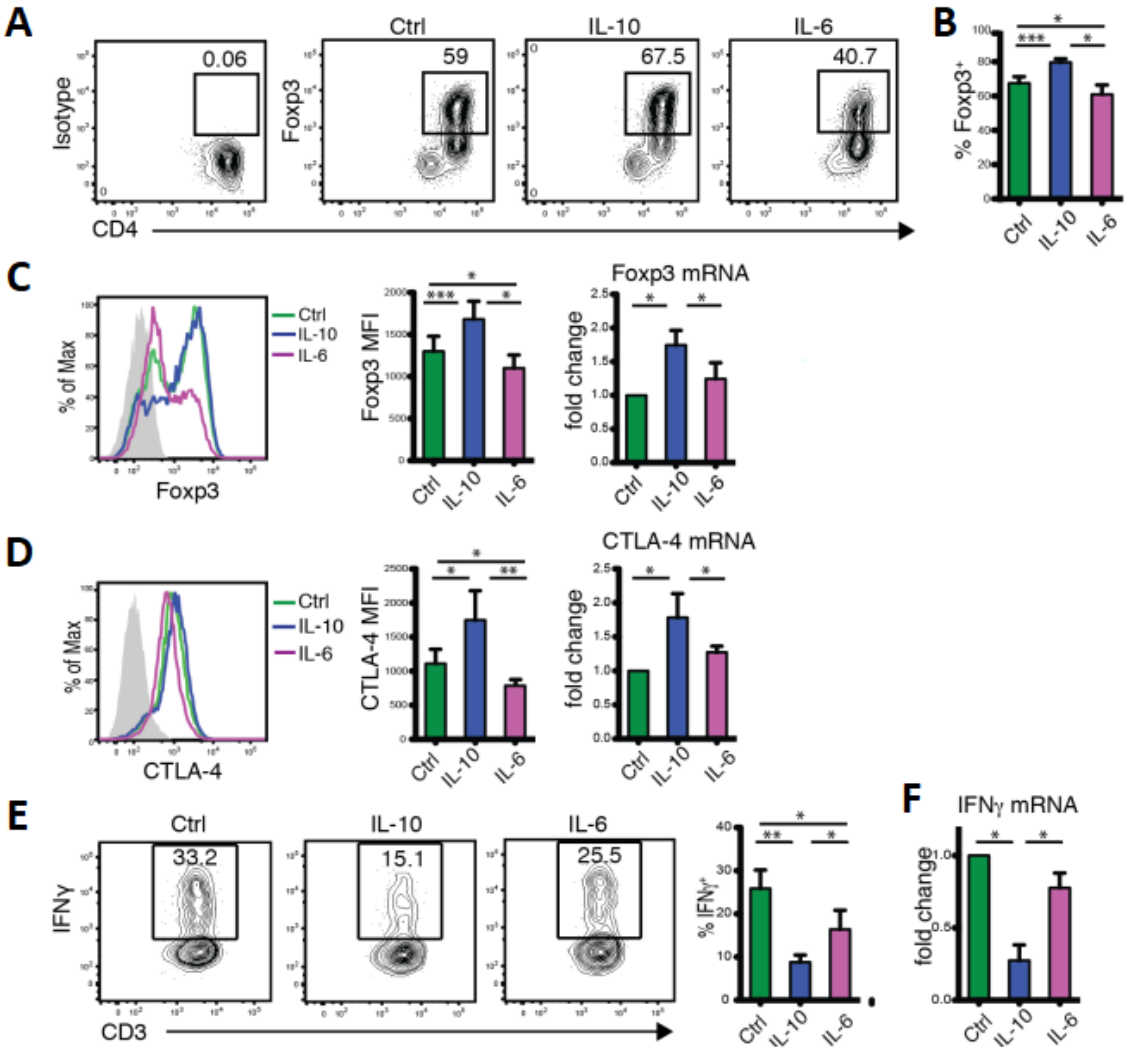

Figure 3.5 IL-10 potentiates human TGF-β-induced iTreg cells.

(A) Representative contour plots gated on live $CD3^+CD4^+$ T cells showing % $Foxp3^+$ cells induced after culture under various conditions: Ctrl (IL-2+TGFβ), IL-10 (IL-2+TGFβ+IL-10) and IL-6 (IL-2+TGFβ+IL-6) compared to isotype control. **(B)** Summary bar graphs showing mean and SEM of % Foxp3 induced under various conditions as indicated (10 independent experiments. *p<0.05, ***p<0.001). Foxp3 **(C)** and CTLA-4 **(D)** expression of live $CD3^+CD4^+$ T cells cultured under various conditions, as shown by representative histogram (left panel), summary bar graph of MFI (10 independent experiments. *p<0.05, **p<0.01) (middle panel) and mRNA expression as fold change

relative to Ctrl (5 independent experiments. *p<0.05) (right panel). **(E)** Representative contour plots showing % IFNγ secreting cells within live $CD3^+CD4^+Foxp3^+$ T cells induced under various conditions and summarized by bar graph (6 independent experiments. *p<0.05, **p<0.01) and confirmed by mRNA expression **(F)** relative to Ctrl. (Figure adapted from (1).)

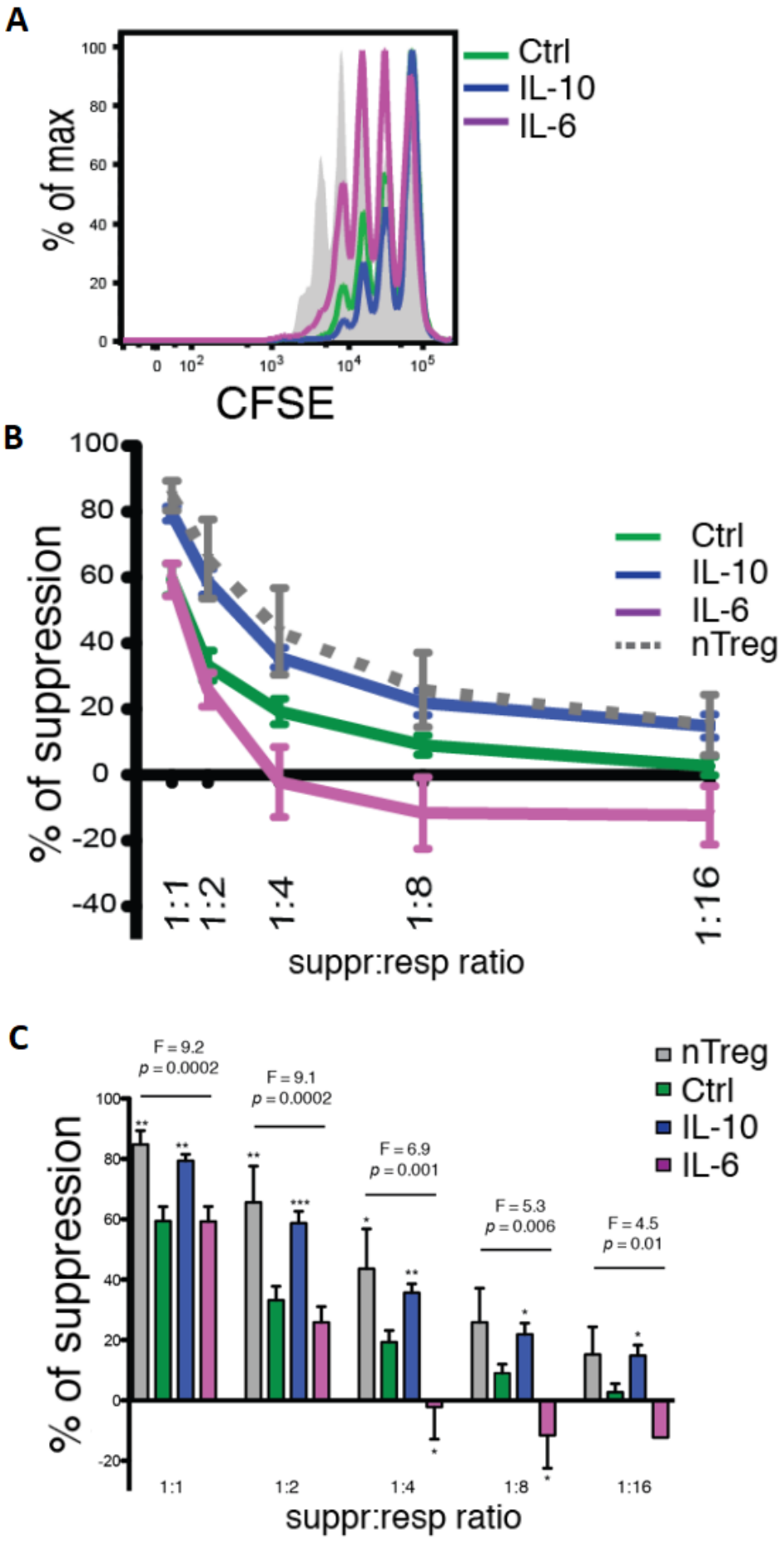
A
% of max
CFSE
Ctrl
IL-10
IL-6
B
% of suppression
suppr:resp ratio
Ctrl
IL-10
IL-6
nTreg
1:1
1:2
1:4
1:8
1:16
C
% of suppression
suppr:resp ratio
nTreg
Ctrl
IL-10
IL-6
F = 9.2
p = 0.0002
F = 9.1
p = 0.0002
F = 6.9
p = 0.001
F = 5.3
p = 0.006
F = 4.5
p = 0.01

Figure 3.6 IL-10 enhances the suppressive capacity of human TGF-β-induced iTreg cells

(A) Representative histograms (at suppressor: responder ratio of 1:4) showing proliferation of CFSE-labelled responder cells alone (shaded) or co-cultured with Ctrl, IL-10 and IL-6 treated iTreg cells. **(B)** Percentage suppression of nTreg cells (dotted line) and iTreg cells (coloured line) cultured under various suppressor: responder ratio and various conditions as labelled. Percentage suppression was calculated as (proliferation of T responder alone – the proliferation of co-cultured T responder) / proliferation of T responder alone x 100. Data show at least 5 independent experiments in each group. **(C)** Statistical analysis of the suppressive capacity of nTreg cells (grey) and iTreg cells (coloured) cultured under various conditions as indicated. ANOVA testing for variance between groups at each suppressor: responder ratio is indicated by F and p values. Data show at least 5 independent experiments in each group. Stars indicate significant p values compared to the Ctrl group based on a student's t-test (*$p<0.05$, ** $p<0.01$, ***$p<0.001$). (Figure adapted from (1).)

3.3.4 Treg Cell Ontogeny during Early Life

Table 3-4 List of contributions for Section 3.2

	Affiliation	Sample Collection and Processing	*In vitro* Experiment	Flow Cytometry	Data Analysis	Manuscript Preparation
Catherine Lai	The Children's Hospital at Westmead	√	√	√	√	√
Peter Hsu	The Children's Hospital at Westmead				√	√
Myself	University of Sydney	√	√	√	√	√

Apart from *in utero* stage, the programming or ontogeny of Treg cells happens after birth as well (333). We first examined the Treg cell ontogeny in terms of three different subsets in healthy children of varying ages. We found that the proportion of $CD45RA^{+}Foxp3^{low}$ resting Treg cells (rTreg) within $CD4^{+}$ T cells slowly decreases with age, whereas the proportion of $CD45RA^{-}Foxp3^{hi}$ activated Treg cells (aTreg) and $CD45RA^{-}Foxp3^{low}$ activated Tconv cells (aTconv) increase with age (Figure 3.7). This is consistent with age-related antigen encounter/activation.

We next The skin homing marker cutaneous lymphocyte antigen (CLA) is expressed on the majority of adult Treg cells (337), whereas there is a higher proportion of gut-homing

α4β7 integrin (made of α4 and β7 subunits) expressing Treg cells in cord blood (338); thus suggesting age-related differences in the Treg cell homing molecule expression. Therefore, we examined the gut and skin tropism of peripheral blood Treg cells. We used β7 integrin as a surrogate marker for gut tropism since almost all $\beta7^+$ T cells (>99%) are also $\alpha4^+$. CLA was used as a marker of skin tropism. Circulating $\beta7^+$ gut homing Treg cells (as a proportion of total circulating $CD4^+$ T cells) were most abundant early in life and decreased with age (Figure 3.8A, B). As a comparison, we next examined skin homing Treg cells and found they were almost absent in cord blood and increased with age (Figure 3.8A, B). We also examined Th2 cells using CRTH2, a well-accepted surface marker for human Th2 cells (340). We then calculated the gut and skin Treg: Th2 ratio by dividing the percentage of gut and skin homing Treg cells with Th2 cells. Here we found that both gut homing and skin homing Treg: Th2 ratios were highest in the first 25 months of life and reduced rapidly with age. In particular, the gut homing Treg: Th2 ratio was higher than the skin homing Treg: Th2 ratio early on but equalised later in life (Figure 3.8C). Overall, the gut homing Treg: Th2 ratio was higher compared to the skin Treg: Th2 ratio (Figure 3.8D). This suggests that the gut homing peripheral T cell population may be more primed towards tolerance acquisition compared to skin-homing T cells, especially early in life.

A higher proportion of $\beta7^+$ Treg cells were also positive for both CD45RA and CD31 (a marker for recent thymic emigrants) (341), compared to CLA^+ Treg cells (Figure 3.9A, B). We then examined the expression of β7 integrin in the thymus. $CD3^+$ thymocytes were gated based on their expression of CD4 and CD8 (Figure 3.9C). Within the $CD4^+Foxp3^+$ cells, approximately 10% of the cells expressed β7 integrin, whereas in the $CD4^+Foxp3^-$ cells, only about 5% of the cells expressed β7 integrin (Figure 3.9C),

compared to the peripheral blood where 60-80% of cord blood Treg and Tconv express β7. This result was confirmed by immunohistochemistry, where there was minimal staining of β7 integrin in the fetal thymus (Figure 3.9D). Collectively, these results suggest that Treg cells likely acquire gut tropism early in their development. However, the induction of β7 expression most likely occurs post-thymic emigration, where they encounter the microbiota metabolites SCFAs.

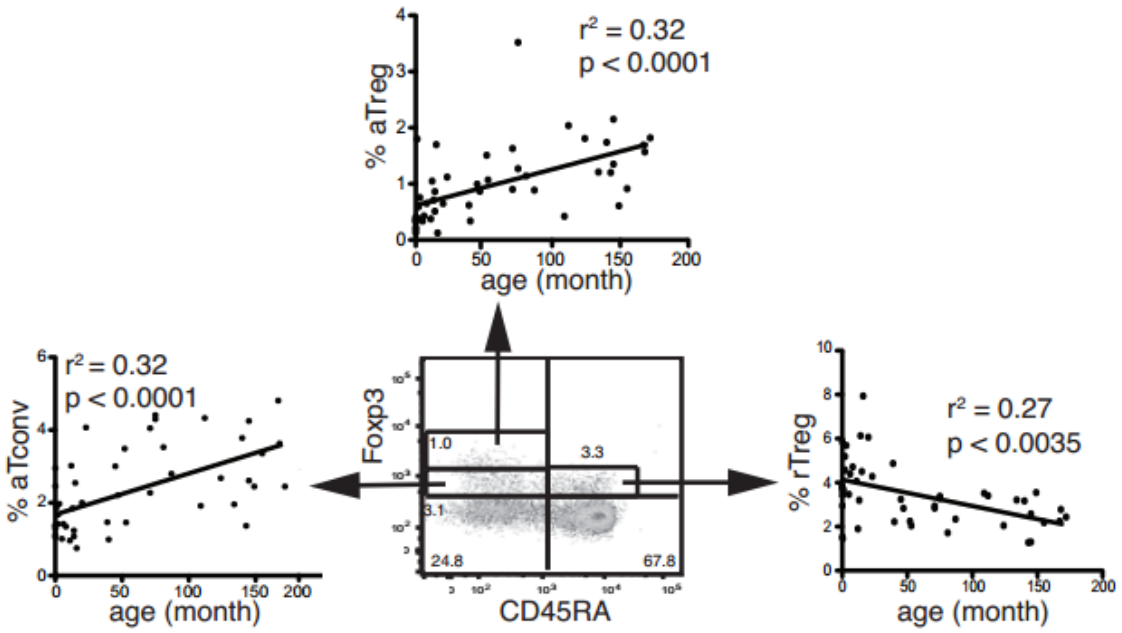

Figure 3.7 Age-dependent changes in Treg cell subsets in children.

$CD4^+Foxp3^+$ cells are subdivided into 3 subsets, $CD45RA^+Foxp3^{low}$ resting Treg (rTreg), $CD45RA^-Foxp3^{hi}$ activated Treg (aTreg) and $CD45RA^-Foxp3^{low}$ activated conventional T cells (aTconv), with their respective age-related change in percentage within $CD4^+$ cells. (Figure adapted from (2).)

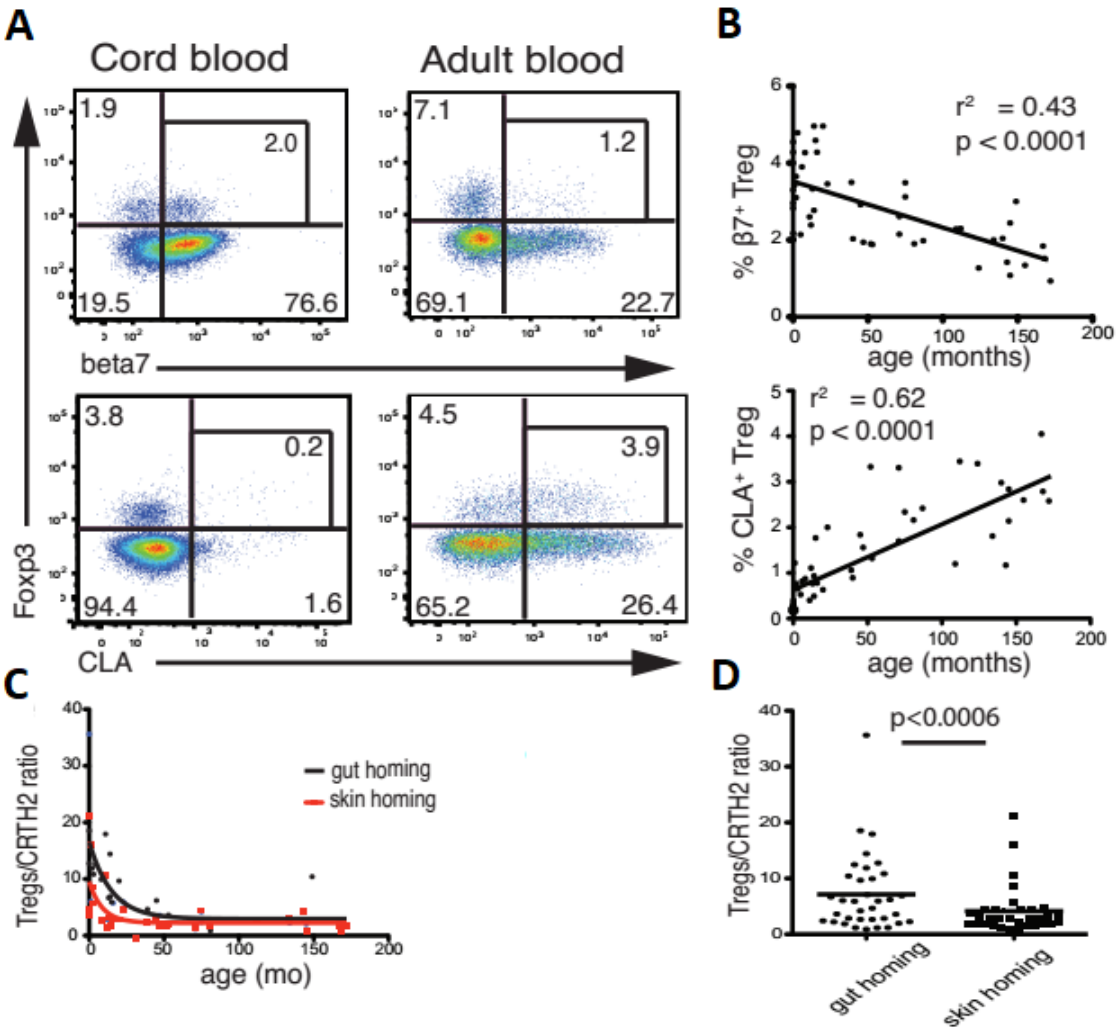

Figure 3.8 Age-related changes in gut and skin homing Treg and Th2 cells in children.

(A) Representative flow plots showing distinct patterns of gut and skin homing expression of Treg cells in cord blood and adult blood. (B) Age-related change in the percentage of gut and skin homing Treg cells within CD4 cells. (C) Age-related changes in gut and skin homing Treg: Th2 ratio. (D) Direct comparison of gut and skin homing Treg/Th2 ratio. (Figure adapted from (2).)

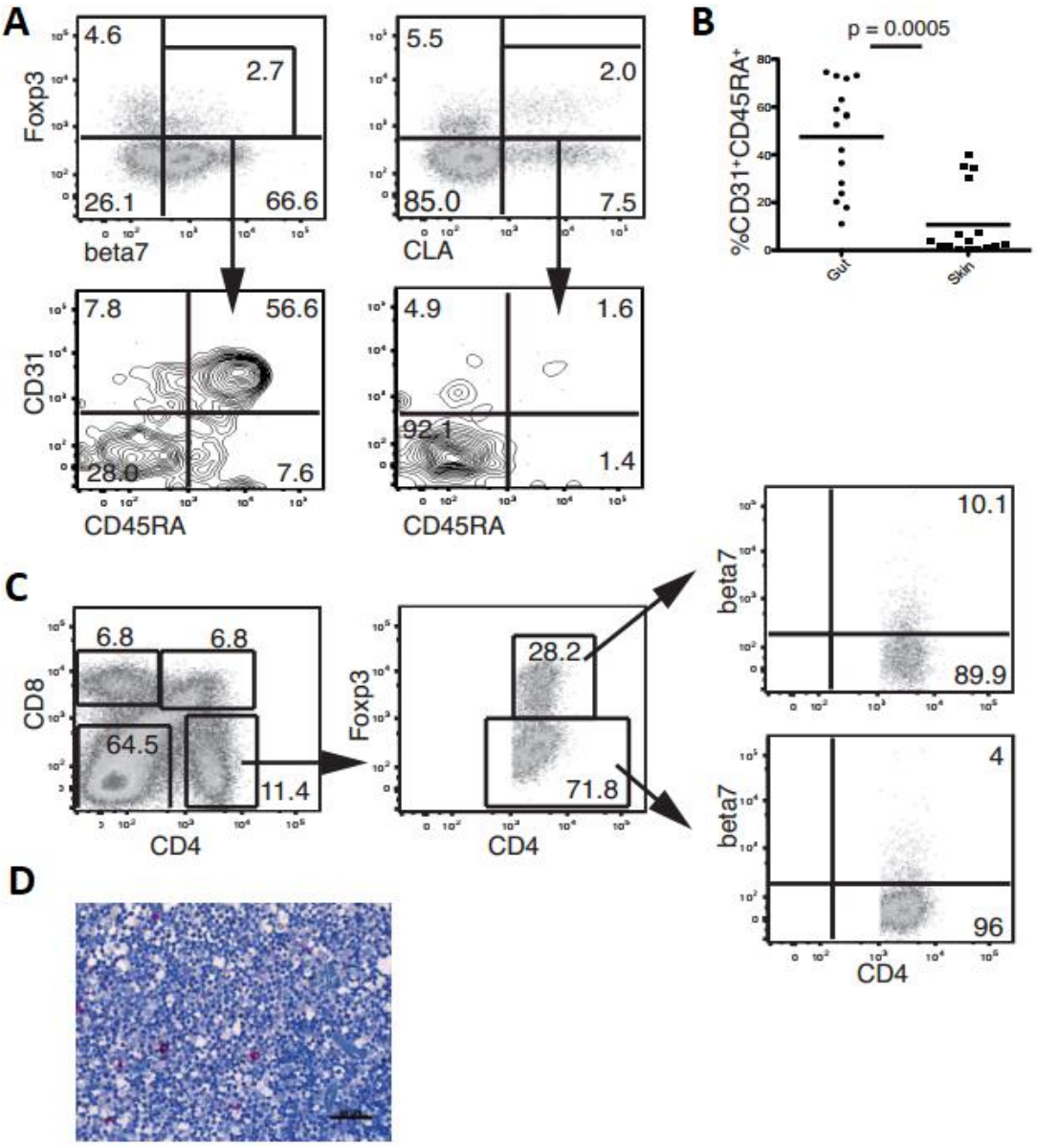

Figure 3.9 Phenotype of gut and skin homing Treg cells.

(A) Representative plot showing the percentage of $CD45RA^{+}CD31^{+}$ cells within gut and skin homing Treg cells in a healthy child. **(B)** Comparison of $CD45RA^{+}CD31^{+}$ cell percentage within gut and skin homing Treg cells. **(C)** Representative flow plot showing β7 expression of $CD4^{+}Foxp3^{+}$ and $CD4^{+}Foxp3^{-}$ cells gated from live CD3+ thymocytes (data representative of two samples). **(D)** Immunohistochemistry showing β7 integrin (pink) and Foxp3 (brown) staining in the human fetal thymus. (Figure adapted from (2).)

3.4 Discussion

Many factors may potentially affect the fetal immune development *in utero*. Previously we showed that IL-10 may be involved in the fetal-maternal alignment of Treg cells (209). In addition to the anti-inflammatory cytokine IL-10, various other environmental cues, especially microbiota metabolites, SCFAs, also contribute to the transplacental programming of Treg cells (331, 342). Therefore, we aim to test whether maternal microbial composition influences fetal thymus and immune development. In the mouse model, we showed that absence of maternal gut microbiome leads to reduced fetal thymus size, fewer thymic $CD4^+$ T cells and $Foxp3^+$ Treg cells. Supplementation of acetate in maternal drinking water, which is the most abundant SCFA in human serum (279), could rescue all the reduction in thymus size and thymic output. These results are also consistent with the fetal-maternal correlation of serum acetate levels we found in human pregnancy and implies that maternal acetate likely crosses the placenta. Collectively, we conclude that maternally acquired acetate plays important roles in shaping fetal thymic development and output, hence exerting its influences on fetal immunity.

The TCR repertoires in neonates showed no bias toward either maternal or paternal repertoires. TCR overlap was minimal and comparative when overlaying either maternal or paternal datasets of memory and naïve T cells. The most surprising observation of the study was the level of TCR sharing between genetically unrelated neonates. Approximately 1-in-50 clonotypes were shared when analysing the most abundant clonotypes in the memory $CD8^+$ T cell compartment and naïve $CD4^+$ and $CD8^+$ T compartments. Collectively, these results suggest that antigen receptor immunity is not "inherited", but driven by other factors, such as environmental cues.

Given that IL-10 and SCFAs contribute to the transplacental programming of Treg cells, we aim to prove that IL-10 and SCFAs (refer to Chapter 4) could potentiate the generation of human Treg cells. IL-10 exerts its immunosuppressive actions at multiple levels of the immune system, including modulation of APCs and inhibition of innate immunity (343, 344), inhibition of T cell proliferation (345, 346), and maintenance of the function and stability of established Treg cells (347, 348). The results presented here extend the role of IL-10 and demonstrate that in addition to TGF-β, IL-10 augments iTreg cell differentiation and function. One of the unresolved issues arising from our study is whether IL-10 signalling in naïve $CD4^+$ T cells is important for pTreg cell differentiation *in vivo*. Nevertheless, our current results prove that in humans, in addition to TGF-β, IL-10 could promote Treg cell generation, which explains the mechanisms of transplacental programming of Treg cells via IL-10 *in utero*, where immune tolerance is dominant.

Tissue homing of T cells is an important aspect of immune function and regulation (349). The results of this chapter suggest that human naïve Treg and Tconv cells may be primed in early life for gut tropism, which reinforces the important role of early gut microbial colonization in shaping the developing immune system. Interestingly, β7 integrin was expressed largely by naïve rTreg cells and the proportion of $\beta7^+$ Treg cells inversely correlated with age, suggesting that Treg cells acquired gut tropism early in life. Consistent with this, notable but variable proportion of peripheral blood $\beta7^+$ Treg cells were $CD31^+$ recent thymic emigrants (RTE), which is consistent with animal data where murine thymocytes acquired gut homing molecules at the RTE stage, although this study did not examine Treg cells specifically (350). Furthermore, only a small proportion of human $CD4^+Foxp3^+$ thymocytes expressed β7 integrin. A previous study suggested that murine RTEs undergo further progressive development in secondary lymphoid organs to

become “mature” naïve T cells (351). Following on from this, it seems likely that human naïve Treg cells also likely acquire their gut homing molecules outside the thymus, where they encounter environmental cues, such as SCFAs.

In summary, our results provide another evidence of Treg cell transplacental programming *in utero* and postnatally. Moreover, we also explain in detail how the environmental factors (IL-10 and acetate) contribute to this progress.

Chapter 4 – Short Chain Fatty Acids Augment the Differentiation and Function of Human Induced Regulatory T Cells via Histone Deacetylation Inhibition

4.1 Introduction

As discussed in the previous chapter, it is known that in addition to IL-10, SCFAs also play an essential role in the transplacental programming of Treg cells. In the animal models, it has already been proven that SCFAs contribute greatly to the pTreg induction *in vivo*, as well as iTreg induction *in vitro* (276-278, 331). SCFAs regulate the differentiation between effector and regulatory T cell lineage commitment by increasing the cellular ATP levels, thus activating the mTOR pathway (318). However, the major mechanism proposed for the regulatory effect of SCFAs on T cells is HDAC inhibition. SCFAs, especially butyrate, promote the generation of Treg cells by enhancing histone H3 acetylation at both promoter and CNS3 regions of the *Foxp3* gene locus and the Foxp3 protein via HDAC inhibition (276, 278). With their significant role in Treg cell generation, SCFAs have an integral contribution to immune tolerance and the protection against various diseases, including asthma (229-231), allergies (110, 230), inflammatory bowel disease (334-336), and Type 1 diabetes (352).

Despite their profound effects on the Treg cells in mice, there is very limited evidence of the effects of SCFAs in humans, both *in vivo* or *in vitro*. To date, there has been only one publication on the generation of human Treg cells *in vitro* via SCFAs (acetate was not tested). Unfortunately, mouse findings were not reproducible in humans (353). Butyrate, but not propionate, did enhance the Foxp3 expression when cultured together with TGF-β and IL-2. However, iTregs treated with butyrate had nearly no TSDR demethylation and showed no *in vitro* suppressive capacity. The addition of butyrate also increased the production of pro-inflammatory cytokine INF-γ.

In addition, there is still no agreement regarding the markers for human iTreg cells. Foxp3 is a surrogate transcriptional marker for tTregs. However, growing evidence suggests that in humans, some $CD4^+$ and $CD8^+$ T cells can transiently up-regulate Foxp3 expression upon *in vitro* stimulation without acquiring Treg cell suppressive activities (60, 61). In addition, there is also a $CD4^+Foxp3^+$ subpopulation in human peripheral blood with no suppressive activity, which even produces pro-inflammatory IL-17 upon activation (354). Thus, the Foxp3 expression is normal following T cell activation, thus not a specific marker for human iTregs *in vitro*. Apart from Foxp3, various markers have been proposed to define human iTreg cells, including CTLA-4, CD127, HLA-DR, PD-1, PD-L1, CD39, GITR and ICOS (Refer to Section 1.2.1.6 for more details).

Therefore, the aims of this chapter are to: a) compare the induction patterns of CBMCs and adult PBMCs; b) explore the precise role of SCFAs (including sodium acetate, butyrate and propionate) in human Treg cell induction, c) investigate the mechanism of SCFAs-mediated Treg induction, and d) identify the potential phenotypic marker for human iTregs.

4.2 Subjects

To determine the effect of SCFAs on Treg cell differentiation from naïve non-Treg cells, in addition to as adult PBMCs, CBMCs were also used in the study, since they are the perfect model for *in utero* transplacental programming. Immune cells from cord blood have a much more pronounced “naive” compartment, which have not been exposed to large amounts of antigens from outer environments, except for intrauterine stimuli.

In total 16 healthy adult volunteers and 12 healthy term pregnant women were recruited after informed consent was obtained. Cord blood samples were collected immediately after elective caesarean section from the umbilical vein. Individuals with any history of autoimmune diseases or allergies were excluded.

4.3 Results

4.3.1 Differential Induction Patterns in the Generation of Human Tregs *in vitro* via SCFAs

In order to compare the iTreg cell induction patterns of CBMCs and adult PBMCs, FACS sorted naïve non-Treg cells ($CD4^+CD45RO^-CD25^-CD127^{hi}$) from both CBMCs and adult PBMCs were stimulated with anti-CD3/anti-CD28 in the presence of IL-2 and TGF-β, with or without SCFAs for 5 days (Section 2.2.3.1).

Induction patterns differed between CBMCs and adult PBMCs in terms of their activation status. Naïve non-Tregs from adult PBMCs were unable to fully differentiate into Treg cells (Figure 4.1A, B). Gated on viable cells, there was a significant population of cells with smaller size and lack of the CD25 expression (Figure 4.1A), representing non-activated cells. Activated cells, as opposed to non-activated cells, were much bigger in size and expressed a high level of CD25. The percentage of activated cells varied significantly across the study population and under different culture conditions (Figure 4.1B). In particular, iTregs treated with butyrate had the smallest proportion of activated cells, roughly half of the proportion of other types of iTregs. In contrast, nearly all the naïve non-Tregs from CBMCs differentiated into Treg cells (Figure 4.1C).

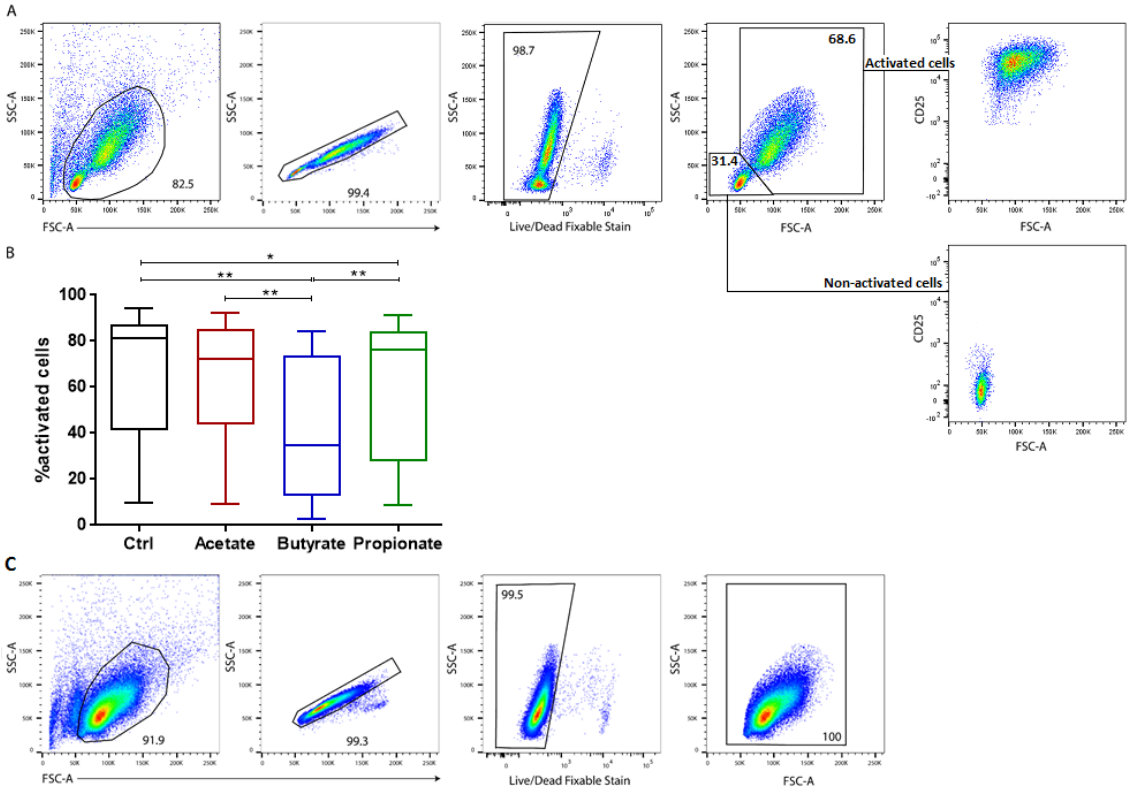

Figure 4.1 Differential induction patterns in the generation of human Tregs *in vitro* via SCFAs.

(**A**) Flow cytometric gating strategy for activated cells gated on viable cells after Treg induction from adult naive $CD4^+$ cells. (**B**) Summary box and whisker graph showing Mean and SEM of the percentage of activated cells after induction from adult naive $CD4^+$ cells under various conditions as indicated (13 independent experiments). (**C**) Flow cytometric gating strategy for activated cells gated on viable cells after Treg induction from CB naive $CD4^+$ cells. *$p < 0.05$, **$p < 0.01$.

4.3.2 Butyrate and Propionate, but not Acetate, Potentiate the Expression of Phenotypic Markers of Human TGF-β–induced Tregs *in vitro*

To determine the precise role of SCFAs (including sodium acetate, butyrate and propionate) in human Treg cell induction, FACS sorted naïve non-Treg cells ($CD4^+CD45RO^-CD25^-CD127^{hi}$) were stimulated with anti-CD3/anti-CD28 in the presence of IL-2 and TGF-β, with or without SCFAs for 5 days (Section 2.2.3.1).

There were obvious differences between non-activated cells and activated cells generated from adult PBMCs in terms of the expression levels of various phenotypic markers, an example shown in flow cytometric gating strategy (Figure 4.2). The expressions of all the phenotypic markers tested were significantly different between non-activated and activated cells under various culture conditions (Figure 4.3), except for PD-L1 and CD127 expressions in control and acetate treated iTregs. Activated cells had a much higher expression of Foxp3, HLA-DR, CD39, GITR, ICOS, PD-1 and CTLA-4; whereas CD127 was the only marker being down-regulated after activation. The flow cytometric gating strategy for iTregs generated from CBMCs (Figure 4.4) showed a similar pattern as activated iTreg cells from adult PBMCs.

Due to the significantly higher percentage of non-activated cells, butyrate-treated iTregs from adult PBMCs had the least Foxp3 expression and highest CD127 expression compared to other iTregs. The expression levels of Foxp3 and CD127 were similar among groups when analysing only the activated cells (Figure 4.5B and Figure 4.6B), as well as iTregs cells generated from CBMCs (Figure 4.5C and Figure 4.6C), except that butyrate-treated iTregs from CBMCs had higher CD127 expression.

As for CD39 (Figure 4.7), GITR (Figure 4.8), ICOS (Figure 4.9), and PD-L1 expressions (Figure 4.10), the trend was the same for both activated iTregs from adult PBMCs and iTregs from CBMCs. Butyrate-treated iTregs had the highest expression for these four markers, followed by propionate-treated iTregs, though not always at statistically significant levels. The expression levels of these markers of iTregs treated with acetate were either the same or slightly higher compared to control.

Butyrate/Propionate-treated iTregs generated from CBMCs had higher expression of PD-1 than acetate-treated or control iTreg (Figure 4.11C). However, this trend was not seen in iTregs from adult PBMCs (Figure 4.11B). There were no significant differences in the expressions of CTLA-4 (Figure 4.12) and HLA-DR (Figure 4.13) across all groups.

These results suggested that a) Foxp3 is an activation marker for human iTregs; b) GITR, ICOS, CD39, PD-1 and PD-L1 are potential candidate markers for human iTregs; c) Butyrate and propionate, but not acetate, potentiate the expression of phenotypic markers of human TGF-β induced Treg cells *in vitro*.

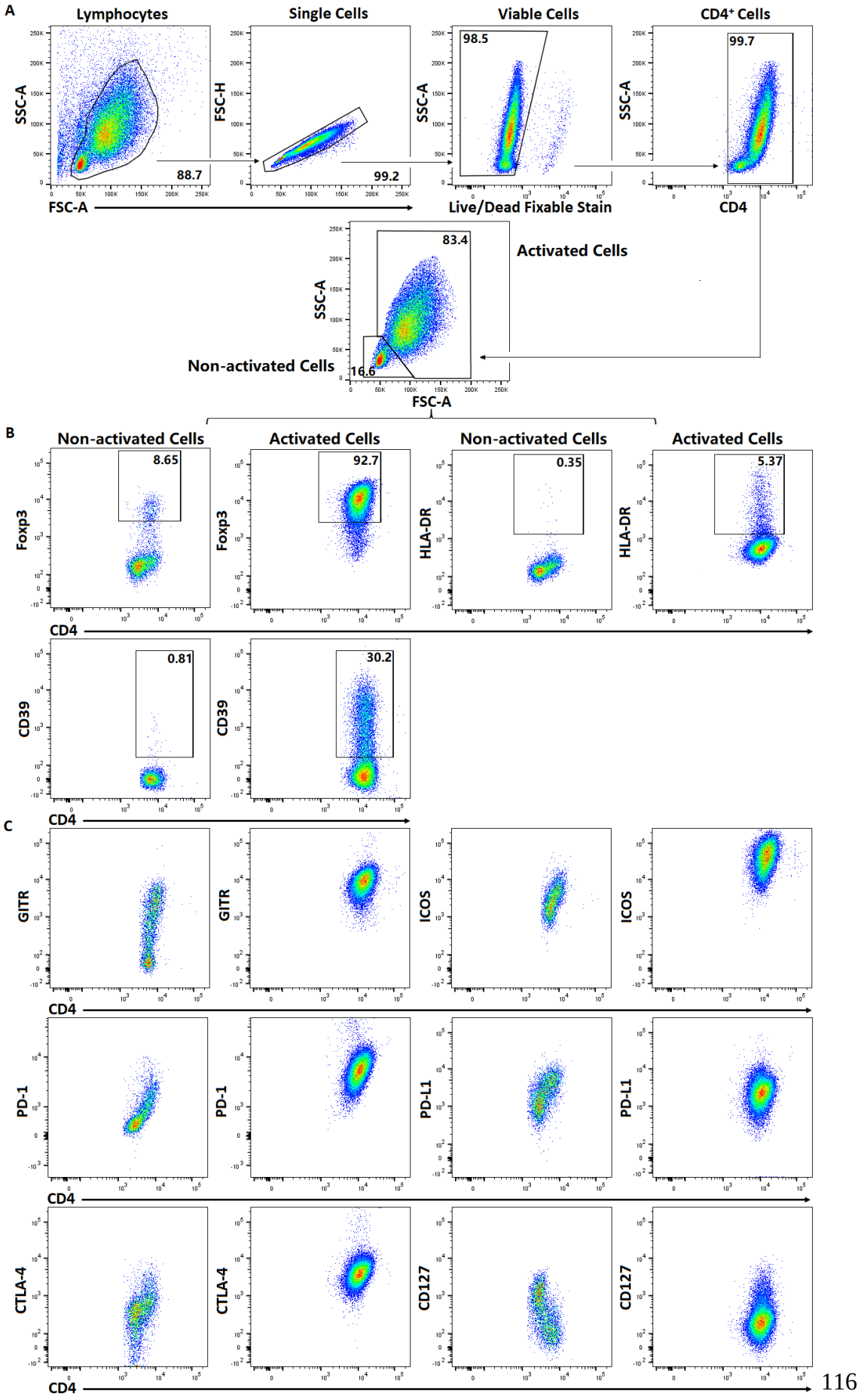
A
Lymphocytes
Single Cells
Viable Cells
CD4⁺ Cells
SSC-A
FSC-A
FSC-H
SSC-A
Live/Dead Fixable Stain
SSC-A
CD4
88.7
99.2
98.5
99.7
Activated Cells
Non-activated Cells
83.4
16.6
FSC-A
B
Non-activated Cells
Activated Cells
Non-activated Cells
Activated Cells
Foxp3
Foxp3
HLA-DR
HLA-DR
CD4
8.65
92.7
0.35
5.37
CD39
CD39
CD4
0.81
30.2
C
GITR
GITR
ICOS
ICOS
CD4
PD-1
PD-1
PD-L1
PD-L1
CD4
CTLA-4
CTLA-4
CD127
CD127
CD4

Figure 4.2 Flow cytometric gating strategy for the phenotypic markers of iTreg generated from adult naive CD4$^+$ cells.

(A) Flow cytometric gating strategy for lymphocytes, single cells, viable cells, CD4$^+$ cells, non-activated and activated iTregs generated from adult naive CD4$^+$ cells. **(B)** The representative dot plots showing the percentage of Foxp3, HLA-DR, and CD39 gated on either non-activated (left panels) or activated (right panels) iTreg cells. **(C)** The representative dot plots showing GITR, ICOS, PD-1, PD-L1, CTLA-4 and CD127 expression patterns on either non-activated (left panels) or activated (right panels) iTreg cells.

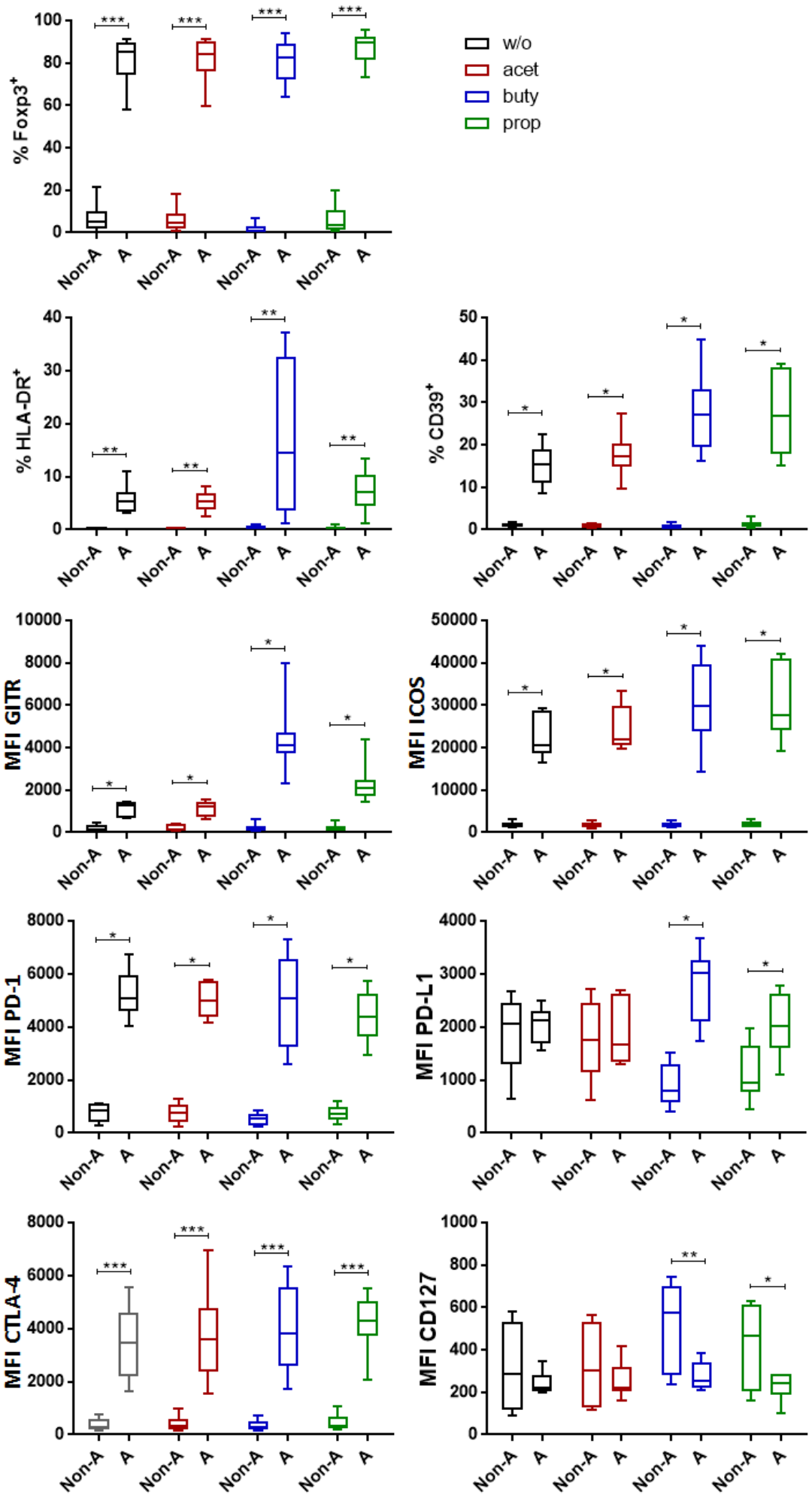
w/o
acet
buty
prop
% Foxp3+
% HLA-DR+
% CD39+
MFI GITR
MFI ICOS
MFI PD-1
MFI PD-L1
MFI CTLA-4
MFI CD127
Non-A
A

Figure 4.3 Enhanced expression of phenotypic markers in activated cells generated from adult naive CD4$^+$ cells.

Summary box and whisker graphs showing %Foxp3$^+$, %HLA-DR+, %CD39$^+$, and MFI of GITR, ICOS, PD-1, PD-L1, CTLA-4 and CD127 gated on non-activated cells (Non-A) and activated cells (A) generated from adult naive CD4$^+$ cells under various conditions. All cells were cultured in the presence of IL-2, TGF-β and additional with: control (black), acetate (red), butyrate (blue), and propionate (green). Data are from 13 independent experiments. *$p < 0.05$, **$p < 0.01$, ***$p < 0.001$.

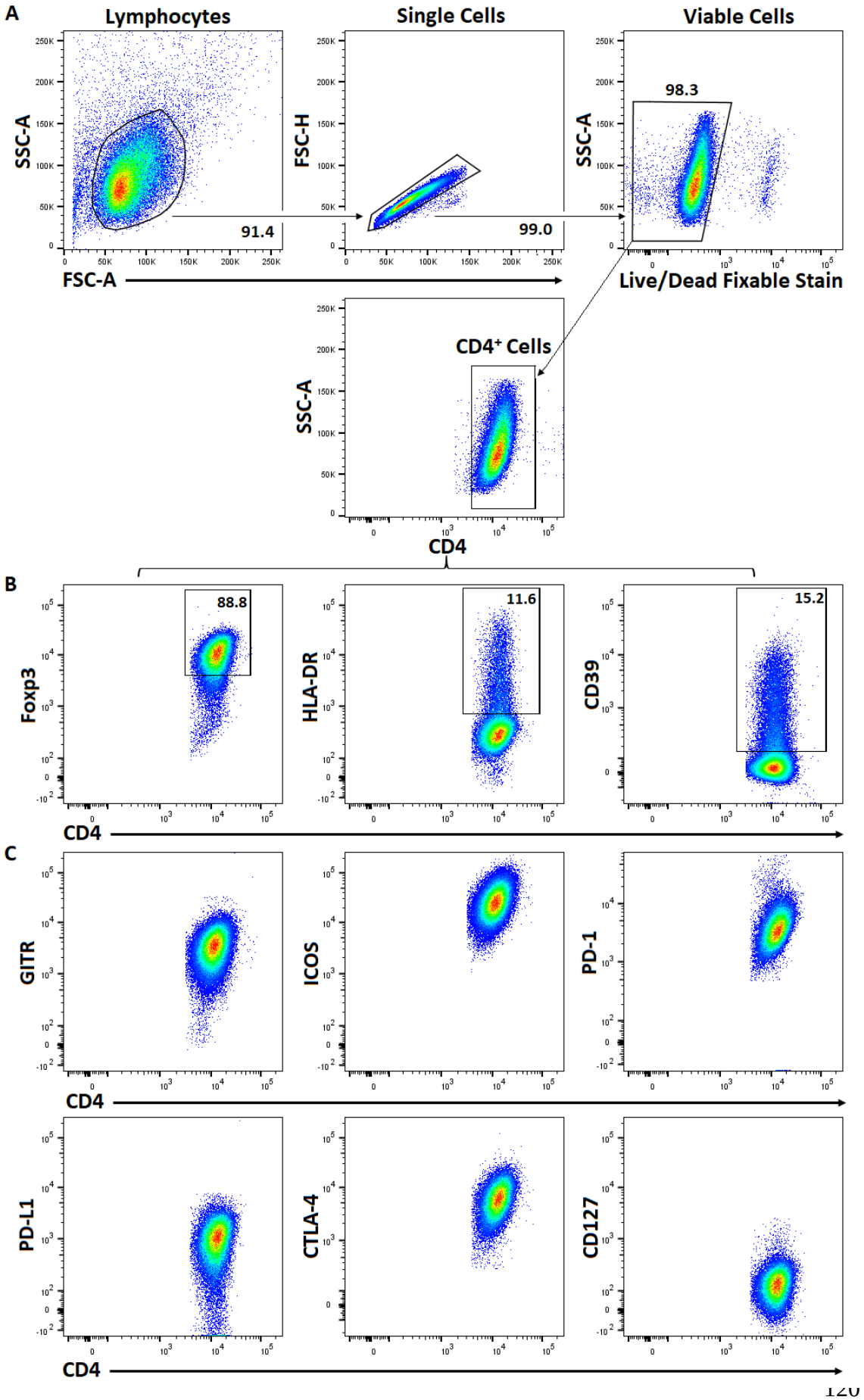
A
Lymphocytes
Single Cells
Viable Cells
SSC-A
FSC-A
FSC-H
SSC-A
Live/Dead Fixable Stain
91.4
99.0
98.3
CD4⁺ Cells
SSC-A
CD4
B
Foxp3
HLA-DR
CD39
88.8
11.6
15.2
CD4
C
GITR
ICOS
PD-1
CD4
PD-L1
CTLA-4
CD127
CD4

Figure 4.4 Flow cytometric gating strategy for various phenotypic markers of iTreg generated from Cord Blood.

(A) Flow cytometric gating strategy for lymphocytes, single cells, viable cells, and $CD4^+$ iTregs. **(B)** The representative dot plots showing the percentage of Foxp3, HLA-DR, and CD39 gated on iTreg cells generated from CB naive $CD4^+$ cells. **(C)** The representative dot plots showing GITR, ICOS, PD-1, PD-L1, CTLA-4 and CD127 expression patterns.

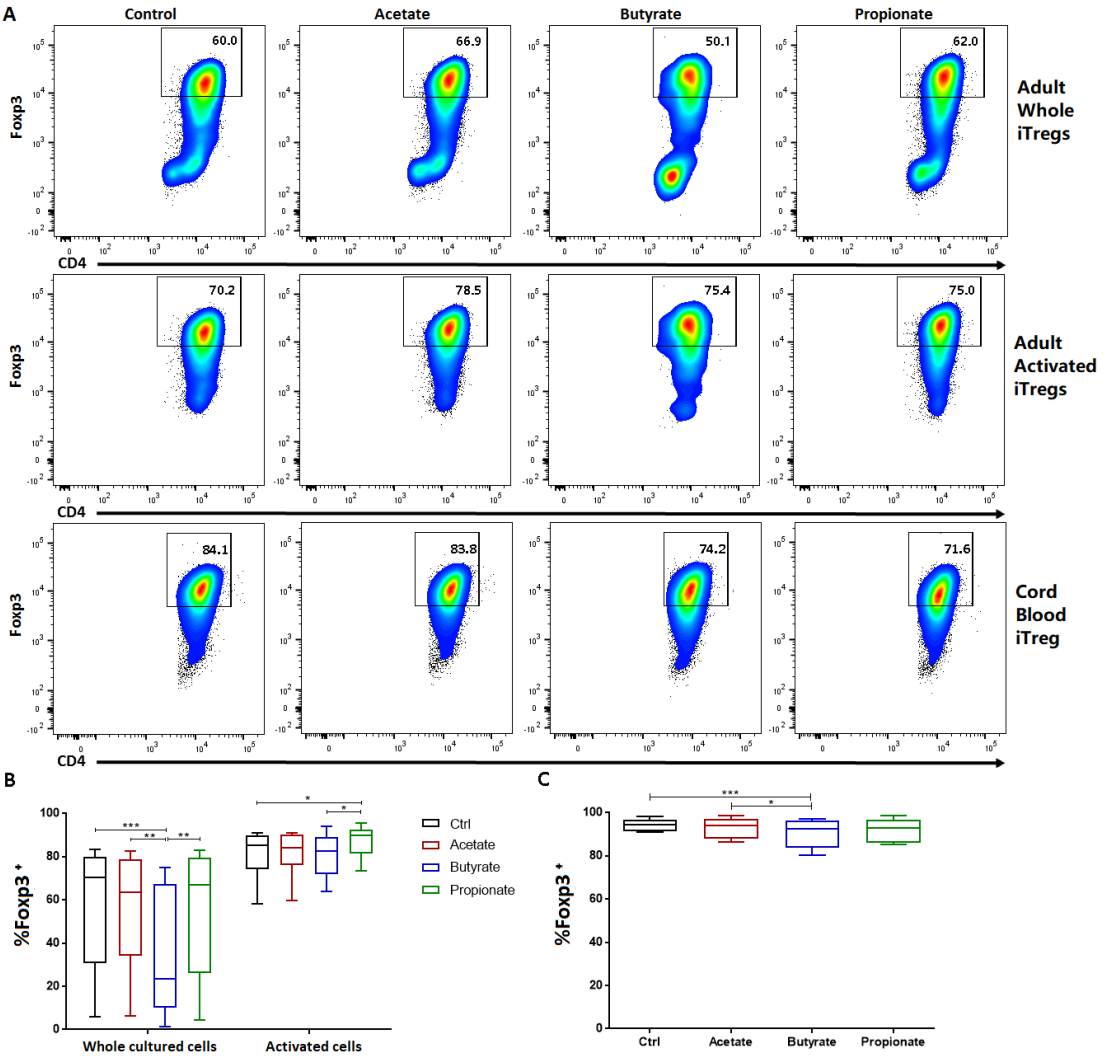

Figure 4.5 The effect of SCFAs on the Foxp3 expression of human iTregs.

(**A**) Representative dot plots showing percentage of Foxp3$^+$ cells gated on adult whole iTregs (top panel), adult activated iTregs (middle panel) and CB iTregs (bottom panel) generated under various conditions. All cells were cultured in the presence of IL-2, TGF-β and additional with: control (black), acetate (red), butyrate (blue), and propionate (green). (**B**) Summary box and whisker graphs showing %Foxp3$^+$ gated on whole iTregs (left panel) and only activated cells (right panel) from adult naive CD4$^+$ cells (n=13). (**C**) Summary box and whisker graphs showing %Foxp3$^+$ of iTregs from CB naive CD4$^+$ cells (n=12). *$p < 0.05$, **$p < 0.01$, ***$p < 0.001$.

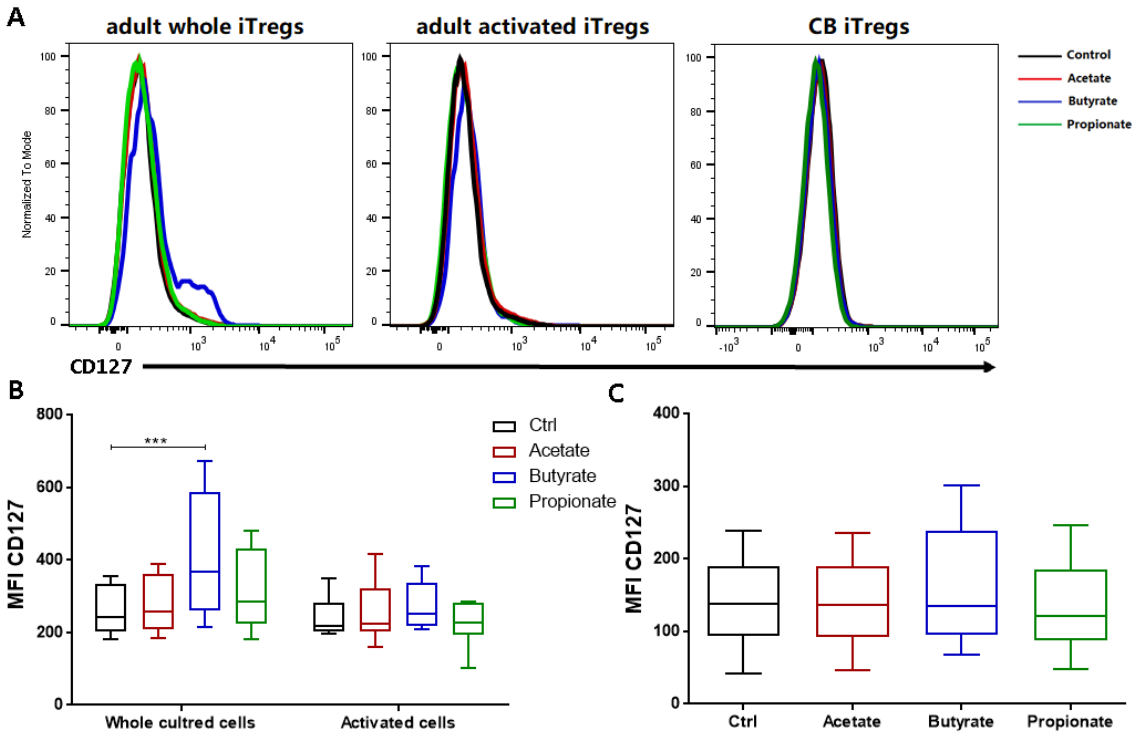

Figure 4.6 The effect of SCFAs on the CD127 expression of human iTregs.

(**A**) Representative histogram showing MFI CD127 of adult whole iTregs (left panel), adult activated iTregs (middle panel) and CB iTregs (right panel) generated under various conditions. All cells were cultured in the presence of IL-2, TGF-β and additional with: control (black), acetate (red), butyrate (blue), and propionate (green). (**B**) Summary box and whisker graphs showing MFI CD127 of whole iTregs (left panel) and only activated cells (right panel) from adult naive $CD4^+$ cells (n=9). (**C**) Summary box and whisker graphs showing MFI CD127 of iTregs from CB naive $CD4^+$ cells (n=10). ***$p < 0.001$.

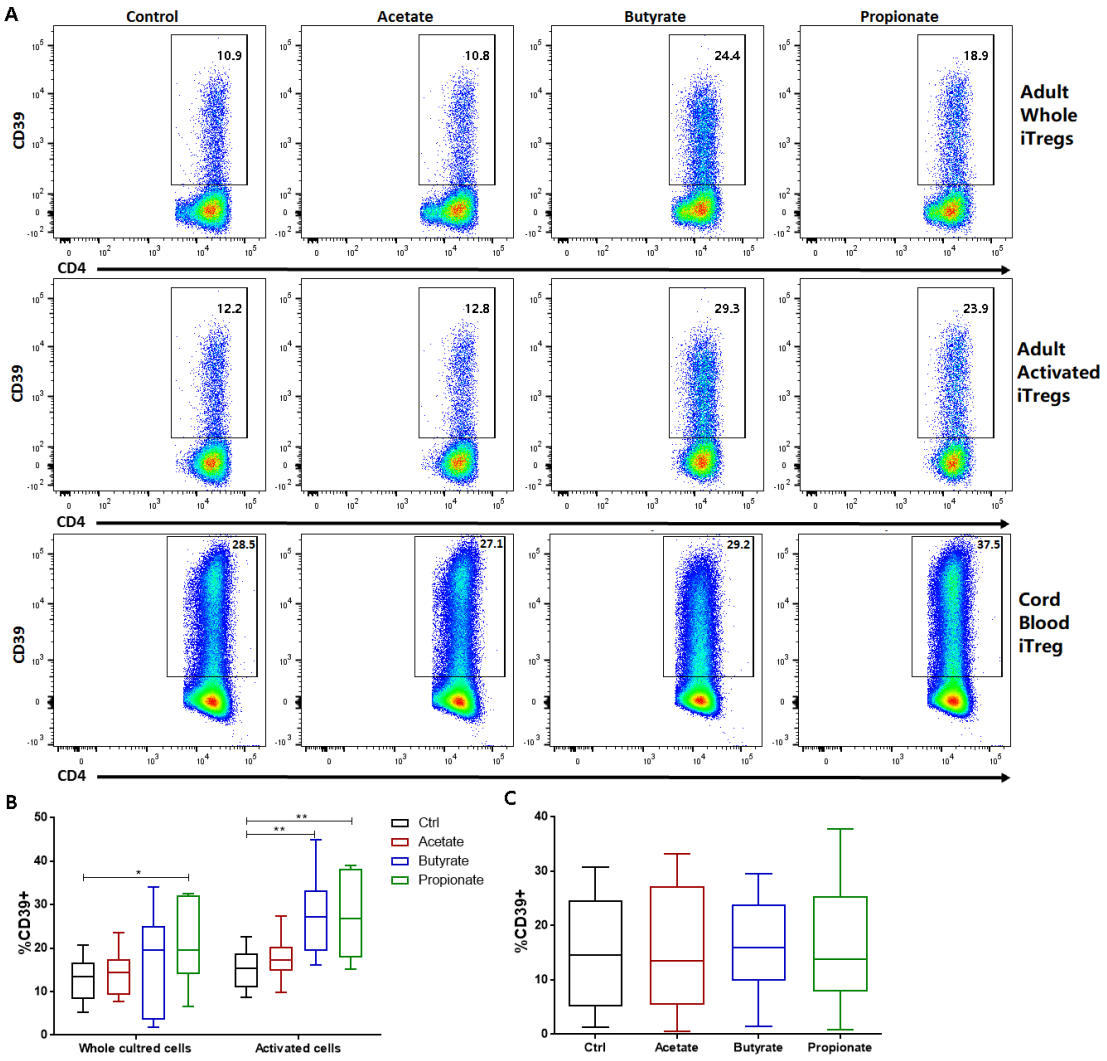

Figure 4.7 The effect of SCFAs on the CD39 expression of human iTregs.

(**A**) Representative histogram showing the percentage of $CD39^+$ cells gated on adult whole iTregs (top panel), adult activated iTregs (middle panel) and CB iTregs (bottom panel) generated under various conditions. All cells were cultured in the presence of IL-2, TGF-β and additional with: control (black), acetate (red), butyrate (blue), and propionate (green). (**B**) Summary box and whisker graphs showing $\%CD39^+$ gated on whole iTregs (left panel) and only activated cells (right panel) from adult naive $CD4^+$ cells (n=7). (**C**) Summary box and whisker graphs showing $\%CD39^+$ of iTregs from CB naive $CD4^+$ cells (n=10). $*p < 0.05$, $**p < 0.01$.

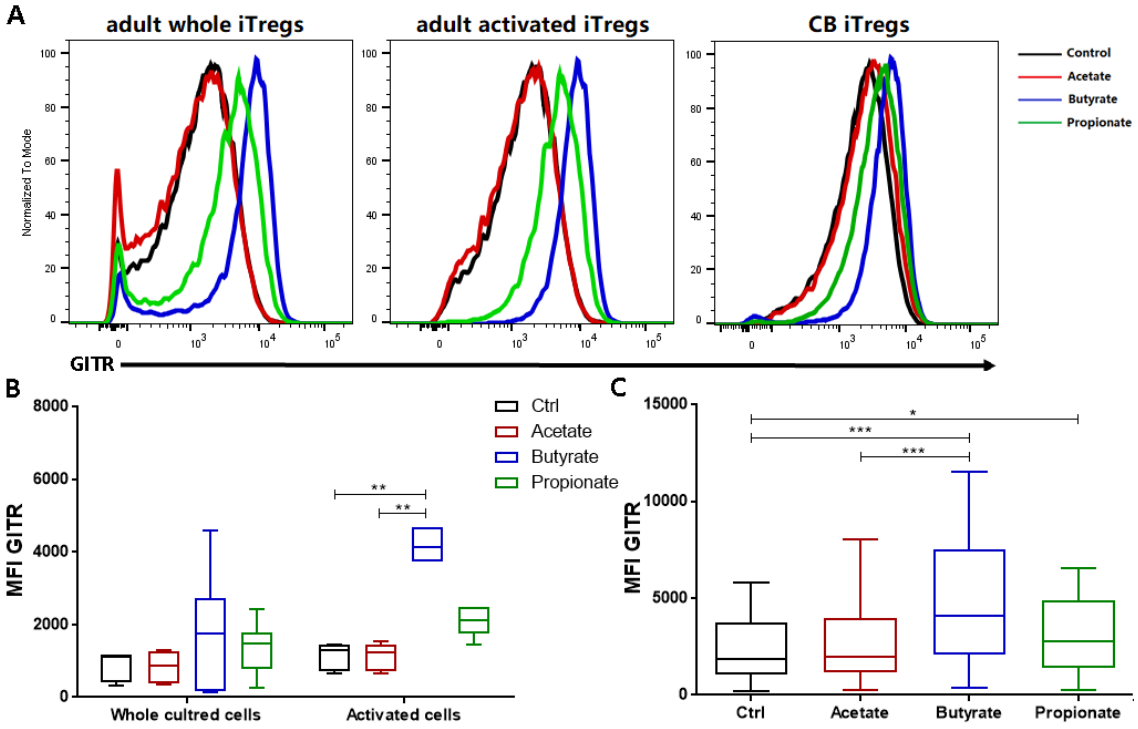

Figure 4.8 The effect of SCFAs on the GITR expression of human iTregs.

(**A**) Representative histogram showing MFI GITR of adult whole iTregs (left panel), adult activated iTregs (middle panel) and CB iTregs (right panel) generated under various conditions. All cells were cultured in the presence of IL-2, TGF-β and additional with: control (black), acetate (red), butyrate (blue), and propionate (green). (**B**) Summary box and whisker graphs showing MFI GITR of whole iTregs (left panel) and only activated cells (right panel) from adult naive $CD4^+$ cells (n=7). (**C**) Summary box and whisker graphs showing MFI GITR of iTregs from CB naive $CD4^+$ cells (n=10). $*p < 0.05$, $**p < 0.01$, $***p < 0.001$.

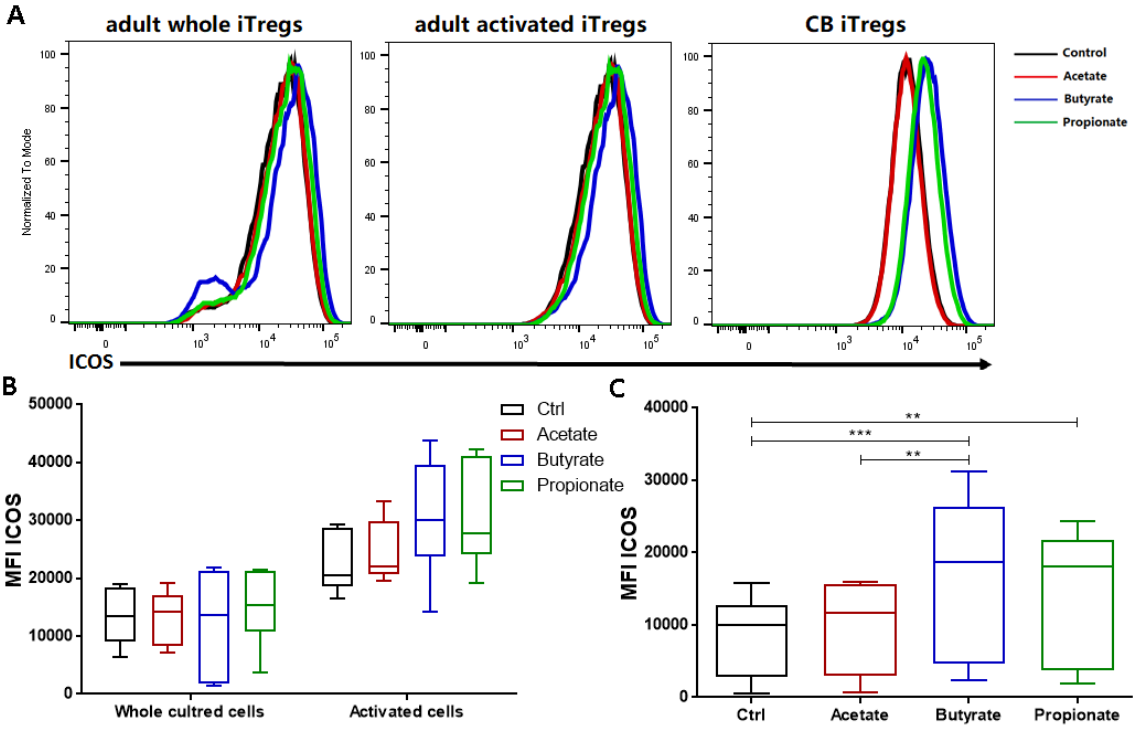

Figure 4.9 The effect of SCFAs on the ICOS expression of human iTregs.

(**A**) Representative histogram showing MFI ICOS of adult whole iTregs (left panel), adult activated iTregs (middle panel) and CB iTregs (right panel) generated under various conditions. All cells were cultured in the presence of IL-2, TGF-β and additional with: control (black), acetate (red), butyrate (blue), and propionate (green). (**B**) Summary box and whisker graphs showing MFI ICOS of whole iTregs (left panel) and only activated cells (right panel) from adult naive $CD4^+$ cells (n=6). (**C**) Summary box and whisker graphs showing MFI ICOS of iTregs from CB naive $CD4^+$ cells (n=10). $^{**}p < 0.01$, $^{***}p < 0.001$.

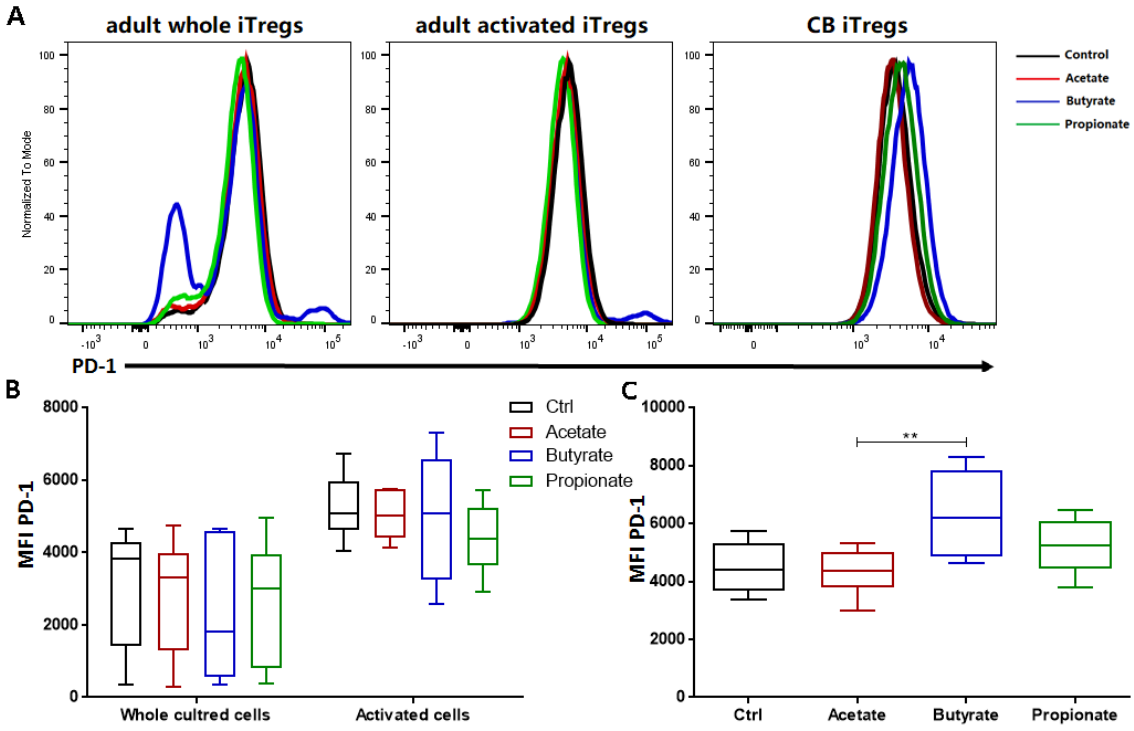

Figure 4.10 The effect of SCFAs on the PD-1 expression of human iTregs.

(**A**) Representative histogram showing MFI PD-1 of adult whole iTregs (left panel), adult activated iTregs (middle panel) and CB iTregs (right panel) generated under various conditions. All cells were cultured in the presence of IL-2, TGF-β and additional with: control (black), acetate (red), butyrate (blue), and propionate (green). (**B**) Summary box and whisker graphs showing MFI PD-1 of whole iTregs (left panel) and only activated cells (right panel) from adult naive $CD4^+$ cells (n=6). (**C**) Summary box and whisker graphs showing MFI PD-1 of iTregs from CB naive $CD4^+$ cells (n=6). $^{**}p < 0.01$.

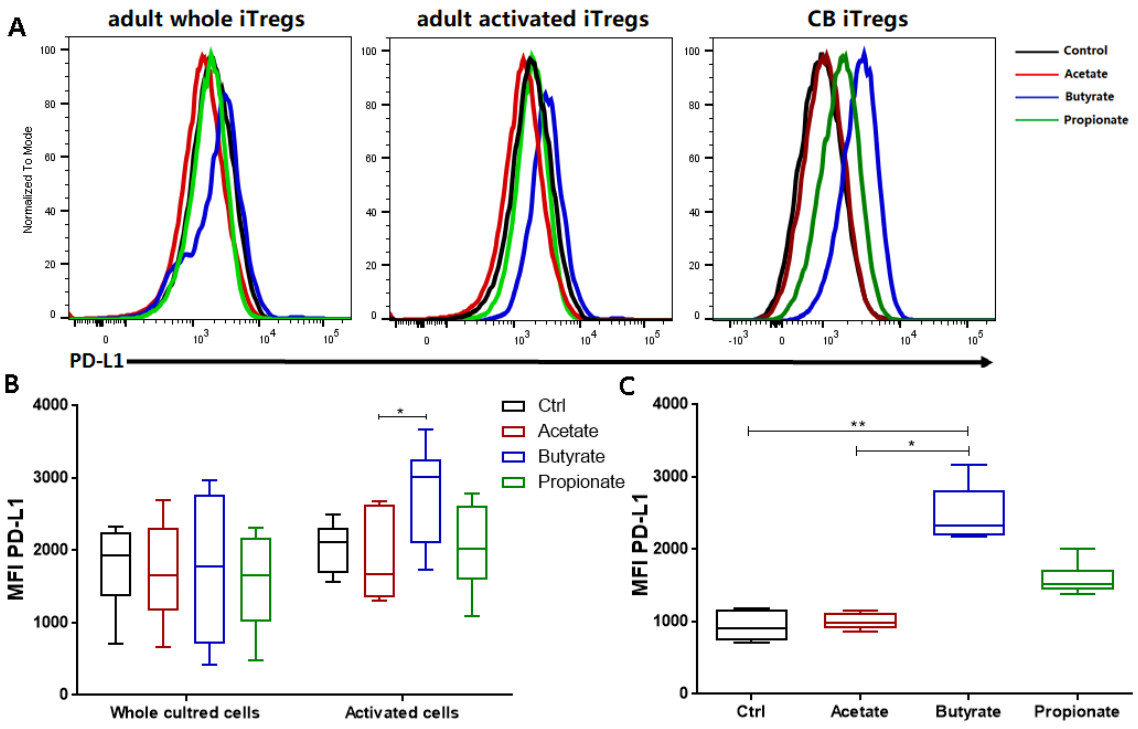

Figure 4.11 The effect of SCFAs on the PD-L1 expression of human iTregs.

(**A**) Representative histogram showing MFI PD-L1 of adult whole iTregs (left panel), adult activated iTregs (middle panel) and CB iTregs (right panel) generated under various conditions. All cells were cultured in the presence of IL-2, TGF-β and additional with: control (black), acetate (red), butyrate (blue), and propionate (green). (**B**) Summary box and whisker graphs showing MFI PD-L1 of whole iTregs (left panel) and only activated cells (right panel) from adult naive $CD4^+$ cells (n=6). (**C**) Summary box and whisker graphs showing MFI PD-L1 of iTregs from CB naive $CD4^+$ cells (n=6). $*p < 0.05$, $**p < 0.01$.

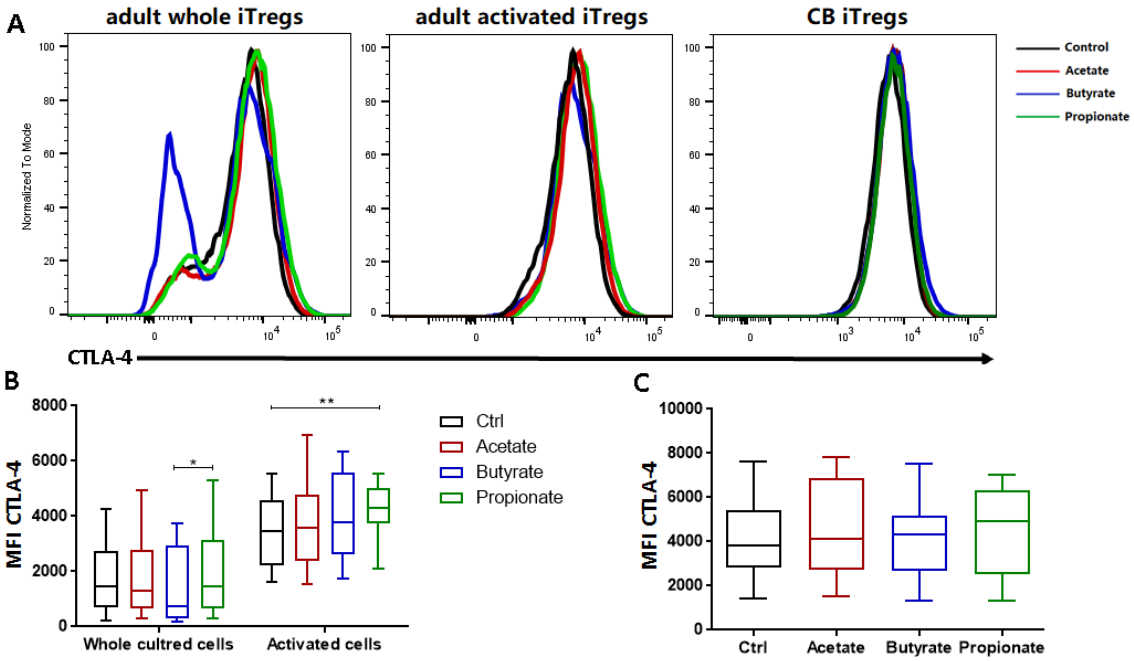

Figure 4.12 The effect of SCFAs on the CTLA-4 expression of human iTregs.

(**A**) Representative histogram showing MFI CTLA-4 of adult whole iTregs (left panel), adult activated iTregs (middle panel) and CB iTregs (right panel) generated under various conditions. All cells were cultured in the presence of IL-2, TGF-β and additional with: control (black), acetate (red), butyrate (blue), and propionate (green). (**B**) Summary box and whisker graphs showing MFI CTLA-4 of whole iTregs (left panel) and only activated cells (right panel) from adult naive $CD4^+$ cells (n=12). (**C**) Summary box and whisker graphs showing MFI CTLA-4 of iTregs from CB naive $CD4^+$ cells (n=12). *$p < 0.05$, **$p < 0.01$.

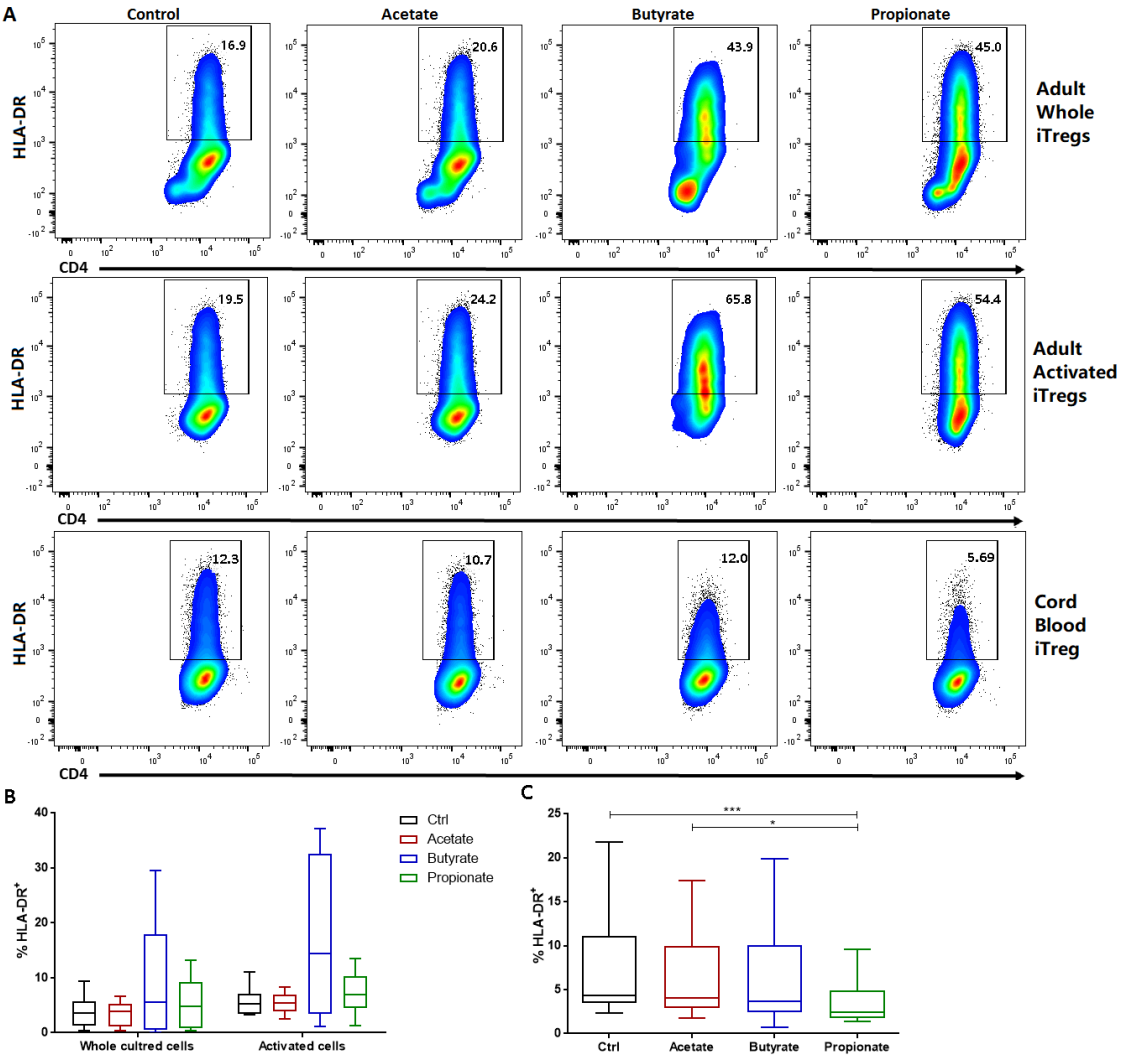

Figure 4.13 The effect of SCFAs on the HLA-DR expression of human iTregs.

(**A**) Representative histogram showing the percentage of HLA-DR$^+$ cells gated on adult whole iTregs (top panel), adult activated iTregs (middle panel) and CB iTregs (bottom panel) generated under various conditions. All cells were cultured in the presence of IL-2, TGF-β and additional with: control (black), acetate (red), butyrate (blue), and propionate (green). (**B**) Summary box and whisker graphs showing %HLA-DR$^+$ gated on whole iTregs (left panel) and only activated cells (right panel) from adult naive CD4$^+$ cells (n=10). (**C**) Summary box and whisker graphs showing %HLA-DR$^+$ of iTregs from CB naive CD4$^+$ cells (n=11). *$p < 0.05$, ***$p < 0.001$.

4.3.3 Butyrate and Propionate, but not Acetate, Enhance the Suppressive Capacity of Human TGF-β–induced Tregs *in vitro*

To test the suppressive capacity of iTreg cells treated with different SCFAs, these iTreg cells were cocultured with autologous CFSE-labelled $CD4^+CD25^-$ responder cells (freshly beads-isolated) under various ratios *in vitro*. Then on day 3, the differences in the proliferation of responder cells were compared (section 2.2.3.2).

Firstly, the suppressive capacity of the whole cultured cells generated from adult naive $CD4^+$ cells was tested. There were no significant differences between SCFAs-treated iTregs and control iTregs (Figure 4.14). Only propionate-treated iTregs showed significantly higher suppressive capacities compared to acetate-treated iTregs at the suppressor: responder cell ratios 1:4, 1:8 and 1:16.

Next, we wanted to test the suppressive capacity of activated iTreg cells generated from adult naive $CD4^+$ cells, considering the significantly different activation status observed in section 4.3.1. Whole cultured cells incubated under various conditions were subjected to CD25 MicroBeads positive selection, to isolate purified $CD25^{high}$ cells (activated cells) for *in vitro* suppression assay. When comparing activated cells and their pair-matched whole cultured cells, the differences in the suppressive capacity were greater in butyrate-treated iTregs, compared to iTregs cultured under other conditions (Figure 4.15). These increases between activated cells and whole cultured cells were significant for butyrate-treated iTregs at the suppressor: responder cell ratios 1:2, 1:8 and 1:16.

In addition, we found that results of the suppression assay for activated iTreg cells were very promising for the first time in human studies. Butyrate-treated iTreg cells reduced the *in vitro* proliferation of autologous $CD4^+CD25^-$ responder cells compared to both

control and acetate-treated iTreg cells (Figure 4.17). This was statistically significant and consistent at all suppressor: responder cell ratios from 1:2 to 1:16. Additionally, propionate-treated iTreg cells also had increased suppressive capacity compared to control iTreg cells, only to a lesser extent and did not reach significance at all cell ratios. On the contrary, the addition of acetate failed to achieve a similar effect.

Finally, we tested the suppressive capacity of iTreg cells generated from CB naive $CD4^+$ cells. The results mimicked the same trend found in activated iTregs generated from adult naive $CD4^+$ cells. The addition of butyrate and propionate increased the suppressive capacity of iTregs at all suppressor: responder cell ratios from 1:1 to 1:16. Significant differences were found at ratios from 1:4 to 1:16 for both butyrate-treated and propionate-treated iTregs. Like the activated iTregs generated from adult naive $CD4^+$ cells, the addition of acetate was unable to increase the suppressive capacity of iTreg cells generated from CB naive $CD4^+$ cells.

These results demonstrate that the addition of butyrate and propionate, but not acetate, augments the suppressive capacity of *in vitro* induced human Treg cells.

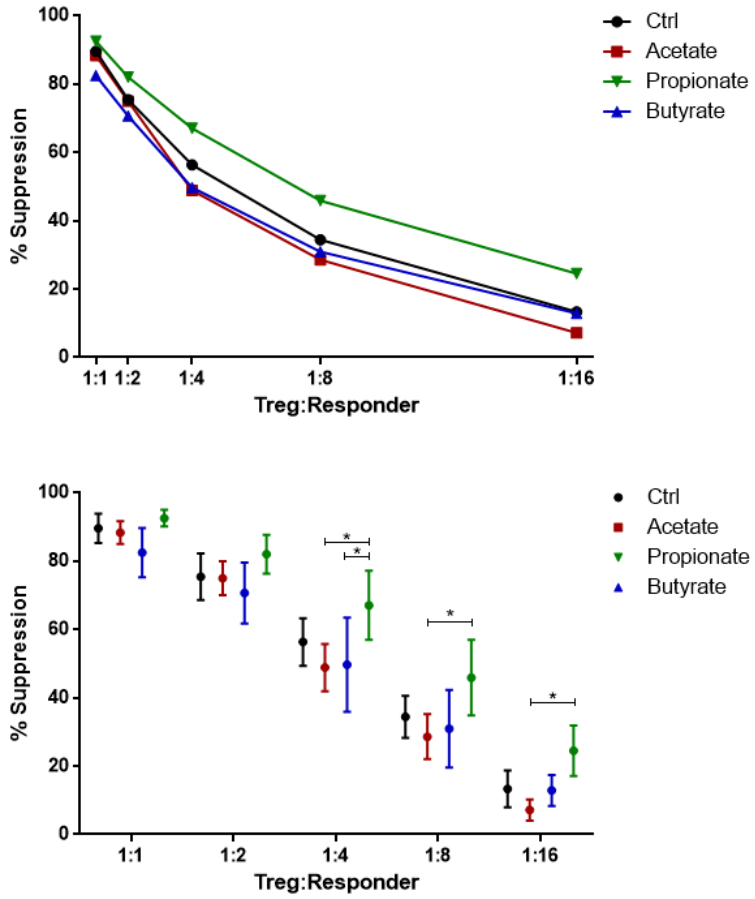

Figure 4.14 The suppressive capacity of iTreg cells generated from adult naive CD4$^+$ cells.

Line graph (upper panel) showing percentages of suppression using whole iTreg cells generated from adult PB naive CD4$^+$ cells under various conditions. All cells were cultured in the presence of IL-2, TGF-β and additional with: control (black), acetate (red), butyrate (blue), and propionate (green). Various suppressor: responder ratios ranging from 1:1 to 1:16 were applied. Summary dot plots (lower panel) showing the statistical analysis of the suppressive capacity of whole iTreg cells as indicated. Percentage of suppression was calculated as (proliferation of T responder alone – the proliferation of co-cultured T responder) / proliferation of T responder alone x 100. Data represent 8 independent experiments in each group. *$p < 0.05$.

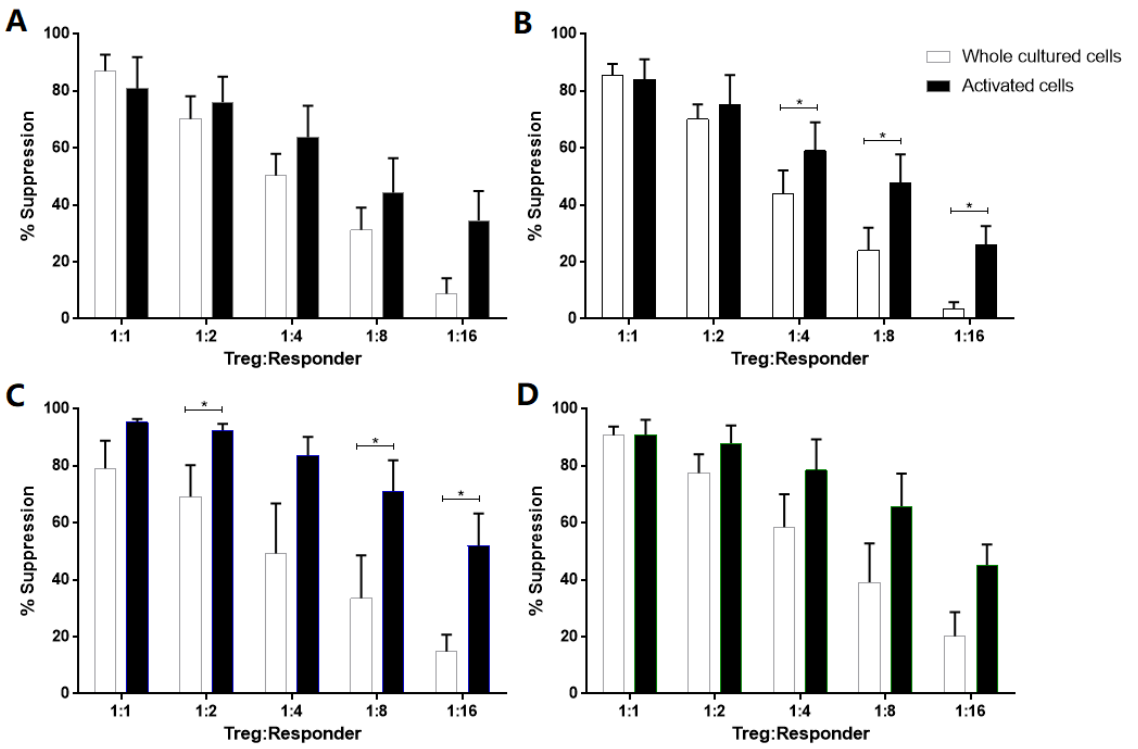

Figure 4.15 Improved suppressive capacity of activated iTregs generated from adult naive CD4$^+$ cells.

Summary bar graphs showing percentages of suppression using whole cultured iTregs (blank) versus activated iTreg cells (black, whole cultured iTregs went through CD25 MicroBeads positive selection) generated from adult naive CD4$^+$ cells under normal conditions. Cells were cultured in the presence of IL-2, TGF-β and additional with: (**A**) control, (**B**) acetate, (**C**) butyrate, and (**D**) propionate. Data represent 6 independent experiments in each group. *$p < 0.05$.

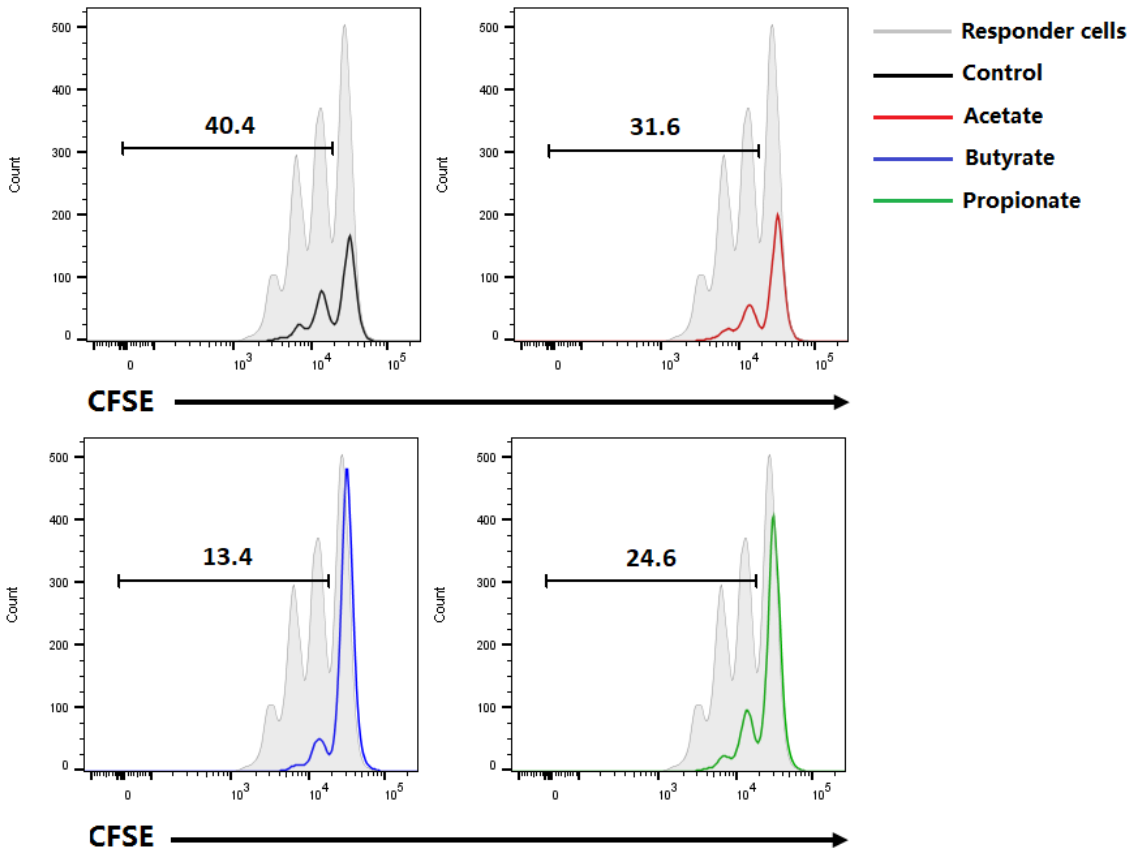

Figure 4.16 The effects of SCFAs-treated iTregs on the proliferation of responder cells.

Representative histograms showing reduced proliferation of CFSE-labelled responder cells by activated iTregs cultured in the presence of IL-2, TGF-β and additional with: acetate (red), butyrate (blue) and propionate (green), compared to iTregs cultured under normal conditions in the absence of SCFAs (Ctrl, black). The proliferation of responder cells alone is shown in the grey background. Data show suppressor: responder ratio of 1:8.

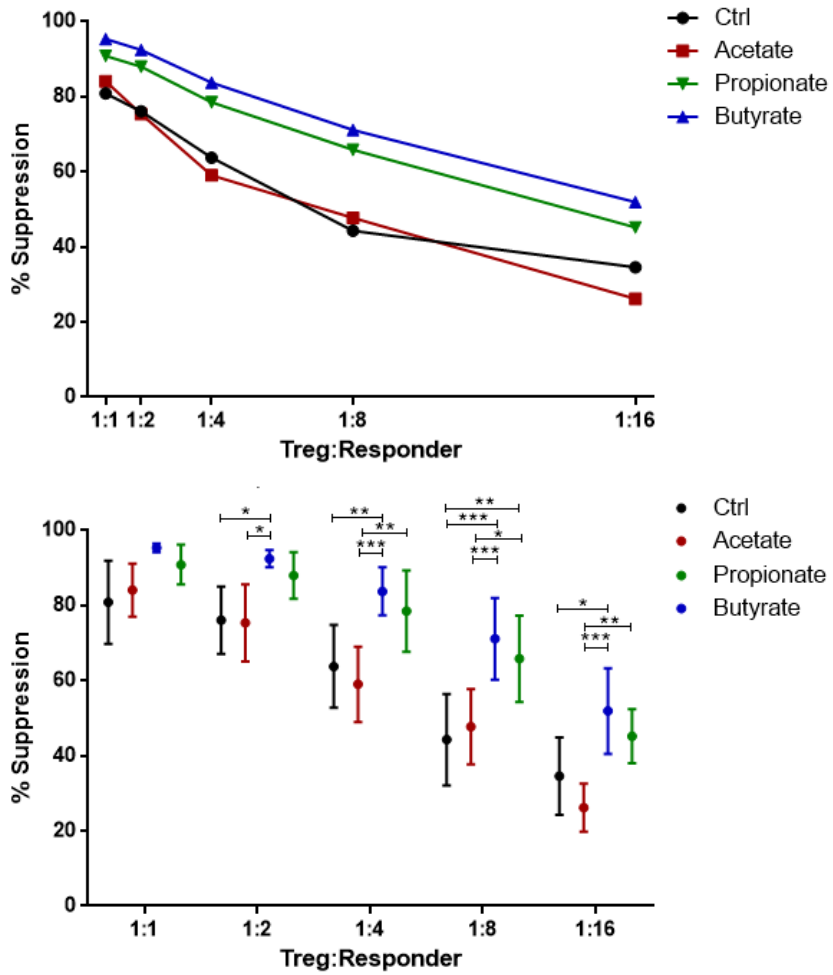

Figure 4.17 Butyrate and propionate enhance the suppressive capacity of activated iTregs generated from Adult naive CD4$^+$ cells.

Line graph (upper panel) showing percentages of suppression using activated iTreg cells (whole cultured iTregs went through CD25 MicroBeads positive selection) generated from adult PB naive CD4$^+$ cells. All cells were cultured in the presence of IL-2, TGF-β and additional with: control (black), acetate (red), butyrate (blue), and propionate (green). Various suppressor: responder ratios ranging from 1:1 to 1:16 were applied. Summary dot plots (lower panel) showing the statistical analysis of the suppressive capacity of activated iTreg cells as indicated. Data represent 6 independent experiments in each group. *$p < 0.05$, **$p < 0.01$, ***$p < 0.001$.

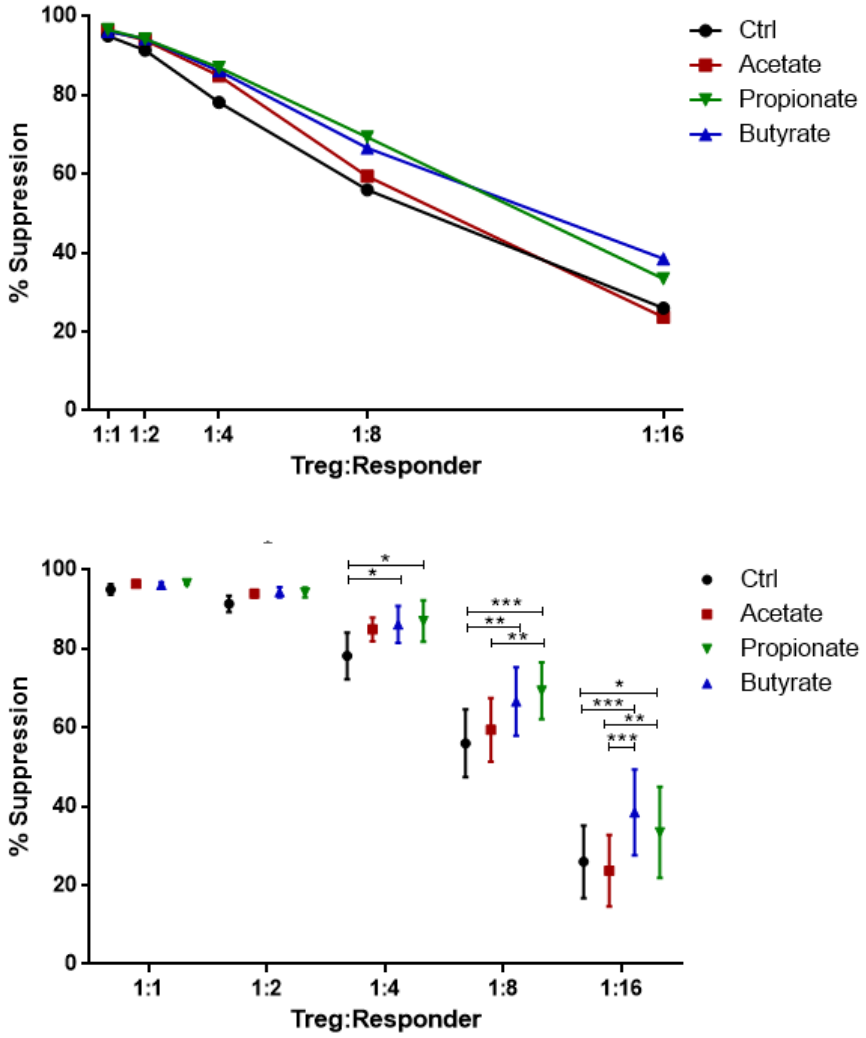

Figure 4.18 Butyrate and propionate enhance the suppressive capacity of iTregs generated from CB naive CD4$^+$ cells.

Line graph (upper panel) showing percentages of suppression using iTreg cells generated from CB naive CD4$^+$ cells under various conditions. All cells were cultured in the presence of IL-2, TGF-β and additional with: control (black), acetate (red), butyrate (blue), and propionate (green). Various suppressor: responder ratios ranging from 1:1 to 1:16 were applied. Summary dot plots (lower panel) showing the statistical analysis of the suppressive capacity of iTreg cells as indicated. Data represent 10 independent experiments in each group. *$p < 0.05$, **$p < 0.01$, ***$p < 0.001$.

4.3.4 Butyrate and Propionate Augment iTreg cell Phenotype and Function through Histone Deacetylation Inhibition

To understand the mechanism of SCFAs-mediated augmentation of iTreg cells, $CD4^+$ cells generated from adult naive non-Tregs were harvest on day 3, while $CD4^+$ cells generated from cord blood were harvest on day 1 and day 3 respectively. Cells were then processed for ChIP-qPCR analysis (Section 2.2.6). As SCFAs treatment inhibits global histone deacetylation (refer to Section 1.5.3 for more details), the values within each sample were initially subjected to cross-sample adjustment based on the read counts of the housekeeping gene (refer to Section 2.2.6.3 for more details). Then the relative enrichment for the seven genes tested was compared as a whole or separately.

In terms of the total and average relative enrichment of all the seven genes tested (Table 4-1 and Figure 4.19), we found that butyrate treated cells of both adult and cord blood origins had the highest amounts of acetylated histones, followed by propionate treated cells. On the contrary, the addition of acetate had less or no effects on the histone acetylation. It was also interesting to notice that histone 4 experienced more acetylation changes compared to histone 3. In addition, the levels of acetylated histones were comparable between cells harvested on day3 of adult origin and day1 of cord blood origin; whereas cells from CB day3 had reduced histone acetylation compared to day1. Looking at chromatin modifications in seven different gene loci (Figure 4.20 to 4.26), the trends were similar to the protein expression of the corresponding gene.

Collectively, these results indicate that a) butyrate, propionate and acetate (to a lesser extent) enhanced histone 3 and histone 4 acetylation of different gene loci, thus augmenting the expressions of these genes; b) the epigenetic modification due to SCFAs

treatment initiated much later in adult cells compared to cord blood cells, another evidence supporting differential induction patterns.

Table 4-1 Sums of Relative Enrichment of Acetylated Histone 3 and 4 of Human iTregs with or without SCFAs.

			Control	Acetate	Butyrate	Propionate
Adult (n=7)	Day3	Histone 3	3.328	3.443	4.838	3.986
		Histone 4	4.318	5.139	9.330	10.393
Cord Blood (n=6)	Day1	Histone 3	1.747	6.410	6.765	6.279
		Histone 4	6.973	5.582	10.918	8.184
	Day3	Histone 3	2.988	2.150	5.581	2.226
		Histone 4	2.811	3.376	4.186	6.278

Data are shown as the sums of relative enrichment of acetylated histone 3 or histone 4 at seven different gene loci, including *Foxp3*, *CD39*, *GITR*, *ICOS*, *PD-1*, *PD-L1* and *CTLA-4*.

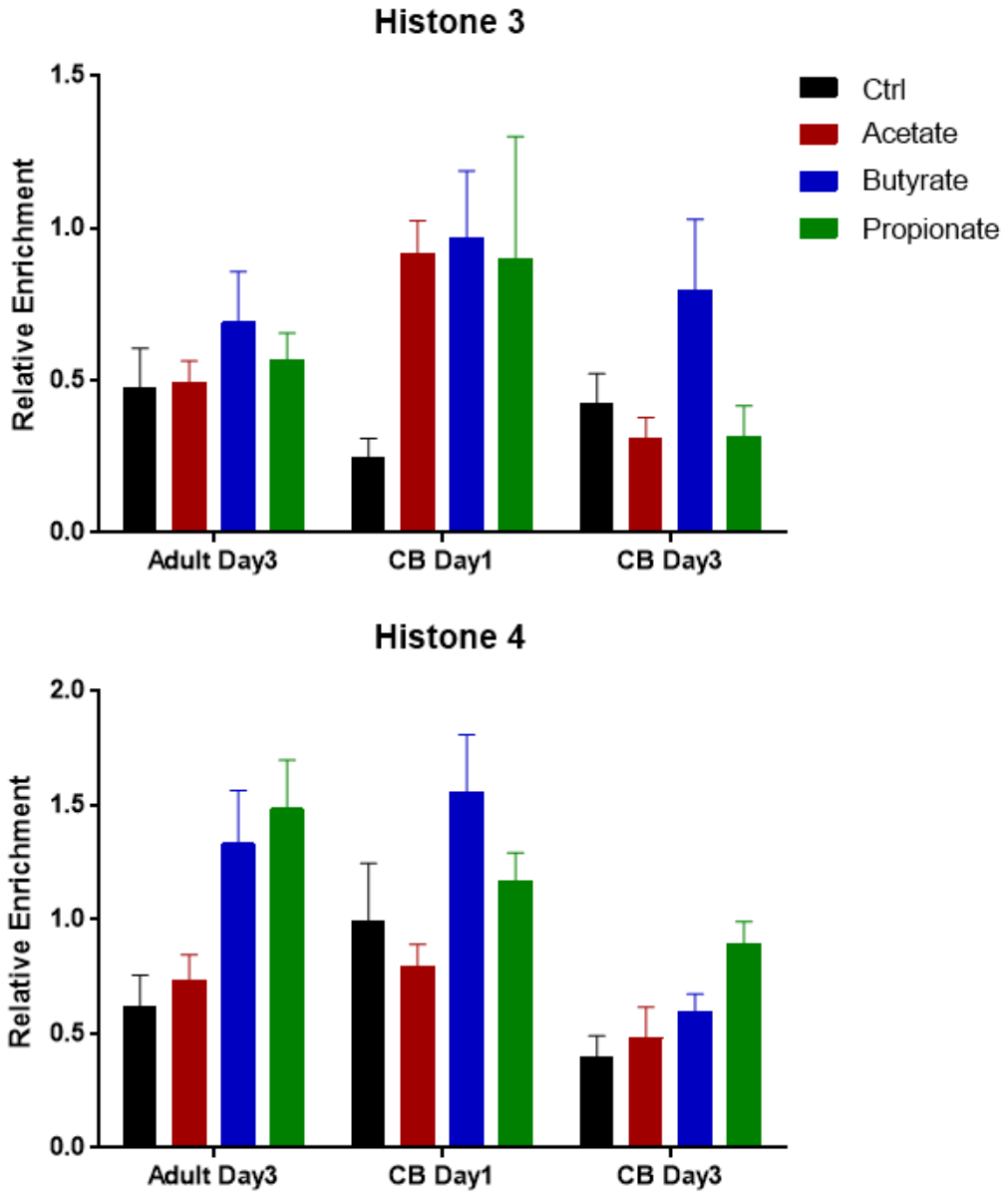

Figure 4.19 Average of Relative Enrichment of Acetylated Histone 3 and 4 of Human iTregs with or without SCFAs

Summary bar graphs showing the average relative enrichment of acetylated histone 3 (top panel) and histone 4 (bottom panel) at seven different gene loci, including *Foxp3*, *CD39*, *GITR*, *ICOS*, *PD-1*, *PD-L1* and *CTLA-4*. Cells generated from adult PB naive $CD4^+$ cells for 3 days (n=7), CB naive $CD4^+$ cells for 1 day (n=6), and CB naive $CD4^+$ cells for 3 days (n=6).

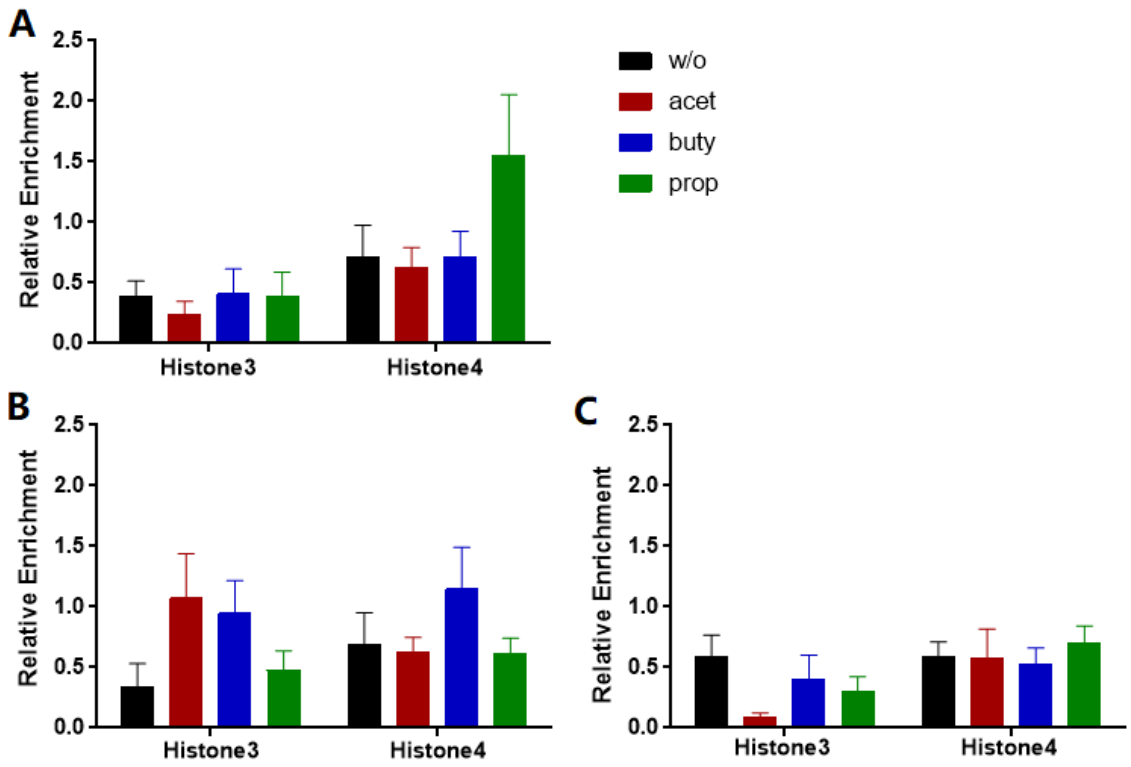

Figure 4.20 Chromatin modification at the *Foxp3* locus by SCFAs.

ChIP-qPCR analysis of the *Foxp3* locus was performed in $CD4^+$ T cells cultured in the absence (black) or presence of acetate (red), butyrate (blue), and propionate (green) using anti-AcH3 and anti-AcH4 antibody. Summary bar graphs showing the relative enrichment of acetylated histone 3 (left panel) and histone 4 (right panel) of cells generated from **(A)** adult PB naive $CD4^+$ cells for 3 days, **(B)** CB naive $CD4^+$ cells for 1 day, and **(C)** CB naive $CD4^+$ cells for 3 days.

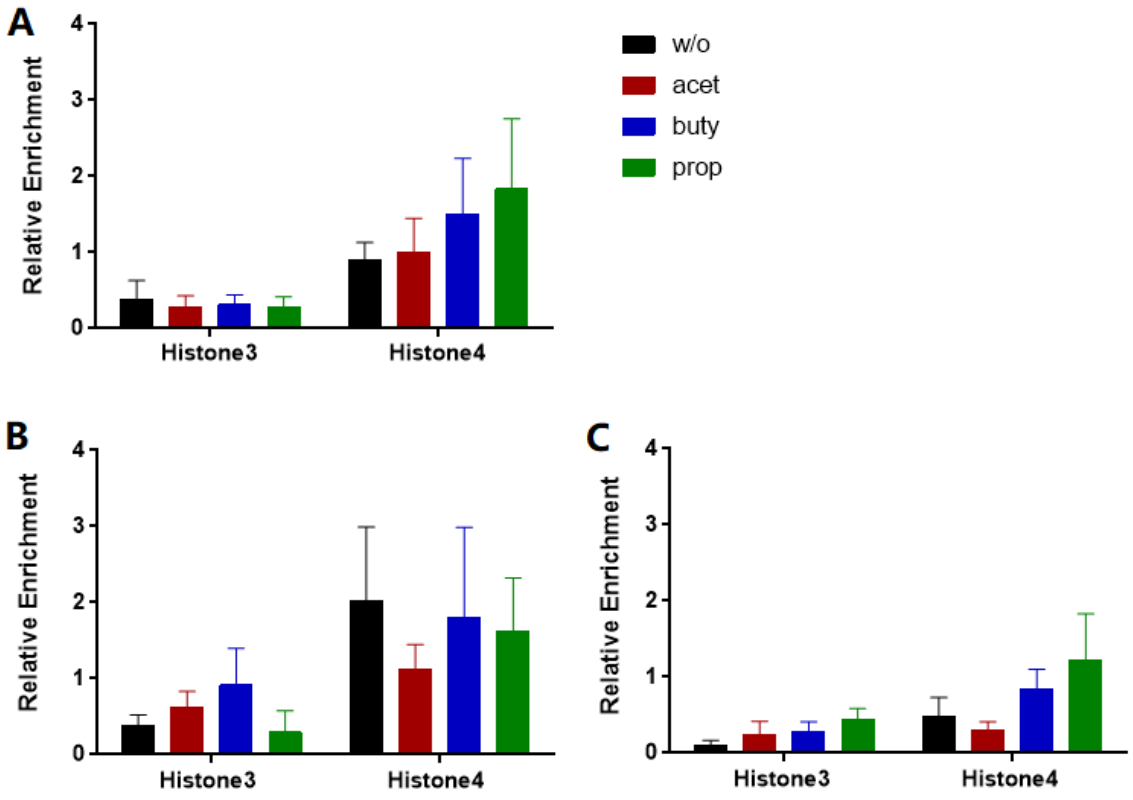

Figure 4.21 Chromatin modification at the CD39 locus by SCFAs.

ChIP-qPCR analysis of the *CD39* locus was performed in $CD4^+$ T cells cultured in the absence (black) or presence of acetate (red), butyrate (blue), and propionate (green) using anti-AcH3 and anti-AcH4 antibody. Summary bar graphs showing the relative enrichment of acetylated histone 3 (left panel) and histone 4 (right panel) of cells generated from **(A)** adult PB naive $CD4^+$ cells for 3 days, **(B)** CB naive $CD4^+$ cells for 1 day, and **(C)** CB naive $CD4^+$ cells for 3 days.

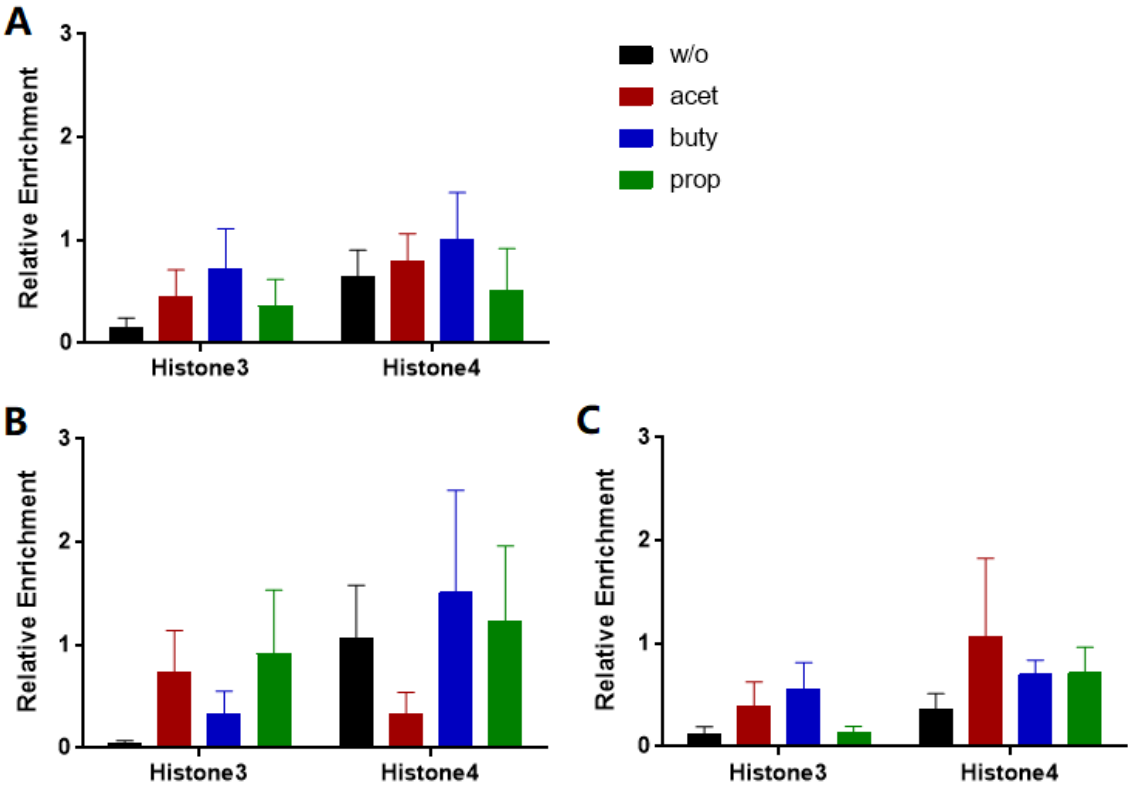

Figure 4.22 Chromatin modification at the *GITR* locus by SCFAs.

ChIP-qPCR analysis of the *GITR* locus was performed in $CD4^+$ T cells cultured in the absence (black) or presence of acetate (red), butyrate (blue), and propionate (green) using anti-AcH3 and anti-AcH4 antibody. Summary bar graphs showing the relative enrichment of acetylated histone 3 (left panel) and histone 4 (right panel) of cells generated from **(A)** adult PB naive $CD4^+$ cells for 3 days, **(B)** CB naive $CD4^+$ cells for 1 day, and **(C)** CB naive $CD4^+$ cells for 3 days.

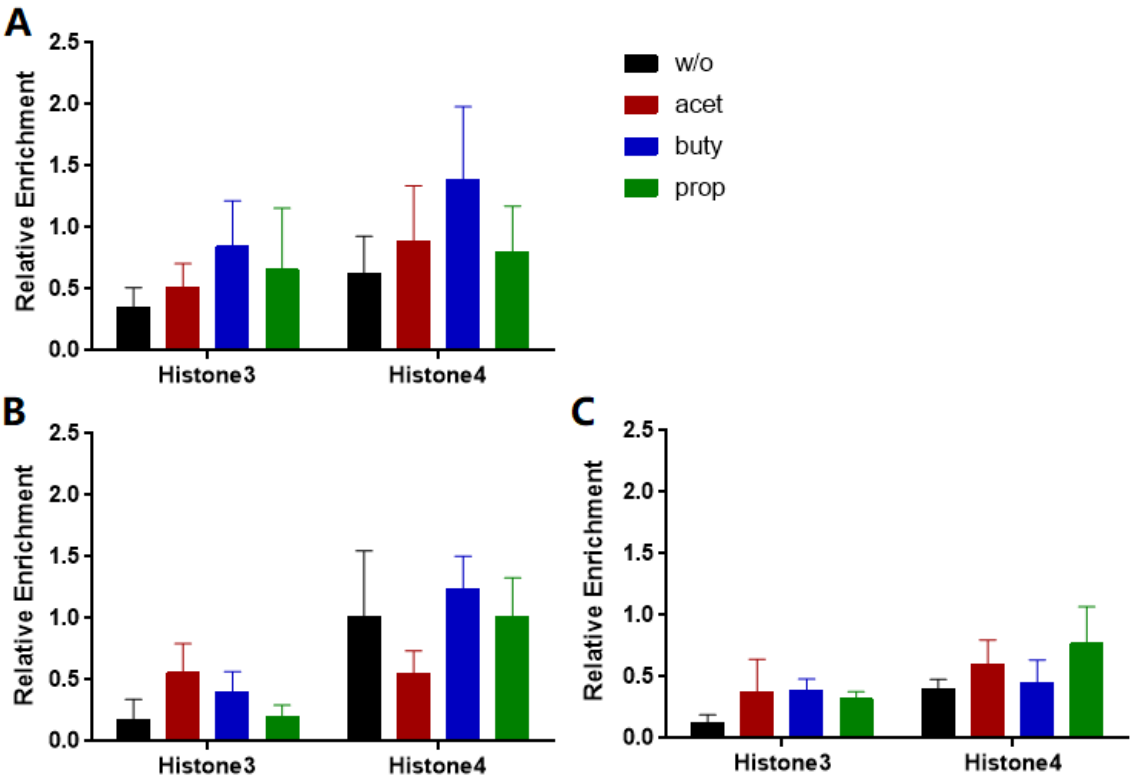

Figure 4.23 Chromatin modification at the *ICOS* locus by SCFAs.

ChIP-qPCR analysis of the *ICOS* locus was performed in $CD4^+$ T cells cultured in the absence (black) or presence of acetate (red), butyrate (blue), and propionate (green) using anti-AcH3 and anti-AcH4 antibody. Summary bar graphs showing the relative enrichment of acetylated histone 3 (left panel) and histone 4 (right panel) of cells generated from **(A)** adult PB naive $CD4^+$ cells for 3 days, **(B)** CB naive $CD4^+$ cells for 1 day, and **(C)** CB naive $CD4^+$ cells for 3 days.

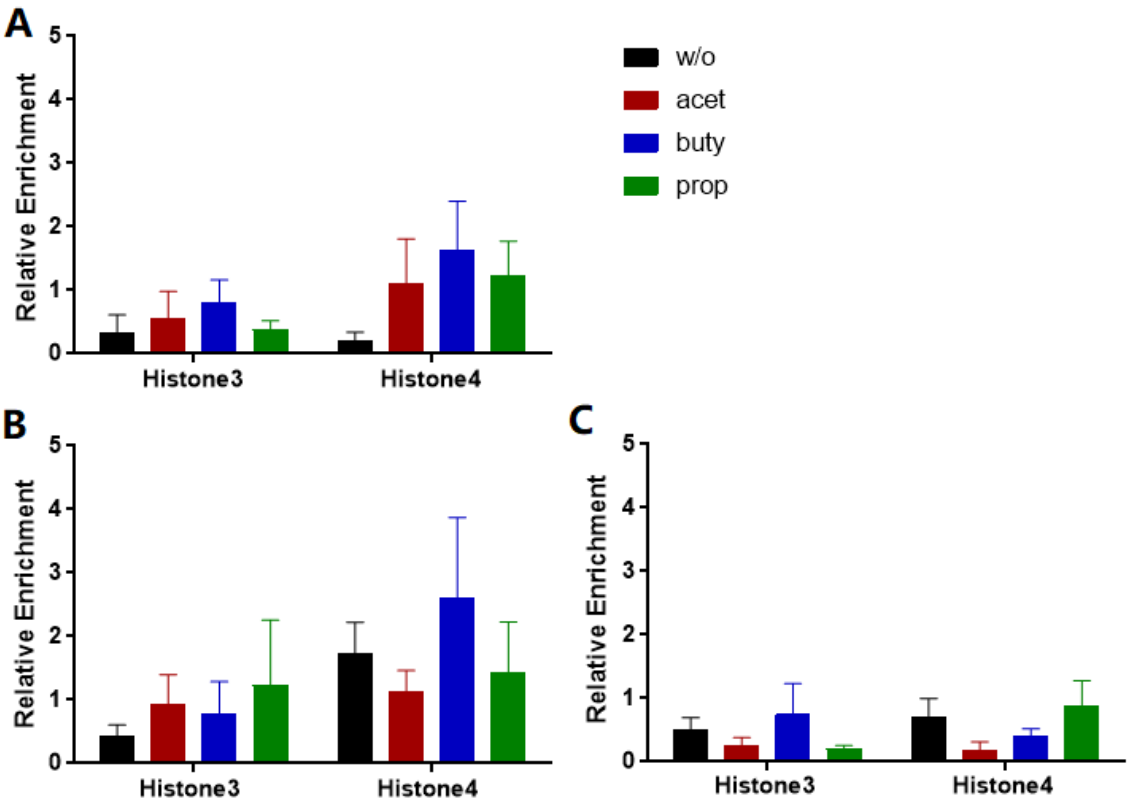

Figure 4.24 Chromatin modification at the *PD-1* locus by SCFAs.

ChIP-qPCR analysis of the *PD-1* locus was performed in $CD4^+$ T cells cultured in the absence (black) or presence of acetate (red), butyrate (blue), and propionate (green) using anti-AcH3 and anti-AcH4 antibody. Summary bar graphs showing the relative enrichment of acetylated histone 3 (left panel) and histone 4 (right panel) of cells generated from **(A)** adult PB naive $CD4^+$ cells for 3 days, **(B)** CB naive $CD4^+$ cells for 1 day, and **(C)** CB naive $CD4^+$ cells for 3 days.

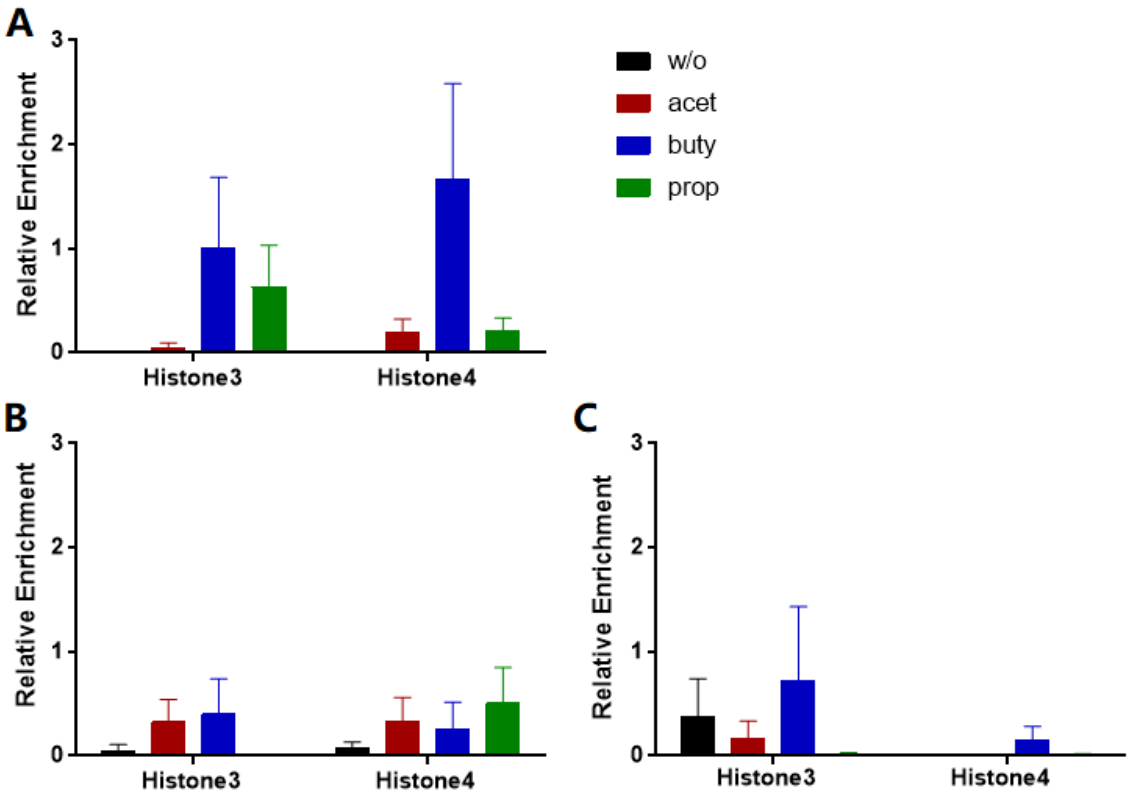

Figure 4.25 Chromatin modification at the *PD-L1* locus by SCFAs.

ChIP-qPCR analysis of the *PD-L1* locus was performed in $CD4^+$ T cells cultured in the absence (black) or presence of acetate (red), butyrate (blue), and propionate (green) using anti-AcH3 and anti-AcH4 antibody. Summary bar graphs showing the relative enrichment of acetylated histone 3 (left panel) and histone 4 (right panel) of cells generated from **(A)** adult PB naive $CD4^+$ cells for 3 days, **(B)** CB naive $CD4^+$ cells for 1 day, and **(C)** CB naive $CD4^+$ cells for 3 days.

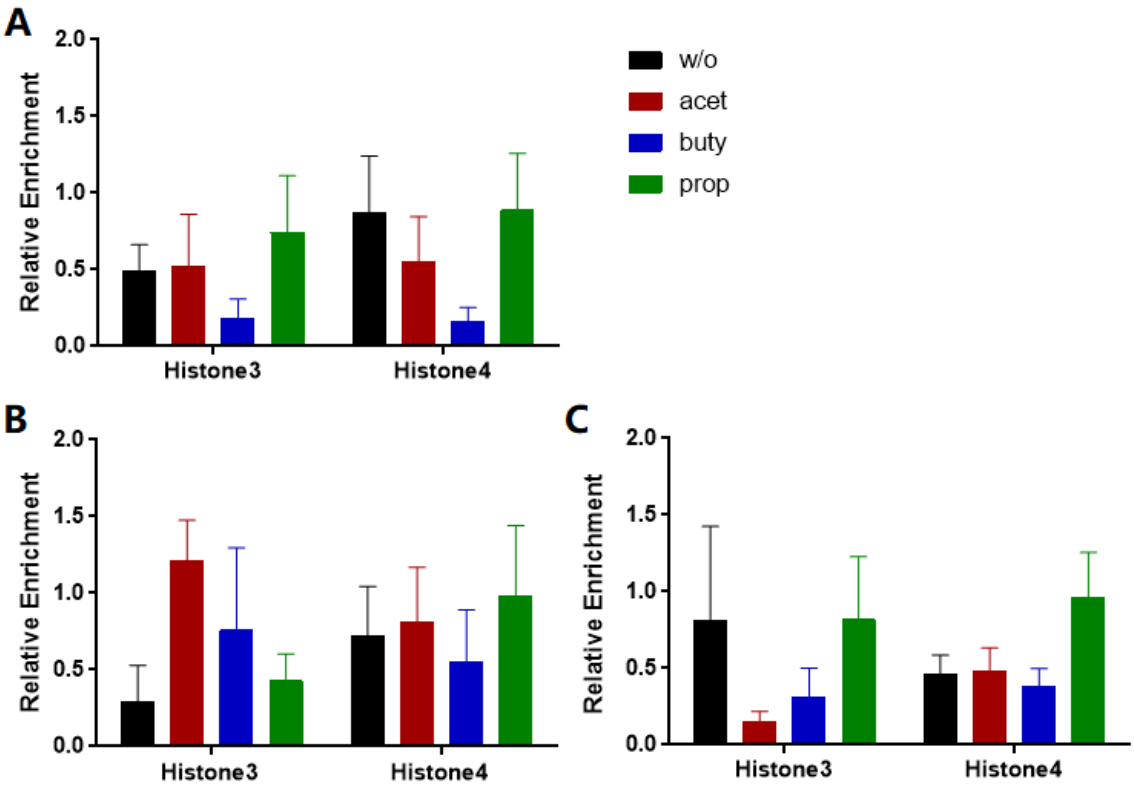

Figure 4.26 Chromatin modification at the *CTLA-4* locus by SCFAs.

ChIP-qPCR analysis of the *CTLA-4* locus was performed in $CD4^+$ T cells cultured in the absence (black) or presence of acetate (red), butyrate (blue), and propionate (green) using anti-AcH3 and anti-AcH4 antibody. Summary bar graphs showing the relative enrichment of acetylated histone 3 (left panel) and histone 4 (right panel) of cells generated from **(A)** adult PB naive $CD4^+$ cells for 3 days, **(B)** CB naive $CD4^+$ cells for 1 day, and **(C)** CB naive $CD4^+$ cells for 3 days.

4.4 Discussion

SCFAs have been well established as essential immune regulators for pTreg and iTreg cell induction in animals (276-278, 331). SCFAs exert their effects on Treg cells via three different mechanisms: a) energy metabolism, b) HDAC inhibition, and c) indirectly via APCs. Firstly, SCFAs are converted to Acetyl-CoA during energy metabolism (316), which then increase the cellular ATP levels (317). Thus, the ATP sensing mTOR pathway is activated to regulate the differentiation of Treg cells (318, 319). Second, the major mechanism proposed is HDAC inhibition, considering the lack of significant levels of GPRs on the T cell surface (288-290). SCFAs promote the generation of pTregs by enhancing Histone 3 acetylation at both promoter and CNS3 regions of the *Foxp3* gene locus and the Foxp3 protein via HDAC inhibition (276, 278). In addition, the expressions of IL-10, IFN-γ and IL-17 are also elevated in T cells (290). Lastly, SCFAs also exert their regulatory effects on Treg cells via APCs. They suppress the expression of pro-inflammatory cytokines of DCs via HDAC inhibition, thus promoting Treg induction (276). Alternatively, the activation of GPR109a by butyrate can skew colonic macrophages and dendritic cells towards tolerogenic phenotype to promote the differentiation of Treg cell and IL-10 producing cells (295).

The biggest questions about human *in vitro* induced Treg cells were a) whether they were stable for long periods; and b) if they had an equivalent suppressive capacity compared to *ex vivo* nTreg cells (86, 107, 355). Neither of these problems was seen in mice (356). To solve this challenge, various reagents, in addition to IL-2 and TGF-β, have been described to improve the suppressive capacity of human iTreg cells *in vitro*. These included retinoic acid (353, 357, 358), rapamycin (353, 358, 359), vitamin D (360), and

IL-10 (1). However, only one paper has been published describing the effects of butyrate and propionate on the generation of human Treg cells *in vitro*, and it failed to prove their efficacy (353).

In view of these recent advances, our results in this chapter showed the novel role of SCFAs in the generation of human iTregs for the first time. The addition of butyrate and propionate, but not acetate, significantly enhanced the suppressive capacity of iTregs. In particular, this conclusion is applied to not only activated iTregs generated from adult naive $CD4^+$ T cells, but also iTregs of cord blood origin. This differential induction pattern was observed previously using completely different methodology (361). This group found that a significantly higher percentage (2.7±0.5-fold, $p<0.002$) of CB $CD4^+CD25^+$ cells were induced upon allogeneic MUTZ3-iDC stimulation (not TGF-β plus anti-CD3/anti-CD28), compared to that from Adult PB $CD4^+CD25^-$ cells (not naive cells). Hence, the differences should attribute to the much higher percentage of naive "inducible" cells in CB.

We postulated that this differential induction patterns of adult iTregs might explain the controversy of the effectiveness of human iTregs as well as the concealment of the effects of SCFAs on adult iTregs. In our study, naïve non-Tregs isolated from adult $CD4^+$ cells were unable to fully differentiate into Treg cells, and there was a significant non-activated subpopulation displaying a smaller cell size. Among all the culture conditions, butyrate treated iTregs had the most non-activated cells, around 40% of the whole cultured cells. We speculated that this population was nonresponsive and did not share iTreg characters. Indeed, these cells had the minimal expression of all the phenotypic markers, except for CD127 (which expressed at higher levels). We then compared the suppressive capacity between activated iTreg cells and their pair-matched whole cultured cells generated from

adult naive $CD4^+$ cells. As expected, the activated iTregs had a higher percentage of suppression compared to their counterparts. The differences were much greater in butyrate-treated iTregs when taking into account the large proportion of non-activated cells. Interestingly, this differential induction pattern was not present in the iTregs generated from CB naïve $CD4^+$ cells. All naïve non-Tregs sorted from CB naïve $CD4^+$ cells were fully differentiated into iTregs. Another evidence for this differential induction pattern is that the epigenetic histone acetylation due to SCFAs treatment was initiated much later in adult cells compared to cord blood cells. Therefore, when analysing iTregs generated from CB naïve $CD4^+$ cells and the activated rather than the whole iTregs generated from adult PB naïve $CD4^+$ cells, we were able to conclude the same finding discovered in animal studies.

Since the only difference in the methodology is the origin of naïve $CD4^+$ T cells and only adult iTregs show partial proliferation, it raises the question as to whether $CD45RO^-$ T cells are really "naïve" in adults compared to cord blood. Although the size and scope of the naïve $CD4^+$ T cell pool are maintained by both thymic output and peripheral homeostatic proliferation throughout adulthood (362, 363), there are functional alterations in these naive T cells. TCR sequencing studies have shown that clonal expansion also happens in human naive T cells, and most of these clonally expanded cells still retain a naive phenotype with the expression of CD45RA, CD28, CD27, and CCR7 (364). In addition, telomere attrition, DNA damage, as well as changes in microRNAs, occur in naive T cells when ageing, which partially account for defective T cell responses (365, 366). However, there is missing data on the conclusive transcriptional and epigenetic profiling exploring the influence of ageing on naive T cells in humans.

The ChIP-qPCR results demonstrated the possible mechanism of butyrate and propionate mediated augmentation of human iTreg cells. Butyrate, propionate and to a lesser extent acetate, enhanced histone 3 and histone 4 acetylation of different gene loci via histone deacetylation inhibition, thus increasing the accessibility of these genes and initiation of protein expression. The delayed histone acetylation in adult iTregs also provided evidence of lower responsiveness and proliferation of adult naive $CD4^+$ T cells. However, we could not exclude the possibility that SCFAs can also contribute in other ways, such as energy metabolism.

Consistent with previous studies, the expression of Foxp3 and CD127 of iTregs in our experiment proved that they were only activation markers for human iTregs. Additionally, we showed that the expression patterns of GITR, ICOS, CD39, PD-1 and PD-L1 on iTregs treated with SCFAs were similar to that of the functional assay results, suggesting that GITR, ICOS, CD39, PD-1 and PD-L1 are potential candidate markers for human *in vitro* induced Treg cells.

In summary, the current results show that in addition to IL-2 and TGF-β, SCFAs enhance gene transcription of potential iTreg candidate genes. This is achieved by acetylation of Histone 3 and Histone 4 via HDAC inhibition, which increases the accessibility of these genes for transcription. These proteins, in turn, potentiate the differentiation of iTreg cells and bestow them with suppressive capacity. This novel role of SCFAs on iTregs is seen for the first time in a human study, providing evidence for future therapeutic and preventative dietary modification strategies for several immune diseases.

Chapter 5 – Short Chain Fatty Acids Skew Monocyte-Derived Dendritic Cells towards a Tolerogenic Status

5.1 Introduction

The results from the previous chapter suggest that in addition to IL-2 and TGF-β, SCFAs (butyrate and propionate, but not acetate) potentiate the induction of human iTregs and enhance the suppressive capacity of these iTregs via HDAC inhibition. This is the first time that this novel role of SCFAs on iTregs has been seen in a human study. Apart from Treg cells, SCFAs can also affect APCs to modulate immune tolerance.

DCs play an essential role in directing the immune response towards either immunity or tolerance, depending on the context of antigen exposure and different environmental stimuli. Several signals are required for DCs to activate T cell responses in addition to MHC-II complexes, such as upregulated co-stimulatory factors on the DC cell surface and the cytokine milieu (164). Therefore, the expressions of costimulatory factors and MHC molecules, as well as cytokine production, are of vital importance to distinguish tolerogenic DCs from immunogenic DCs. SCFAs suppress the expression of pro-inflammatory cytokines by murine DCs, thus promoting Treg induction (276). Butyrate can also activate the GPR109a signalling pathway, thus skewing murine colonic macrophages and DCs towards a tolerogenic phenotype to promote the differentiation of Treg cell and IL-10 producing cells (295).

The effect of butyrate on DCs has been thoroughly examined in human MoDCs, including their differentiation, maturation, cytokine production and immune-stimulatory capacity. The addition of butyrate during the MoDC differentiation process downregulated the expression of costimulatory factors, such as CD80, CD83, CD86, CD40, and ICAM-1 (CD54) of immature MoDCs and to a much greater extent, mature MoDCs (325, 367-369). The expressions of MHC class including HLA-A/B/C and HLA-DR/DQ, as well as

group 1 CD1 family (CD1a, CD1b and CD1c), were also reduced by butyrate treatment (325, 367-369). Taken together, this profound downregulation of costimulatory factors and antigen presentation MHC molecules by butyrate indicated that both the differentiation and maturation of DCs were compromised. Moreover, butyrate significantly reduced the production of pro-inflammatory cytokines (IL-12, IL-6, and TNF-α) and chemokines (for example, CXCL9) (368, 369), while increasing IL-10 production (367). The presence of butyrate also resulted in less T cell stimulatory activity (325, 367). Other types of HDAC inhibitors, like VPA and MS-275, showed similar influence on human DCs (370). However, there is very limited research on the effects of other SCFAs (acetate and propionate) on human DCs. Woetmann et al. found that acetate only exerted minimal effects on the gene expression of human MoDCs, whereas propionate strongly reduced the production of pro-inflammatory chemokines CXCL9 and CCL19 (369).

Therefore, the aims of this chapter are to: a) explore the precise role of SCFAs (including sodium acetate, butyrate and propionate) on human MoDCs, including the expression of costimulatory factors, adhesion factors, migration factors, MHC-II molecule, chemokines, and cytokines; b) investigate how SCFA-treated MoDCs influence the proliferation of autologous $CD4^+$ T cells; and c) compare the suppressive capacity of $CD4^+$ T cells cocultured with SCFA-treated MoDCs.

5.2 Subjects

To determine the effect of SCFAs on the human MoDCs, a total of 14 healthy adult volunteers were recruited. For MoDC flow cytometric analysis, eight adult PBMCs were used, while for functional analysis, peripheral blood samples were collected twice over

two consecutive weeks from six healthy adults. Individuals with any history of autoimmune disease or allergies were excluded.

5.3 Results

5.3.1 SCFAs Skew Human Monocyte-Derived Dendritic Cells towards a Tolerogenic Phenotype

To understand the precise role of SCFAs (including sodium acetate, butyrate and propionate) on human MoDCs (Section 2.2.3.3), bead selected $CD14^+$ monocytes were cultured in the presence of GM-CSF and IL-4 with or without SCFAs for 7 days to induce immature MoDCs (im-MoDCs). LPS was added to selected cultures to induce MoDC maturation (m-MoDCs) 24 hours prior to harvesting.

First, we examined whether the addition of LPS could successfully induce the MoDC maturation. There was significant upregulation of the costimulatory factors in both control and SCFAs-treated m-MoDCs, including CD80, CD83, CD86, and PD-L1 (Figure 5.1). In addition, the expression of MHC class (HLA-DR) was also significantly increased in m-MoDCs, while the expression of CD1a was decreased (Figure 5.2). The changes in CD1a expression was diminished in butyrate-treated m-MoDCs compared to im-DCs. The trend was similar for other DC markers (DC-Sign, CD11c) and migration markers (lymph node homing receptor CCR7) (Figure 5.3). m-MoDCs had significant higher expressions of CD11c, TLR-4, and CCR7. However, it was not always significant for butyrate or propionate treated MoDCs. DC-Sign was downregulated after the addition of LPS, and CD14 expression slightly increased. As for the cytokine signature, LPS significantly increased the expressions of chemokines and cytokines, such as CXCL9, IL-12 p35, and IL-12/23 p40 determined by flow cytometric analysis (Figure 5.4). The level

of CXCL9 was similar for butyrate treated MoDCs. However, we failed to find significant changes in TNF-α and TGF-β expressions.

Next, we tested the effects of SCFAs on both immature and mature MoDCs. The expressions of CD80, CD83, CD86, HLA-DR, and PD-L1 were at very low levels in im-MoDCs (Figure 5.5 to Figure 5.7). As for m-MoDCs, butyrate and propionate treatment reduced the expression of these markers compared to control and acetate treated groups. There was a significant decrease in CD1a (a nonclassical antigen presenting molecule (371)) expression for butyrate and propionate treated MoDCs in both immature and mature groups (Figure 5.7 right panel). Butyrate and propionate also reduced the expressions of CD11c in the m-MoDC group (Figure 5.8 left panel). As for DC-Sign, TLR-4, and CCR7, there were no significant differences compared to control MoDCs (Figure 5.9 and 5.10). The expression of CD14 shared the same trend found in CD1a (Figure 5.10). The upregulation of CXCL9 was least in the butyrate and propionate treated m-MoDCs, and these cells also had the highest expression of TGF-β (Figure 5.11). However, the flow cytometric results for the other cytokine signatures were not consistent with the previously published ELISA results.

Taken together, these results indicated that both butyrate and propionate, but not acetate, could inhibit the differentiation and maturation of MoDCs, skewing towards immature or tolerogenic status. In addition, butyrate and propionate also modulate cytokine production by MoDCs.

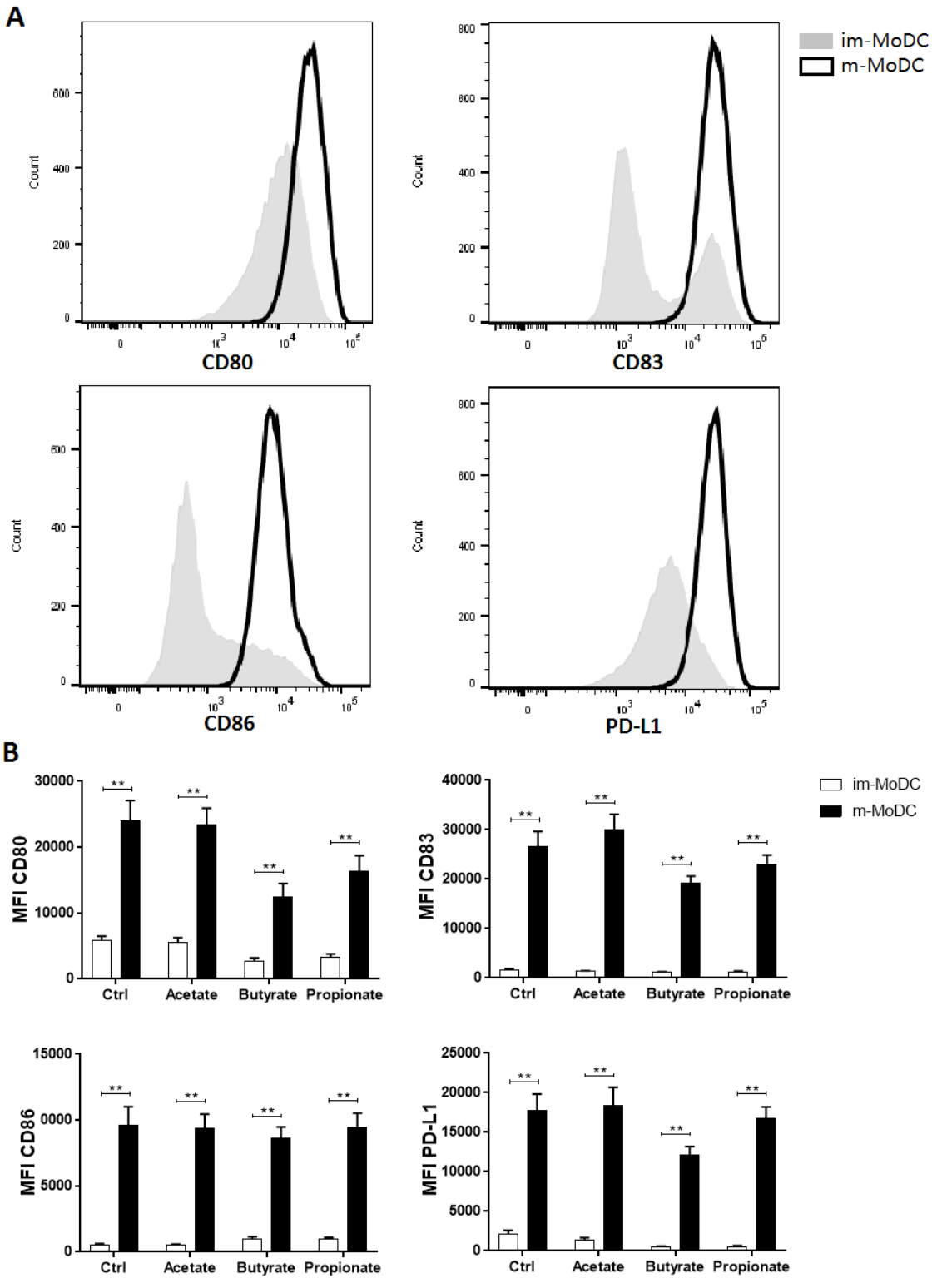

Figure 5.1 The expression of costimulatory factors in human immature and mature MoDCs.

(**A**) Representative histograms showing the expressions of CD80, CD83, CD86, and PD-L1 of both im-MoDCs (grey shade) and mature MoDCs (maturation with LPS for 24 hours, black thick line) cultured under normal conditions (GM-CSF+IL-4). (**B**) Bar graphs showing the MFI of CD80, CD83, CD86, and PD-L1 of both im-MoDCs (white) and mature MoDCs (black) cultured under various conditions: Ctrl (GM-CSF+IL-4), acetate (GM-CSF+IL-4+acetate), butyrate (GM-CSF+IL-4+butyrate), and propionate (GM-CSF+IL-4+propionate). Data represent 8 independent experiments. $^{**}p < 0.01$.

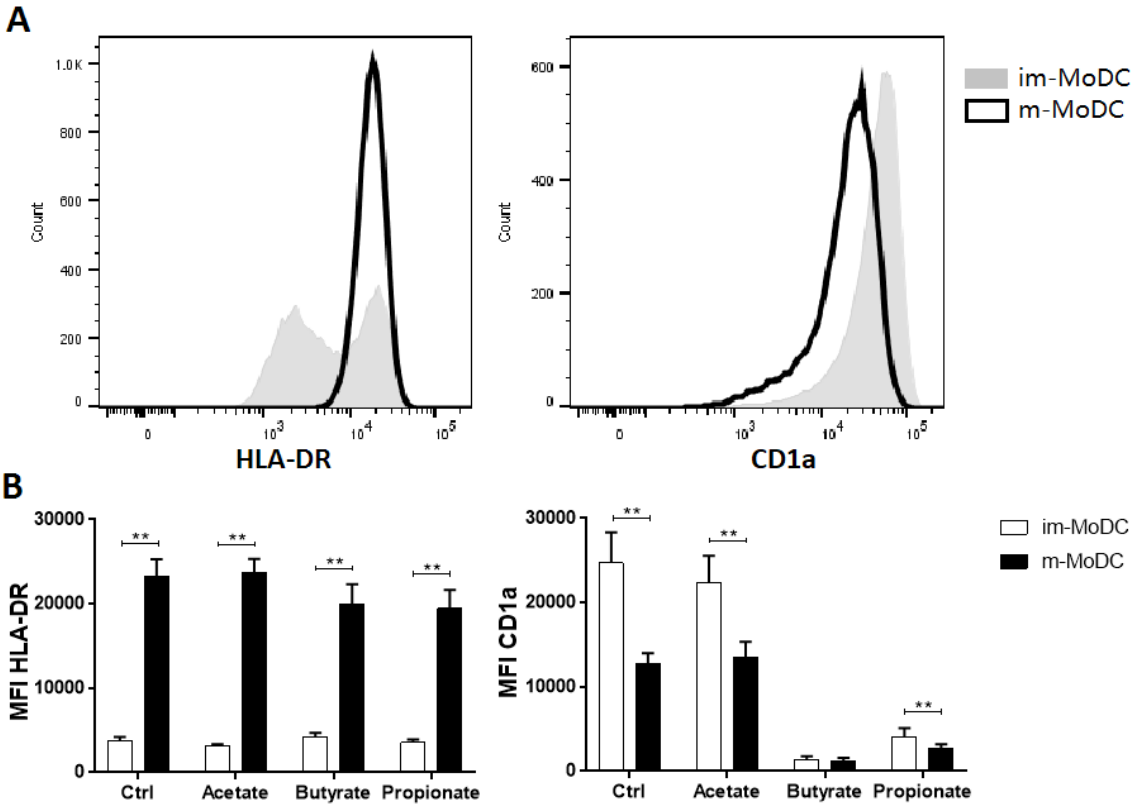

Figure 5.2 The expression of HLA-DR and CD1a in human immature and mature MoDCs.

(**A**) Representative histograms showing the expressions of HLA-DR and CD1a of both im-MoDCs (grey shade) and mature MoDCs (maturation with LPS for 24 hours, black thick line) cultured under normal conditions (GM-CSF+IL-4). (**B**) Bar graphs showing the MFI of HLA-DR and CD1a of both im-MoDCs (white) and mature MoDCs (black) cultured under various conditions: Ctrl (GM-CSF+IL-4), acetate (GM-CSF+IL-4+acetate), butyrate (GM-CSF+IL-4+butyrate), and propionate (GM-CSF+IL-4+propionate). Data represent 8 independent experiments. $^{**}p < 0.01$.

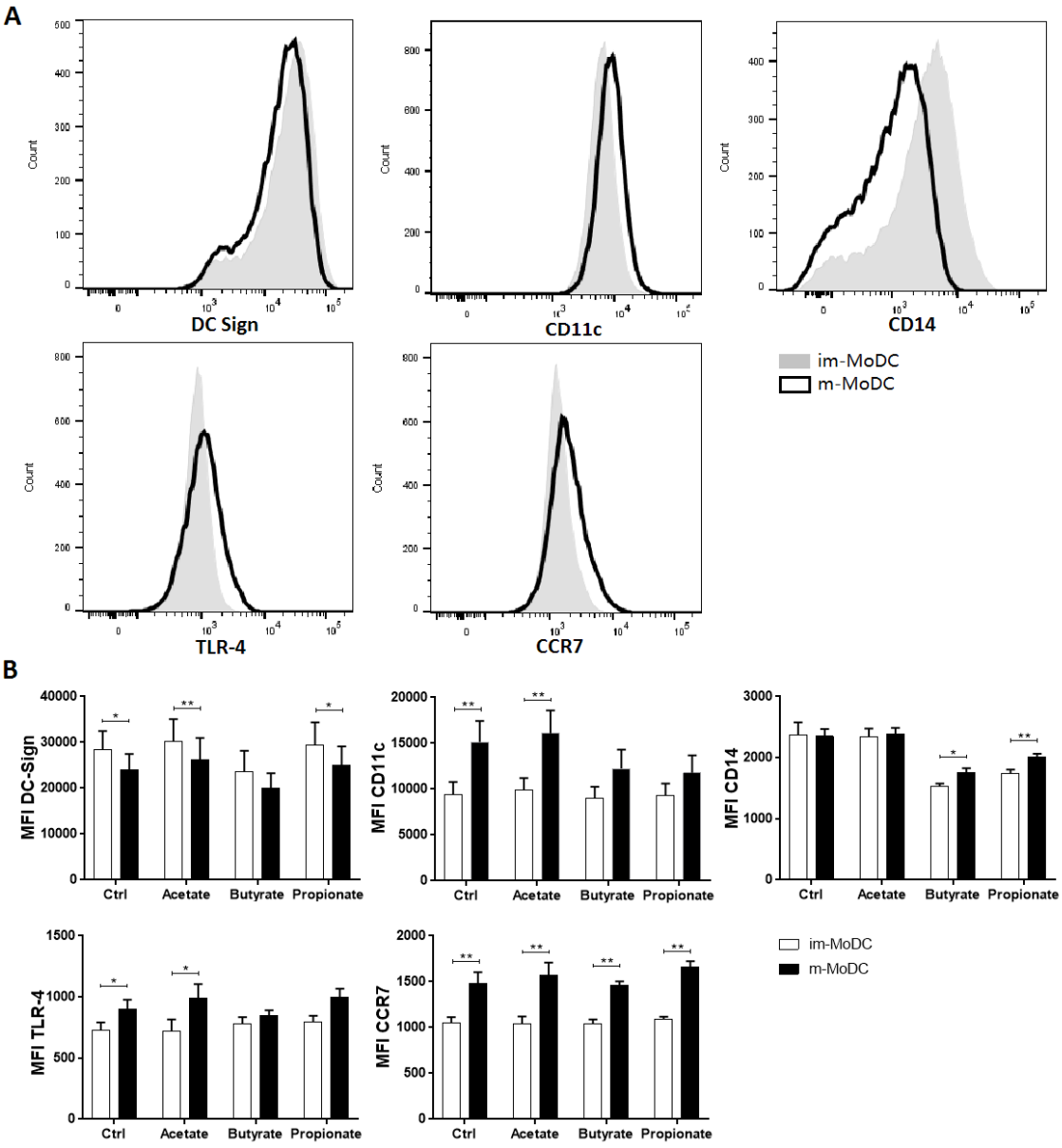

Figure 5.3 The expression of DC markers and migration markers in human immature and mature MoDCs.

(**A**) Representative histograms showing the expressions of DC-Sign, CD11c, CD14, TLR-4, and CCR7 of both im-MoDCs (grey shade) and mature MoDCs (maturation with LPS for 24 hours, black thick line) cultured under normal conditions (GM-CSF+IL-4). (**B**) Bar graphs showing the MFI of DC-Sign, CD11c, CD14, TLR-4, and CCR7 of both im-MoDCs (white) and mature MoDCs (black) cultured under various conditions: Ctrl

(GM-CSF+IL-4), acetate (GM-CSF+IL-4+acetate), butyrate (GM-CSF+IL-4+butyrate), and propionate (GM-CSF+IL-4+propionate). Data represent 8 independent experiments. *$p < 0.05$, **$p < 0.01$.

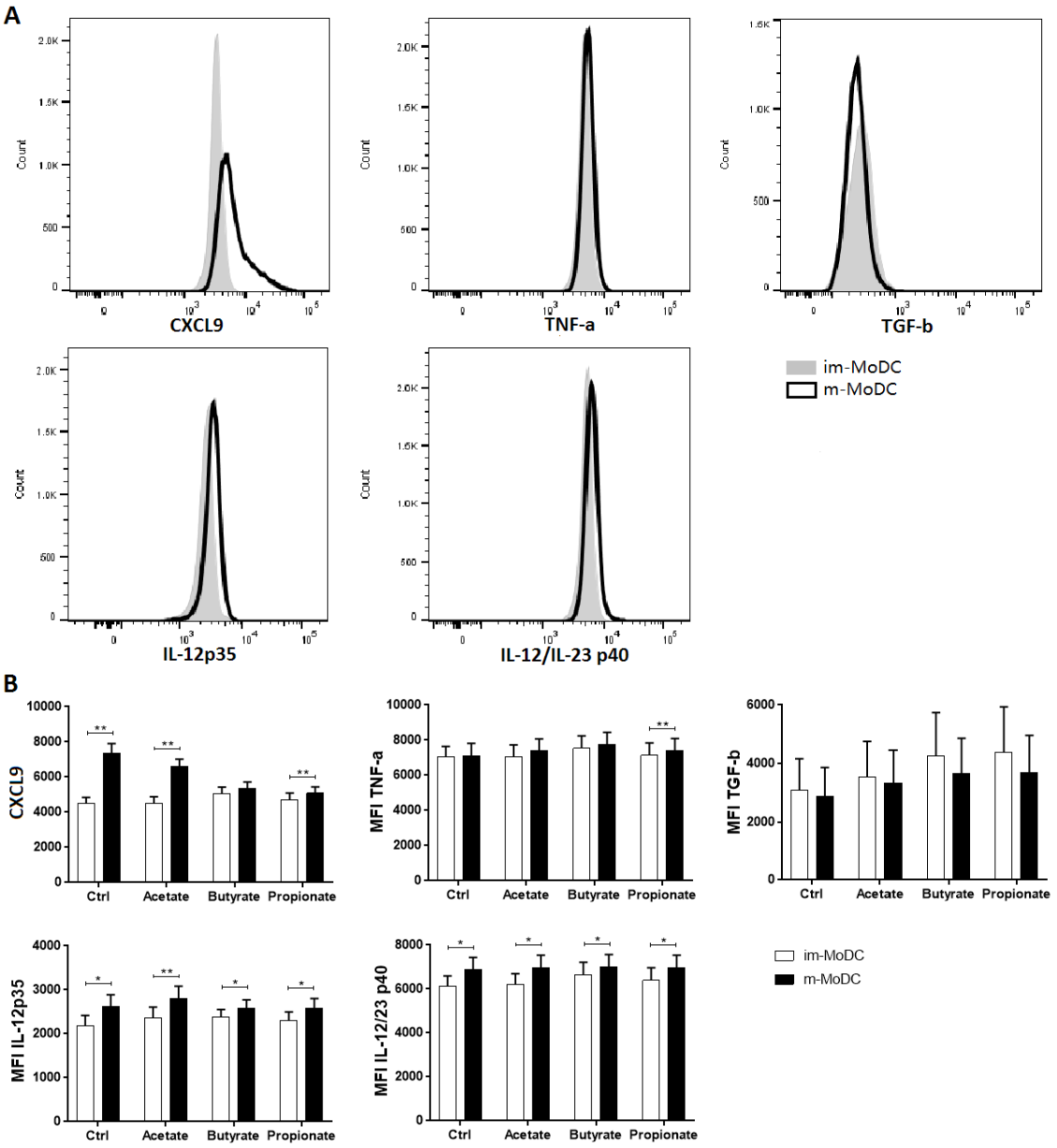

Figure 5.4 The expression of cytokine signatures in human immature and mature MoDCs.

(**A**) Representative histograms showing the expression of CXCL9, TNF-α, TGF-β, IL-12 p35, and IL-12/35 p40 of both im-MoDCs (grey shade) and mature MoDCs (maturation with LPS for 24 hours, black thick line) cultured under normal conditions (GM-CSF+IL-4). (**B**) Bar graphs showing the MFI of CXCL9, TNF-α, TGF-β, IL-12 p35, and IL-12/35

p40 of both im-MoDCs (white) and mature MoDCs (black) cultured under various conditions: Ctrl (GM-CSF+IL-4), acetate (GM-CSF+IL-4+acetate), butyrate (GM-CSF+IL-4+butyrate), and propionate (GM-CSF+IL-4+propionate). Data represent 8 independent experiments. *$p < 0.05$, **$p < 0.01$.

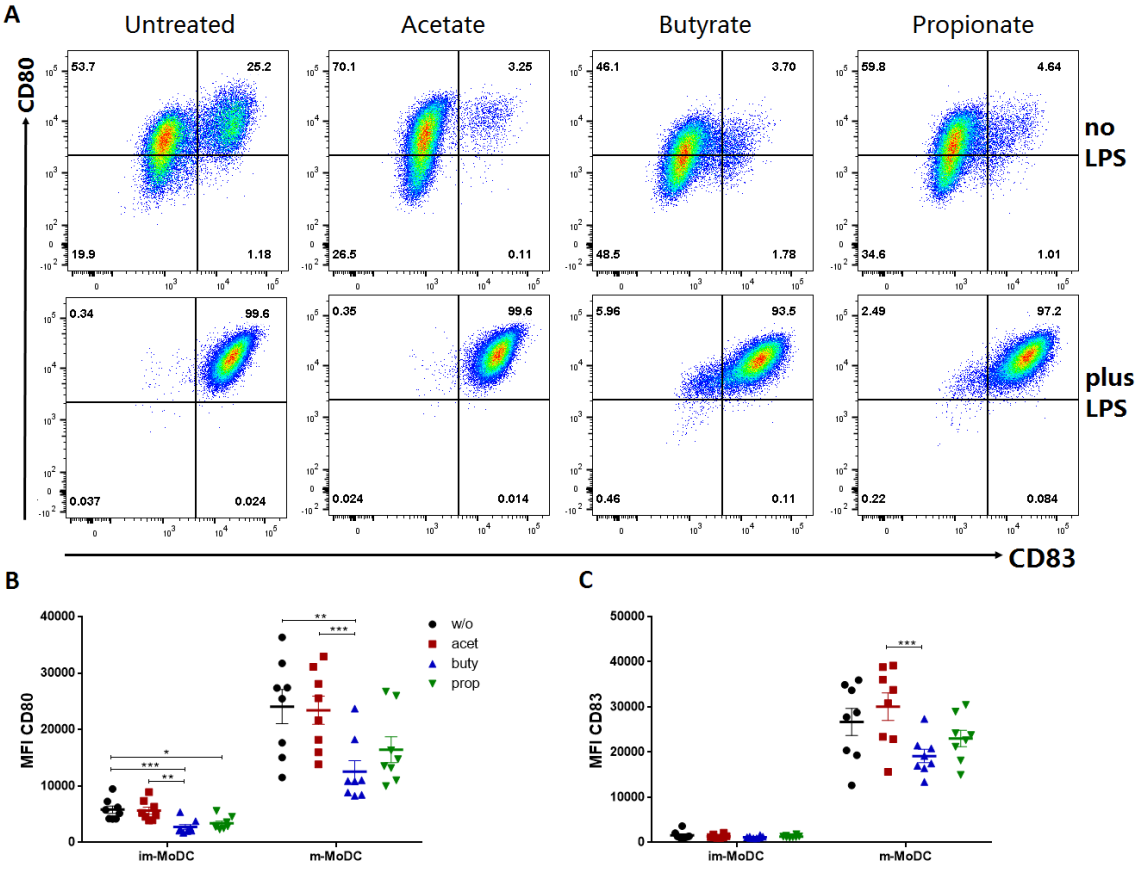

Figure 5.5 The effects of SCFAs on the expression of CD80 and CD83 in human MoDCs.

(**A**) Representative pseudocolour dot plots showing the effects of SCFAs on the expression of CD80 and CD83 of both im-MoDCs (upper) and mature MoDCs (maturation with LPS for 24 hours, lower). Scattered dot plots showing the MFI of (**B**) CD80 and (**C**) CD83 of both im-MoDCs (left panel) and mature MoDCs (right panel) cultured under various conditions: Ctrl (GM-CSF+IL-4, black), acetate (GM-CSF+IL-4+acetate, red), butyrate (GM-CSF+IL-4+butyrate, blue), and propionate (GM-CSF+IL-4+propionate, green). Data are from 8 independent experiments. *$p < 0.05$, **$p < 0.01$, ***$p < 0.001$.

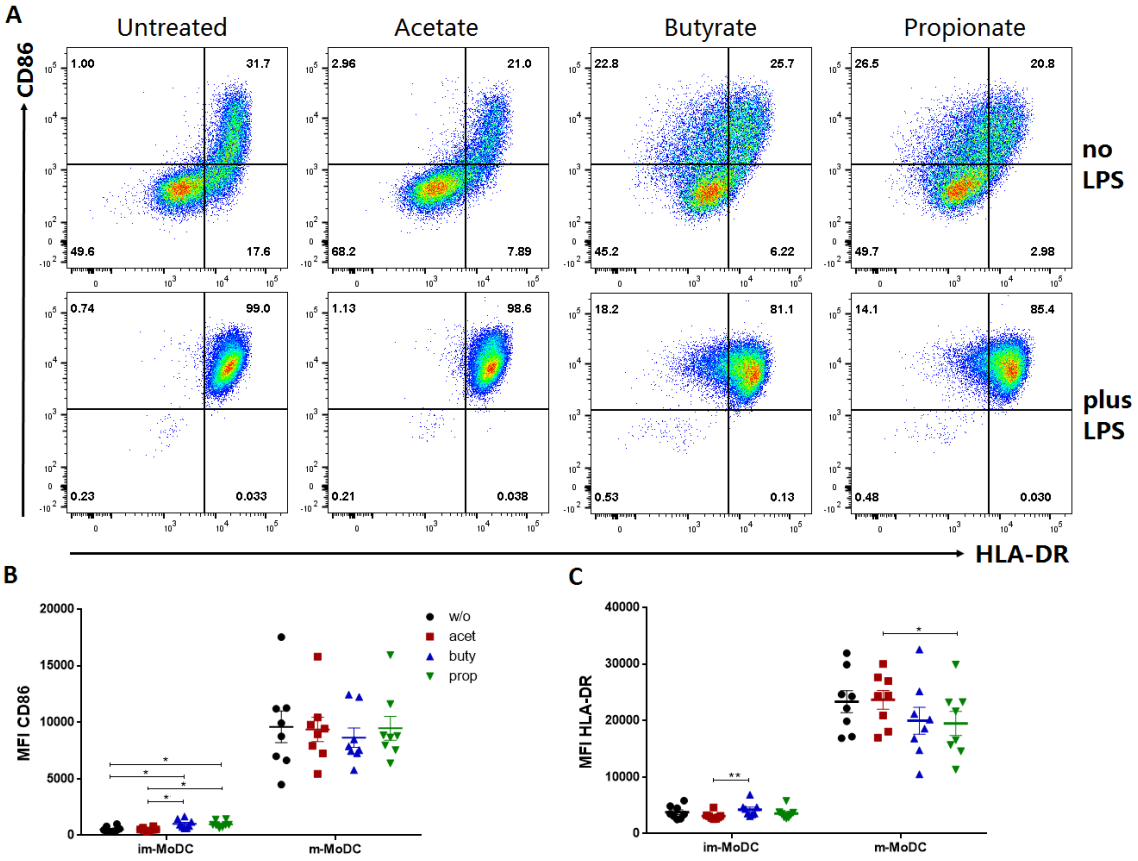

Figure 5.6 The effects of SCFAs on the expression of CD86 and HLA-DR in human MoDCs.

(**A**) Representative pseudocolour dot plots showing the effects of SCFAs on the expression of CD86 and HLA-DR of both im-MoDCs (upper) and mature MoDCs (maturation with LPS for 24 hours, lower). Scattered dot plots showing the MFI of (**B**) CD86 and (**C**) HLA-DR of both im-MoDCs (left panel) and mature MoDCs (right panel) cultured under various conditions: Ctrl (GM-CSF+IL-4, black), acetate (GM-CSF+IL-4+acetate, red), butyrate (GM-CSF+IL-4+butyrate, blue), and propionate (GM-CSF+IL-4+propionate, green). Data are from 8 independent experiments. *$p < 0.05$, **$p < 0.01$.

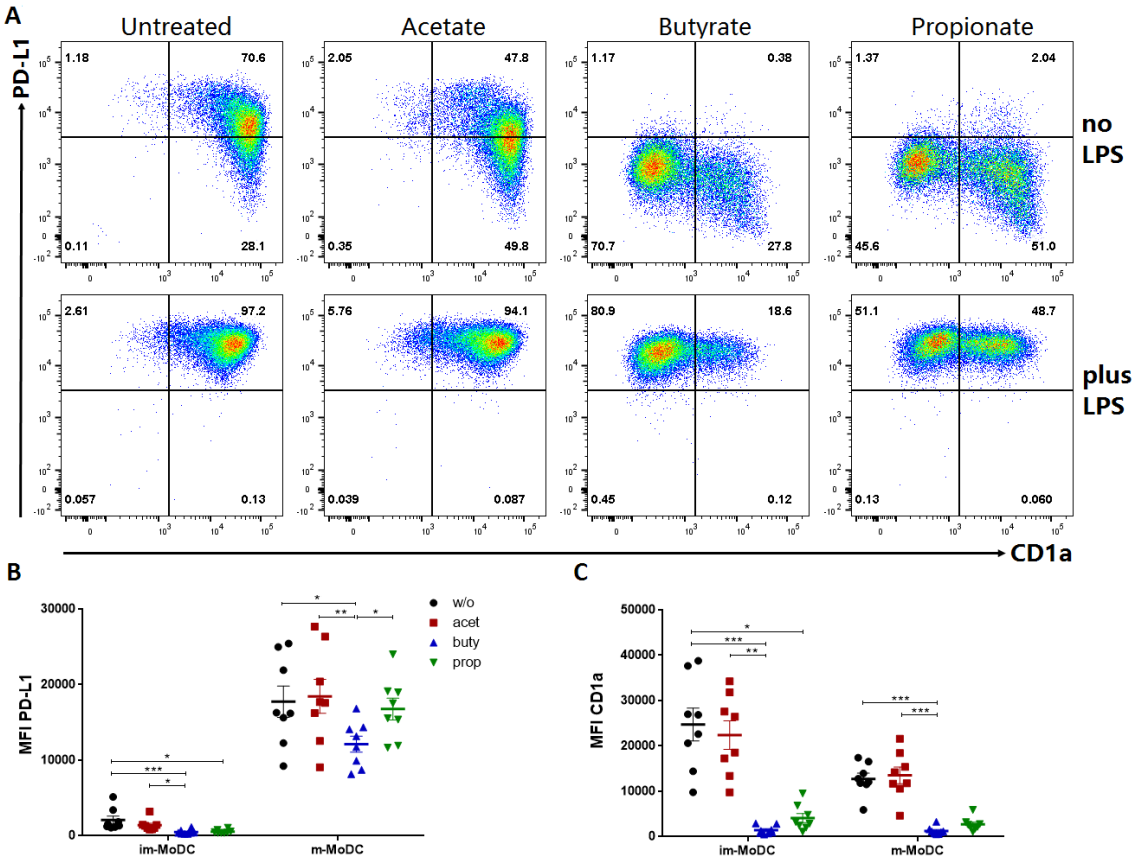

Figure 5.7 The effects of SCFAs on the expression of PD-L1 and CD1a in human MoDCs.

(**A**) Representative pseudocolour dot plots showing the effects of SCFAs on the expression of PD-L1 and CD1a of both im-MoDCs (upper) and mature MoDCs (maturation with LPS for 24 hours, lower). Scattered dot plots showing the MFI of (**B**) PD-L1 and (**C**) CD1a of both im-MoDCs (left panel) and mature MoDCs (right panel) cultured under various conditions: Ctrl (GM-CSF+IL-4, black), acetate (GM-CSF+IL-4+acetate, red), butyrate (GM-CSF+IL-4+butyrate, blue), and propionate (GM-CSF+IL-4+propionate, green). Data are from 8 independent experiments. *$p < 0.05$, **$p < 0.01$, ***$p < 0.001$.

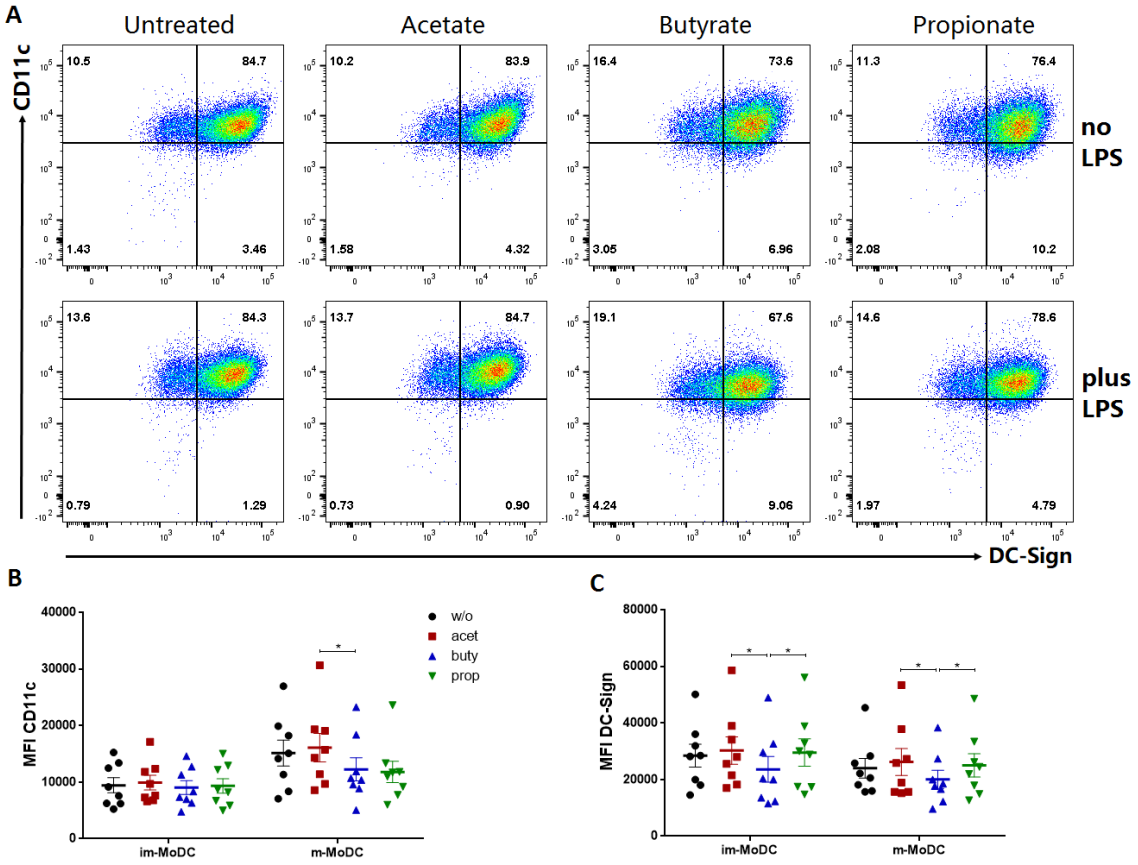

Figure 5.8 The effects of SCFAs on the expression of CD11c and DC-Sign in human MoDCs.

(**A**) Representative pseudocolour dot plots showing the effects of SCFAs on the expression of CD11c and DC-Sign of both im-MoDCs (upper) and mature MoDCs (maturation with LPS for 24 hours, lower). Scattered dot plots showing the MFI of (**B**) CD11c and (**C**) DC-Sign of both im-MoDCs (left panel) and mature MoDCs (right panel) cultured under various conditions: Ctrl (GM-CSF+IL-4, black), acetate (GM-CSF+IL-4+acetate, red), butyrate (GM-CSF+IL-4+butyrate, blue), and propionate (GM-CSF+IL-4+propionate, green). Data are from 8 independent experiments. *$p < 0.05$.

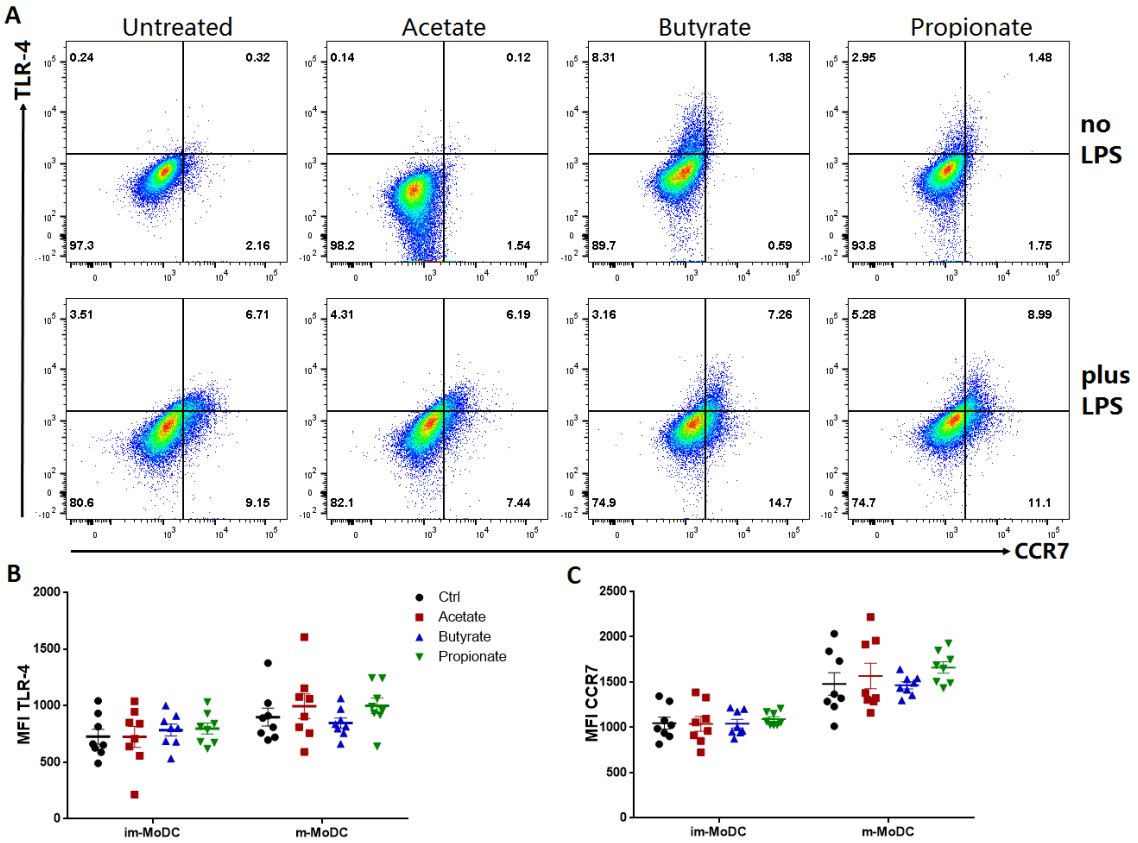

Figure 5.9 The effects of SCFAs on the expression of TLR-4 and CCR7 in human MoDCs.

(**A**) Representative pseudocolour dot plots showing the effects of SCFAs on the expression of TLR-4 and CCR7 of both im-MoDCs (upper) and mature MoDCs (maturation with LPS for 24 hours, lower). Scattered dot plots showing the MFI of (**B**) TLR-4 and (**C**) CCR7 of both im-MoDCs (left panel) and mature MoDCs (right panel) cultured under various conditions: Ctrl (GM-CSF+IL-4, black), acetate (GM-CSF+IL-4+acetate, red), butyrate (GM-CSF+IL-4+butyrate, blue), and propionate (GM-CSF+IL-4+propionate, green). Data are from 8 independent experiments. *$p < 0.05$, **$p < 0.01$.

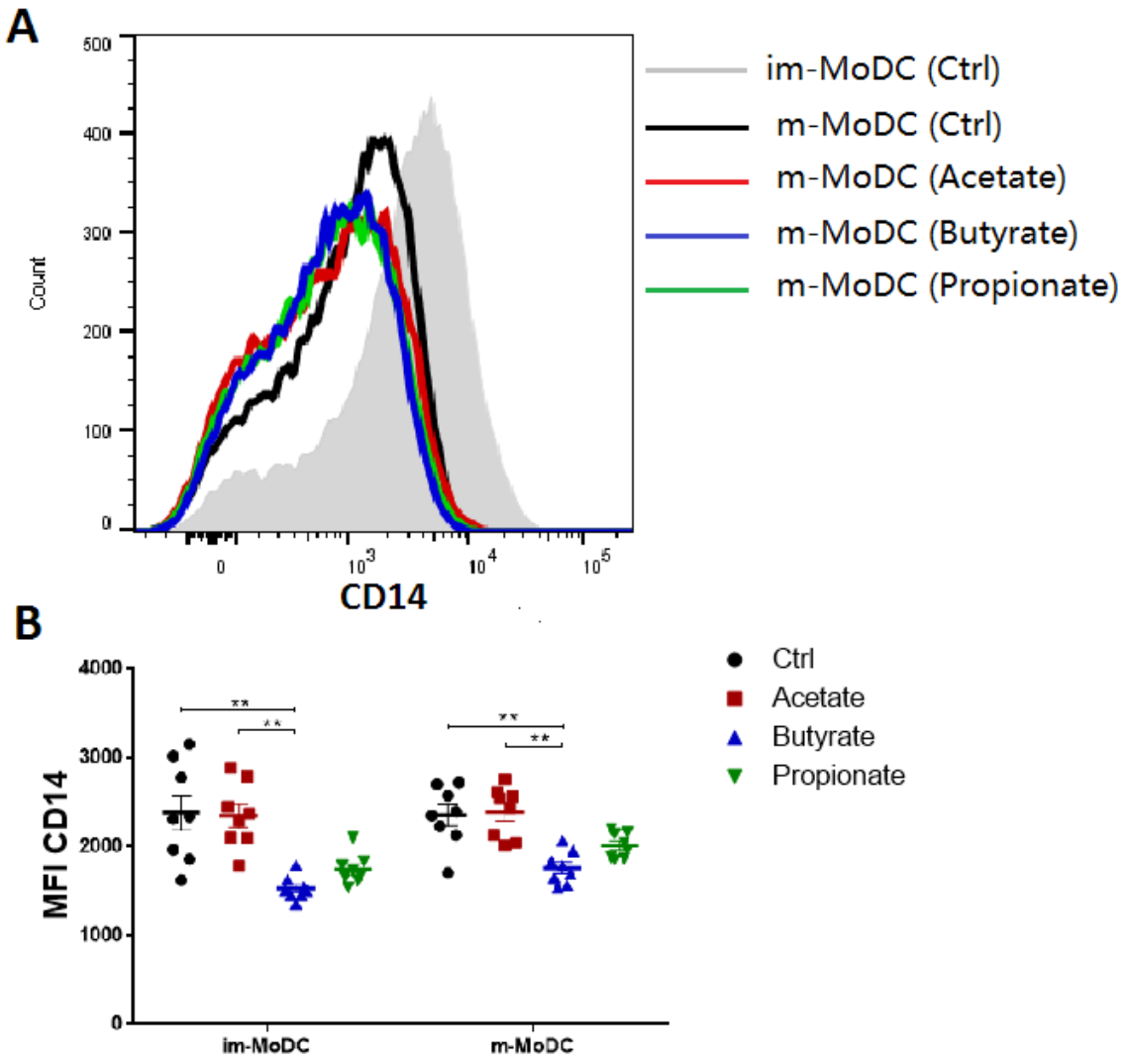

Figure 5.10 The effects of SCFAs on the expression of CD14 in human MoDCs.

(**A**) Representative histogram showing the effects of SCFAs on the expression of CD86 and HLA-DR of im-MoDCs (grey shade) and mature MoDCs (maturation with LPS for 24 hours, different colour lines). (**B**) Scattered dot plots showing the MFI of CD14 of both im-MoDCs (left panel) and mature MoDCs (right panel) cultured under various conditions: Ctrl (GM-CSF+IL-4, black), acetate (GM-CSF+IL-4+acetate, red), butyrate (GM-CSF+IL-4+butyrate, blue), and propionate (GM-CSF+IL-4+propionate, green). Data are from 8 independent experiments. $^{**}p < 0.01$.

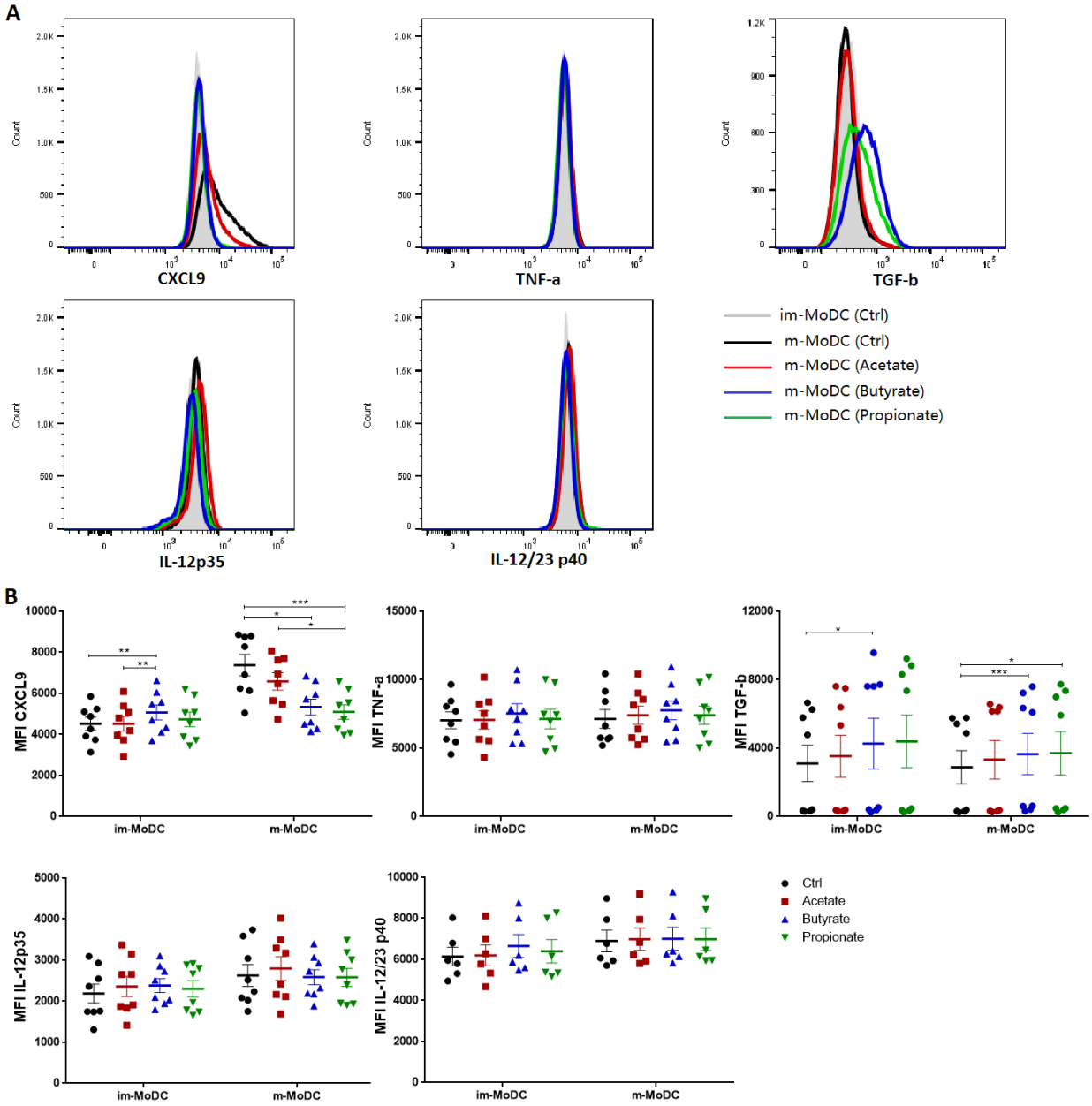

Figure 5.11 The effects of SCFAs on the expression of cytokine signatures in human MoDCs.

(**A**) Representative histogram showing the effects of SCFAs on the expression of CXCL9, TNF-α, TGF-β, IL-12 p35, and IL-12/35 p40 of im-MoDCs (grey shade) and mature MoDCs (maturation with LPS for 24 hours, different colour lines). (**B**) Scattered dot plots showing the MFI of CXCL9, TNF-α, TGF-β, IL-12 p35, and IL-12/35 p40 of both im-

MoDCs (left panel) and mature MoDCs (right panel) cultured under various conditions: Ctrl (GM-CSF+IL-4, black), acetate (GM-CSF+IL-4+acetate, red), butyrate (GM-CSF+IL-4+butyrate, blue), and propionate (GM-CSF+IL-4+propionate, green). Data are from 8 independent experiments. *$p < 0.05$, **$p < 0.01$, ***$p < 0.001$.

5.3.2 The Proliferation of Naïve CD4$^+$ T Cells were Influenced by SCFA-treated Monocyte-Derived Dendritic Cells

We learnt from the previous section that SCFAs, especially butyrate and propionate, affected the proliferation, maturation of MoDCs. Next, we wanted to test the function of these SCFA-treated MoDCs and how they influence the proliferation of autologous naive CD4$^+$ T cells. So, MoDCs were first pulsed with anti-CD3, then added to the FACS sorted autologous naïve CD4$^+$ cells at a ratio of 1:4-5, in the presence of IL-2 only for 5 days (Section 2.2.3.4). The same phenotypic markers used for iTregs were also tested for the proliferated CD4$^+$ T cells, since these markers were closely related to immune tolerance.

CD4$^+$ T cells differentiated from naive CD4$^+$ cells in the presence of butyrate and propionate treated im-MoDCs had higher expression levels of Foxp3, GITR, ICOS, HLA-DR, PD-1, PD-L1, and CTLA-4, whereas the expression of these markers was similarly lower in CD4$^+$ cells cultured with control or acetate treated im-MoDCs (Figure 5.12 and 5.13). CD127 expression, on the contrary, was least in butyrate and propionate treated groups. There was no difference in the expression of CD39. All these results were not significant (small sample size, n=6).

Naive CD4$^+$ T cells were also cultured in the presence of m-MoDCs treated under various conditions. The same trend of upregulated immune tolerance markers was found in these settings as well (Figure 5.14). Cells differentiated in the presence of butyrate-treated m-MoDCs had the highest expression of ICOS, PD-1, PD-L1, and CTLA-4; followed by propionate treated cells. The expression of Foxp3 and HLA-DR was also higher in CD4$^+$ cells cultured with butyrate and propionate treated m-MoDCs, while CD127 expression

was least in butyrate and propionate treated groups. There was no difference in the expression of CD39 and GITR.

These results suggested: a) all the immune tolerance related phenotypic markers were upregulated in the $CD4^+$ T cells cultured with butyrate and propionate treated MoDCs; and b) butyrate and propionate treated MoDCs (both im-MoDCs and m-MoDCs) were more tolerogenic, compared to control and acetate treated MoDCs.

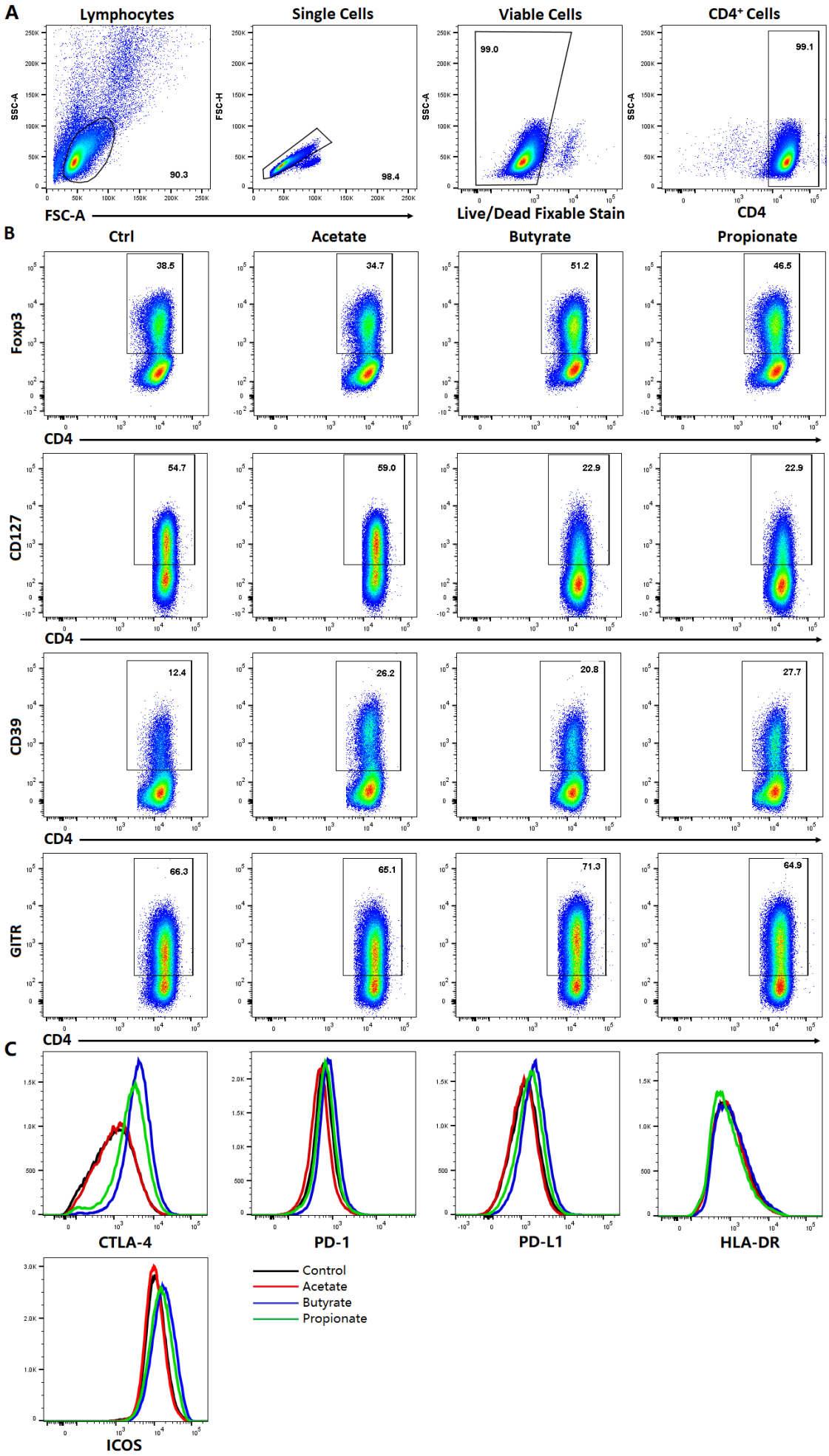
A
Lymphocytes
Single Cells
Viable Cells
CD4⁺ Cells
SSC-A
FSC-H
SSC-A
SSC-A
90.3
98.4
99.0
99.1
FSC-A
Live/Dead Fixable Stain
CD4
B
Ctrl
Acetate
Butyrate
Propionate
Foxp3
38.5
34.7
51.2
46.5
CD4
CD127
54.7
59.0
22.9
22.9
CD4
CD39
12.4
26.2
20.8
27.7
CD4
GITR
66.3
65.1
71.3
64.9
CD4
C
CTLA-4
PD-1
PD-L1
HLA-DR
ICOS
Control
Acetate
Butyrate
Propionate

Figure 5.12 The effects of SCFAs treated MoDCs on the proliferation of naive $CD4^+$ T cells.

(A) Flow cytometric gating strategy for lymphocytes, single cells, viable cells, and $CD4^+$ T cells. **(B)** The representative pseudocolour dot plots showing the percentage of Foxp3, CD127, CD39, and GITR gated on $CD4^+$ T cells cocultured with autologous MoDCs treated under different conditions (from left to right: control, acetate, butyrate, and propionate). **(C)** The representative histograms showing CTLA-4, PD-1, PD-L1, HLA-DR, and ICOS expression of $CD4^+$ T cells cocultured with autologous MoDCs treated under different conditions: control (black line), acetate (red line), butyrate (blue line), and propionate (green line).

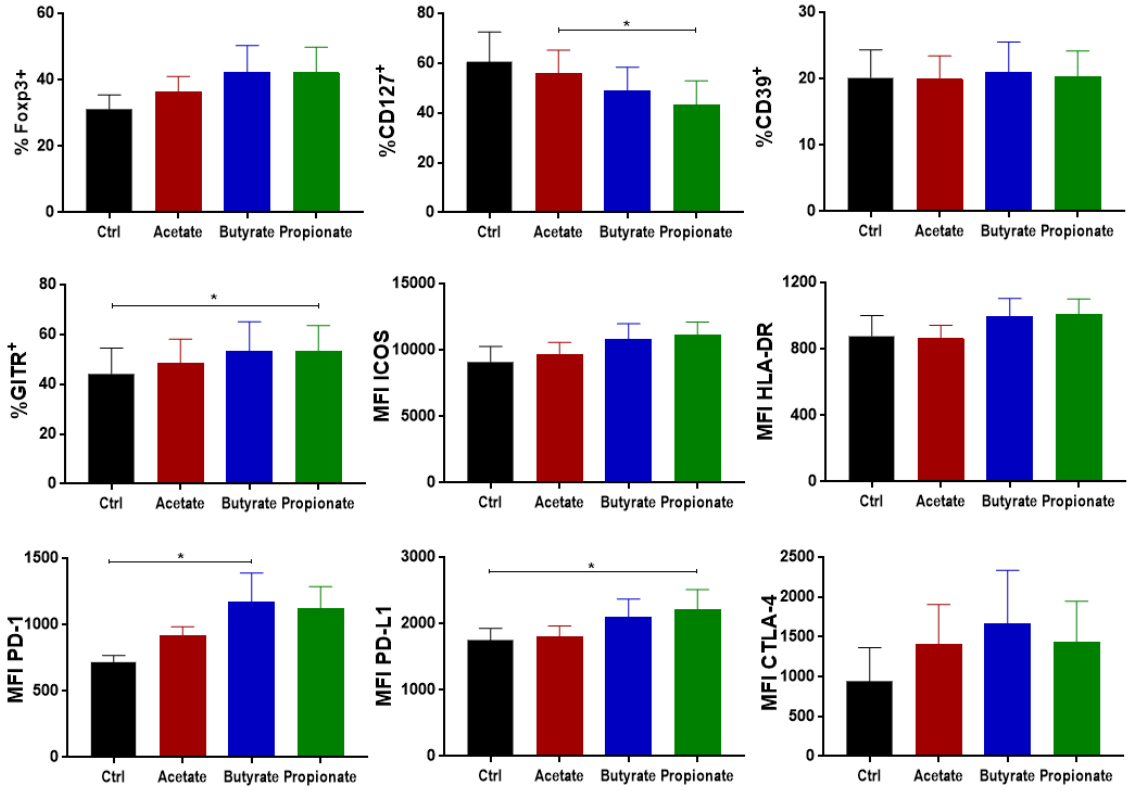

Figure 5.13 The effects of SCFAs treated im-MoDCs on the proliferation of naive CD4$^+$ T cells.

The summary bar graphs showing the % Foxp3$^+$, % CD127$^+$, % CD39$^+$, % GITR$^+$, MFI ICOS, MFI HLA-DR, MFI PD-1, MFI PD-L1, and MFI CTLA-4 of CD4$^+$ T cells cocultured with autologous im-MoDCs treated under different conditions (from left to right): control (black), acetate (red), butyrate (blue), and propionate (green). Data represent 6 independent experiments. *$p < 0.05$.

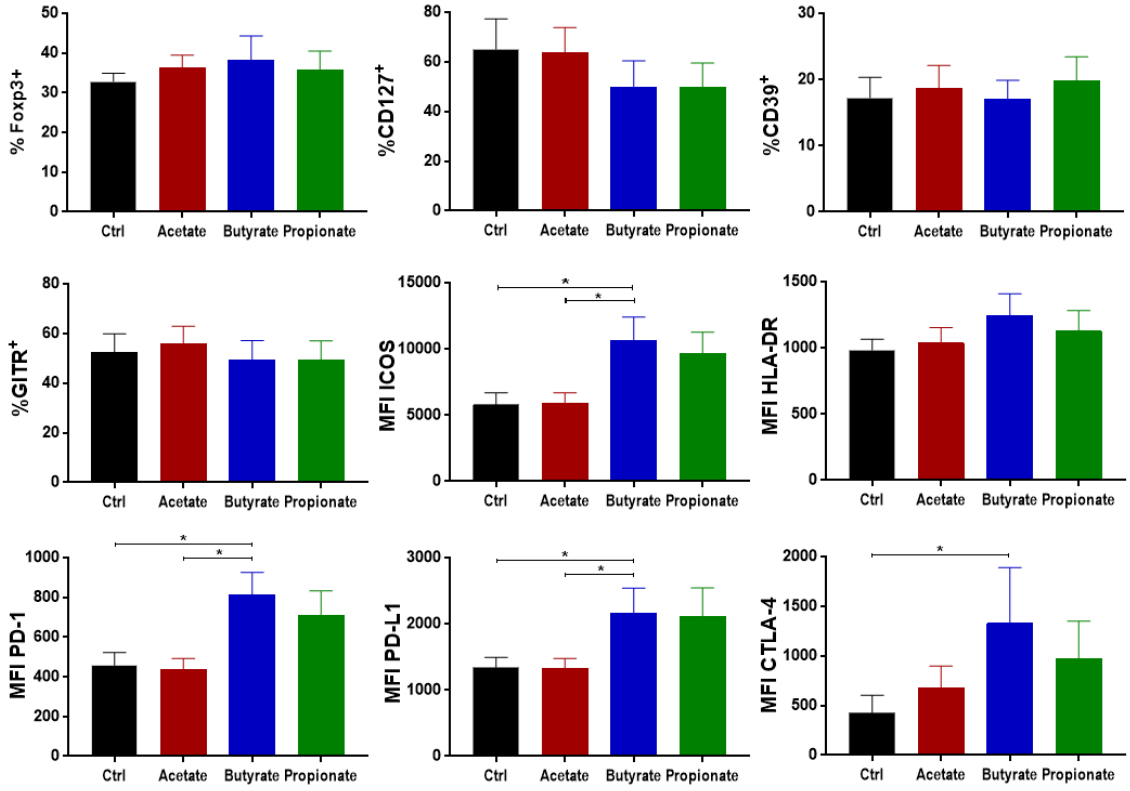

Figure 5.14 The effects of SCFAs treated m-MoDCs on the proliferation of naive CD4$^+$ T cells.

The summary bar graphs showing the % Foxp3$^+$, % CD127$^+$, % CD39$^+$, % GITR$^+$, MFI ICOS, MFI HLA-DR, MFI PD-1, MFI PD-L1, and MFI CTLA-4 of CD4$^+$ T cells cocultured with autologous m-MoDCs treated under different conditions (from left to right): control (black), acetate (red), butyrate (blue), and propionate (green). Data represent 6 independent experiments. *$p < 0.05$.

5.3.3 $CD4^+$ T Cells cocultured with SCFA-treated Monocyte-Derived Dendritic Cells Had Enhanced Suppressive Capacity

We learnt from the previous section that all the immune tolerance related phenotypic markers were upregulated in the $CD4^+$ T cells cultured with butyrate and propionate treated MoDCs. To test whether these $CD4^+$ T cells were tolerogenic or immunogenic, we cocultured them with freshly bead-isolated autologous CFSE-labelled $CD4^+CD25^-$ responder cells under various ratios for 3 days *in vitro*, then compared the differences in the proliferation of responder cells (section 2.2.3.2).

$CD4^+$ cells cultured in the presence of SCFA-treated im-MoDCs reduced the *in vitro* proliferation of autologous $CD4^+CD25^-$ cells, compared to cells cultured with control im-MoDCs (Figure 5.15 and 5.16). Butyrate-treated cells had the highest suppressive capacity, followed by propionate and acetate. However, it was only statistically significant at suppressor: responder cell ratio 1:2.

The results of $CD4^+$ cells cultured in the presence of SCFA-treated m-MoDCs mimicked the same trend found above. Compared to the cells cultured with control m-MoDCs, SCFA-treated MoDCs increased the suppressive capacity of $CD4^+$ cells at all suppressor: responder cell ratios from 1:1 to 1:4. However, only butyrate-treated cells reached significance at suppressor: responder cell ratios 1:2 and 1:4.

These results demonstrate that a) T cells induced with SCFA-treated MoDCs had increased suppressive capacity; b) addition of SCFAs, including acetate, butyrate and propionate, did skew MoDCs towards tolerogenic status.

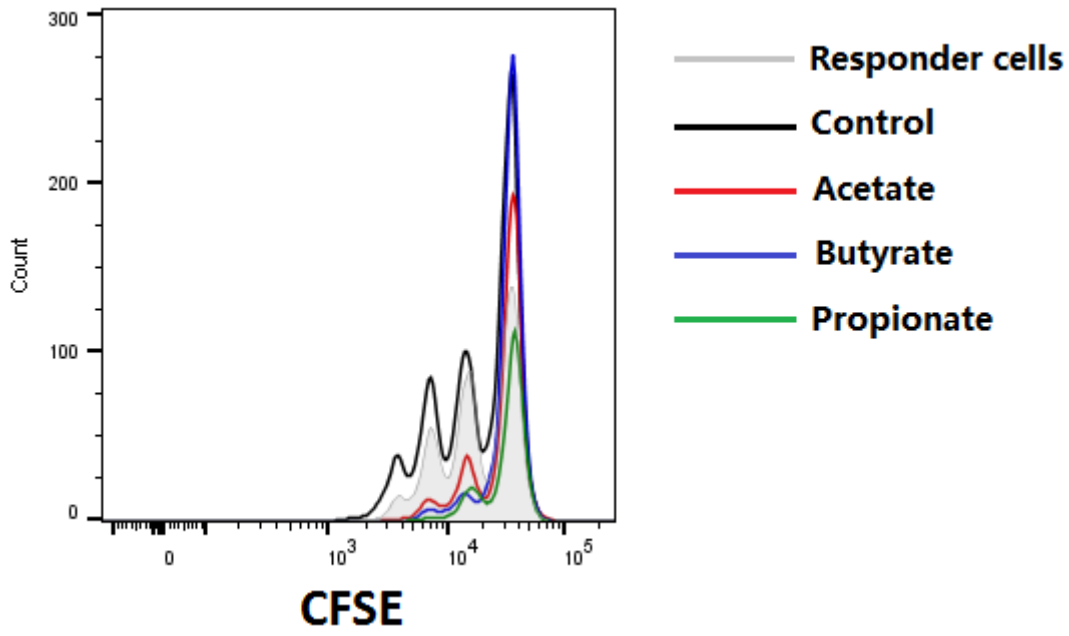

Figure 5.15 The effects of CD4$^+$ T cells cocultured with SCFAs treated MoDCs on the proliferation of responder cells.

Representative histogram showing the proliferation of responder cells alone (grey shaded) and compared with CD4$^+$ cells cultured from naïve CD4$^+$ cells in the presence of im-MoDCs treated under different conditions: control (black line), acetate (red line), butyrate (blue line), and propionate (green line). Data show suppressor: responder ratio of 1:2.

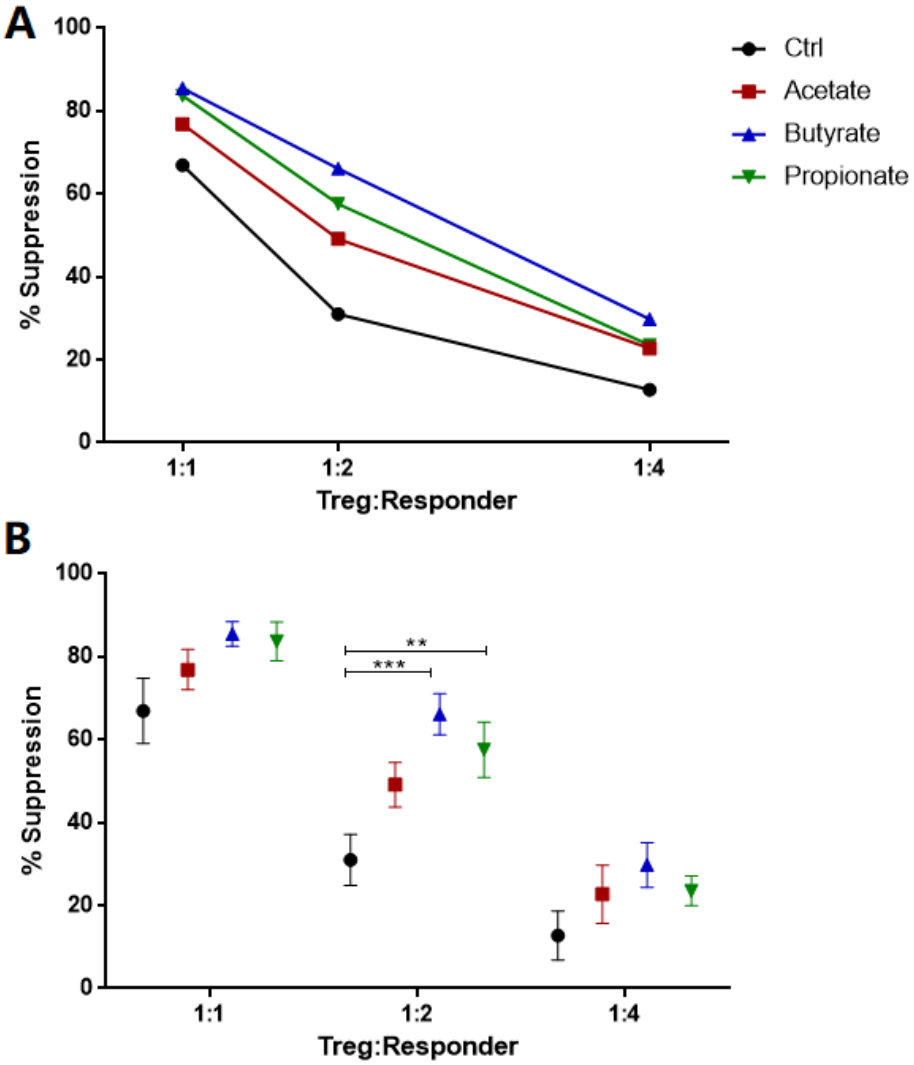

Figure 5.16 CD4$^+$ T Cells cocultured with SCFAs treated im-MoDCs Had Enhanced Suppressive Capacity.

(**A**) Line graph showing percentages of suppression using CD4$^+$ cells cultured from naïve CD4$^+$ cells in the presence of im-MoDCs treated under different conditions: control (black line), acetate (red line), butyrate (blue line), and propionate (green line). Various suppressor/responder ratios ranging from 1:1 to 1:4 were applied. (**B**) Summary dot plots (down) showing the statistical analysis of the suppressive capacity of these im-MoDC induced CD4$^+$ cells. Data represent 6 independent experiments in each group. $^{**}p < 0.01$, $^{***}p < 0.001$.

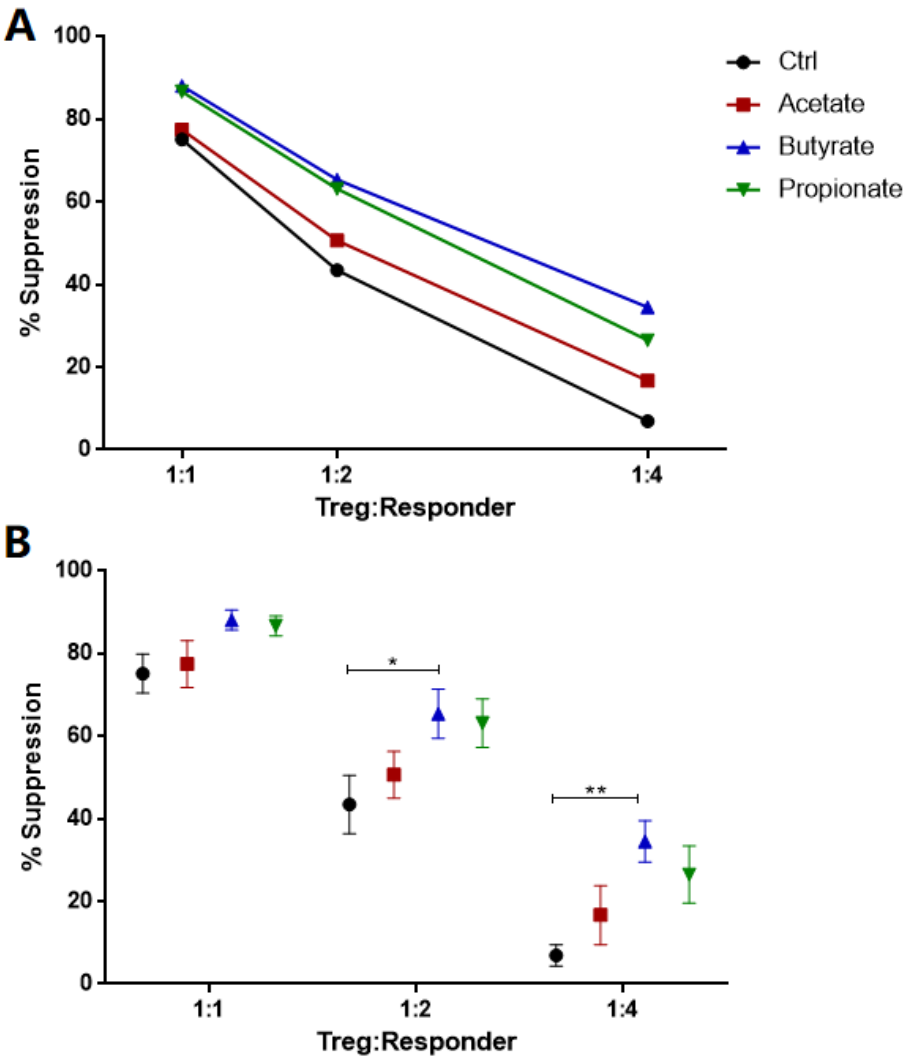

Figure 5.17 CD4$^+$ T Cells cocultured with SCFAs treated m-MoDCs Had Enhanced Suppressive Capacity.

(**A**) Line graph showing percentages of suppression using CD4$^+$ cells cultured from naïve CD4$^+$ cells in the presence of m-MoDCs treated under different conditions: control (black line), acetate (red line), butyrate (blue line), and propionate (green line). Various suppressor/responder ratios ranging from 1:1 to 1:4 were applied. (**B**) Summary dot plots (down) showing the statistical analysis of the suppressive capacity of these m-MoDC induced CD4$^+$ cells. Data represent 6 independent experiments in each group. *$p < 0.05$, **$p < 0.01$.

5.4 Discussion

In this chapter, we thoroughly investigated the precise role of SCFAs on DCs, and extended the existing understanding from butyrate to other two major types of SCFAs. Our observations were consistent with previous studies on butyrate. We found that both butyrate and propionate could significantly inhibit the differentiation and maturation of MoDCs, while the addition of acetate again was less effective. In addition, butyrate and propionate also modulate cytokine production by downregulating the secretion of chemokines and pro-inflammatory cytokines. Therefore, butyrate and propionate skewed MoDCs towards a tolerogenic status.

The functional capacity of these SCFA-treated MoDCs was also tested. *In vitro* suppression assays demonstrated that $CD4^+$ T cells cocultured with SCFA-treated MoDCs (both immature and mature MoDCs) had significantly higher suppressive capacities compared to control MoDCs. We also tested the expression of immune tolerance related phenotypic markers, such as GITR, CD39, ICOS, PD-1, and PD-L1. The flow cytometric analyses suggested that all these markers were upregulated on $CD4^+$ T cells co-cultured with butyrate and propionate treated MoDCs (both immature and mature MoDCs), compared to control and acetate treated MoDCs.

It is postulated that SCFAs exert their regulatory effects on macrophages and DCs via either HDAC inhibition or GPRs-mediated signalling. SCFAs act as HDAC inhibitor to reduce the expression of NF-kB transcriptional factor and suppress the expression of pro-inflammatory cytokines of DCs, thus promoting Treg induction (276, 323-325). In addition, the GPR109a signalling pathway could also be activated by butyrate, skewing

murine colonic macrophages and dendritic cells towards tolerogenic phenotype to promote the differentiation of Treg cell and IL-10 producing cells (295).

However, it has recently been questioned whether HDAC inhibition and GPR109a signalling were mandatory for butyrate to effectively promote a tolerogenic phenotype in human DCs (372). Only the simultaneous addition of both niacin and TSA could replicate the effects of butyrate, whereas single niacin (another GPR109a ligand) or TSA (a general HDAC inhibitor) treatment was insufficient to induce tolerogenic MoDCs. In addition, silencing of GPR109a led to the ineffectiveness of butyrate.

In contrast to these observations, the results presented in this chapter showed that propionate also had similar tolerogenic effects as butyrate and to a lesser extent, acetate. Most importantly, both propionate and acetate are not GPR109a ligands (293). Therefore, we assumed that GPR109a signalling is only a complementary mechanism for butyrate, and HDAC inhibition is the major pathway for SCFA-mediated tolerogenicity. Unfortunately, there is still a paucity in the understanding of underlying mechanisms of how SCFAs induce tolerogenic DCs and prime Treg cell induction, thus further studies are warranted.

Collectively, our results proved that the addition of SCFAs, especially butyrate and propionate, skewed MoDCs towards tolerogenic status in humans. They influenced the function of DCs via significantly reduced co-stimulation, MHC presentation and pro-inflammatory cytokines. These tolerogenic DCs upregulated immune tolerance related genes, and in turn influenced T cell polarization (the ratio between Treg cells and Teff cells), hence resulting in a higher suppressive capacity of the $CD4^+$ T cells. To our knowledge, this is for the first time that butyrate, as well as propionate and acetate, has

been shown to effectively induce tolerogenic DCs and these DCs can prime T cell responses towards a tolerogenic status. In addition to Treg cells, this chapter provides *in vitro* evidence of the effects of SCFAs on another type of immune cells.

Chapter 6 – Short Chain Fatty Acids Regulate Immune Tolerance related Gene Expression in Human Peripheral Mononuclear Cells *in vitro*

6.1 Introduction

PBMCs consists of various types of immune cells, including B cells, T cells, NK cells, monocytes, and very rare dendritic cells (<2%). Due to the presence of these highly sophisticated immune cells and their crosstalk networks, PBMCs have been widely used in immunological studies. Research had been recently conducted on the effects of SCFAs on human PBMCs, but restricted mainly to their effects on cytokine production. PBMCs are capable of producing pro-inflammatory cytokines (such as TNF-α, IL-12 and IFN-γ) in response to different stimuli. Meanwhile, anti-inflammatory cytokines (such as IL-10 and TGF-β1) are released as well. Asarat et al. measured the cytokine levels (including IL-1β, IL-2, IL-6, IL-12, IL-17, IL-21, IL-23, TNF-α, IFN-γ, and TGF-β1) produced by PBMCs in the presence of LPS with or without SCFAs using ELISA. The addition of SCFAs significantly reduced the production of pro-inflammatory IL-1β, IL-2, IL-6, IL-12, IL-17, IL-21, TNF-α, and IFN-γ, with a lesser reduction of IL-23 and TGF-β1. Moreover, IL-10 secretion was augmented by SCFAs, particularly butyrate (373, 374).

SCFAs also exert their influence on the numbers of Th17 and Treg cells in human PBMCs. Asarat et al. found that the percentage of Th17 cells was reduced, while the percentage of Treg cells was increased in the presence of SCFAs. Among SCFAs, butyrate was the most effective inducer for Treg cells (373, 374). The mechanism was not investigated, but the changes in cytokine milieus may play an important role. The expression of the key immune tolerance related markers has not been examined yet.

Our results from the previous two chapters extensively explored the effects of SCFAs on the differentiation of human iTregs and MoDCs *in vitro*. Both these cell types are part of PBMCs. We found that butyrate and propionate, but not acetate, not only potently induced

highly functional iTregs, but also skewed the MoDCs towards a tolerogenic status. These results were concluded based on *in vitro* experiments using a single cell type, which did not mimic the actual *in vivo* environment where cell crosstalk is always present.

Therefore, the aims of this chapter are to: a) explore the effects of SCFAs (including acetate, butyrate and propionate) on human PBMCs, in terms of phenotypic expression; b) assess and compare the expression of phenotypic markers related to Treg-mediated immune tolerance on other T cell subsets.

6.2 Subjects

To determine the effect of SCFAs on the human PBMCs, a total of 7 healthy adult volunteers were recruited. Individuals with any history of autoimmune disease or allergies were excluded.

6.3 Results

To explore the effects of SCFAs (including acetate, butyrate and propionate) on human PBMCs in terms of phenotypic expression, and to assess and compare the expression of phenotypic markers related to Treg-mediated immune tolerance on other T cell subsets, freshly isolated PBMCs were stimulated with anti-CD3/anti-CD28 in the presence of IL-2, with or without SCFAs for 5 days (Section 2.2.3.5).

6.3.1 The tolerogenic effects of SCFAs (including acetate, butyrate and propionate) on human PBMCs

Figure 6.1 showed the gating strategy for all the T cell subsets, including $CD4^+$ cells, $CD4^+Foxp3^+$ cells, $CD4^+Foxp3^-$ cells, $CD8^+$ cells, $CD8^+Foxp3^+$ cells, and $CD8^+Foxp3^-$

cells. The percentage of $Foxp3^+$ cells within $CD4^+$ cells was much lower when treated with butyrate and propionate, compared to cells treated under normal condition or with acetate (approximately 22% versus 27%) (Figure 6.2). The addition of propionate resulted in the least amount of $Foxp3^+$ cells within $CD8^+$ cells, followed by butyrate, control and acetate. As for the expression of CD39 and CD127, the addition of SCFAs did not make any difference to the expression in any of the T cell subsets (Figure 6.3 and 6.4).

As for other phenotypic markers related to immune tolerance, the expression of PD-1, PD-L1, CTLA-4, GITR and ICOS were consistently higher in all T cell subsets when treated with butyrate compared to control (Figure 6.4). The effects of acetate were similar to that of propionate, both of which were to a lesser extent compared to butyrate.

These results suggested that SCFAs could potentiate the expression of immune tolerance related phenotypic markers on human PBMCs *in vitro*, and these SCFA-induced differential expression patterns were the same regardless of the Foxp3 expression or type of T cells.

6.3.2 The same effects of SCFAs on different T cell subsets

Next, we wanted to assess and compare the expression of phenotypic markers related to Treg-mediated immune tolerance on other T cell subsets. It was interesting to find that there was a comparable frequency of $Foxp3^+$ cells within $CD8^+$ cells (20-30%) to that within $CD4^+$ cells (Figure 6.2). Another finding was that around 60% of $CD8^+$ cells expressed CD39, whereas in $CD4^+$ cells, this number dropped to 20% (Figure 6.3). Interestingly, in both $CD4^+$ and $CD8^+$ cells, the percentages of $CD39^+$ cells were only slightly higher in $Foxp3^+$ cells, compared to $Foxp3^-$ cells. CD127 expression was slightly

less in the $CD4^+Foxp3^+$ subset, while there were no differences found in other subsets (Figure 6.4).

The expression was generally higher for other Treg-related immune tolerance markers in $CD4^+$ cells compared to $CD8^+$ cells, but to a different extent (Figure 6.4). The biggest difference was in the expression of PD-L1, followed by GITR, PD-1, ICOS and CTLA-4. In terms of the influence by the Foxp3 expression, the phenotypic expression of PD-1, GITR, ICOS and CTLA-4 were all upregulated in $Foxp3^+$ cells compared to $Foxp3^-$ cells, whereas PD-L1 expression remained unchanged.

To conclude, all the immune tolerance related phenotypic markers were expressed in different T cell subsets. Most of them were relatively rich in $CD4^+$ T cells, whereas the expression of CD39 was much less. These markers were also upregulated in the $Foxp3^+$ cells upon *in vitro* stimulation.

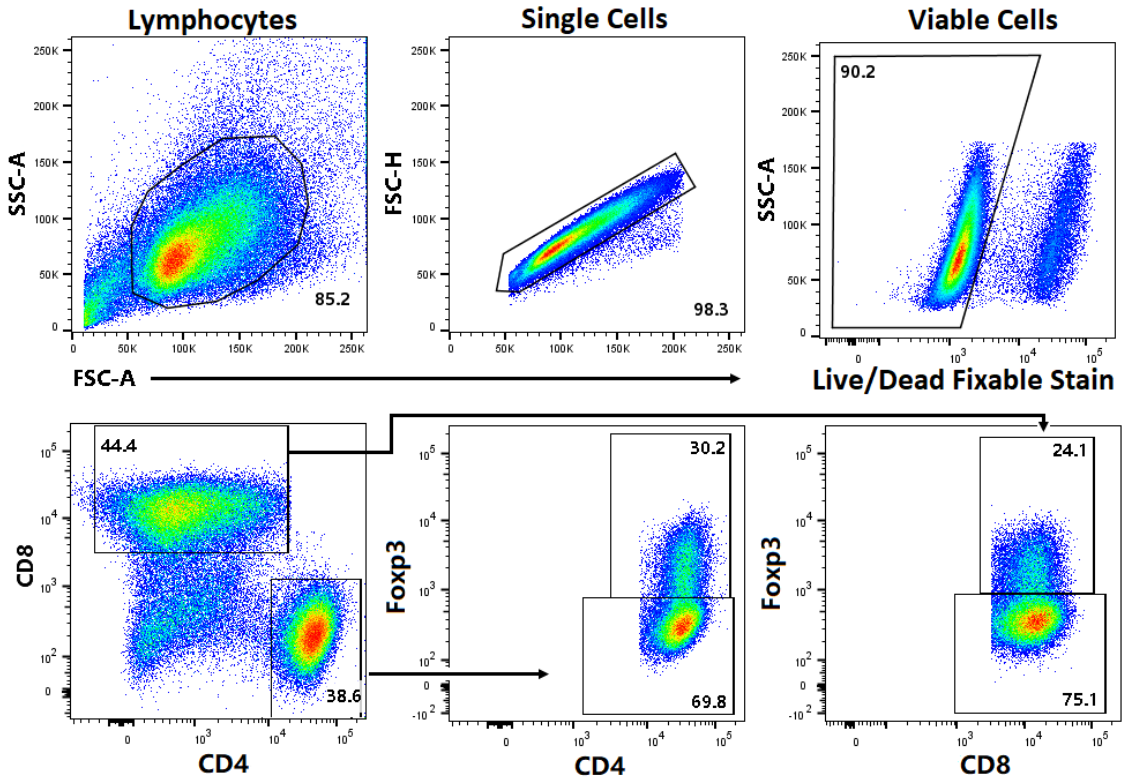

Figure 6.1 Flow cytometric gating strategy.

Flow cytometric gating strategy for lymphocytes, single cells, viable cells, $CD4^+$ cells, $CD8^+$ cells and $Foxp3^+$ cells gated on $CD4^+$ and $CD8^+$ cells after adult PBMCs culture.

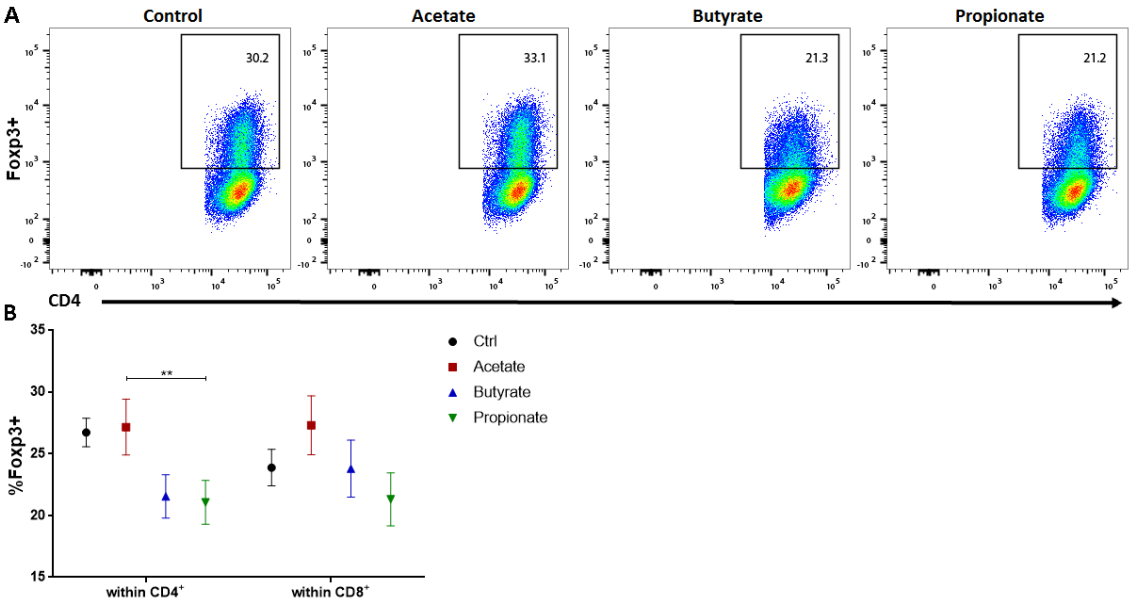

Figure 6.2 The effect of SCFAs on the Foxp3 expression of human PBMCs.

(**A**) Representative pseudocolour plots showing percentage of $Foxp3^+$ cells gated on $CD4^+$ cells cultured from adult PBMCs under various conditions: control (IL-2), acetate (IL-2+acetate), butyrate (IL-2+butyrate), and propionate (IL-2+propionate). (**B**) Summary dot plots showing $\%Foxp3^+$ gated on $CD4^+$ cells (left panel) and $CD8^+$ cells (right panel) from adult PBMCs (n=7). $*p < 0.05$.

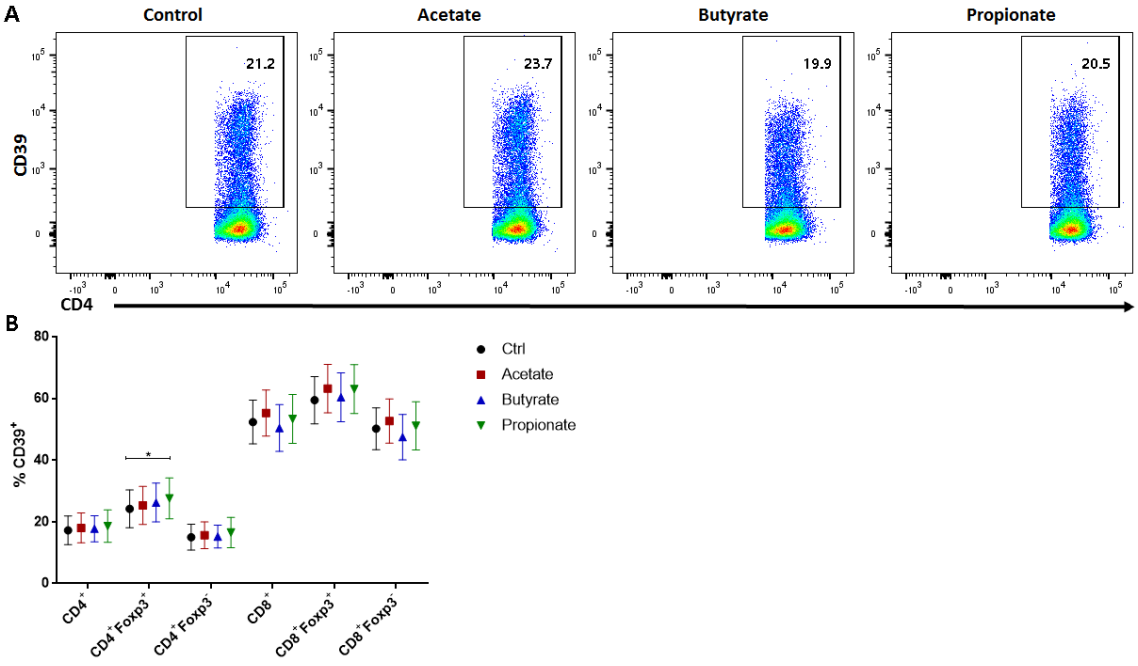

Figure 6.3 The effect of SCFAs on the CD39 expression of human PBMCs.

(**A**) Representative pseudocolour plots showing percentage of $CD39^+$ cells gated on $CD4^+$ cells cultured from adult PBMCs under various conditions: control (IL-2), acetate (IL-2+acetate), butyrate (IL-2+butyrate), and propionate (IL-2+propionate). (**B**) Summary dot plots showing $\%CD39^+$ gated on $CD4^+$ cells, $CD4^+Foxp3^+$ cells, $CD4^+Foxp3^-$ cells, $CD8^+$ cells, $CD8^+Foxp3^+$ cells, and $CD8^+Foxp3^-$ cells (from left to right) from adult PBMCs (n=7). $*p < 0.05$.

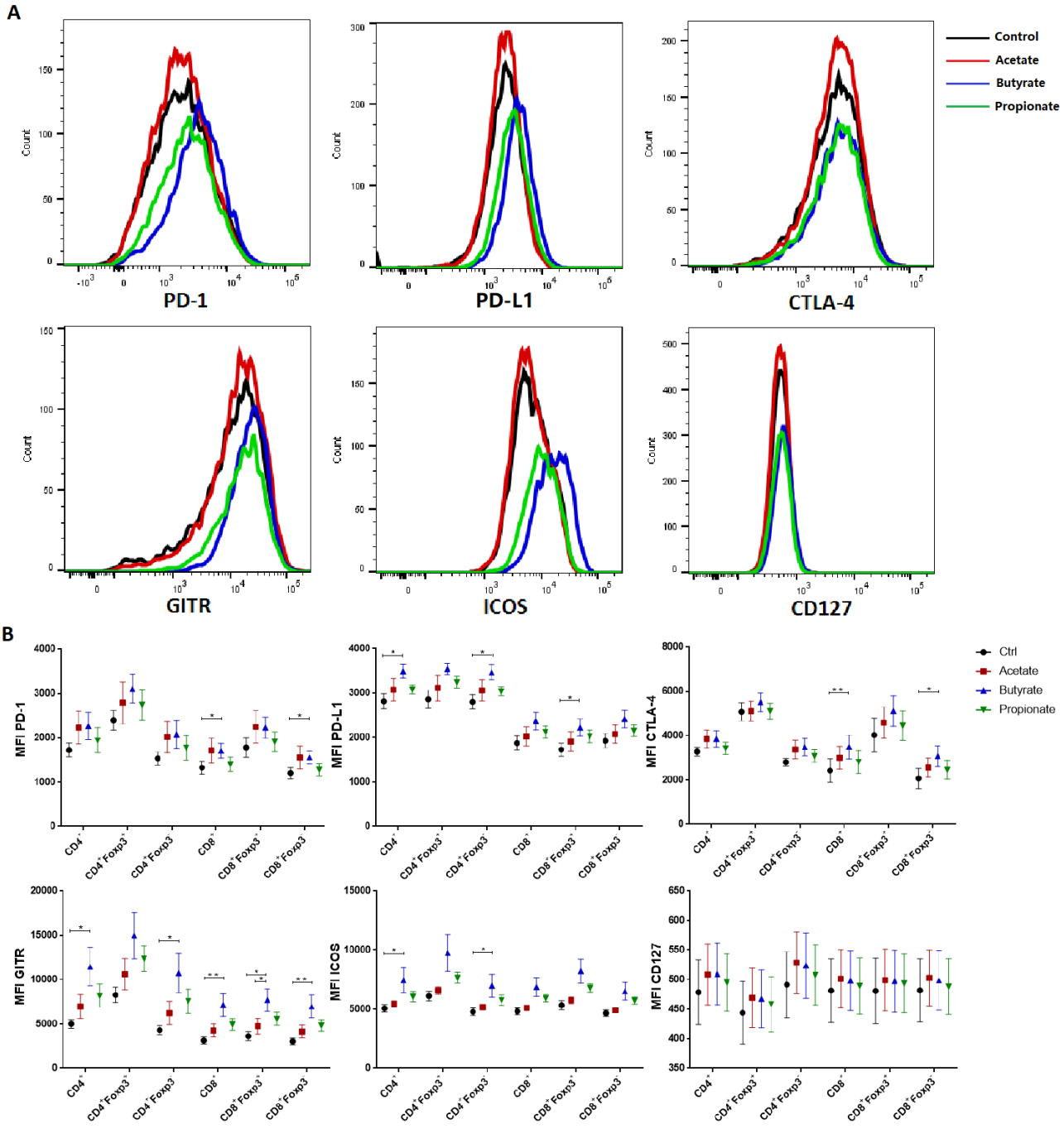

Figure 6.4 The effect of SCFAs on the expression of phenotypic markers of human PBMCs.

(**A**) Representative histograms showing PD-1, PD-L1, CTLA-4, GITR, ICOS and CD127 expression of $CD4^+$ cells cultured from adult PBMCs under various conditions: control

(IL-2), acetate (IL-2+acetate), butyrate (IL-2+butyrate), and propionate (IL-2+propionate). (**B**) Summary dot plots showing MFI PD-1, PD-L1, CTLA-4, GITR, ICOS and CD127 of $CD4^+$ cells, $CD4^+Foxp3^+$ cells, $CD4^+Foxp3^-$ cells, $CD8^+$ cells, $CD8^+Foxp3^+$ cells, and $CD8^+Foxp3^-$ cells (from left to right) from adult PBMCs (n=7). *$p < 0.05$, **$p < 0.01$.

6.4 Discussion

It was clearly demonstrated in the previous two chapters that SCFAs exerted their tolerogenic effects on human iTregs as well as MoDCs *in vitro*. In this chapter, we extended our understanding of SCFAs to PBMCs, which simulate the *in vivo* environment with cell crosstalk. We were able to show that SCFAs could potentiate the expression of phenotypic markers related to Treg-mediated immune tolerance in different T cell subsets apart from Tregs *in vitro*. These SCFA-induced differential expressions were consistent regardless of the Foxp3 expression. Moreover, the expression of all phenotypic markers related to Treg-mediated immune tolerance was not restricted to only $CD4^+$ T cells, and they also had a relatively lower expression in $CD8^+$ T cells, except for CD39. These markers were likely to be upregulated in $Foxp3^+$ cells upon *in vitro* stimulation.

It was postulated that SCFAs regulate T cells directly via either HDAC inhibition (288-290) or energy metabolism by converting to Acetyl-CoA (316). Our ChIP-qPCR results from Chapter Four demonstrated the possible mechanism of HDAC inhibition. However, SCFAs could also exert their regulatory effects on T cells indirectly by other immune cells. They suppressed the expression of pro-inflammatory cytokines of DCs via HDAC inhibition, thus changing T cell polarization conditions (276). Alternatively, the activation of GPR109a by butyrate skewed colonic macrophages and dendritic cells towards tolerogenic phenotype to promote the T cell differentiation (295).

A previous study on human PBMCs showed that the addition of SCFAs significantly reduced the production of pro-inflammatory cytokines while it increased the IL-10 secretion (373, 374). It proved that the immunological cytokine milieu was altered by SCFAs in order to favour T cell differentiation towards a tolerogenic status (more Treg

cells and IL-10 producing cells than effector T cells). Our findings provide another perspective as to how SCFAs manipulate immune cells *in vitro*. We have shown that in addition to cytokine changes, SCFAs also modify the expression of genes related to Treg-mediated immune tolerance in T cell subsets other than Treg cells, mostly via HDAC inhibition. Among the three types of SCFAs, butyrate is the most effective in promoting the regulatory effects. Previous chapters have already demonstrated the close interlink between gene expressions and the *in vitro* suppressive capacity of T cells. Therefore, SCFAs also exert their tolerogenic effects on human PBMCs *in vitro*.

Moreover, it was noticed that the percentage of $Foxp3^+$ cells within $CD8^+$ cells was similar to that within $CD4^+$ cells, between 20% and 30%. Since the percentage of $CD8^+$ Tregs was normally much less (0.1–1%) in *ex vivo* human PBMCs (42), it was another proof that Foxp3 was only an activation marker, but not an iTreg specific marker.

In summary, our findings of the broad tolerogenic effects of SCFAs on T cell phenotypes, together with the previous cytokine results, indicate that through the production of anti-inflammatory cytokines and the induction of immune tolerance related gene expression, SCFAs have *in vitro* anti-inflammatory effects and exert their tolerogenic effects on immune tolerance in peripheral blood.

Chapter 7 – General Discussion and Conclusions

7.1 Treg cell transplacental programming during early life

Whilst there is abundant indirect evidence from clinical observations for transplacental immune programming (215-217), there is a paucity of direct mechanistic data. It is known that appropriate stimulation to the maternal immune system *in utero* may educate and shape the fetal immune system, specifically Treg cells. In BALB/c mouse models, maternal Th1 and regulatory immune responses to schistosome infection could protect the offspring from the onset of allergic airway inflammation. Associated schistosome-specific cytokine and gene expression changes were also seen within the fetal-maternal interface (228). In addition, the offspring of tolerised mice were completely protected against asthma due to the transplacental transfer of allergen-specific IgG (218). Furthermore, microbial stimulation of the pregnant mice could lead to decreased levels of atopic sensitisation and asthma in the offspring (229-231). Chapter 3 summarises collaborative works to prove that Treg cell transplacental immune programming occurs, and partially explained the mechanism behind this phenomenon.

Our group previously made a surprising discovery that there was a specific and significant correlation of Treg cells between maternal-fetal dyads (209). Gene microarray analysis suggested that IL-10 pathway may contribute to the Treg alignment between maternal-fetal dyads and it was confirmed by the specific alignment of serum IL-10 at a protein level (209). The mechanism by which IL-10 contributes to Treg generation was investigated in section 3.3. We showed that in addition to TGF-β, IL-10 enhanced the phenotype of iTreg cells and augmented the suppressive capacity of these iTreg cells *in vitro* (1). However, whether IL-10 signalling in naïve $CD4^+$ T cell differentiation is dispensable for pTreg cell differentiation *in vivo* remained unclear.

In addition to anti-inflammatory cytokine IL-10, various other environmental factors, such as pregnancy-related hormones or microbiota metabolites-SCFAs, also contribute to the transplacental programming of Treg cells (331, 342). In section 3.1.1, our collaborators were able to demonstrate how the maternal microbial composition influences fetal thymus and Treg cell development. The absence of maternal gut microbiota (GF mice) led to significantly reduced fetal thymus size, fewer thymic $CD4^+$ T cells and $Foxp3^+$ Treg cells. Supplementation of acetate in maternal drinking water, which is the most abundant SCFA in human serum (279), could rescue all these reductions in thymus size and thymic output. These results are also consistent with the fetal-maternal correlation of serum acetate levels we found in human pregnancy, which implies that maternal acetate likely crosses the placenta. TCR sequencing data in section 3.1.2 from our collaborators also suggests that fetal antigen receptor immunity is not inherited, but rather driven by local immunomodulatory factors. Taken together, it can be concluded that maternally acquired metabolites (acetate) play an important role in shaping fetal thymic development and output, hence exerting their influences on fetal immunity.

Apart from *in utero* stage, the programming of T cells happens after birth as well (333). (375). Together with our collaborators from the Children's Hospital at Westmead, we found that circulating $\beta7^+$ gut homing Treg cells were most abundant early in life and decreased with age. Treg cells probably acquire gut tropism early in their development. However, the induction of β7 expression mostly occurs after thymic emigration. Furthermore, *in vitro* experiment done by myself showed that IL-2 specifically skews the expression of human Treg cell homing molecules to favour gut homing. Overall, section 3.2 indicates that human naïve Treg cells are primed early in life for gut tropism, which reinforces the important role of early gut microbial colonization in shaping the developing

immune system. It seems likely that human naïve Treg cells also likely acquire their gut homing molecules outside the thymus, where they encounter environmental cues, such as SCFAs.

The concept of Treg cell transplacental programming provides a new perspective for non-pharmaceutical approach during pregnancy. Maternal dietary interventions, prebiotic intakes or direct SCFAs supplementation, may alleviate or treat various non-communicable diseases, or even prevent the development of autoimmune diseases in early life. Mouse models have confirmed the beneficial effects of maternal SCFAs supplementation on the development of allergic airway disease, asthma and haematopoiesis in the offspring (221, 376). Additionally, butyrate or propionate supplementation commenced antenatally ameliorated and interfered with the course of Type 1 diabetes in the offspring of rats (377). Moreover, the relationship between maternal butyrate supplementation and improved lipid metabolisms, insulin resistance and mitochondria biogenesis have also been studied in rats (378-380).

However, there were only observational studies in humans, showing the association between maternal SCFAs and diseases. One prospective cohort study with 1,538 pregnant women showed that increased dietary fibre intake in early pregnancy was associated with decreased preeclampsia risk (381). Dietary modification during pregnancy is mainly designed to alleviate gestational diabetes (382). The specific preventive mechanisms induced by different SCFA supplementation approaches are still poorly understood.

7.2 The tolerogenic effects of SCFAs on immune tolerance, particularly Treg cell differentiation

In addition to the context of pregnancy, SCFAs also have profound regulatory effects on immune tolerance. Although their effects have been consistently proven in different animal models, their efficacy in modulating immune cells in humans still remains unclear. Therefore, we conducted *in vitro* experiments using primary cells from humans to show the precise role of SCFAs in different types of immune cells, especially Treg cells. The results presented in Chapter 4, 5 and 6 highlight the important role of SCFAs in immune tolerance, particularly in Treg cell physiology.

The most essential finding is that we are the first to demonstrate the effectiveness of SCFAs in Treg cell differentiation *in vitro* in humans. The addition of butyrate and propionate, but not acetate, potentiated the expression of phenotypic markers and augmented the suppressive capacity of induced human Treg cells. Compared to CBMCs, adult PBMCs had a completely different induction pattern with a reduced level of activation. We postulated that this differential induction patterns of adult iTregs may account for the inconsistent effectiveness of human iTregs as well as the concealment of SCFAs' effects, considering the higher proportion of non-activated iTregs in adults. ChIP analyses also provided additional evidence for the observed differential induction patterns in adults. The epigenetic histone acetylation due to SCFAs treatment initiated much later in adult cells compared to cord blood cells.

Additionally, we have also proved the tolerogenic effects of SCFAs on other immune cells in humans, including MoDCs and different T cell subsets. We showed that both butyrate and propionate, but not acetate, inhibited the differentiation and maturation of

MoDCs, skewing them towards immature or tolerogenic status. When cocultured with naive $CD4^+$ T cells, these tolerogenic MoDCs upregulated the immune tolerance related phenotypic markers and increased the suppressive capacity of cultured $CD4^+$ T cells. These tolerogenic effects of SCFAs also applied to different T cell subsets regardless of their Foxp3 expression *in vitro*.

Another interesting finding is that acetate, which is the most abundant SCFA in human serum (279, 285, 286), only showed reduced or almost no effects on Treg cell and MoDC differentiation. In animal models, acetate also failed to promote the generation of pTregs and tolerogenic DCs *in vivo*, but could still promote the accumulation of Treg cells in the colon (276-278). Moreover, Woetmann et al. found that acetate (1mM) only exerted minimum effects on the gene expression of human MoDCs *in vitro* (369). We postulated that the inefficiency of HDAC inhibition by acetate contributed to this result. Acetate normally has a little effect on the HDAC activity (383). However, this lack of HDAC inhibition by acetate might change depending on the cell type and the concentration used in the experiments. In HeLa Mad 38 cells transfected with an HDAC-dependent reporter gene construct, acetate was unable to trigger HDAC inhibition at all concentrations tested (0-20mM) (326). On the contrary, T cells were shown to be suppressed by acetate in a dose-dependent manner. Acetate had significant HDAC inhibitor activity at concentrations (10mM) much higher than butyrate and propionate (290). In our experiments, the concentration used for acetate was only 1mM (same as Woetmann's group), which is much lower than the concentration needed to be effective. This specific concentration was chosen because it did not affect the cell viability and it was more similar to the concentration found in peripheral blood rather than colon concentration.

Finally, we confirmed that Foxp3 is only an *in vitro* activation marker rather than a surrogate human iTregs marker. It is always upregulated upon different types of *in vitro* stimulation (such as anti-CD3) and correlates to the activation status. Our findings are consistent with previous findings in humans. $CD4^+$ and $CD8^+$ T cells can transiently up-regulate the Foxp3 expression upon *in vitro* stimulation without acquiring Treg cell suppressive activity (60, 61). In addition, there is also a $CD4^+Foxp3^+$ subpopulation in human peripheral blood with no suppressive activity which even produces pro-inflammatory IL-17 upon activation (354). Whilst Foxp3 is not suitable for defining iTregs, the expression patterns of GITR, ICOS, CD39, PD-1 and PD-L1 of iTregs treated with SCFAs were in accordance with functional assay results. It was demonstrated in our MoDC and PBMCs cultures that SCFAs induced the same expression patterns of these markers on other immune cells. Collectively, these results suggest that GITR, ICOS, CD39, PD-1 and PD-L1 are potential candidate markers for the human *in vitro* induced Treg cells, and their expression levels are closely related to the SCFA-mediated immune tolerance.

In conclusion, butyrate and propionate can potentiate the expression of immune tolerance related phenotypic markers via HDAC inhibition, promote the differentiation of tolerogenic human iTregs and MoDCs *in vitro*, and augment the suppressive capacity of iTregs.

7.3 SCFAs as new immune therapeutic manipulation

Immune therapy has developed rapidly during the past two decades. Treg cell immunotherapy (adoptive Treg cell transfer) have been promising for treating human autoimmune diseases and preventing GVHDs (106). Compared to non-specific immunosuppressive drugs, Tregs are safer, more effective, and have fewer side effects. Due to limited numbers of Tregs and instability of the *in vitro* induced human Tregs, *ex vivo* expanded nTregs are most commonly used for immunotherapy. However, there are several problems encountered during the process, including difficulty in isolating adequate amounts of nTregs and deterioration of the function after several rounds of proliferation. Therefore, new immune therapeutic manipulation methods are needed.

It is well known that gut microbiota and its metabolites, SCFAs, have profound tolerogenic effects on immune homeostasis, thus play a beneficial role in various diseases. Since diet is closely interlinked with the composition of gut microbiota and SCFAs production, various human and animal studies have been conducted to reveal the therapeutic effects of SCFAs on the prevention and treatment of autoimmune and inflammatory diseases by dietary modification or direct SCFAs supplementation.

In mice, it was proved that a high fibre diet altered the gut microbiota and increased the production of SCFAs, particularly acetate and butyrate (384). It promoted oral tolerance and protected mice from the peanut allergy. This effect was dependant on mucosal $CD103^+$ DCs, which promote differentiation of Treg cells via epithelial GPR43 and immune cell GPR109a. Specialised diets designed to release acetate or butyrate also provided protection against Type 1 diabetes in NOD mice (352). Since key features of this autoimmune disease were inversely associated with SCFAs concentrations, NOD

mice were fed with different types of diets offering acetate, or butyrate, or combined acetate and butyrate production. Combination feeding achieved complete protection, whereas acetate or butyrate feeding only had partial effects, thus suggesting that acetate and butyrate might operate through distinct mechanisms. They found that acetate affected auto-reactive T cells in lymphoid tissues through B cells while butyrate augmented Treg cells. Apart from allergies and Type 1 diabetes, high fibre diet and acetate supplementation significantly reduced blood pressure, cardiac and renal fibrosis, and left ventricular hypertrophy in a hypertensive mouse model (385).

In humans, dietary intervention studies have been carried out within different populations, including obese men and women, IBD remission patients (Australian Clinical Trial Registry Number 12614000271606, http://www.anzctr.org.au) (386), irritable bowel syndrome patients (Australian Clinical Trial Registry Number 12614000271606, http://www.anzctr.org.au) (387), and healthy individuals (388). These dietary interventions resulted in changes in the gut microbiota composition and faecal or serum SCFAs concentrations. However, the prognosis of disease was not significantly influenced. There are also clinical trials investigating the beneficial effects of butyrate enema on colonic health (National Clinical Trial 02451189, https://www.clinicaltrials.gov). The role of acetate and propionate has also been studied on the satiety and glucose homeostasis for obese population. A double-blind, randomized clinical trial was conducted to investigate the effects of adjunct butyrate therapy in shigellosis (389). Butyrate enema alleviated the symptoms due to an early decline in inflammatory cells of rectal mucosa and pro-inflammatory cytokines in the stool. More clinical trials have been registered and started their recruitment. For example, an

investigation about the effects of sodium butyrate on the cognitive function in schizophrenia (National Clinical Trial 03010865, https://www.clinicaltrials.gov).

In conclusion, SCFAs offer a new approach as immune therapeutic manipulation. This new intervention is effective and non-pharmaceutical, aiming to lessen immunological defects and treat autoimmune and inflammatory diseases. Our results about the tolerogenic effects of SCFAs on human immune cells provide further theoretical support to this manipulation.

7.4 Limitations and future directions

7.4.1 Limitations

This thesis mainly focused on human studies. In contrast to animal models, human studies are limited by multiple cofounders, which are difficult to account for. In this thesis, we did not control for factors such as diet, age, gender, socioeconomic status and ethnicity. Moreover, the results from each chapter are from different cohorts, and we infer that these results from different cohorts would be consistent if applied to a single cohort.

7.4.2 Future directions

Our observational studies showed promising results of the tolerogenic effects of SCFAs, hence it might indicate that a high fibre diet, which would fuel the production of SCFAs, might be used as an intervention to prevent or treat allergies and autoimmune diseases. This simple dietary approach would have the potential to transform treatment for these aberrant immune responses in the future.

APPENDICES

Table S-1 Primers used for quantitative assessment of H3 or H4 histone acetylation by PCR following ChIP.

Target	Forward primer	Reverse primer
***FOXP3* promoter**	TTCTTTCCCCAGAGACCCTC	AGGGCTCATGAGAAACCACA
***FOXP3* CNS-2**	TACCACATCCACCAGCACC	TCCGCCATTGACGTCATG
***FOXP3* CNS-3**	CCTTTACTGTGGCACTGGG	GGATTTTCTTGGCCCTGCAA
***CTLA-4* promoter**	TGCCTAGACAAATCCTGCCA	TCCTGGAGTACAAGGGTCCT
***CD39* promoter**	GTCCTGTCCCACATCCAGAA	TGACAGTGTGAGACCCTGTC
***GITR* promoter**	GGCTCCATGGTTGAGGCTCT	GCGGCGTTTATAGCACCTTGT
***ICOS* promoter**	TGATTCAGAGAAGTAGGGTGGT	TGCTGGAAAGGAAGTGGGTT
***PD1* promoter**	AAGATCTGGAACTGTGGCCA	CTCAACCCCACTCCCATTCT
***PD-L1* promoter**	TCTTCCCGGTGAAAATCTCATT	TTCCTGACCTTCGGTGAAATC
RPL32 (control gene)	GGAAGTGCTTGCCTTTTTCC	GGATTGCCACGGATTAACAC

The Journal of Immunology

IL-10 Potentiates Differentiation of Human Induced Regulatory T Cells via STAT3 and Foxo1

Peter Hsu,*,† Brigitte Santner-Nanan,* Mingjing Hu,* Kristen Skarratt,* Cheng Hiang Lee,‡ Michael Stormon,‡ Melanie Wong,† Stephen J. Fuller,* and Ralph Nanan*

Foxp3$^+$ regulatory T cells (Tregs) play essential roles in maintaining the immune balance. Although the majority of Tregs are formed in the thymus, increasing evidence suggests that induced Tregs (iTregs) may be generated in the periphery from naive cells. However, unlike in the murine system, significant controversy exists regarding the suppressive capacity of these iTregs in humans, especially those generated in vitro in the presence of TGF-β. Although it is well known that IL-10 is an important mediator of Treg suppression, the action of IL-10 on Tregs themselves is less well characterized. In this article, we show that the presence of IL-10, in addition to TGF-β, leads to increased expansion of Foxp3$^+$ iTregs with enhanced CTLA-4 expression and suppressive capability, comparable to that of natural Tregs. This process is dependent on IL-10R–mediated STAT3 signaling, as supported by the lack of an IL-10 effect in patients with IL-10R deficiency and dominant-negative STAT3 mutation. Additionally, IL-10–induced inhibition of Akt phosphorylation and subsequent preservation of Foxo1 function are critical. These results highlight a previously unrecognized function of IL-10 in human iTreg generation, with potential therapeutic implications for the treatment of immune diseases, such as autoimmunity and allergy. ***The Journal of Immunology*****, 2015, 195: 3665–3674.**

Interleukin-10 is a pleiotropic cytokine that acts on various immune cells via IL-10R, which is composed of IL-10RA and IL-10RB (1). IL-10 signaling is critical for gut homeostasis, as demonstrated in patients with IL-10R or IL-10 loss-of-function mutations, who develop early-onset, severe inflammatory bowel disease (2, 3). Although it is well known that IL-10 is an important mediator of regulatory T cell (Treg) suppression (4, 5), the action of IL-10 on Tregs themselves is less well characterized. A previous study showed that IL-10 acts on Tregs through STAT3 to amplify Treg IL-10 production, which, in turn, is important for suppression of Th17 cell–induced inflammation in the gut (6). Another study suggested that IL-10 from gut APCs maintains Foxp3 expression of Tregs in the murine colitis model (7). Both of these murine studies focused on the role of IL-10 in established Tregs and not in the process of induced Treg (iTreg) induction.

Interestingly, although both IL-10 and IL-6 signal through phosphorylation of STAT3, they have distinct anti- and proinflammatory functions, with IL-6 being critical for Th17 cell induction (8) and unfavorable for iTreg induction (9, 10). In this context, the role of IL-10 in iTreg induction remains unanswered.

Importantly, there is significant contextual cross-talk between IL-10 and TGF (TGF-β) (11), with the latter being a well-known factor important for iTreg induction (12, 13). Of particular interest is that naive CD4$^+$ human, but not murine, T cells cultured in the presence of IL-2 and TGF-β appear to have poor suppressive function, despite Foxp3 expression (14, 15). This suggests that other factors may be required to bestow these induced Foxp3$^+$ cells with suppressive capability in humans. Indeed several factors, some natural [e.g., retinoic acid (16) and vitamin D (17)] and some pharmacological [e.g., rapamycin (18)], were identified to enhance human TGF-β–induced iTreg function.

Lastly, in a recent study, Shouval et al. (19) showed that defective IL-10 signaling in innate immune cells causes a profound defect in the generation of functional Tregs. This was associated with a diminished expression of IL-10 by M2 macrophages. In light of these findings, we explore the possibility that IL-10 may potentiate the generation of functional human iTregs.

Materials and Methods

Human subjects

Peripheral blood was obtained from healthy adult volunteers (n = 20), one patient with IL-10RA deficiency, and one patient with dominant-negative STAT3 mutation (hyper IgE syndrome [HIES]), as well as from their respective age- and sex-matched healthy controls. Mononuclear cells were isolated by Ficoll-Hypaque (Amersham Pharmacia, Piscataway, NJ) gradient centrifugation. The Ethics Committee of the Sydney West Area Health Service approved this project, according to the Declaration of Helsinki.

Flow cytometry

Surface Ab and intracellular staining for Foxp3 and cytokines was performed as described previously (20). For in vitro–cultured human cells, dead cells were excluded from the analysis using the LIVE/DEAD Fixable Dead Cell Stain Kit (Invitrogen, Carlsbad, CA.) For phospho-flow cytometry, cells were serum starved for 2–12 h before stimulation. For p-Stat3 analysis, cells were stimulated with IL-6 (100 ng/ml) at 37°C for 20 min, whereas for p-Foxo1 and p-Akt analysis, cells were activated through TCR-mediated signaling. On day 7, cells were activated by addition of anti-CD3 (OKT3, 0.1 μg/ml) and anti-CD28 (0.5 μg/ml, both

*Charles Perkins Centre Nepean, The University of Sydney, Kingswood, New South Wales 2751, Australia; †Department of Allergy and Immunology, Children's Hospital at Westmead, Westmead, New South Wales 2145, Australia; and ‡Department of Gastroenterology, Children's Hospital at Westmead, Westmead, New South Wales 2145, Australia

Received for publication November 19, 2014. Accepted for publication August 5, 2015.

This work was supported by the Nepean Medical Research Foundation of The University of Sydney and the Australian Women and Children's Research Foundation.

Address correspondence and reprint requests to Prof. Ralph Nanan, Charles Perkins Centre Nepean, Nepean Hospital, Kingswood, NSW 2751, Australia. E-mail address: Ralph.Nanan@sydney.edu.au

The online version of this article contains supplemental material.

Abbreviations used in this article: HIES, hyper IgE syndrome; iTreg, induced Treg; MFI, mean fluorescence intensity; nTreg, natural Treg; Treg, regulatory T cell; TSDR, Treg-specific demethylated region.

www.jimmunol.org/cgi/doi/10.4049/jimmunol.1402898

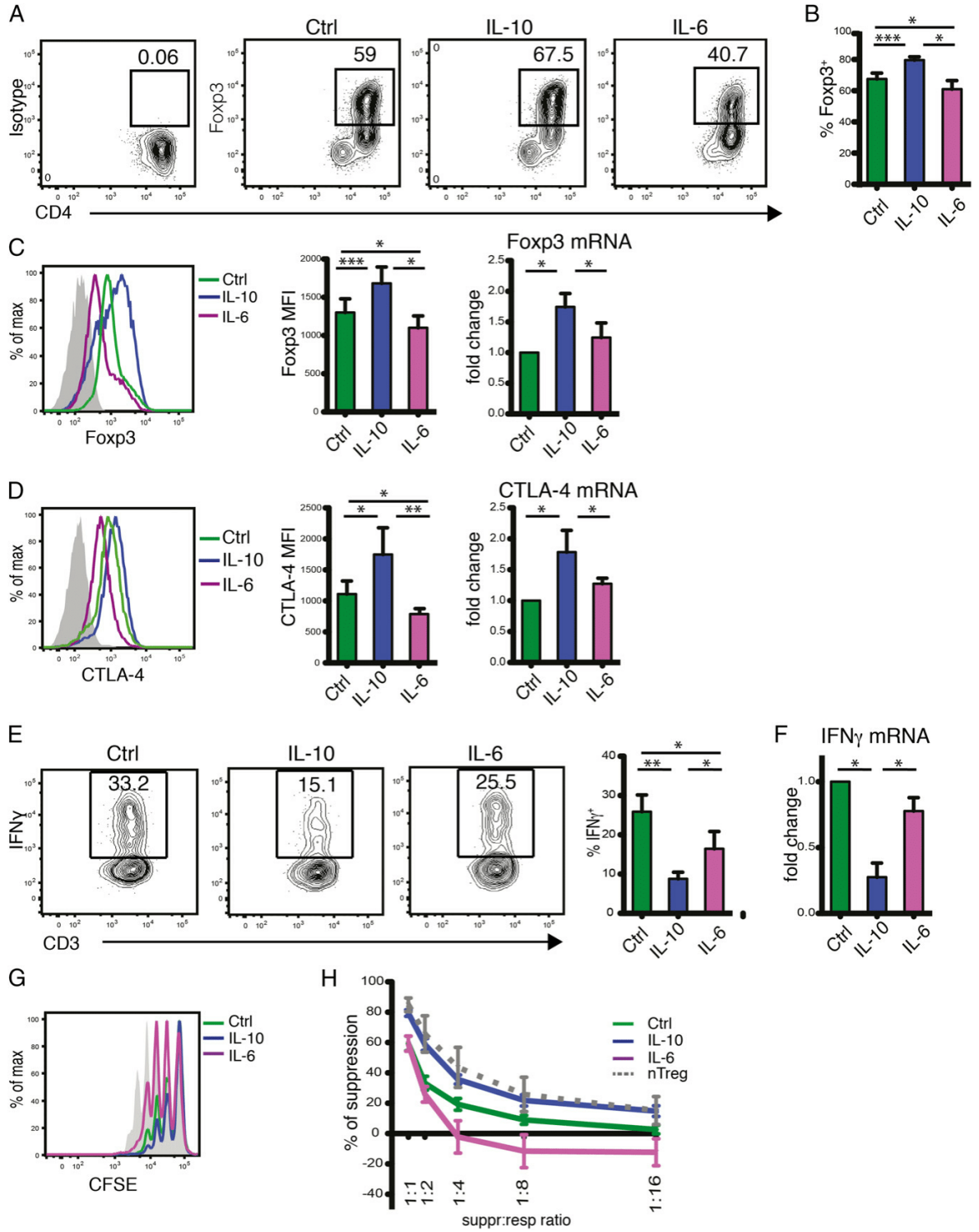

FIGURE 1. IL-10 potentiates human TGF-β–induced iTregs. (**A**) Representative contour plots gated on live $CD3^+CD4^+$ T cells showing percentage of $Foxp3^+$ cells induced after culture under various conditions: Ctrl (IL-2 + TGF-β), IL-10 (IL-2 + TGF-β + IL-10), and IL-6 (IL-2 + TGF-β + IL-6) compared with isotype control. (**B**) Summary bar graph showing mean and SEM of percentage of Foxp3 induced under various conditions (10 independent experiments). Foxp3 (**C**) and CTLA-4 (**D**) expression of live $CD3^+CD4^+$ T cells cultured under various conditions, as shown by representative histograms (left panels), summary bar graph of MFI (10 independent experiments) (*middle panels*), and mRNA expression as fold change relative to Ctrl (five independent experiments) (*right panel*). (**E**) Representative contour plots showing the percentage of IFN-γ–secreting cells within live $CD3^+CD4^+Foxp3^+$ T cells induced under various conditions and summarized by bar graph (*right panel*). (**F**) Data in (E) were confirmed by mRNA (*Figure legend continues*)

from eBioscience, San Diego, CA). Cells were washed once, and the primary mAbs were cross-linked by addition of anti-mouse IgG $F(ab')_2$ (20 μg/ml; Jackson ImmunoResearch, West Grove, PA) at 37°C for 20 min. An untreated/unstimulated sample was kept for each condition as control. Cells were fixed with BD Cytofix and permeabilized with Perm-Buffer III (both from BD Biosciences). Consecutive staining was performed according to the manufacturer's instructions. Data were read on a FACSVerse (BD Pharmingen), and data files were analyzed using FlowJo software (TreeStar, San Carlos, CA).

FACS

For flow cytometric sorting, human PBMCs were pre-enriched for $CD4^+$ T cells using the human $CD4^+$ T Cell Isolation Kit II (Miltenyi Biotec). Subsequently, cells were stained using a combination of FITC–anti-CD127, PerCp–eFluor 710–anti-CD45RO, BDV500–anti-CD4, and allophycocyanin–anti-CD25. Cells were sorted on a FACSAria cell sorter.

Generation of iTregs

Cells were cultured in RPMI 1640 supplemented with 10% FCS, L-glutamine (2 mM), penicillin (100 U/ml), and streptomycin (100 μg/ml). For in vitro Treg differentiation, flow cytometry–sorted naive non-Tregs ($CD4^+CD45RA^+CD25^-CD127^{hi}$) and Tregs ($CD4^+CD25^+CD127^{lo}$) were stimulated for 5 d with plate-bound anti-CD3 (OKT3, 10 μg/ml) and soluble anti-CD28 (CD28.2, 2 μg/ml; both from eBioscience) in the presence of rIL-2 (50 U/ml) or TGF-β (5 ng/ml) and in select cultures of IL-6 (10 ng/ml, all from PeproTech) or IL-10 (100 ng/ml; BD Pharmingen). Cells were cultured at 37°C in 48-well plates in supplemented RPMI 1640, at a concentration of 5×10^5 cells/ml. Cytokines were added on days 0 and 3. Cells were rested on day 5 in supplemented RPMI 1640 and IL-2 (50 U/ml) and harvested on day 7. Inhibitor of STAT3, StatticV (50 ng/ml), and inhibitor of Foxo1, AS1842856 (35 ng/ml; both from Millipore), were added to the indicated cultures.

For iTreg induction in the presence of monocytes, $CD14^+$ cells were enriched from PBMCs with magnetic bead selection and subsequently stimulated with LPS (100 ng/ml; Sigma-Aldrich). After 24 h, monocytes were harvested, washed twice, and cultured with FACS-sorted naive $CD4^+CD45RA^+CD25^-CD127^{hi}$ T cells at a ratio of 1:4. Cells were stimulated with plate bound anti-CD3, with the addition of TGF-β and IL-2, in the presence or absence of anti–IL-10 Ab (10 μg/ml; eBioscience). Subsequent cell treatment was the same as described above. Anti–IL-10 was added on days 0 and 3 of culture.

Suppression assays

Autologous bead-selected $CD4^+CD25^+$ cell–depleted cells were labeled with CFSE and cocultured at a concentration of 4×10^4 cells/well with ex vivo Tregs or iTregs at a ratio of 1:1 to 1:16. For suppression assays using iTregs from the IL-10RA patient, HIES patient, and healthy control, iTregs were cocultured with allogeneic responder cells. Cocultures were stimulated with magnetic bead–coated biotinylated CD3/CD28 at a cell/bead ratio of 4:1 (MicroBeads) or 60:1 (Dynabeads). At day 4, cells were analyzed by flow cytometry. Percentage of suppression was determined as the difference in proliferation between the negative control ($CD4^+CD25^-$ responder cells alone) and the coculture, expressed as a percentage of the former. Percentage of change in suppression was expressed as the difference in suppressive capacity between iTregs induced with or without IL-10 under both conditions (in the presence or absence of Foxo1 inhibitor).

Immunofluorescence microscopy

In vitro–generated Tregs were harvested on day 5, rested for 24 h, and stimulated with the indicated concentrations of anti-CD3 at 37°C for 20 min; controls were left untreated. Cell suspensions of 5×10^4 cells were added to each slide. Cells were fixed with 4% paraformaldehyde and permeabilized with Foxp3/Fixation Permeabilization Buffer and 3% BSA, according to the manufacturer's instructions. After blocking with Permeabilization Buffer and 3% BSA, cells were incubated with 1:400 diluted mouse anti-Foxo1 Ab (Abcam), followed by Alexa Fluor 555 anti-mouse secondary Ab. The slides were then incubated with mouse Alexa Fluor 488 anti-Foxp3 Ab. Subsequently, slides were incubated with DAPI for nuclear staining. Cover slips were placed and sealed, and images were acquired with a Nikon Eclipse 80i Fluorescence microscope.

Real-time PCR

Stimulated cells were stored at −80°C in RNA protect buffer (QIAGEN). RNA was extracted from cell pellets using an RNeasy Mini Kit (QIAGEN). RNA was retro-transcribed using a Tetro cDNA synthesis kit (Bioline). For real-time PCR reactions, a SensiMix SYBR No-ROX Kit (Bioline) was used. The ΔΔ cycle threshold method was used to quantify changes in expression relative to GAPDH. Sequences for suitable real-time PCR primers were sourced from the OriGene Web site, and primers were manufactured by Sigma-Aldrich.

Statistical analysis

Normality of distribution was determined by the Shapiro-Wilk test using SPSS software. For normally distributed data, the Student *t* test was used to assess statistically significant difference between two samples. For data with a nonnormal distribution, the Mann–Whitney test and the Wilcoxon signed-rank test was used for unpaired and paired data, respectively. Pearson's correlation coefficient was used for correlation studies. A p value < 0.05 was deemed statistically significant. For ANOVA in a group with multiple independent variables, a univariate ANOVA was used to determine statistical significance.

Results

IL-10, but not IL-6, enhances Foxp3 and CTLA-4 expression of human TGF-β–induced Tregs without affecting Foxp3 demethylation

To examine the role of IL-10 and IL-6 in human iTreg induction, FACS-sorted naive $CD4^+CD45RO^-CD25^-CD127^{hi}$ T cells (>97% purity; Supplemental Fig. 1A) were stimulated with anti-CD3/CD28 in the presence of IL-2 and TGF-β, with or without IL-10 or IL-6. On day 7, there was a modest, but significant, increase in the percentage of $Foxp3^+$ cells in cultures treated with IL-10 (Fig. 1A, 1B), which was associated with significantly enhanced Foxp3 and CTLA-4 expression, as assessed by mean fluorescence intensity (MFI). This was confirmed on the mRNA level (Fig. 1C, 1D). IL-6 had the opposite effect, causing reduced Foxp3 and CTLA-4 expression. We further show that IL-10–treated $Foxp3^+$ cells, and to a lesser extent, IL-6–treated $Foxp3^+$ cells, expressed significantly less IFN-γ, with reduced IFN-γ mRNA levels (Fig. 1E, 1F). Therefore, unlike IL-6, IL-10 enhances the phenotype of iTregs. IL-10 also significantly enhanced intracellular TGF-β, but not IL-10, expression (Supplemental Fig. 1B–E). We then examined the Foxp3 Treg-specific demethylated region (TSDR) demethylation status in four donors and found that TGF-β–induced cells had minimal TSDR demethylation, consistent with a previous study (21). The addition of IL-10 did not enhance this demethylation (Supplemental Fig. 1F), nor did it enhance the stability of Foxp3 expression 14 d after induction (data not shown).

IL-10 enhances, whereas IL-6 diminishes, the suppressive capacity of human TGF-β–induced iTregs

We next tested the suppressive function of cultured cells in vitro. IL-10–treated iTregs suppressed the in vitro proliferation of autologous $CD4^+CD25^-$ cells significantly better than did non-IL-10–treated iTregs. This was true at all suppressor/responder cell ratios (Fig. 1G, 1H) and was highly statistically significant (Supplemental Fig. 2A). The suppressive capability of IL-10–treated iTregs was comparable to that of FACS-sorted $CD4^+$

expression relative to Ctrl (bar graph; *right panel*) (six independent experiments). (**G**) Representative histograms (at suppressor/responder ratio of 1:4) showing proliferation of CFSE-labeled responder cells alone (shaded) or cocultured with Ctrl-, IL-10–, and IL-6–treated iTregs. (**H**) Percentage suppression of iTregs cultured under various suppressor/responder ratio and various conditions. Data show at least five independent experiments in each group. $*p < 0.05$, $**p < 0.01$, $***p < 0.001$.

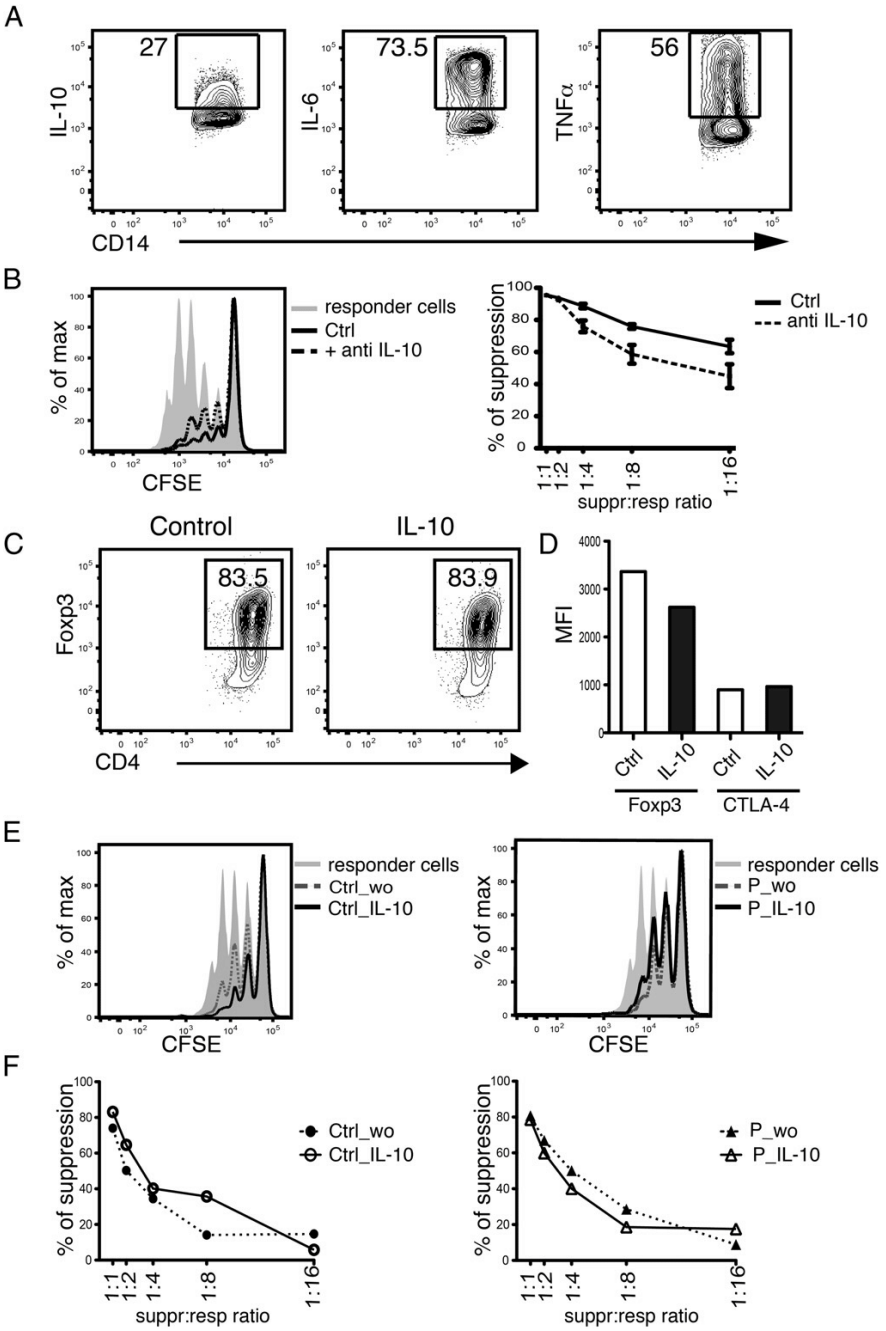

FIGURE 2. Monocyte-derived IL-10 enhances the suppressive function of iTregs. (**A**) Intracellular cytokine staining of peripheral blood monocytes after LPS stimulation. (**B**) Suppressive function of iTregs induced with LPS-stimulated monocytes in the presence (dashed line) or absence (solid line) of anti–IL-10 Ab. (**C**) In vitro Treg induction from naive $CD4^+$ T cells from an IL-10RA–deficient patient with impaired IL-10 signaling. Contour plots showing intracellular staining for Foxp3 in Treg cultures induced in the presence and absence of IL-10. (**D**) Bar graph of Foxp3 and CTLA-4 MFI from IL-10RA–deficient patient–derived iTregs. (**E**) Suppressive function of iTregs induced in the absence and presence of IL-10 in the IL-10RA–deficient patient (P_wo and P_IL-10) compared with a healthy donor (Ctrl_wo, Ctrl_IL-10). A representative histogram from a healthy donor and the patient (suppressor/responder ratio 1:8) is shown along with their respective suppression graph (**F**).

$CD25^+CD127^{lo}$ natural Tregs (nTregs) isolated from the same donor (≥97% purity; Supplemental Fig. 2B) and stimulated/rested in vitro for the same period (Fig. 1H). In stark contrast, IL-6 significantly reduced the suppressive function of TGF-β–induced iTregs (Fig. 1G, 1H). The same results presented as proliferation, rather than percentage suppression, are shown in Supplemental Fig. 2C. Anti–IL-10, anti–CTLA-4, and anti–TGF-β Abs each partially reversed the suppression mediated by these IL-10–treated iTregs, consistent with the suppressive mechanism of Tregs (Supplemental Fig. 2D, 2E). A separate set of

experiments was performed comparing Treg induction cultures in the presence or absence of TGF-β. Cells cultured without TGF-β exhibited less suppressive capacity; however, IL-10 also enhanced suppression in the absence of TGF-β (Supplemental Fig. 2F). Overall, these results demonstrate that, in contrast to IL-6, IL-10 augments the suppressive function of iTregs.

Monocyte-derived IL-10 enhances the suppressive function of iTregs

LPS stimulation of monocytes and gut tissue macrophages leads to the production of proinflammatory cytokines, as well as IL-10, which is thought to serve as a brake in this proinflammatory response (22). Therefore, we hypothesized that IL-10 secreted by monocytes can similarly enhance iTreg function. We first showed by flow cytometry that LPS-stimulated human peripheral blood monocytes express high levels of IL-10, in addition to TNF-α and IL-6 (Fig. 2A). We then cultured these LPS-stimulated monocytes with autologous naive $CD4^+$ T cells under Treg-skewing conditions, in the presence of IL-2, TGF-β, and CD3 stimulation. In this system, the addition of IL-10–blocking Ab to the cultures led to an increase in IFN-γ–producing cells (Supplemental Fig. 3B) and a reduction in the suppressive function of iTregs (Fig. 2B), despite comparable induction of Foxp3 (Supplemental Fig. 3). The lack of Foxp3 enhancement in these cultures may be related to the variable amounts of cytokines, such as IL-6 and TNF-α, present in this system, which may influence iTreg induction (9, 19).

To ascertain that the augmentative effect on iTreg induction was truly mediated by IL-10, an in vitro iTreg-induction experiment (without monocytes) was performed on a patient with early-onset inflammatory bowel disease resulting from an IL-10RA mutation and impaired IL-10 signaling (23). Addition of IL-10 to this patient's cells failed to enhance Foxp3 or CTLA-4 expression (Fig. 2C, 2D) and, more importantly, failed to augment iTreg suppression (Fig. 2E, 2F). These results suggest that monocyte-derived IL-10 signaling through its receptor may be important for iTreg function, particularly in the gut microenvironment.

IL-10 enhances iTreg phenotype and function through STAT3

Because IL-10 mediates most of its action through activation/phosphorylation of STAT3 (24), we hypothesized that loss of STAT3 function would abrogate the ability of IL-10 to bestow these cultured cells with suppressive phenotype and function. Although silencing of STAT3 using siRNA with viral transfection was considered, we decided against this, as transfection of primary human T cells is difficult and, by modern standards, still requires significant manipulation (activation and/or cytokine addition), which may jeopardize the purity and naivety of the starting cell population. Hence, to test our hypothesis, we used the small molecule inhibitor of STAT3, StatticV, which was shown to specifically inhibit STAT3 phosphorylation (25). Not surprisingly, IL-10–treated iTregs showed enhanced STAT3 phosphorylation after 7 d of culture (Supplemental Fig. 4A). This STAT3 phosphorylation could be inhibited by 50 ng/ml of StatticV, a concentration used in human primary lymphocytes in a previous study (26). In cultures in which StatticV was added along with IL-10, no enhancement of Foxp3 or CTLA-4 expression was observed compared with cells cultured without IL-10 (Fig. 3A–C). In addition, there was partial, but not complete, reversion of the repressed IFN-γ expression observed with IL-10 addition (Fig. 3D, 3E). Importantly, iTregs cultured in the presence of both IL-10 and StatticV failed to acquire enhanced suppressive capacity (Fig. 4A, 4B).

To confirm these results, we isolated naive $CD4^+$ T cells from a patient with autosomal-dominant HIES. This patient has a previously reported heterozygous mutation in the SH2 domain of the STAT3 gene (27), which prevents STAT3 phosphorylation (28). In contrast to the healthy control, IL-10 did not enhance Foxp3 induction or the suppressive capacity of iTregs in this patient (Fig. 4C–E). Together, these data indicate that the ability of IL-10 to enhance the suppressive function of human iTregs is largely mediated through STAT3.

IL-10 inhibits PI3K/Akt pathway and enhances Foxo1 nuclear localization and function

In addition to STAT3 phosphorylation, IL-10 can inhibit the PI3K/Akt signal in T cells (29). Because downstream pathways of Akt phosphorylation regulate Foxo1 (30), which, in turn, controls Treg function (31), we hypothesized that IL-10–treated iTregs may have enhanced Foxo1 nuclear localization and function. Using immunofluorescence, we showed that IL-10–treated cells had increased nuclear retention of Foxo1 after low-dose anti-CD3 stimulation

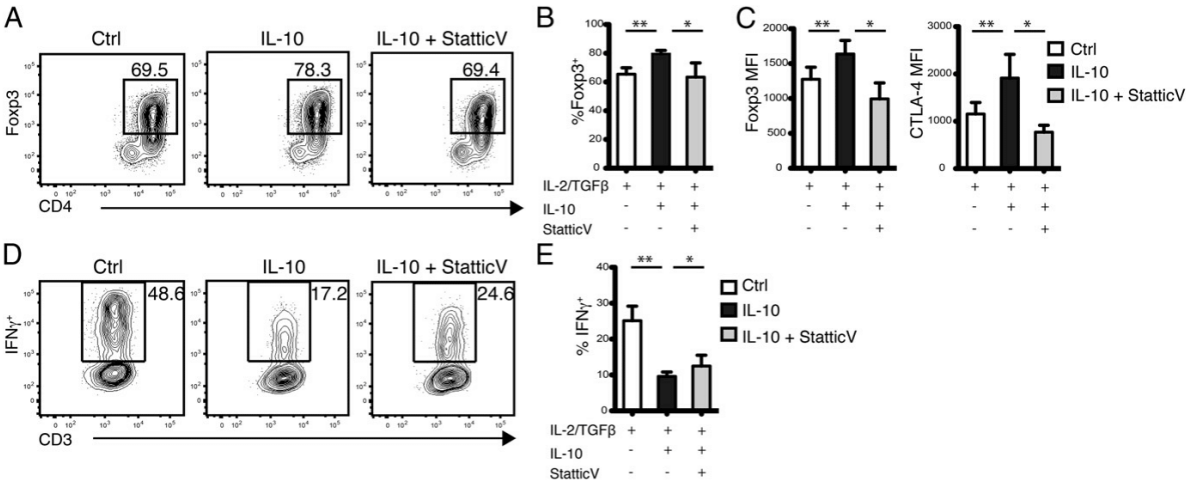

FIGURE 3. IL-10 enhances iTreg phenotype through STAT3. (**A**) Representative contour plots showing Foxp3 expression in cells cultured under various conditions. (**B**) Bar graph (mean + SEM) showing percentage of $Foxp3^+$ cells within various culture conditions. (**C**) Foxp3 and CTLA-4 MFI of cells cultured under various conditions. Data represent six independent experiments. Representative contour plots (**D**) and bar graph (mean + SEM) (**E**) showing the percentage of $IFN\gamma^+$ cells in iTregs induced under various conditions. Data are from six independent experiments. $*p < 0.05$, $**p < 0.01$.

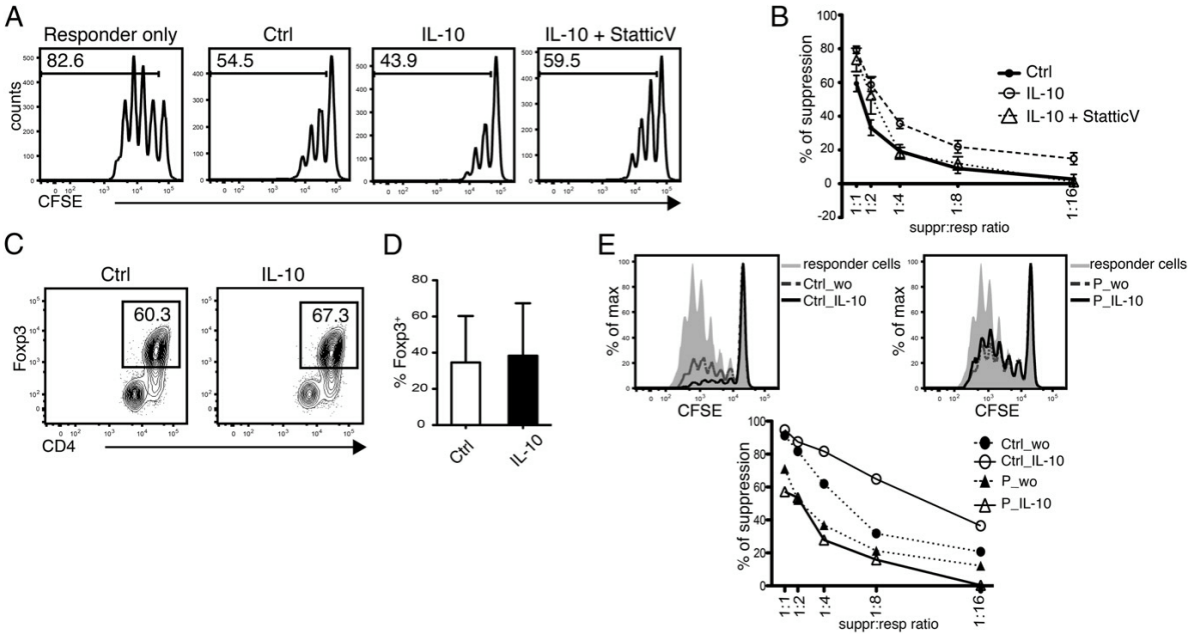

FIGURE 4. STAT3 is crucial for IL-10–potentiated iTreg function. (**A**) Representative histograms showing proliferation of responder cells alone and compared with iTregs cultured under various conditions (data show suppressor/responder ratio of 1:4). (**B**) Percentage of suppression by iTregs cultured under various conditions and suppressor/responder ratios. Data are representative of six independent experiments. (**C**) iTreg induction from naive $CD4^+$ T cells from a patient with autosomal-dominant HIES. Contour plots show Foxp3 expression after Treg induction in the presence and absence of IL-10. (**D**) Bar graph shows percentage of $Foxp3^+$-expressing cells analyzed on day 7 of Treg induction. (**E**) Suppressive capacity of iTregs generated from the patient (P_wo and P_IL-10) compared with a healthy donor (Ctrl_wo and Ctrl_IL-10). A representative graph from a healthy donor and the patient (suppressor/responder ratio 1:8) is shown along with suppression graph. Data are representative of two independent experiments.

compared with control cells. This effect was lost upon stimulation with a higher dose of anti-CD3 (Fig. 5). This was supported by flow cytometry, showing reduced p-Foxo1 expression (both in terms of the percentage of $pFoxo1^+$ cells and p-Foxo1 MFI) in CD3/CD28-stimulated IL-10–treated cells compared with cells cultured without IL-10 (Fig. 6A, 6B, Supplemental Fig. 4B showing gating strategy). As expected, most cells expressed total Foxo1; however, IL-10–treated cells had slightly higher total Foxo1 expression compared with control cells at rest (Fig. 6C, 6D, Supplemental Fig. 4C, showing gating strategy). Real-time PCR also showed increased mRNA expression of Foxo1 and $p27^{kip1}$, a cyclin-dependent kinase inhibitor upregulated by Foxo1 (32), in IL-10–treated cells (Fig. 6E). These results are consistent with a previous report demonstrating that ex vivo Tregs retain Foxo1 after stimulation more efficiently than do non-Tregs (31). We next examined the PI3K/Akt pathway in cultured cells. All cells naturally expressed unphosphorylated Akt; however, after resting and restimulation with anti-CD3/CD28, IL-10–treated iTregs expressed consistently less p-Akt compared with control cells (Fig. 6F–H, Supplemental Fig. 4D, showing gating strategy). These results suggest that IL-10 inhibits the PI3K/Akt pathway and enhances Foxo1 expression and function in differentiating iTregs.

Foxo1 is critical for iTreg induction and mediates the augmentation of iTreg function by IL-10

To examine the effect of Foxo1 on differentiating iTregs, we used a Foxo1 inhibitor (AS1842856) that was shown previously to specifically block Foxo1 DNA binding (33). The dose of the Foxo1 inhibitor was titrated against CCR7 expression in cultured $CD4^+$ naive T cells and the degree of cell death, because CCR7 is in-

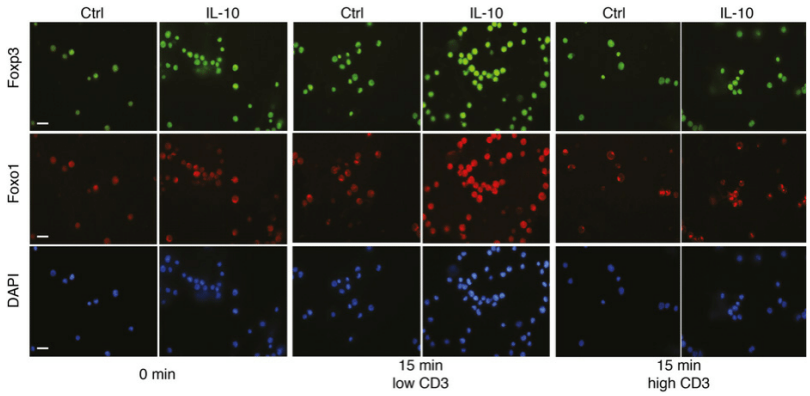

FIGURE 5. IL-10 enhances Foxo1 nuclear retention. Representative immunofluorescence images showing Foxp3 (*top panels*) and Foxo1 (*middle panels*) expression. Slides were counterstained for DAPI (blue; *bottom panels*). Images show iTregs induced under Ctrl (IL-2 + TGF-β) and IL-10 (IL-2 + TGF-β + IL-10) conditions. Cells at rest (*left panels*). Cells stimulated with 0.01 μg/ml anti-CD3 for 15 min (*middle panels*). Cells stimulated with 0.1 μg/ml anti-CD3 for 15 min (*right panels*). Images are representative of two independent experiments. Scale bars, 20 μm.

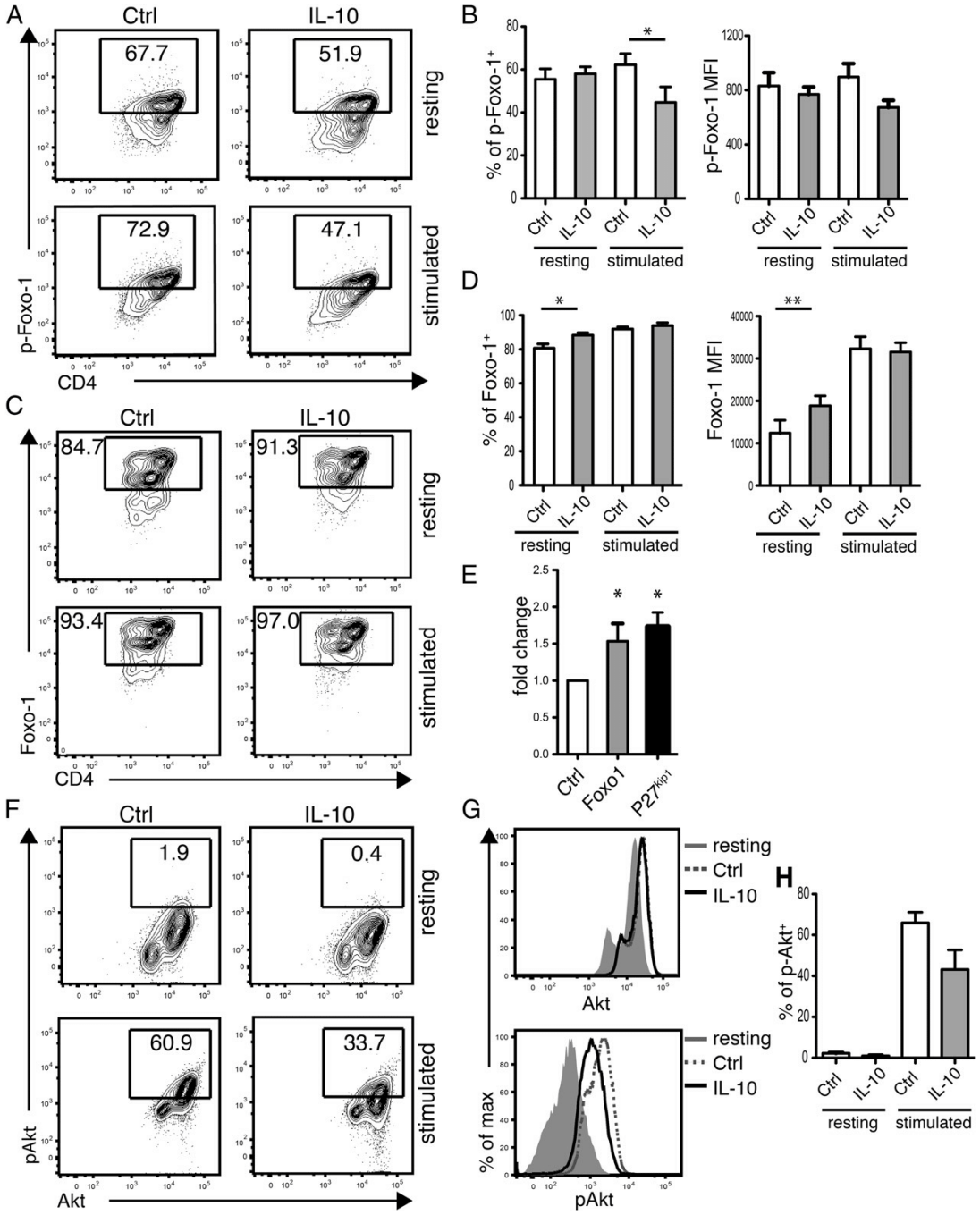

FIGURE 6. IL-10 reduces Akt and Foxo1 phosphorylation. (**A**) Representative contour plots showing p-Foxo1 expression in CD4$^+$ iTregs induced under Ctrl (*left panels*) and IL-10 (*right panels*) conditions, either under resting conditions (*upper panels*) or stimulated with anti-CD3/CD28 (*lower panels*). (**B**) Summary bar graphs showing percentage of p-Foxo1 along with MFI of p-Foxo1. (**C**) Representative contour plots showing total Foxo1 expression gated on CD4$^+$ iTregs under Ctrl (*left panels*) and IL-10 (*right panels*) conditions, either resting (*upper panels*) or stimulated (*lower panels*). (**D**) Bar graph representing the percentage of Foxo1 and Foxo1 MFI under the indicated conditions. Data shown are representative of three independent experiments. (**E**) Foxo1 and p27^{kip1} mRNA expression in IL-10–treated cells compared with control. Bars represent mean and SEM of fold change compared with control. Data represent four independent experiments. (**F**) Analysis of Akt phosphorylation/activation. Representative contour plots showing total Akt (Akt) and p-Akt expression in control Foxp3$^+$ iTregs (*left panels*) and IL-10–treated Foxp3$^+$ iTregs (*right panels*), under resting conditions (*upper panels*) or stimulated with anti-CD3/CD28 (*lower panels*). (**G**) Histograms of Akt (*upper panel*) and p-Akt (*lower panel*) expression in control (dotted line) and IL-10 (solid line)-treated iTregs after stimulation compared with resting conditions (shaded graph). (**H**) Summary bar graph showing percent of pAkt$^+$ cells in various conditions as indicated. Data show two independent experiments. $*p < 0.05$, $**p < 0.01$.

duced by Foxo1 (34), and too much Foxo1 inhibitor led to significant cell death in vitro. Naive $CD4^+$ T cells were stimulated with anti-CD3/CD28 in the presence of Foxo1 inhibitor, at doses ranging from 5 to 50 ng/ml, for 3 d. The optimal concentration of Foxo1 inhibitor was selected to be 35 ng/ml, based on the reduction of cell surface CCR7 expression and minimal cell death (Supplemental Fig. 4E, 4F). In cultures treated with Foxo1 inhibitor, a reduction in $p27^{kip1}$ mRNA was noted, confirming blockade of Foxo1 function (Supplemental Fig. 4G).

Foxo1 inhibition led to a significant reduction in Foxp3 expression in naive T cells cultured under Treg-skewing conditions, with or without IL-10 (Fig. 7A, 7B). IL-10 was unable to enhance the Foxp3 or CTLA-4 expression of Foxo1-inhibited cells, as determined by the percentage change in Foxp3 or CTLA-4 expression (Fig. 7B–D). Furthermore, in the presence of Foxo1 inhibition, IL-10 could not enhance the suppressive activity of iTregs (Fig. 7E, 7F). This is clearly shown in the average percentage of change in suppression, where under conditions without Foxo1 inhibitor, addition of IL-10 resulted in a >2-fold increase in suppression compared with a reduction of 20% suppression in the presence of Foxo1 inhibitor (Fig. 7G). Collectively, these data suggest that IL-10 augments iTreg phenotype and function via Foxo1.

Discussion

IL-10 exerts its immunosuppressive actions at multiple levels of the immune system, including modulation of APCs (35), inhibition of T cell proliferation (36), and, more recently, maintaining the function/stability of established Tregs (6, 7). The results presented in this study extend the role of IL-10 and demonstrate that, in addition to TGF-β, IL-10 augments iTreg differentiation and function. This offers one plausible explanation as to why gut IL-10Rβ–deficient M2 macrophages with reduced IL-10 production may fail to generate functional Tregs (19). Furthermore, this function of IL-10 is in keeping with the copresence of TGF-β and IL-10 in various contexts of immune tolerance and emphasizes the synergistic role of TGF-β and IL-10 in tolerance induction (37–39). Importantly, we demonstrate in this study that this potentiating effect of IL-10 is likely mediated through the STAT3 and Foxo1 pathway.

Our results reveal a novel role for IL-10 as a physiological regulator of PI3K/Akt and Foxo1 signaling in iTreg differentiation. Previous studies showed that IL-10 inhibits PI3K/Akt signaling (29, 40), which is consistent with the current results showing that IL-10–treated iTregs have reduced Akt phosphorylation in response to stimulation, a characteristic of established Tregs. In congruence with this, IL-10–treated iTregs have enhanced Foxo1 nuclear

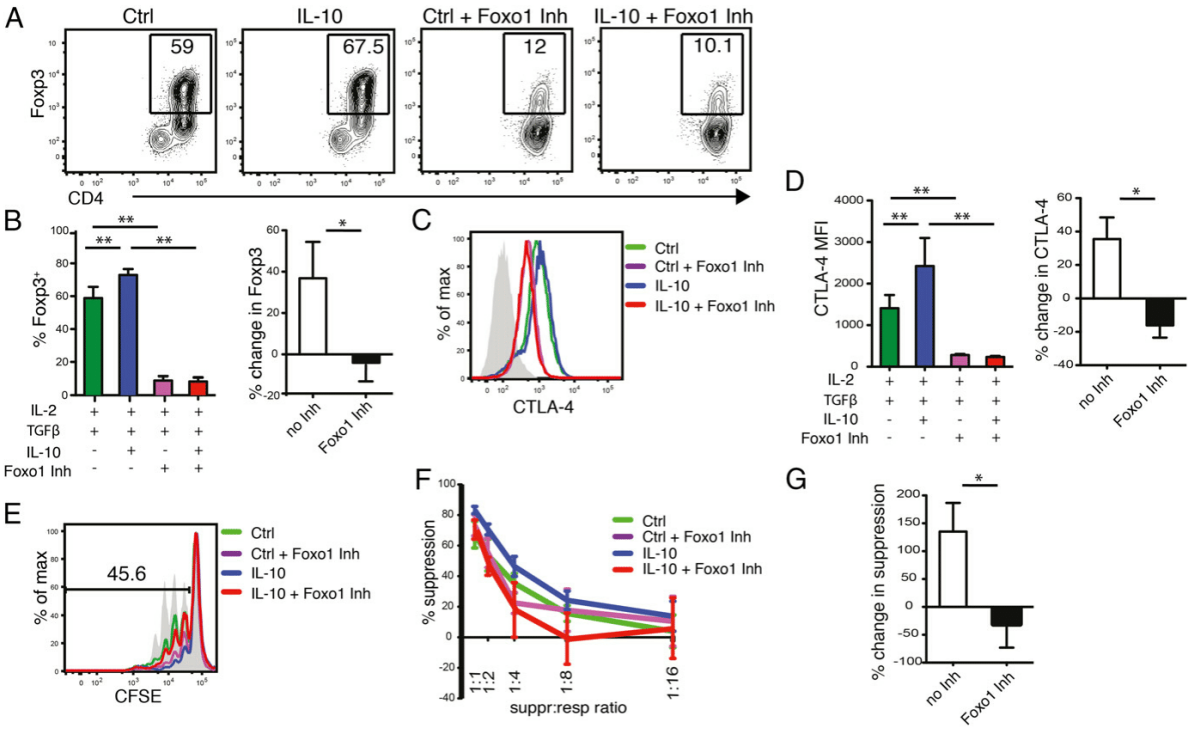

FIGURE 7. The role of Foxo1 in iTreg induction and potentiation by IL-10. (**A**) Representative contour plots showing Foxp3 expression in Ctrl (IL-2 + TGF-β), IL-10 (IL-2 + TGF-β + IL-10), Ctrl + Foxo1 Inh (IL-2 + TGF-β + AS1842856), and IL-10 + Foxo1 Inh (IL-2 + TGF-β + IL-10 + AS1842856). Data are representative of four independent experiments. (**B**) Bar graph (mean + SEM) showing percentage of $Foxp3^+$ cells induced under various conditions (*left panel*). Percentage change in the proportion of $Foxp3^+$ cells in cultures treated with IL-10 (IL-2 + TGF-β + IL-10) compared with Ctrl (IL-2 + TGF-β), within pairs with no Inh or with Foxo1 Inh (*right panel*). Data show at least four independent experiments in each group. (**C**) Representative histograms showing CTLA-4 expression in Ctrl, IL-10–treated, Ctrl + Foxo Inh–treated, and IL-10 + Foxo Inh–treated cells. (**D**) Bar graph (mean + SEM) showing CTLA-4 MFI of cells cultured under various conditions (*left panel*). Percentage change in CTLA-4 MFI in cultures treated with IL-10 (IL-2 + TGF-β + IL-10) compared with Ctrl (IL-2 + TGF-β), within pairs with and without Foxo1 Inh (*right panel*). Data are representative of at least four independent experiments in each group. (**E**) Histograms showing proliferation of responder cells alone (shaded) compared with iTregs cultured under various conditions (data represent suppressor/responder ratio of 1:8). (**F**) Percentage suppression by iTregs cultured under various conditions and suppressor/responder ratios. (**G**) Bar graph showing percentage change in suppressive activity between Ctrl-treated and IL-10–treated cells, with or without Inh. Percentage changes in suppression between IL-10–treated and Ctrl-treated cells at each suppressor/responder ratio were used as individual data points. Data are representative of four independent experiments. $*p < 0.05$, $**p < 0.01$. Inh, inhibitor.

retention and activity with increased $p27^{kip1}$ mRNA expression. Inhibition of Foxo1 activity by a small molecule Foxo1 inhibitor expectedly impaired Foxp3 induction; however, more importantly, it abrogated the ability of IL-10 to enhance iTreg differentiation and function. Therefore, the potentiating effect of IL-10 on iTregs is dependent on activation of Foxo1. This fits in well with the now well-established role of Foxo1 as a crucial factor for Treg differentiation and suppressive function (31, 41, 42).

Importantly, inhibition of IL-10–induced STAT3 phosphorylation by StatticV also inhibited the ability of IL-10 to enhance iTreg differentiation. This was confirmed in a patient with dominant-negative STAT3 mutation (HIES), which suggests that, in addition to the impaired ability of IL-10–unresponsive APCs to induce iTregs in HIES (43), naive STAT3-defective $CD4^+$ T cells may respond to IL-10 poorly, leading to poor functional capacity of the induced Tregs, thereby contributing to the immune dysregulation seen in this disease. Interestingly, a previous murine study demonstrated an important role for STAT3 in iTreg differentiation (44), whereas a more recent study suggested that STAT3 signaling inhibits iTreg generation in a murine graft-versus-host disease model (45). However, in the latter study, the proinflammatory environment, and primarily IL-6–mediated STAT3 signaling, impaired iTreg generation in this context. Indeed, our results also showed that, in contrast to IL-10, IL-6 impaired iTreg generation and function in vitro. Therefore, despite both acting through STAT3, the divergent role of IL-10 and IL-6 as anti- and proinflammatory cytokines is clearly manifest. This differential effect may be due to the fact that IL-6–induced STAT3 activation is more sensitive to SOCS3 inhibition (46) and that IL-6 causes a more transient STAT3 activation compared with IL-10 (47). Alternatively, differential STAT3-independent pathways activated by these cytokines may also contribute. These issues need to be addressed in future studies.

The reason for this STAT3-mediated augmentation of iTreg cells is unclear; however, given that the enhancing effect of IL-10 can be completely blocked by Foxo1 inhibition, it is likely that STAT3 may also act through Foxo1. Indeed, recent evidence showed that STAT3 phosphorylation is important for nuclear retention and hence activation of Foxo factors, where deficiency of STAT3 in mice resulted in both reduced Foxo1 expression and the cytoplasmic localization/inactivation of Foxo1 (48). Our present results demonstrating increased Foxo1 and $p27^{kip1}$ mRNA in IL-10–treated iTregs associated with enhanced STAT3 phosphorylation are consistent with these findings.

Importantly, IL-10 did not enhance TSDR demethylation, which suggests that the potentiating effect of IL-10 is not due to improvement of iTreg stability. This is in keeping with our results showing that IL-10 likely augments iTreg function through Foxo1, which is required for Foxp3 induction but not its maintenance (41, 49). Although other studies reported enhancement of TGF-β–induced human iTreg function [e.g., by addition of rapamycin (50)], to our knowledge, it is not possible to induce Foxp3 demethylation in vitro. Previous murine studies yielded controversial results regarding the TSDR demethylation status of in vivo–induced iTregs (51), and it remains unknown whether human iTregs are demethylated at the TSDR region. This is a particular challenge, because no surface markers exist to identify human iTregs in vivo. Nevertheless, it remains possible that an unidentified factor could induce TSDR demethylation of human iTregs in vivo, because sustained peripheral tolerance to foreign Ags is important for immune homeostasis.

One of the unresolved issues arising from our study is whether IL-10 signaling in naive CD4 T cells is important for iTreg function at the microbiota-rich gut interface. Previous murine studies focused on the role of IL-10 in the maintenance and function of established Tregs (6, 7), but the importance of IL-10 signaling in Treg induction in vivo remains unknown. This aspect of gut immunology is particularly difficult to tease out, because the relative contribution of nTregs and iTregs to gut homeostasis is unknown, although evidence suggests that both nTregs and iTregs are required for gut immune tolerance (52). Additionally, the lack of surface markers to distinguish nTregs and iTregs in humans precludes the ex vivo functional study of human iTregs.

In conclusion, our results show that, in the context of human iTreg induction, IL-10 promotes STAT3 phosphorylation, inhibits PI3K/Akt signaling, and enhances Foxo1 activity. Foxo1, in turn, endows these differentiating iTregs with potent suppressive capacity. This novel role of IL-10 is likely important for generating iTregs at mucosal surfaces, such as the gut and the decidua, where tolerance to foreign Ags is paramount. The divergent role of IL-10 and IL-6 in iTreg generation demonstrated in this study, and, therefore, the balance of IL-10 and IL-6, is likely to be important in determining the immune outcome at mucosal surfaces, especially in the face of immune activation and inflammation. Lastly, our results suggest that IL-10 may enhance the therapeutic potential of in vitro–generated human iTregs for the treatment of immune diseases, such as autoimmunity and allergy, although further studies are required to address the instability of in vitro–generated iTregs.

Acknowledgments

We thank the staff of the Centenary Institute Flow Cytometry Facility and the Westmead Research Hub Cell Sorting Service for excellent assistance with cell sorting. We also acknowledge the individuals who participated in this study. We thank Andrew Martin, statistician at the National Health and Medical Research Council Trial Center (University of Sydney), for input on statistical analysis.

Disclosures

The authors have no financial conflicts of interest.

References

1. Mosser, D. M., and X. Zhang. 2008. Interleukin-10: new perspectives on an old cytokine. *Immunol. Rev.* 226: 205–218.
2. Glocker, E.-O., D. Kotlarz, K. Boztug, E. M. Gertz, A. A. Schäffer, F. Noyan, M. Perro, J. Diestelhorst, A. Allroth, D. Murugan, et al. 2009. Inflammatory bowel disease and mutations affecting the interleukin-10 receptor. *N. Engl. J. Med.* 361: 2033–2045.
3. Kotlarz, D., R. Beier, D. Murugan, J. Diestelhorst, O. Jensen, K. Boztug, D. Pfeifer, H. Kreipe, E.-D. Pfister, U. Baumann, et al. 2012. Loss of interleukin-10 signaling and infantile inflammatory bowel disease: implications for diagnosis and therapy. *Gastroenterology* 143: 347–355.
4. Rubtsov, Y. P., J. P. Rasmussen, E. Y. Chi, J. Fontenot, L. Castelli, X. Ye, P. Treuting, L. Siewe, A. Roers, W. R. Henderson, Jr., et al. 2008. Regulatory T cell-derived interleukin-10 limits inflammation at environmental interfaces. *Immunity* 28: 546–558.
5. Miyara, M., and S. Sakaguchi. 2007. Natural regulatory T cells: mechanisms of suppression. *Trends Mol. Med.* 13: 108–116.
6. Chaudhry, A., R. M. Samstein, P. Treuting, Y. Liang, M. C. Pils, J.-M. Heinrich, R. S. Jack, F. T. Wunderlich, J. C. Brüning, W. Müller, and A. Y. Rudensky. 2011. Interleukin-10 signaling in regulatory T cells is required for suppression of Th17 cell-mediated inflammation. *Immunity* 34: 566–578.
7. Murai, M., O. Turovskaya, G. Kim, R. Madan, C. L. Karp, H. Cheroutre, and M. Kronenberg. 2009. Interleukin 10 acts on regulatory T cells to maintain expression of the transcription factor Foxp3 and suppressive function in mice with colitis. *Nat. Immunol.* 10: 1178–1184.
8. Zhou, L., I. I. Ivanov, R. Spolski, R. Min, K. Shenderov, T. Egawa, D. E. Levy, W. J. Leonard, and D. R. Littman. 2007. IL-6 programs T(H)-17 cell differentiation by promoting sequential engagement of the IL-21 and IL-23 pathways. *Nat. Immunol.* 8: 967–974.
9. Fujimoto, M., M. Nakano, F. Terabe, H. Kawahata, T. Ohkawara, Y. Han, B. Ripley, S. Serada, T. Nishikawa, A. Kimura, et al. 2011. The influence of excessive IL-6 production in vivo on the development and function of Foxp3+ regulatory T cells. *J. Immunol.* 186: 32–40.

10. Doganci, A., T. Eigenbrod, N. Krug, G. T. De Sanctis, M. Hausding, V. J. Erpenbeck, B. Haddad, H. A. Lehr, E. Schmitt, T. Bopp, et al. 2005. The IL-6R alpha chain controls lung CD4+CD25+ Treg development and function during allergic airway inflammation in vivo. *J. Clin. Invest.* 115: 313–325.
11. Li, M. O., and R. A. Flavell. 2008. Contextual regulation of inflammation: a duet by transforming growth factor-beta and interleukin-10. *Immunity* 28: 468–476.
12. Yamagiwa, S., J. D. Gray, S. Hashimoto, and D. A. Horwitz. 2001. A role for TGF-beta in the generation and expansion of CD4+CD25+ regulatory T cells from human peripheral blood. *J. Immunol.* 166: 7282–7289.
13. Tran, D. Q. 2012. TGF-β: the sword, the wand, and the shield of FOXP3(+) regulatory T cells. *J. Mol. Cell Biol.* 4: 29–37.
14. DiPaolo, R. J., C. Brinster, T. S. Davidson, J. Andersson, D. Glass, and E. M. Shevach. 2007. Autoantigen-specific TGFbeta-induced Foxp3+ regulatory T cells prevent autoimmunity by inhibiting dendritic cells from activating autoreactive T cells. *J. Immunol.* 179: 4685–4693.
15. Tran, D. Q., H. Ramsey, and E. M. Shevach. 2007. Induction of FOXP3 expression in naive human CD4+FOXP3 T cells by T-cell receptor stimulation is transforming growth factor-beta dependent but does not confer a regulatory phenotype. *Blood* 110: 2983–2990.
16. Lu, L., J. Ma, Z. Li, Q. Lan, M. Chen, Y. Liu, Z. Xia, J. Wang, Y. Han, W. Shi, et al. 2011. All-trans retinoic acid promotes TGF-β-induced Tregs via histone modification but not DNA demethylation on Foxp3 gene locus. *PLoS One* 6: e24590.
17. Jeffery, L. E., F. Burke, M. Mura, Y. Zheng, O. S. Qureshi, M. Hewison, L. S. K. Walker, D. A. Lammas, K. Raza, and D. M. Sansom. 2009. 1,25-Dihydroxyvitamin D3 and IL-2 combine to inhibit T cell production of inflammatory cytokines and promote development of regulatory T cells expressing CTLA-4 and FoxP3. *J. Immunol.* 183: 5458–5467.
18. Battaglia, M., A. Stabilini, B. Migliavacca, J. Horejs-Hoeck, T. Kaupper, and M.-G. Roncarolo. 2006. Rapamycin promotes expansion of functional CD4+CD25+FOXP3+ regulatory T cells of both healthy subjects and type 1 diabetic patients. *J. Immunol.* 177: 8338–8347.
19. Shouval, D. S., A. Biswas, J. A. Goettel, K. McCann, E. Conaway, N. S. Redhu, I. D. Mascanfroni, Z. Al Adham, S. Lavoie, M. Ibourk, et al. 2014. Interleukin-10 receptor signaling in innate immune cells regulates mucosal immune tolerance and anti-inflammatory macrophage function. *Immunity* 40: 706–719.
20. Santner-Nanan, B., M. J. Peek, R. Khanam, L. Richarts, E. Zhu, B. Fazekas de St Groth, and R. Nanan. 2009. Systemic increase in the ratio between Foxp3+ and IL-17-producing CD4+ T cells in healthy pregnancy but not in preeclampsia. *J. Immunol.* 183: 7023–7030.
21. Baron, U., S. Floess, G. Wieczorek, K. Baumann, A. Grützkau, J. Dong, A. Thiel, T. J. Boeld, P. Hoffmann, M. Edinger, et al. 2007. DNA demethylation in the human FOXP3 locus discriminates regulatory T cells from activated FOXP3(+) conventional T cells. *Eur. J. Immunol.* 37: 2378–2389.
22. Boonstra, A., R. Rajsbaum, M. Holman, R. Marques, C. Asselin-Paturel, J. P. Pereira, E. E. Bates, S. Akira, P. Vieira, Y.-J. Liu, et al. 2006. Macrophages and myeloid dendritic cells, but not plasmacytoid dendritic cells, produce IL-10 in response to MyD88- and TRIF-dependent TLR signals, and TLR-independent signals. *J. Immunol.* 177: 7551–7558.
23. Lee, C. H., P. Hsu, B. Nanan, R. Nanan, M. Wong, K. J. Gaskin, R. W. Leong, R. Murchie, A. M. Muise, and M. O. Stormon. 2014. Novel de novo mutations of the interleukin-10 receptor gene lead to infantile onset inflammatory bowel disease. *J. Crohn's Colitis* 8: 1551–1556.
24. Donnelly, R. P., H. Dickensheets, and D. S. Finbloom. 1999. The interleukin-10 signal transduction pathway and regulation of gene expression in mononuclear phagocytes. *J. Interferon Cytokine Res.* 19: 563–573.
25. Schust, J., B. Sperl, A. Hollis, T. U. Mayer, and T. Berg. 2006. Stattic: a small-molecule inhibitor of STAT3 activation and dimerization. *Chem. Biol.* 13: 1235–1242.
26. Goodman, W. A., A. B. Young, T. S. McCormick, K. D. Cooper, and A. D. Levine. 2011. Stat3 phosphorylation mediates resistance of primary human T cells to regulatory T cell suppression. *J. Immunol.* 186: 3336–3345.
27. Ives, M. L., C. S. Ma, U. Palendira, A. Chan, J. Bustamante, S. Boisson-Dupuis, P. D. Arkwright, D. Engelhard, D. Averbuch, K. Magdorf, et al. 2013. Signal transducer and activator of transcription 3 (STAT3) mutations underlying autosomal dominant hyper-IgE syndrome impair human CD8(+) T-cell memory formation and function. *J. Allergy Clin. Immunol.* 132: 400–411.e9.
28. Renner, E. D., S. Rylaarsdam, S. Anover-Sombke, A. L. Rack, J. Reichenbach, J. C. Carey, Q. Zhu, A. F. Jansson, J. Barboza, L. F. Schimke, et al. 2008. Novel signal transducer and activator of transcription 3 (STAT3) mutations, reduced T (H)17 cell numbers, and variably defective STAT3 phosphorylation in hyper-IgE syndrome. *J. Allergy Clin. Immunol.* 122: 181–187.
29. Taylor, A., M. Akdis, A. Joss, T. Akkoç, R. Wenig, M. Colonna, I. Daigle, E. Flory, K. Blaser, and C. A. Akdis. 2007. IL-10 inhibits CD28 and ICOS costimulations of T cells via src homology 2 domain-containing protein tyrosine phosphatase 1. *J. Allergy Clin. Immunol.* 120: 76–83.
30. Kops, G. J., R. H. Medema, J. Glassford, M. A. Essers, P. F. Dijkers, P. J. Coffer, E. W. Lam, and B. M. Burgering. 2002. Control of cell cycle exit and entry by protein kinase B-regulated forkhead transcription factors. *Mol. Cell. Biol.* 22: 2025–2036.
31. Ouyang, W., W. Liao, C. T. Luo, N. Yin, M. Huse, M. V. Kim, M. Peng, P. Chan, Q. Ma, Y. Mo, et al. 2012. Novel Foxo1-dependent transcriptional programs control T(reg) cell function. *Nature* 491: 554–559.
32. Medema, R. H., G. J. Kops, J. L. Bos, and B. M. Burgering. 2000. AFX-like Forkhead transcription factors mediate cell-cycle regulation by Ras and PKB through p27kip1. *Nature* 404: 782–787.
33. Nagashima, T., N. Shigematsu, R. Maruki, Y. Urano, H. Tanaka, A. Shimaya, T. Shimokawa, and M. Shibasaki. 2010. Discovery of novel forkhead box O1 inhibitors for treating type 2 diabetes: improvement of fasting glycemia in diabetic db/db mice. *Mol. Pharmacol.* 78: 961–970.
34. Kerdiles, Y. M., D. R. Beisner, R. Tinoco, A. S. Dejean, D. H. Castrillon, R. A. DePinho, and S. M. Hedrick. 2009. Foxo1 links homing and survival of naive T cells by regulating L-selectin, CCR7 and interleukin 7 receptor. *Nat. Immunol.* 10: 176–184.
35. de Waal Malefyt, R., J. Abrams, B. Bennett, C. G. Figdor, and J. E. de Vries. 1991. Interleukin 10(IL-10) inhibits cytokine synthesis by human monocytes: an autoregulatory role of IL-10 produced by monocytes. *J. Exp. Med.* 174: 1209–1220.
36. de Waal Malefyt, R., H. Yssel, and J. E. de Vries. 1993. Direct effects of IL-10 on subsets of human CD4+ T cell clones and resting T cells. Specific inhibition of IL-2 production and proliferation. *J. Immunol.* 150: 4754–4765.
37. Jarry, A., C. Bossard, C. Bou-Hanna, D. Masson, E. Espaze, M. G. Denis, and C. L. Laboisse. 2008. Mucosal IL-10 and TGF-beta play crucial roles in preventing LPS-driven, IFN-gamma-mediated epithelial damage in human colon explants. *J. Clin. Invest.* 118: 1132–1142.
38. Fuss, I. J., M. Boirivant, B. Lacy, and W. Strober. 2002. The interrelated roles of TGF-beta and IL-10 in the regulation of experimental colitis. *J. Immunol.* 168: 900–908.
39. Cottrez, F., and H. Groux. 2001. Regulation of TGF-beta response during T cell activation is modulated by IL-10. *J. Immunol.* 167: 773–778.
40. Akdis, C. A., A. Joss, M. Akdis, A. Faith, and K. Blaser. 2000. A molecular basis for T cell suppression by IL-10: CD28-associated IL-10 receptor inhibits CD28 tyrosine phosphorylation and phosphatidylinositol 3-kinase binding. [Published erratum appears in *FASEB J.* 2000 Oct 14(13): 2128.] *FASEB J.* 14: 1666–1668.
41. Ouyang, W., O. Beckett, Q. Ma, J. H. Paik, R. A. DePinho, and M. O. Li. 2010. Foxo proteins cooperatively control the differentiation of Foxp3+ regulatory T cells. *Nat. Immunol.* 11: 618–627.
42. Kerdiles, Y. M., E. L. Stone, D. R. Beisner, M. A. McGargill, I. L. Ch'en, C. Stockmann, C. D. Katayama, and S. M. Hedrick. 2010. Foxo transcription factors control regulatory T cell development and function. *Immunity* 33: 890–904.
43. Saito, M., M. Nagasawa, H. Takada, T. Hara, S. Tsuchiya, K. Agematsu, M. Yamada, N. Kawamura, T. Ariga, I. Tsuge, et al. 2011. Defective IL-10 signaling in hyper-IgE syndrome results in impaired generation of tolerogenic dendritic cells and induced regulatory T cells. *J. Exp. Med.* 208: 235–249.
44. Pallandre, J.-R., E. Brillard, G. Créhange, A. Radlovic, J.-P. Remy-Martin, P. Saas, P.-S. Rohrlich, X. Pivot, X. Ling, P. Tiberghien, and C. Borg. 2007. Role of STAT3 in CD4+CD25+FOXP3+ regulatory lymphocyte generation: implications in graft-versus-host disease and antitumor immunity. *J. Immunol.* 179: 7593–7604.
45. Laurence, A., S. Amarnath, J. Mariotti, Y. C. Kim, J. Foley, M. Eckhaus, J. J. O'Shea, and D. H. Fowler. 2012. STAT3 transcription factor promotes instability of nTreg cells and limits generation of iTreg cells during acute murine graft-versus-host disease. *Immunity* 37: 209–222.
46. Yasukawa, H., M. Ohishi, H. Mori, M. Murakami, T. Chinen, D. Aki, T. Hanada, K. Takeda, S. Akira, M. Hoshijima, et al. 2003. IL-6 induces an anti-inflammatory response in the absence of SOCS3 in macrophages. *Nat. Immunol.* 4: 551–556.
47. Braun, D. A., M. Fribourg, and S. C. Sealfon. 2013. Cytokine response is determined by duration of receptor and signal transducers and activators of transcription 3 (STAT3) activation. *J. Biol. Chem.* 288: 2986–2993.
48. Oh, H.-M., C.-R. Yu, I. Dambuza, B. Marrero, and C. E. Egwuagu. 2012. STAT3 protein interacts with Class O Forkhead transcription factors in the cytoplasm and regulates nuclear/cytoplasmic localization of FoxO1 and FoxO3a proteins in CD4(+) T cells. *J. Biol. Chem.* 287: 30436–30443.
49. Merkenschlager, M., and H. von Boehmer. 2010. PI3 kinase signalling blocks Foxp3 expression by sequestering Foxo factors. *J. Exp. Med.* 207: 1347–1350.
50. Hippen, K. L., S. C. Merkel, D. K. Schirm, C. Nelson, N. C. Tennis, J. L. Riley, C. H. June, J. S. Miller, J. E. Wagner, and B. R. Blazar. 2011. Generation and large-scale expansion of human inducible regulatory T cells that suppress graft-versus-host disease. *Am. J. Transplant.* 11: 1148–1157.
51. Yadav, M., S. Stephan, and J. A. Bluestone. 2013. Peripherally induced tregs - role in immune homeostasis and autoimmunity. *Front. Immunol.* 4: 232.
52. Haribhai, D., J. B. Williams, S. Jia, D. Nickerson, E. G. Schmitt, B. Edwards, J. Ziegelbauer, M. Yassai, S.-H. Li, L. M. Relland, et al. 2011. A requisite role for induced regulatory T cells in tolerance based on expanding antigen receptor diversity. *Immunity* 35: 109–122.

Published May 2, 2018, doi:10.4049/jimmunol.1701533

The Journal of Immunology

IL-2 Enhances Gut Homing Potential of Human Naive Regulatory T Cells Early in Life

Peter S. Hsu,[*,†,‡] Catherine L. Lai,[*,†,§] Mingjing Hu,[§] Brigitte Santner-Nanan,[§] Jane E. Dahlstrom,[¶,‖] Cheng Hiang Lee,[#,] Ayesha Ajmal,[¶] Amanda Bullman,[¶] Susan Arbuckle,[††] Ahmed Al Saedi,[§] Lou Gacis,[*] Reta Nambiar,[*] Andrew Williams,[*] Melanie Wong,[*] Dianne E. Campbell,[*,†,‡] and Ralph Nanan[§]**

Recent evidence suggests early environmental factors are important for gut immune tolerance. Although the role of regulatory T (Treg) cells for gut immune homeostasis is well established, the development and tissue homing characteristics of Treg cells in children have not been studied in detail. In this article, we studied the development and homing characteristics of human peripheral blood Treg cell subsets and potential mechanisms inducing homing molecule expression in healthy children. We found contrasting patterns of circulating Treg cell gut and skin tropism, with abundant β7 integrin$^+$ Treg cells at birth and increasing cutaneous lymphocyte Ag (CLA$^+$) Treg cells later in life. β7 integrin$^+$ Treg cells were predominantly naive, suggesting acquisition of Treg cell gut tropism early in development. In vitro, IL-7 enhanced gut homing but reduced skin homing molecule expression in conventional T cells, whereas IL-2 induced a similar effect only in Treg cells. This effect was more pronounced in cord compared with adult blood. Our results suggest that early in life, naive Treg cells may be driven for gut tropism by their increased sensitivity to IL-2–induced β7 integrin upregulation, implicating a potential role of IL-2 in gut immune tolerance during this critical period of development. ***The Journal of Immunology*****, 2018, 200: 000–000.**

Since the discovery of Foxp3$^+$ regulatory T (Treg) cells, mounting evidence from both mice and humans has confirmed the important role of these cells in maintaining immune tolerance. This tolerance is required for both self-antigens and ubiquitous foreign Ags such as food proteins and commensal microbial agents (1, 2). A primary deficiency of Treg cells in humans leads to immune dysregulation; polyendocrinopathy; enteropathy; X-linked syndrome, with breakdown of tolerance to self-antigens and foreign Ags characterized by systemic autoimmunity; severe enteropathy; and multiple food allergies (3). On a broader scale, deficits in the frequency and function of Treg cells have been documented in patients with autoimmune diseases (4) as well as atopic disorders such as food allergy (5).

Importantly, many cohort and observational studies have identified early environmental factors such as diet and microbial and antibiotic exposure as potential candidates contributing to the rising prevalence of allergies (6) and gut immunopathologies such as inflammatory bowel disease (7, 8) in developed countries. It is proposed that such environmental exposures modulate the development of the immune system with effects on Treg cells. However, few studies have actually examined the development of Treg cells in normal children or in children with gut immune dysregulation. A recent cohort study revealed changes in the proportion of naive/resting and memory/activated Treg (aTreg) cells in healthy control infants in the first 12 mo of life (9). However, the development of tissue tropism in human Treg cell subsets remains unclear. This is particularly important given that Treg cells exert control of immune responses locally. Additionally, increasing evidence suggests that exposure of food Ags via the gut is more likely to promote tolerance compared with exposure through the skin, which is thought to promote sensitization and allergy (10).

A previous study of human Treg cells found that the majority of Treg cells expressed the skin homing marker cutaneous lymphocyte Ag (CLA) (11), whereas a separate study found a high proportion of cord blood human Treg cells expressed gut homing α4β7 integrin (made of α4 and β7 subunits) (12), which suggests age related differences in Treg cell homing molecule expression. The importance of homing molecules for Treg cell function is demonstrated in murine studies in which lack of β7 integrin or its

*Department of Allergy and Immunology, The Children's Hospital at Westmead, Sydney, New South Wales 2145, Australia; †Kids Research Institute, The Children's Hospital at Westmead, Sydney, New South Wales 2145, Australia; ‡Discipline of Paediatrics and Child Health, The University of Sydney, Sydney, New South Wales 2145, Australia; §Charles Perkins Centre Nepean, Nepean, New South Wales 2747, Australia; ¶Department of Anatomical Pathology, Australian Capital Territory Pathology, Canberra Hospital, Garran, Australian Capital Territory 2605, Australia; ‖Australian National University Medical School, Canberra, Australian Capital Territory 0200, Australia; #Department of Gastroenterology, The Children's Hospital at Westmead, Sydney, New South Wales 2145, Australia; **James Fairfax Institute of Paediatric Nutrition, The University of Sydney, Sydney, New South Wales 2006, Australia; and ††Department of Pathology, The Children's Hospital at Westmead, Sydney, New South Wales 2145, Australia

ORCIDs: 0000-0002-4076-0464 (C.L.L.); 0000-0002-0104-2072 (M.H.); 0000-0003-1025-6520 (C.H.L.); 0000-0002-2479-5317 (A.A.S.); 0000-0002-7493-4055 (R. Nambiar).

Received for publication November 7, 2017. Accepted for publication April 11, 2018.

This work was supported by the Nepean Medical Research Foundation, the Allergy and Immunology Foundation of Australasia, and an Early Career Researcher Kickstart grant from The University of Sydney.

P.S.H. conceptualized and designed the project and drafted the manuscript; C.L.L., M.H., B.S.-N., C.H.L., A.A., L.G., R. Nambiar, A.A.S., and A.W. were involved in sample processing, and/or performing flow cytometry experiments, and/or result analysis; J.E.D., A.A., A.B., and S.A. performed the immunohistochemistry; and M.W., D.E.C., and R. Nanan supervised the project and critically reviewed the manuscript.

Address correspondence and reprint requests to Dr. Peter S. Hsu, Department of Allergy and Immunology, The Children's Hospital at Westmead, Hawkesbury Road, Westmead, Sydney 2145, NSW, Australia. E-mail address: peter.hsu@health.nsw.gov.au

The online version of this article contains supplemental material.

Abbreviations used in this article: aTconv, activated Tconv; aTreg, activated Treg; CB, cord blood; CLA, cutaneous lymphocyte Ag; GALT, gut-associated lymphoid tissue; HPF, high power field; RA, retinoic acid; RARa, RA receptor antagonist; RTE, recent thymic emigrant; rTreg, resting Treg; SP, single positive; Tconv, conventional T; Treg, regulatory T.

www.jimmunol.org/cgi/doi/10.4049/jimmunol.1701533

ligand MAdCAM-1 led to failure of oral tolerance induction (13). In terms of the induction of T cell tissue tropism, murine models have shown that in activated/memory T cells, α4β7 integrin is induced in gut-associated lymphoid tissue (GALT) by dendritic cell–derived retinoic acid (RA) (14, 15), whereas CLA can be induced by IL-12 in Th2 cells (16). Interestingly, a previous study of human conventional T (Tconv) cells showed that naive Tconv cells may acquire α4β7 integrin expression early in life because of enhanced response to IL-7 (17). This was further exemplified in HIV patients receiving IL-7 for T cell recovery, where upregulation of α4β7 integrin and gut migration of naive T cells was noted. However, in view of the reduced CD127 (IL-7 receptor α) expression on Treg cells, whether IL-7 has the same effect for Treg cells remains unknown.

In this study, we demonstrate the acquisition of early gut and delayed skin homing potential of peripheral blood Treg cells in healthy children of different ages. We further show that cord blood naive Treg cells are particularly sensitive to IL-2 induced upregulation of β7 integrin compared with their adult/memory counterparts and Tconv cells.

Materials and Methods

Subjects and isolation of mononuclear cells

Peripheral blood was obtained from healthy infants and children aged 0–16 y ($n = 50$) undergoing general anesthetic for elective surgery. Blood samples were collected at the time of cannulation prior to surgical procedures, which included orchidopexy, hypospadias repair, circumcision, hernia repair, and orthopedic surgery. Blood samples were also collected from healthy adult volunteers ($n = 10$) for functional studies. Subjects with known current or past history of allergic diseases (eczema, asthma, allergic rhinitis, food allergies, allergic gastrointestinal diseases), autoimmune diseases, immune deficiencies, or other genetic diagnoses were excluded. PBMC were isolated by Ficoll-Hypaque (Amersham Pharmacia, Piscataway, NJ) gradient centrifugation. Cells were frozen at −196°C and subsequently thawed for analysis by flow cytometry. In a small group of subjects ($n = 7$) who had a normal colonoscopy/biopsy for investigation of abdominal symptoms, peripheral blood and gut biopsies were obtained. For isolation of colonic cells, colon mucosal biopsy samples were washed with normal saline until macroscopically cleared of blood. The samples were incubated in prewarmed HBSS without calcium or magnesium, containing 1 mM EDTA and 1 mM DTT (Sigma-Aldrich) for 15 min; this process was repeated a total of four times. The samples were then transferred in a solution containing Collagenase III (100 U/ml) and DNAse (0.1 mg/ml) (Sigma-Aldrich) and incubated at 37°C for 2 h. At the end of the digestion, the cell suspension was filtered through a 70-μm sieve. Cells were then stained for flow cytometry as described. Thymus samples from two infants <6 mo of age undergoing cardiac surgery for isolated congenital heart disease (with no syndromal diagnosis such as CHARGE or DiGeorge syndrome) were obtained. Samples were processed, and mononuclear cells were isolated by Ficoll, then frozen at −196°C. For immunohistochemistry, available gut and skin sections previously taken from fetuses and children at autopsy or adjacent tissue from other surgical procedures were identified by the pathology department at two institutions. Subjects who had sepsis, known immune deficiency, gut/lung/skin inflammations, or allergic diseases at the time of biopsy were excluded. The Ethics Committee of the Sydney Children's Hospital Network (12/SCHN/33, 13/SCHN/240, 15/SCHN/229) and Sydney West Area Health Service approved this project according to the Declaration of Helsinki.

Flow cytometry

Surface Ab and intracellular staining for Foxp3 was performed as described previously (18). Briefly, surface stains ~1×10^6 PBMC were resuspended with 100 μl of FACS buffer (PBS containing 0.1% FCS and 0.02% sodium azide) in FACS tube. Dead cells were excluded from the analysis using Zombie (eBioscience). After washing, a mixture of appropriate amounts of fluorochrome-conjugated Abs were then added and incubated at 4°C for 25 min in the dark, then washed once with FACS buffer before intracellular staining, which was performed using the anti-human Foxp3 staining set and protocol (BioLegend). Abs used in the study are listed in Supplemental Table I.

Flow-activated cell sorting

For selected experiments, $CD4^+$ T cells were first isolated from cord blood PBMC by magnetic separation using CD4 biotin Ab followed by anti-biotin MACS magnetic MicroBeads (Miltenyi Biotec). Cells were then labeled with CD25 and CD127 (in addition to CD3 and CD4) and sorted into $CD25^+CD127^{lo}$ Treg cells and $CD25^-CD127^{hi}$ Tconv cells to >99% purity using BD Influx cell sorter (The Westmead Institute for Medical Research), then used for subsequent cultures.

In vitro cell cultures

PBMC or sorted Treg/Tconv cells were plated at 37°C in 48-well (1×10^6 cells/ml) or 96-well (1×10^5 cells/ml) plates respectively. RPMI 1640 was supplemented with 10% FCS, L-glutamine (2 mM), penicillin (100 U/ml), and streptomycin (100 mg/ml). For cultures examining the effect of various IL-2 doses and IL-7 on cells, PBMC were cultured for 72 h in the presence or absence of recombinant human IL-2 (50, 100, and 200 U/ml; eBioscience) or recombinant human IL-7 (5 ng/ml; BioLegend) and in selected cultures for anti–IL-2, IL-7–neutralizing Ab MA5-23700 (0.8 μg/ml; Thermo Fisher Scientific), or RA receptor antagonist (RARa), AGN (1 μM; R&D Systems). For cultures examining the effect of STAT5 inhibitor, PBMC were cultured for 24 h in the presence of recombinant human IL-2 (100 U/ml) or recombinant human IL-7 (5 ng/ml) with STAT5 inhibitor (150 mM; Merck Millipore) or DMSO.

Immunohistochemistry

Paraffin-embedded duodenum and skin tissues from each of the five subjects per age group (early second trimester [13–16 wk], late second trimester [20–26 wk], mid–third trimester [30–35 wk], newborn [37–41 w]), 0–3, 4–6, 7–9, 10–12 mo, 1–5 y old, 6–10 y old, 11–15 y old, >16 y) were sectioned and sequentially stained to assess the presence and quantity of CD4- and Foxp3-expressing lymphocytes. $CD4^+$ and $Foxp3^+$ cells were counted over 10 high power fields (HPF) in each section. The average number of cells per HPF was then calculated for each slide, each tissue, and each subject, and results were plotted against age. $Foxp3^+$ and β7 integrin expression in thymic cells were counted over 50 HPF in each section in five fetuses at term (38–40 wk gestation). Immunohistochemistry was performed as described previously (18).

Statistical analyses

For normally distributed data, Student t test was used to assess statistically significant difference between two samples. For data with nonnormal distribution, the Mann–Whitney and Wilcoxon signed-rank test were used for unpaired and paired data respectively. For datasets with multiple comparisons, one-way ANOVA was used to determine whether there was significant variance among groups, followed by post hoc Bonferroni analysis. Pearson correlation coefficient was used for correlation studies. A p value <0.05 was deemed statistically significant. If not specified within graphs, p values are denoted as follows: $*p < 0.05$, $**p < 0.01$, $***p < 0.001$, and $****p < 0.0001$.

Results

The contrasting pattern of development in Treg cell subsets and their tissue homing potential with age

A previous study has shown that $CD45RA^+Foxp3^{lo}$ Treg cells represent naive resting Treg (rTreg) cells with less suppressive capacity but more longevity compared with $CD45RA^-Foxp3^{hi}$ aTreg cells, whereas the $CD45RA^-Foxp3^{lo}$ population mainly consists of activated Tconv (aTconv) cells with promiscuous cytokine production (19). We examined these three subsets of $Foxp3^+$ cells in healthy children of varying ages and found that the proportion of rTreg cells within $CD4^+$ T cells slowly decreases with age, whereas the proportion of aTreg cells and aTconv cells increases with age (Fig. 1A). This is consistent with age-related Ag encounter/activation. We also examined Treg cell subsets based on their expression of Helios, which had been proposed as a marker of natural Treg cells in humans (20). However, later studies seem to suggest that $Helios^+$ Treg cells may represent those that have been alternatively activated (21) or those that are more stable (22). Nevertheless, we found that the proportion of $Helios^+Foxp3^+$ Treg cells remained stable with age, whereas $Helios^-Foxp3^+$ Treg cells increased with age (Fig. 1B).

We next examined the gut and skin homing molecule expression of peripheral blood Treg cells. We used β7 integrin as a surrogate marker for gut tropism because almost all $\beta7^+$ T cells (>99%)

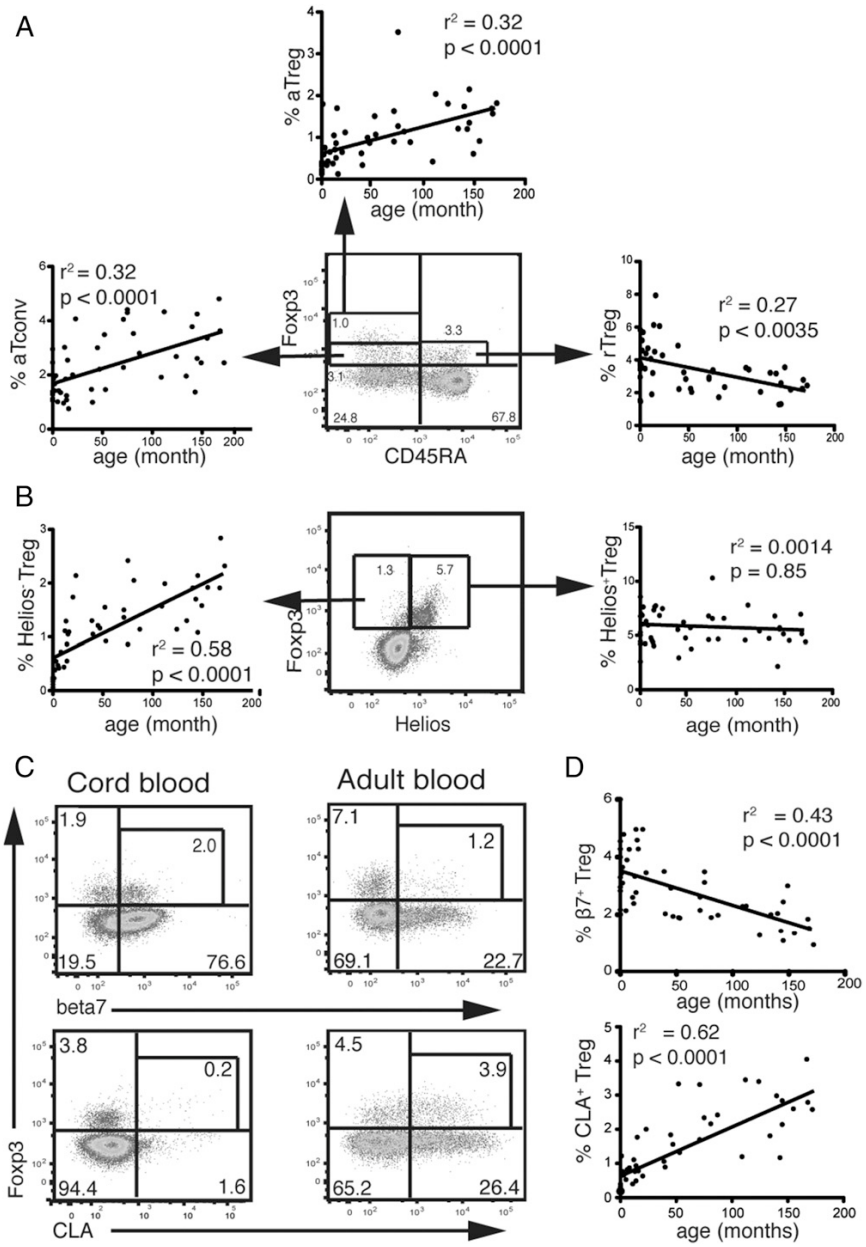

FIGURE 1. Age-dependent changes in Treg cell subsets in children. (**A**) $CD4^+Foxp3^+$ cells are subdivided into three subsets, $CD45RA^+Foxp3^{lo}$ rTreg, $CD45RA^-Foxp3^{hi}$ aTreg, and $CD45RA^-Foxp3^{lo}$ aTconv, with their respective age-related change in percentage (within $CD4^+$ cells). (**B**) Treg cell subsets based on Helios expression and their related age-related change in percentage. (**C**) Representative flow plots showing distinct patterns of gut and skin homing molecule expression of Treg cells in cord blood and adult blood. (**D**) Age-related change in the percentage of $\beta7^+$ and CLA^+ Treg cells within CD4 cells.

were also $\alpha4^+$ (Supplemental Fig. 1a). CLA was used as a marker of skin tropism. Circulating $\beta7^+$ Treg cells (as a proportion of total circulating $CD4^+$ T cells) were most abundant early in life and decreased with age (Fig. 1C, 1D). The same pattern was observed when $\alpha4\beta7^+$ Treg cells were analyzed in a subgroup of patients (Supplemental Fig. 1b). In a small group of children who had endoscopy/biopsy, we also observed a correlation between peripheral blood $\beta7^+Foxp3^+$ Treg cells and gut mucosal $Foxp3^+$ Treg cells (Supplemental Fig. 1c), which suggests that β7 expression in peripheral blood Treg cells is a good surrogate marker for gut mucosal Treg cells. As a comparison, we next examined skin homing Treg cells and found they were almost absent in cord blood and increased with age (Fig. 1C, 1D).

$\beta7^+$ Treg cells are predominantly naive and acquire β7 integrin after thymic emigration

The age-dependent pattern of Treg cell gut and skin tropism appears to parallel the development of rTreg and aTreg cells respectively. Indeed, the proportion of $\beta7^+$ Treg cells correlated significantly with rTreg cells, whereas the proportion of CLA^+ Treg

cells correlated significantly with aTreg cells (Fig. 2A). On further examination, a significant proportion of $\beta7^{+}Foxp3^{+}$ cells were rTreg cells, whereas aTreg cells composed a larger proportion of CLA^{+} $Foxp3^{+}$ cells (Fig. 2B, 2C). Additionally, a higher proportion of $\beta7^{+}$ Treg cells were also positive for both CD45RA and CD31 (a marker for recent thymic emigrants [RTE]) (23), compared with CLA^{+} Treg cells (Fig. 2D, 2E). Given these findings, we then examined the expression of β7 integrin in the thymus. Using flow cytometry, $CD3^{+}$ thymocytes were gated based on their expression of CD4 and CD8 (Fig. 2F). As expected, most $Foxp3^{+}$ cells were CD4 single positive (SP). Within the $CD4SPFoxp3^{+}$ cells, ~10% of the cells expressed β7 integrin, whereas in the $CD4SPFoxp3^{-}$ cells, ~5% of the cells expressed β7 integrin (Fig. 2F), as compared with peripheral blood, where 60–80% of cord blood Treg and Tconv cells express β7. This result was confirmed by immunohistochemistry (Fig. 2G), in which we found very few $\beta7\ integrin^{+}$ cells (mean 2.83 per 50 HPF;

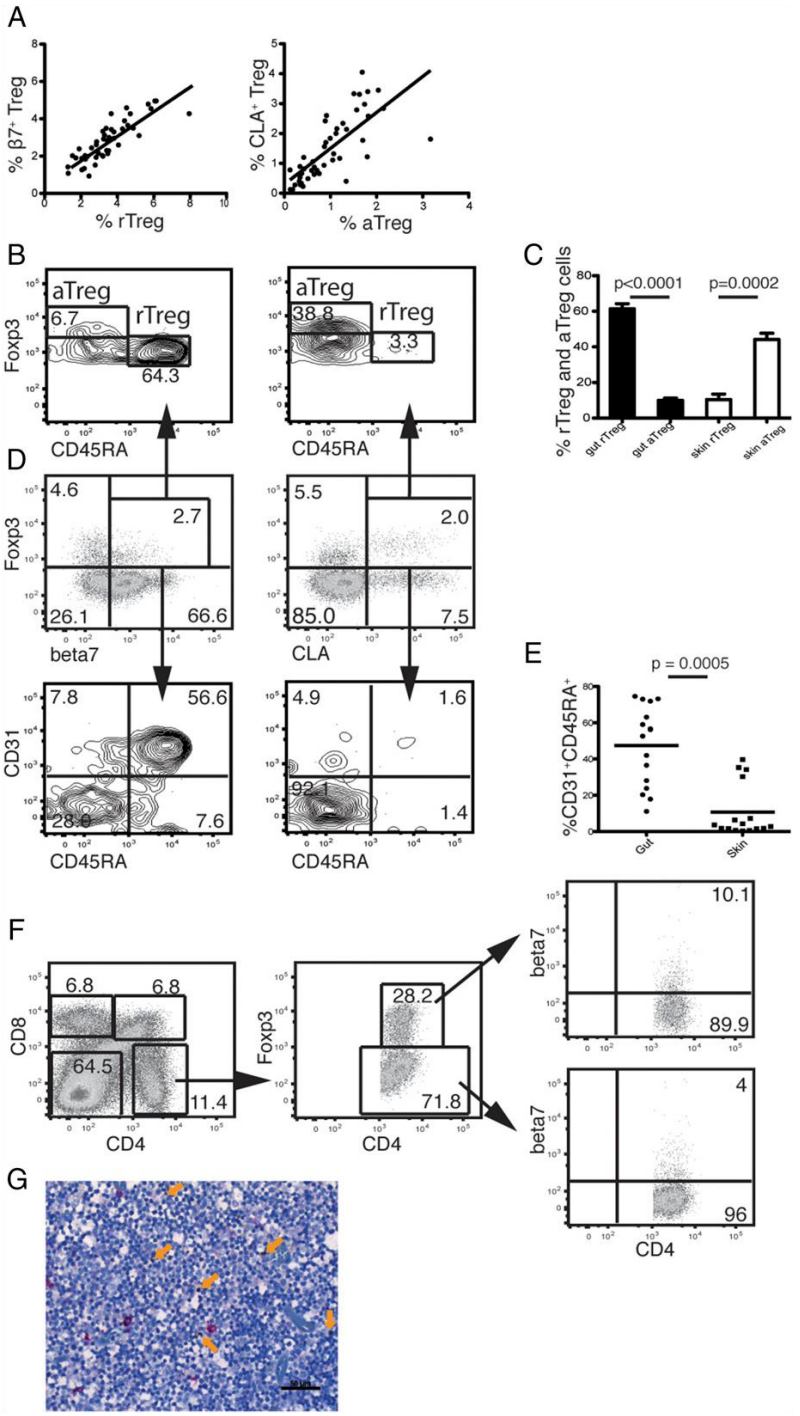

FIGURE 2. Phenotype of gut and skin homing Treg cells. (**A**) Correlation of gut homing Treg cells with rTreg and skin homing Treg cells with aTreg. (**B**) Representative flow plot showing the distribution of gut (left) and skin (right) homing Treg cells in a healthy child. (**C**) Comparison of aTreg and rTreg percentages within gut and skin homing Treg cells. (**D**) Representative plot showing the percentage of $CD45RA^{+}$ $CD31^{+}$ cells within gut and skin homing Treg cells in a healthy child. (**E**) Comparison of $CD45RA^{+}CD31^{+}$ cell percentage within gut and skin homing Treg cells. (**F**) Representative flow plot showing β7 expression of $CD4SPFoxp3^{+}$ and $CD4SPFoxp3^{-}$ cells gated from live $CD3^{+}$ thymocytes (data representative of two samples). (**G**) Representative micrograph (original magnification ×40) of a term fetal thymus showing $Foxp3^{+}$ cells (stained brown marked by yellow arrow) and few $\beta7^{+}$ cells (pink). Scale bar, 50 μg.

95% confidence interval 1.15–4.51) in the fetal thymus from five term infants. No coexpression of β7 integrin and Foxp3 was observed. Collectively, these results suggest that Treg cells likely acquire β7 expression early in their development but after thymic emigration.

Naive Tconv cell show enhanced β7 in response to IL-7

A previous study had shown that naive Tconv cells in particular upregulate their expression of β7 integrin in response to IL-7 (17). However, Treg cells have significantly lower surface expression of CD127, the IL-7 receptor α-chain (24), so whether they respond in the same way is unknown. We found that when adult PBMC were cultured in the presence of IL-7, naive $CD4^+Foxp3^-$ Tconv cells demonstrated significantly more upregulation of β7 expression compared with memory Tconv cells (Fig. 3A, 3B). This was independent of CD127 expression intensity because memory Tconv cells have comparable or slightly higher CD127 expression compared with naive Tconv cells (data not shown). In contrast, adult naive and memory peripheral Treg cells demonstrated minimal upregulation of β7 integrin compared with naive Tconv cells (Fig. 3A, 3B). Similar upregulation of α4 expression was also seen with IL-7 incubation (Supplemental Fig. 2a). Cord blood Tconv (both naive and memory) and naive Treg cells also

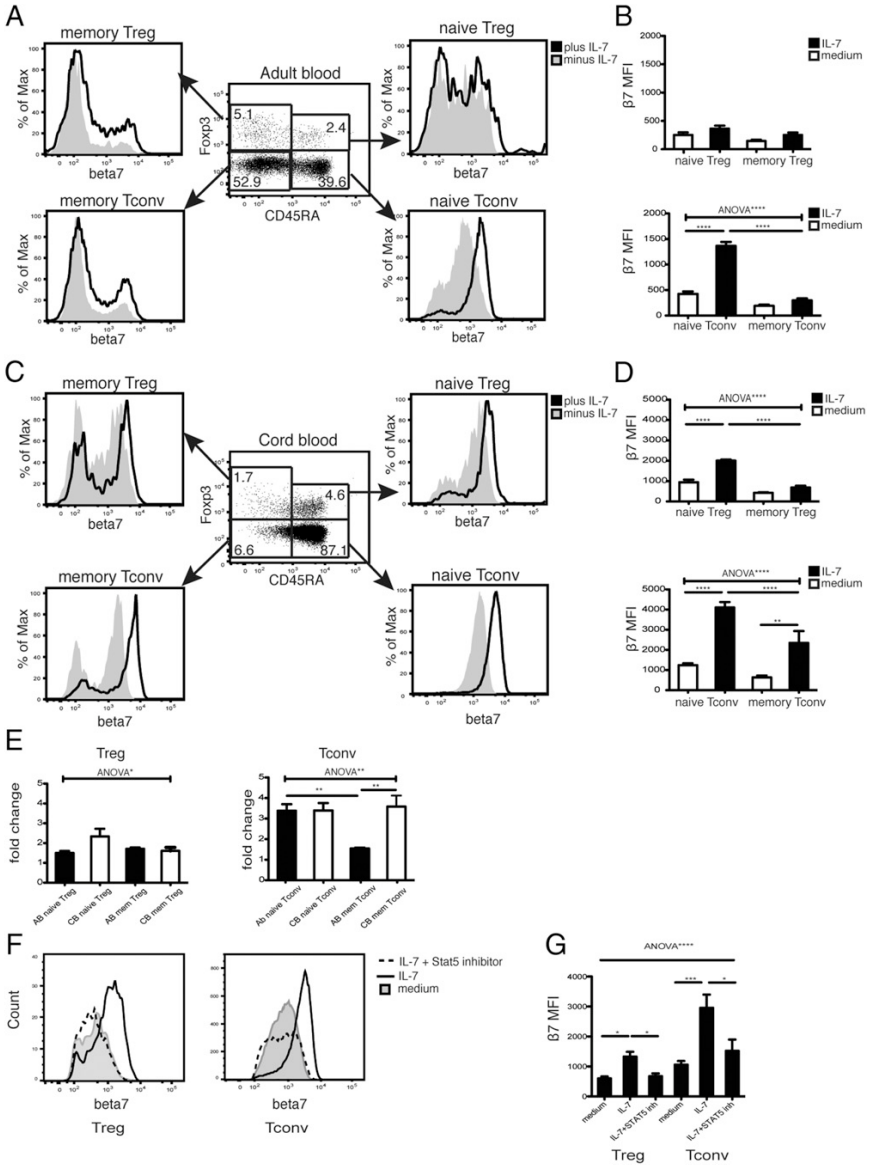

FIGURE 3. IL-7 induces upregulation of β7 integrin in a STAT5-dependent manner. (**A**) Representative histograms showing β7 expression of various $CD4^+$ T cell subsets after 3 d of culture with (black line) or without IL-7 (shaded) in healthy adults, summarized in (**B**) in terms of β7 integrin mean fluorescence intensity (MFI; $n = 5$). (**C**) Representative histograms showing β7 expression of various $CD4^+$ T cell subsets after 3 d of culture with (black line) or without IL-7 (shaded) in cord blood, summarized in (**D**) in terms of β7 integrin MFI ($n = 5$). (**E**) Comparison of the fold change in β7 integrin MFI in Treg and Tconv cell subsets between adult and cord blood PBMC. (**F**) Representative histograms showing the effect of STAT5 inhibition on cord blood Treg and Tconv cells cultured with IL-7 for 1 d. (**G**) Summary bar graph showing the effect of STAT5 inhibition on β7 integrin MFI expression ($n = 4$). $^*p < 0.05$, $^{**}p < 0.01$, $^{***}p < 0.001$, and $^{****}p < 0.0001$.

upregulated β7 integrin in response to IL-7. In comparison with adult cells, cord blood memory Tconv cells and naive Treg cells trended toward increased β7 upregulation based on fold change in β7 expression (Fig. 3C–E). These results were confirmed on sorted Treg and Tconv cells (data not shown). The increase in β7 expression could be suppressed by IL-7 neutralization (Supplemental Fig. 1d) or inhibition of pSTAT5 in Treg and Tconv cells (Fig. 3F, 3G), suggesting this effect is mediated by IL-7–induced STAT5 activation. We also confirm that the effect of IL-7 was not dependent on RA, because addition of RARa did not inhibit IL-7–induced β7 upregulation in naive Tconv cells (Supplemental Fig. 1e). These results are consistent with the report by Cimbro et al. (17). Overall, these data suggest that naive T cells are particularly sensitive to IL-7–induced β7 upregulation.

IL-2 selectively enhanced β7 expression in Treg cells, especially in cord blood

Because Treg cell homeostasis is dependent on another STAT5-activating cytokine (IL-2), with Treg cells having much higher CD25 (IL-2RA) expression compared with Tconv cells (24), we tested the ability of IL-2 to upregulate β7 in both Treg and Tconv cells. Incubation of PBMC alone without any cytokines led to significant increases in Treg cell and to a lesser extent Tconv β7 expression. This spontaneous β7 upregulation could be reversed by the addition of anti–IL-2 in Treg cells but not in Tconv cells (Fig. 4A–C). This suggests that endogenous IL-2 production (likely by Tconv cells) upregulated Treg cell but not Tconv β7 expression in vitro. Importantly, we found that only Treg but not Tconv cells upregulated their β7 expression in response to exogenous IL-2 (Fig. 4A–C). This was true at all IL-2 doses tested

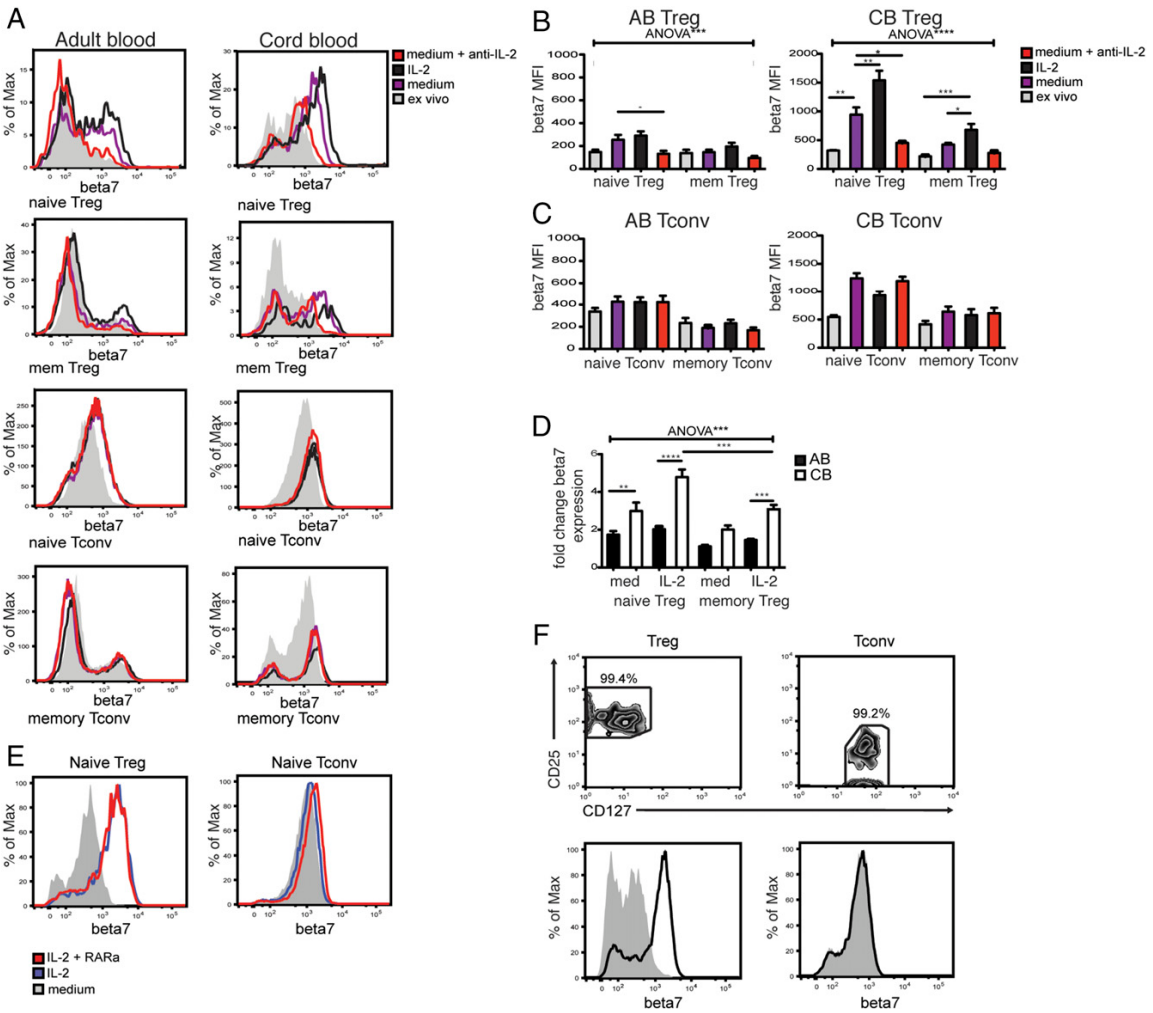

FIGURE 4. IL-2 selectively enhances β7 integrin expression in Treg cells. (**A**) Representative histograms of Treg and Tconv subsets in adult and cord blood, showing β7 integrin expression at day 0 (ex vivo, shaded), at day 3 cultured with (green) or without (blue) IL-2 (50 U/ml), and at day 3 cultured without IL-2 in the presence of anti–IL-2 (red). This is summarized in bar graphs showing adult and cord blood Treg subsets (**B**) and Tconv subsets (**C**) cultured under various conditions as indicated ($n = 5$). (**D**) Fold change in β7 MFI compared with ex vivo condition (day 0) in various Treg and Tconv cell subsets. (**E**) Effect of RARa on β7 expression in Treg and non-Treg cells in response to IL-2 (data representative of three independent experiments). (**F**) Effect of IL-2 (black line) on β7 expression of sorted Treg and non-Treg cells compared with medium alone (shaded) (data representative of three independent experiments). $*p < 0.05$, $**p < 0.01$, $***p < 0.001$, and $****p < 0.0001$.

(50, 100, and 200 U/ml) and was similarly observed for α4 expression (Supplemental Fig. 2b, 2c). The effect of IL-2 was most pronounced in naive Treg cells, especially in the cord blood (Fig. 4D). This correlates with the higher β7 expression observed ex vivo in cord blood naive Treg cells. Addition of RARa did not inhibit IL-2–induced β7 upregulation (Fig. 4E), suggesting that this effect is RA independent. Furthermore, the same effect of IL-2 on β7 expression in Treg and non-Treg cells was observed in isolated cultures of sorted Treg and non-Treg cells in the absence of APCs (Fig. 4F), which are the likely producers of RA. Overall, our data suggest IL-2 selectively upregulates β7 expression (especially in cord blood), independent of RA.

Enhanced IL-2 production and response in cord blood

We then examined the ability of $CD4^+Foxp3^-$ Tconv cells to produce IL-2. Stimulating PBMC with PMA and ionomycin, we found that a higher proportion of cord blood Tconv cells produced IL-2 compared with adult Tconv cells (Fig. 5A). In fact, it was clear that the proportion of IL-2–secreting Tconv cells was significantly higher in cord blood compared with PBMC from any other age group (Fig. 5B). To assess whether cord blood Treg cells had enhanced responses to IL-2 compared with adult blood, we cultured cord and adult blood PBMC in the presence of IL-2 without stimulation for 3 h, then assessed pSTAT5 in naive Treg cells. IL-2 induced a modest but significant increase in the proportion of $pSTAT^+$ cells in cord blood compared with adult blood naive Treg cells (Fig. 5C). This was associated with an increased pSTAT5 expression in cord blood naive Treg cells (Fig. 5D). However, cord blood (CB) Treg cells did not respond more quickly to IL-2 (Fig. 5E) or better to lower doses of IL-2 (data not shown). Additionally, we show that Treg cells in cord blood have a higher expression of CD25 (Fig. 5F, 5G), consistent with the enhanced pSTAT5 seen in cord blood. Overall these results suggest that in cord blood, there is both an increased propensity for IL-2 production by Tconv cells and an enhanced responsiveness of naive Treg cells to IL-2.

IL-2 and IL-7 paradoxically downregulate CLA expression

To examine whether IL-2 and IL-7 specifically upregulate β7, we also examined CLA expression in the cultured cells. We found that both IL-2 and IL-7 downregulated CLA expression in vitro. Unlike with β7, the effect of IL-2 was not limited to Treg cells but also reduced CLA expression in Tconv cells (Fig. 6A, 6B), although to a lesser extent than IL-7 (Fig. 6C). Likewise, IL-7 induced CLA downregulation in both Tconv and Treg cells (Fig. 6A, 6B). In contrast with β7, there was no obvious differential effect of IL-2 or IL-7 on CLA expression in cord blood compared with adult blood or in naive compared with memory T cells (Fig. 6C). Of note, IL-2 and IL-7 did not significantly alter CCR7 or αE integrin (CD103) expression in Treg or Tconv cells, respectively (Fig. 6D). Overall, these results suggest that IL-2 and IL-7 specifically skew the expression of human T cell homing molecules to favor gut but not skin homing.

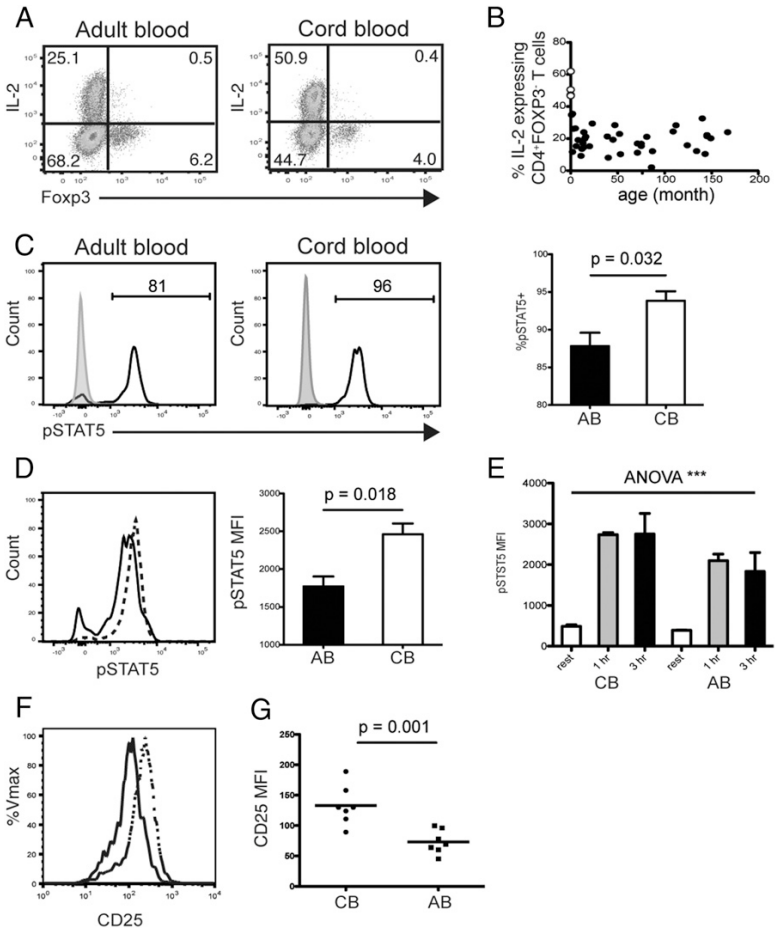

FIGURE 5. Increased IL-2 production and response to IL-2 in cord blood. PBMC was stimulated by PMA/ionomycin for 5 h and intracellular cytokine expression analyzed by flow cytometry (**A**) Representative flow plots gated on $CD3^+CD8^-$ T cells showing the proportion of IL-2–expressing $Foxp3^-$ Tconv cells in adult blood and cord blood. (**B**) The proportion of IL-2–expressing $CD3^+CD8^-Foxp3^-$ Tconv cells plotted against age (white circle = cord blood). (**C**) Representative histograms and summary bar graphs showing the proportion of $pSTAT5^+$ cells within CB and adult blood (AB) naive Treg cells after 3 h of IL-2 stimulation (solid line) compared with cultures without addition of IL-2 (shaded), $n = 4$. (**D**) Representative histograms and summary bar graphs showing the expression of pSTAT5 in CB (dashed line) and AB (solid line) naive Treg cells after 3 h of IL-2 stimulation ($n = 4$). (**E**) pSTAT5 expression in CB and AB Treg cells 1 and 3 h after incubation with IL-2; data represent three independent experiments. (**F**) Representative histogram showing CD25 expression in CB (dashed) and AB (solid) Treg cells. (**G**) Summary dot plot showing Treg cell CD25 mean fluorescence intensity (MFI) in CB and AB. $***p < 0.001$.

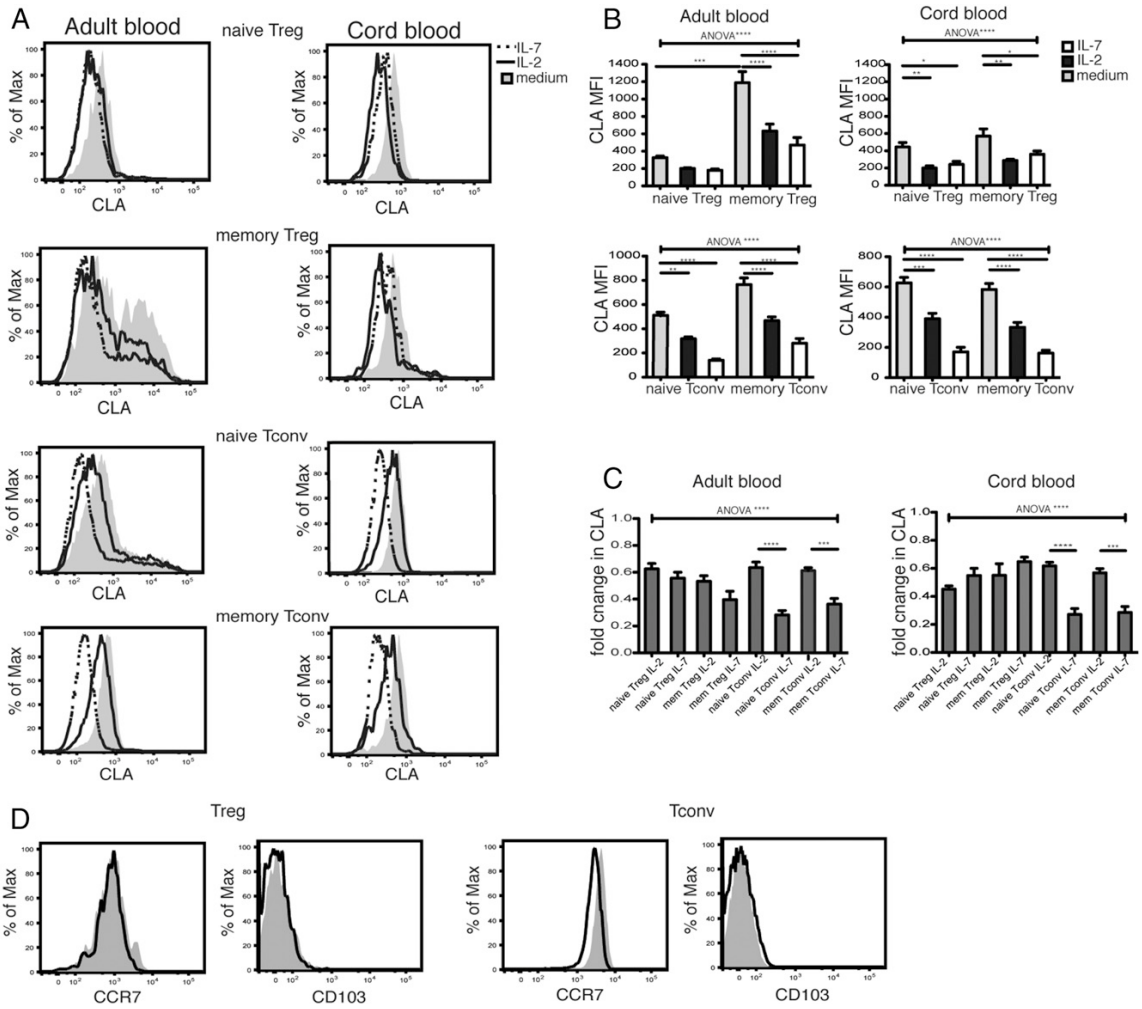

FIGURE 6. IL-2 and IL-7 downregulates CLA expression. (**A**) Representative histograms showing CLA expression in various adult and cord blood Treg and Tconv subsets cultured for 3 d without cytokine (shaded), with IL-2 (black), or with IL-7 (dashed). (**B**) Summary bar graphs showing CLA expression in Treg and Tconv subsets cultured for 3 d without cytokine, with IL-2, or with IL-7 ($n = 5$). (**C**) Fold change in CLA expression of cells cultured with IL-2 or IL-7 relative to cells cultured without cytokines for 3 d ($n = 5$). (**D**) Effect of IL-2 (black line) on Treg cells and IL-7 (black line) on Tconv cells in terms of CCR7 and CD103 expression compared with medium alone (shaded) (data representative of three independent experiments). $*p < 0.05$, $**p < 0.01$, $***p < 0.001$, and $****p < 0.0001$.

Age-dependent gut and skin distribution of Treg cells in children

In addition to examining tissue homing of Treg cells in peripheral blood, we sought to examine the actual tissue distribution of Treg cells in the duodenum and skin from the second trimester to 16 y of age using tissue immunohistochemistry (Fig. 7A, 7B).

In both the duodenum and skin, $CD4^+$ T cells were observed from mid–second trimester and increased rapidly in the early postnatal period, then remained stable with age (Fig. 7C). Similarly, occasional Treg cells were observed in the skin and duodenum in the second and third trimester; however, the number of Treg cells increased dramatically in the early postnatal period and remained stable (Fig. 7D). When looking at the number of $Foxp3^+$ cells per HPF as a percentage of the number of $CD4^+$ cells per HPF in each section, we found that in the first 6 mo of life, the duodenum harbored a significantly higher percentage of $Foxp3^+$ cells compared with the skin and this difference disappeared after 6 mo of age (Fig. 7E). This is consistent with the age dependent pattern of Treg homing molecule expression in the peripheral blood, in that the percentage of $\beta7^+$ Treg cells was highest early in life.

Discussion

Tissue homing of both memory and naive T cells is an important aspect of immune function and regulation (25). The results of this study suggest that human naive Treg and Tconv cells may be primed early in life for gut tropism, which reinforces the important role of early gut microbial colonization and oral/gut Ag exposure in shaping the developing immune system. Importantly, we explored the potential mechanisms for the induction of gut tropism and demonstrated distinct Treg and Tconv responses to the lymphopoietic cytokines IL-2 and IL-7.

IL-7 plays an important role in lymphopoiesis and peripheral homeostasis of T cells (26). This is evidenced by the human severe combined immune deficiency disorder caused by IL-7 receptor deficiency, in which there is failure of T cell development (27).

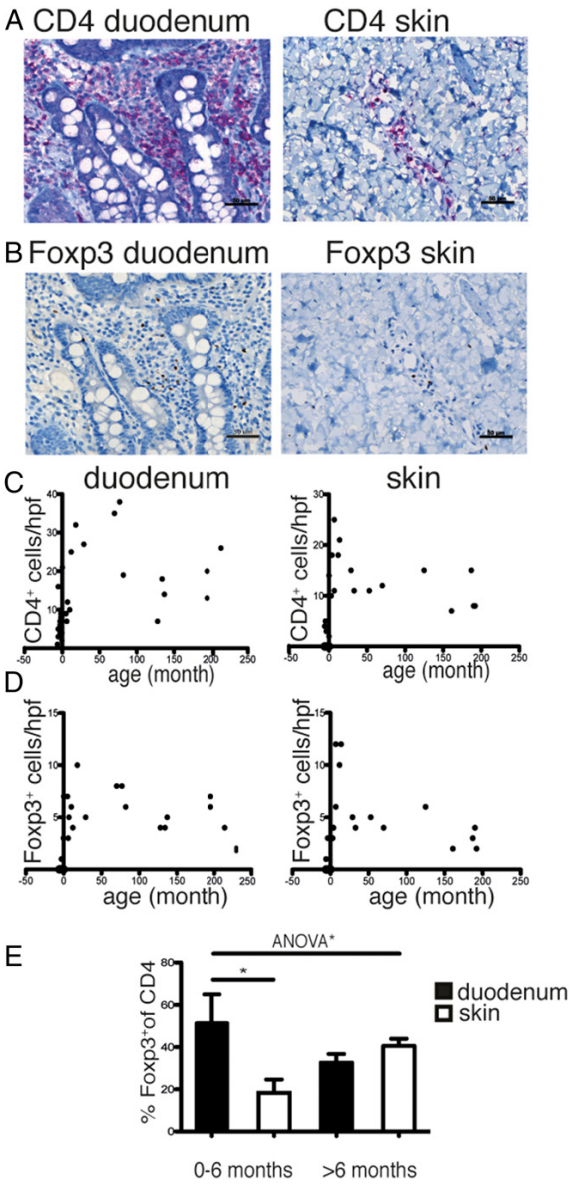

FIGURE 7. Tissue distribution of Foxp3$^+$ and CD4$^+$ cells in the gut and skin. Representative immunohistochemistry micrographs showing (**A**) CD4$^+$ (alkaline phosphatase, red) cells or (**B**) Foxp3$^+$ (3,3′-diaminobenzidine, brown) cells in the duodenum (left) and skin (right). Scale bars, 50 μm. The numbers of CD4$^+$ cells (**C**) and Foxp3$^+$ cells (**D**) per HPF were counted and plotted against age (months), where ages below 0 represent months before full term (40 wk gestation). (**E**) Relative percentage of Foxp3$^+$ cells per HPF against CD4$^+$ cells per HPF in the duodenum and skin grouped according to age (0–6 mo, >6 mo). *$p < 0.05$.

Our study demonstrated that IL-7 was able to bias Tconv cells toward a gut homing phenotype, which included upregulation of the β7 (and α4) integrin and downregulation of CLA. Consistent with a previous study, β7 integrin upregulation was most pronounced in naive Tconv cells (17) but was comparable between adult and cord blood. This implies that IL-7 may act to ensure a consistent supply of naive T cells directed to the gut throughout life and suggests that GALT may be an important target of naive T cell homing, in keeping with the fact that GALT is the largest lymphoid organ and an important interface for Ag encounter. Interestingly, the response of adult Treg cells to IL-7 was minimal compared with Tconv cells, perhaps owing to the reduced CD127 expression in Treg cells, although a modest response to IL-7 could be observed with cord blood naive Treg cells.

However, it was IL-2 that had the most pronounced effect on Treg cells for gut tropism. IL-2 is now well recognized to be a critical cytokine for Treg cell generation, homeostasis, and function (28). Human monogenetic disorders that lead to defective responses to IL-2, such as CD25 deficiency, STAT5 deficiency, and STAT3 gain of function mutations, give rise to primary immune deficiencies similar to the immune dysregulation, polyendocrinopathy, enteropathy, X-linked syndrome with pronounced gastrointestinal symptoms, and immunodeficiency (29–31), suggesting a potential role for IL-2 in gut immune tolerance.

In this study, we showed that IL-2 selectively enhanced β7 (and α4) integrin expression in Treg cells but not in Tconv cells. Moreover, this effect was most prominent in cord blood naive Treg cells. Interestingly, endogenous IL-2 production by unstimulated Tconv cells was sufficient to enhance β7 expression in vitro, which suggests this is a physiological effect. Indeed, we showed that a significantly higher proportion of cord blood non-Treg cells produced IL-2 compared with other age groups, consistent with a previous study (32). Furthermore, we show that cord blood Treg cells have a higher expression of IL-2RA (CD25). This likely leads to enhanced IL-2–induced pSTAT5 in cord blood naive Treg cells. Together, these results suggest an important role for IL-2 in shaping the Treg cell population early in life.

In addition to the cytokine environment, the timing and site of β7 acquisition by naive Treg cells is clearly of interest. Our results showed that β7 integrin was expressed largely by naive rTreg cells, and the proportion of β7$^+$ Treg cells inversely correlated with age. This suggests that Treg cells acquired gut tropism early in life. Consistent with this, a notable but variable proportion of peripheral blood β7$^+$ Treg cells were CD31$^+$ RTE, which is consistent with animal data in which murine thymocytes acquired gut homing molecules at the RTE stage, although this study did not examine Treg cells specifically (33). Furthermore, we showed that only a small proportion of human CD4SPFoxp3$^+$ thymocytes expressed β7 integrin, which suggests that naive human Treg cells likely acquired their gut homing phenotype after they emigrated from the thymus. As a previous study suggested that murine RTE undergo further progressive development in secondary lymphoid organs to become "mature" naive T cells (34), it seems likely that the gut homing molecules are acquired in these peripheral lymphoid tissues.

Although RA produced by gut-derived CD103$^+$ APCs is known to induce gut homing molecules in mesenteric node T cells, this does not appear to be selective for Treg cells (35). In contrast, our current results indicate that IL-2 selectively upregulates α4 and β7 integrin in naive Treg cells, especially early in life. Furthermore, previous reports suggest that RA requires TCR engagement/activation to exert its effect on T cell α4 and β7 expression (17, 35), whereas in our current study, we show that IL-2 was able to upregulate α4 and β7 expression without any stimulation. This suggests that IL-2 may be important for priming thymus-derived naive/unstimulated Treg cells for gut homing to promote early mucosal tolerance, whereas RA is important for homing of Ag-induced/aTreg cells to the gut. Indeed, the importance of thymic Treg cells for intestinal immune tolerance is supported by a previous murine study, showing that thymus-derived Treg cells constitute the majority of gut Treg cell compartments (36). However, recent data also suggest that a distinct population of Helios-RORγt$^+$ Treg cells, likely induced later in life by certain members of the gut microbiome, are present in both the

murine and human colon and promote tolerance to commensal microorganisms (37). Therefore, intestinal Treg cells are likely derived from both the thymic and peripheral naive T cell pool and probably play differential but overlapping roles in controlling immune responses to self-antigens and foreign/microbial Ags, respectively (38). In view of our results, we propose that an early wave of naive thymic/natural Treg cells may be driven by IL-2 for gut migration to establish early mucosal tolerance, in preparation for progressive microbial/foreign Ag exposure, which likely leads to induction and gut homing of extrathymic memory/aTreg cells under the influence of RA. Clearly, further investigations are required to test this hypothesis.

We concede that expression of peripheral blood tissue homing markers does not necessarily equate to actual tissue homing. In vivo cell trafficking studies would be required to confirm this association. This is currently not possible in human studies. There is, however, substantial indirect evidence that $\alpha4\beta7$ expression by human T cells correlates to gut homing. In particular, vedolizumab, a mAb that blocks the interaction of $\alpha4\beta7$ integrin with MAdCAM-1, has been used effectively in humans to treat ulcerative colitis by blocking T cell entry to the gut (39). This effect was supported by reduced gut T cell infiltrates in vedolizumab-treated patients in addition to other histological recovery (40). Notably, the inhibition of gut homing by vedolizumab was observed in both Treg and T effector cells (Tconv) in patients with ulcerative colitis (41), suggesting that $\alpha4\beta7$ integrin mediates both Treg and T effector trafficking to the gut. Consistent with this, in a small group of subjects, we found a correlation between peripheral blood $\beta7^+$ Treg cells and colonic $Foxp3^+$ Treg cells. Furthermore, we assessed tissue Treg cells in a separate cohort using immunohistochemistry. We showed that the proportion of $Foxp3^+$ cells (relative to $CD4^+$ cells) was higher in the gut in the first 6 mo of life, consistent with the higher proportion of peripheral blood $\beta7^+$ Treg cells in early life. Therefore, our results suggest that in healthy individuals, Treg cells likely acquire gut homing potential early in life.

This has important implications for diseases in which impairment of gut tolerance is thought to play a role, such as food allergies and inflammatory bowel disease. Indeed, a recent study suggested that suppression of IL-2 production may contribute to the early reduction of naive Treg cells observed in children who later develop food allergies (42). However, whether Treg cell gut homing is impaired in children with food allergies requires further investigation. Notably, our results showing the early acquisition of Treg gut homing potential supports the notion that early oral introduction of food within a critical window may be important for establishment of oral tolerance and for allergy prevention (due to a favorable gut immune milieu), a concept which is well supported by recent clinical trials (43–45). In contrast, the delayed acquisition of skin homing potential in Treg cells could favor early allergen sensitization through the skin, especially when there is impairment of skin barrier, such as in atopic dermatitis (46). These findings are of interest to the study of allergic disease development and may be further tested in future well-designed longitudinal cohort studies. Similarly, such studies may also be helpful for examining the development of inflammatory bowel disease because enhanced mucosal type 2 immune responses have also been noted in ulcerative colitis compared with Crohn's disease and controls (47), although how early such changes occur is unknown.

Lastly, our results highlight a previously unrecognized function of IL-2, which may be of interest in view of the emerging role of low dose IL-2 as a potential therapy for diseases of immune dysregulation such as in systemic lupus erythematosus (48) and hepatitis C–induced vasculitis (49). Although no human studies have examined the role of low-dose IL-2 in atopic disorders, in mice, low-dose IL-2 therapy was able to protect against development of allergy via expansion of Treg cells in gut-associated tissues (8), supporting the potential role of IL-2 in allergy prevention. We are also aware of an ongoing clinical trial examining the effect of low-dose IL-2 in human ulcerative colitis. Early results indicate expansion of Treg cells in the peripheral blood of a treated patient (50). It would be interesting to examine whether there are any alterations in gut Treg cell proportion in this context.

In summary, our study showed that IL-2 biases Treg cells to upregulate $\beta7$ expression, especially early in life. This function correlates with the increased sensitivity of neonatal Treg cells to IL-2 and the increased Treg expression of $\beta7$ integrin in early life and suggests a potential role of IL-2 in regulating Treg cell gut tropism and mucosal immune tolerance during this critical period.

Acknowledgments

We would like to acknowledge Alvin Benig (Immunology Laboratory, The Children's Hospital at Westmead) for help processing and storing the peripheral blood samples. We thank Prof. Stephen Alexander and Prof. Stuart Tangye for providing the thymus samples. We also thank Dr. Suat Dervish at the Westmead Institute of Medical Research for assistance with flow-activated cell sorting.

Disclosures

The authors have no financial conflicts of interest.

References

1. Haribhai, D., J. B. Williams, S. Jia, D. Nickerson, E. G. Schmitt, B. Edwards, J. Ziegelbauer, M. Yassai, S.-H. Li, L. M. Relland, et al. 2011. A requisite role for induced regulatory T cells in tolerance based on expanding antigen receptor diversity. *Immunity* 35: 109–122.
2. Wing, K., and S. Sakaguchi. 2010. Regulatory T cells exert checks and balances on self tolerance and autoimmunity. *Nat. Immunol.* 11: 7–13.
3. Torgerson, T. R., and H. D. Ochs. 2007. Immune dysregulation, polyendocrinopathy, enteropathy, X-linked: forkhead box protein 3 mutations and lack of regulatory T cells. *J. Allergy Clin. Immunol.* 120: 744–750; quiz 751–752.
4. Grant, C. R., R. Liberal, G. Mieli-Vergani, D. Vergani, and M. S. Longhi. 2015. Regulatory T-cells in autoimmune diseases: challenges, controversies and–yet–unanswered questions. [Published erratum appears in 2015 *Autoimmun. Rev.* 14: 845–846.] *Autoimmun. Rev.* 14: 105–116.
5. Noval Rivas, M., and T. A. Chatila. 2016. Regulatory T cells in allergic diseases. *J. Allergy Clin. Immunol.* 138: 639–652.
6. Prescott, S. L. 2013. Early-life environmental determinants of allergic diseases and the wider pandemic of inflammatory noncommunicable diseases. *J. Allergy Clin. Immunol.* 131: 23–30.
7. Molodecky, N. A., I. S. Soon, D. M. Rabi, W. A. Ghali, M. Ferris, G. Chernoff, E. I. Benchimol, R. Panaccione, S. Ghosh, H. W. Barkema, and G. G. Kaplan. 2012. Increasing incidence and prevalence of the inflammatory bowel diseases with time, based on systematic review. *Gastroenterology* 142: 46–54.e42; quiz e30.
8. Abegunde, A. T., B. H. Muhammad, O. Bhatti, and T. Ali. 2016. Environmental risk factors for inflammatory bowel diseases: evidence based literature review. *World J. Gastroenterol.* 22: 6296–6317.
9. Collier, F. M., M. L. Tang, D. Martino, R. Saffery, J. Carlin, K. Jachno, S. Ranganathan, D. Burgner, K. J. Allen, P. Vuillermin, and A. L. Ponsonby. 2015. The ontogeny of naïve and regulatory CD4(+) T-cell subsets during the first postnatal year: a cohort study. *Clin. Transl. Immunology* 4: e34.
10. Chinthrajah, R. S., J. D. Hernandez, S. D. Boyd, S. J. Galli, and K. C. Nadeau. 2016. Molecular and cellular mechanisms of food allergy and food tolerance. *J. Allergy Clin. Immunol.* 137: 984–997.
11. Hirahara, K., L. Liu, R. A. Clark, K. Yamanaka, R. C. Fuhlbrigge, and T. S. Kupper. 2006. The majority of human peripheral blood CD4+CD25high-Foxp3+ regulatory T cells bear functional skin-homing receptors. *J. Immunol.* 177: 4488–4494.
12. Grindebacke, H., H. Stenstad, M. Quiding-Järbrink, J. Waldenström, I. Adlerberth, A. E. Wold, and A. Rudin. 2009. Dynamic development of homing receptor expression and memory cell differentiation of infant CD4+CD25high regulatory T cells. *J. Immunol.* 183: 4360–4370.
13. Cassani, B., E. J. Villablanca, F. J. Quintana, P. E. Love, A. Lacy-Hulbert, W. S. Blaner, T. Sparwasser, S. B. Snapper, H. L. Weiner, and J. R. Mora. 2011. Gut-tropic T cells that express integrin $\alpha4\beta7$ and CCR9 are required for induction of oral immune tolerance in mice. *Gastroenterology* 141: 2109–2118.
14. Kang, S. G., J. Park, J. Y. Cho, B. Ulrich, and C. H. Kim. 2011. Complementary roles of retinoic acid and TGF-$\beta1$ in coordinated expression of mucosal integrins by T cells. *Mucosal Immunol.* 4: 66–82.

15. Scott, C. L., A. M. Aumeunier, and A. M. Mowat. 2011. Intestinal CD103+ dendritic cells: master regulators of tolerance? *Trends Immunol.* 32: 412–419.
16. Biedermann, T., G. Lametschwandtner, K. Tangemann, J. Kund, S. Hinteregger, N. Carballido-Perrig, A. Rot, C. Schwärzler, and J. M. Carballido. 2006. IL-12 instructs skin homing of human Th2 cells. *J. Immunol.* 177: 3763–3770.
17. Cimbro, R., L. Vassena, J. Arthos, C. Cicala, J. H. Kehrl, C. Park, I. Sereti, M. M. Lederman, A. S. Fauci, and P. Lusso. 2012. IL-7 induces expression and activation of integrin α4β7 promoting naive T-cell homing to the intestinal mucosa. *Blood* 120: 2610–2619.
18. Hsu, P., B. Santner-Nanan, J. E. Dahlstrom, M. Fadia, A. Chandra, M. Peek, and R. Nanan. 2012. Altered decidual DC-SIGN+ antigen-presenting cells and impaired regulatory T-cell induction in preeclampsia. *Am. J. Pathol.* 181: 2149–2160.
19. Miyara, M., Y. Yoshioka, A. Kitoh, T. Shima, K. Wing, A. Niwa, C. Parizot, C. Taflin, T. Heike, D. Valeyre, et al. 2009. Functional delineation and differentiation dynamics of human CD4+ T cells expressing the FoxP3 transcription factor. *Immunity* 30: 899–911.
20. Thornton, A. M., P. E. Korty, D. Q. Tran, E. A. Wohlfert, P. E. Murray, Y. Belkaid, and E. M. Shevach. 2010. Expression of Helios, an Ikaros transcription factor family member, differentiates thymic-derived from peripherally induced Foxp3+ T regulatory cells. *J. Immunol.* 184: 3433–3441.
21. Gottschalk, R. A., E. Corse, and J. P. Allison. 2012. Expression of Helios in peripherally induced Foxp3+ regulatory T cells. *J. Immunol.* 188: 976–980.
22. Kim, H. J., R. A. Barnitz, T. Kreslavsky, F. D. Brown, H. Moffett, M. E. Lemieux, Y. Kaygusuz, T. Meissner, T. A. Holderried, S. Chan, et al. 2015. Stable inhibitory activity of regulatory T cells requires the transcription factor Helios. *Science* 350: 334–339.
23. Kimmig, S., G. K. Przybylski, C. A. Schmidt, K. Laurisch, B. Möwes, A. Radbruch, and A. Thiel. 2002. Two subsets of naive T helper cells with distinct T cell receptor excision circle content in human adult peripheral blood. *J. Exp. Med.* 195: 789–794.
24. Seddiki, N., B. Santner-Nanan, J. Martinson, J. Zaunders, S. Sasson, A. Landay, M. Solomon, W. Selby, S. I. Alexander, R. Nanan, et al. 2006. Expression of interleukin (IL)-2 and IL-7 receptors discriminates between human regulatory and activated T cells. *J. Exp. Med.* 203: 1693–1700.
25. Cose, S. 2007. T-cell migration: a naive paradigm? *Immunology* 120: 1–7.
26. Fry, T. J., and C. L. Mackall. 2005. The many faces of IL-7: from lymphopoiesis to peripheral T cell maintenance. *J. Immunol.* 174: 6571–6576.
27. Puel, A., S. F. Ziegler, R. H. Buckley, and W. J. Leonard. 1998. Defective IL7R expression in T(-)B(+)NK(+) severe combined immunodeficiency. *Nat. Genet.* 20: 394–397.
28. Cheng, G., A. Yu, M. J. Dee, and T. R. Malek. 2013. IL-2R signaling is essential for functional maturation of regulatory T cells during thymic development. *J. Immunol.* 190: 1567–1575.
29. Caudy, A. A., S. T. Reddy, T. Chatila, J. P. Atkinson, and J. W. Verbsky. 2007. CD25 deficiency causes an immune dysregulation, polyendocrinopathy, enteropathy, X-linked-like syndrome, and defective IL-10 expression from CD4 lymphocytes. *J. Allergy Clin. Immunol.* 119: 482–487.
30. Bernasconi, A., R. Marino, A. Ribas, J. Rossi, M. Ciaccio, M. Oleastro, A. Ornani, R. Paz, M. A. Rivarola, M. Zelazko, and A. Belgorosky. 2006. Characterization of immunodeficiency in a patient with growth hormone insensitivity secondary to a novel STAT5b gene mutation. *Pediatrics* 118: e1584–e1592.
31. Milner, J. D., T. P. Vogel, L. Forbes, C. A. Ma, A. Stray-Pedersen, J. E. Niemela, J. J. Lyons, K. R. Engelhardt, Y. Zhang, N. Topcagic, et al. 2015. Early-onset lymphoproliferation and autoimmunity caused by germline STAT3 gain-of-function mutations. *Blood* 125: 591–599.
32. Kibler, R., M. J. Hicks, A. L. Wright, and L. M. Taussig. 1986. A comparative analysis of cord blood and adult lymphocytes: interleukin-2 and interferon production, natural killer cell activity, and lymphocyte populations. *Diagn. Immunol.* 4: 201–208.
33. Guy-Grand, D., P. Vassalli, G. Eberl, P. Pereira, O. Burlen-Defranoux, F. Lemaitre, J. P. Di Santo, A. A. Freitas, A. Cumano, and A. Bandeira. 2013. Origin, trafficking, and intraepithelial fate of gut-tropic T cells. [Published erratum appears in 2013 *J. Exp. Med.* 210: 2493.] *J. Exp. Med.* 210: 1839–1854.
34. Houston, E. G., Jr., R. Nechanitzky, and P. J. Fink. 2008. Cutting edge: contact with secondary lymphoid organs drives postthymic T cell maturation. *J. Immunol.* 181: 5213–5217.
35. Iwata, M., A. Hirakiyama, Y. Eshima, H. Kagechika, C. Kato, and S. Y. Song. 2004. Retinoic acid imprints gut-homing specificity on T cells. *Immunity* 21: 527–538.
36. Cebula, A., M. Seweryn, G. A. Rempala, S. S. Pabla, R. A. McIndoe, T. L. Denning, L. Bry, P. Kraj, P. Kisielow, and L. Ignatowicz. 2013. Thymus-derived regulatory T cells contribute to tolerance to commensal microbiota. *Nature* 497: 258–262.
37. Sefik, E., N. Geva-Zatorsky, S. Oh, L. Konnikova, D. Zemmour, A. M. McGuire, D. Burzyn, A. Ortiz-Lopez, M. Lobera, J. Yang, et al. 2015. MUCOSAL IMMUNOLOGY. Individual intestinal symbionts induce a distinct population of RORγ$^+$ regulatory T cells. *Science* 349: 993–997.
38. Tanoue, T., K. Atarashi, and K. Honda. 2016. Development and maintenance of intestinal regulatory T cells. *Nat. Rev. Immunol.* 16: 295–309.
39. Feagan, B. G., P. Rutgeerts, B. E. Sands, S. Hanauer, J. F. Colombel, W. J. Sandborn, G. Van Assche, J. Axler, H. J. Kim, S. Danese, et al; GEMINI 1 Study Group. 2013. Vedolizumab as induction and maintenance therapy for ulcerative colitis. *N. Engl. J. Med.* 369: 699–710.
40. Arijs, I., G. De Hertogh, B. Lemmens, L. Van Lommel, M. de Bruyn, W. Vanhove, I. Cleynen, K. Machiels, M. Ferrante, F. Schuit, et al. 2018. Effect of vedolizumab (anti-alpha4beta7-integrin) therapy on histological healing and mucosal gene expression in patients with UC. *Gut*. 67: 43–52. http://gut.bmj.com/content/67/1/43. PubMed
41. Fischer, A., S. Zundler, R. Atreya, T. Rath, C. Voskens, S. Hirschmann, R. López-Posadas, A. Watson, C. Becker, G. Schuler, et al. 2016. Differential effects of α4β7 and GPR15 on homing of effector and regulatory T cells from patients with UC to the inflamed gut in vivo. *Gut* 65: 1642–1664.
42. Zhang, Y., F. Collier, G. Naselli, R. Saffery, M. L. Tang, K. J. Allen, A. L. Ponsonby, L. C. Harrison, and P. Vuillermin, BIS Investigator Group. 2016. Cord blood monocyte-derived inflammatory cytokines suppress IL-2 and induce nonclassic "T(H)2-type" immunity associated with development of food allergy. *Sci. Transl. Med.* 8: 321ra8.
43. Du Toit, G., G. Roberts, P. H. Sayre, H. T. Bahnson, S. Radulovic, A. F. Santos, H. A. Brough, D. Phippard, M. Basting, M. Feeney, et al; LEAP Study Team. 2015. Randomized trial of peanut consumption in infants at risk for peanut allergy. *N. Engl. J. Med.* 372: 803–813.
44. Perkin, M. R., K. Logan, A. Tseng, B. Raji, S. Ayis, J. Peacock, H. Brough, T. Marrs, S. Radulovic, J. Craven, et al; EAT Study Team. 2016. Randomized trial of introduction of allergenic foods in breast-fed infants. *N. Engl. J. Med.* 374: 1733–1743.
45. Wei-Liang Tan, J., C. Valerio, E. H. Barnes, P. J. Turner, P. A. Van Asperen, A. M. Kakakios, and D. E. Campbell. 2017. A randomized trial of egg introduction from 4 months of age in infants at risk for egg allergy. *J. Allergy Clin. Immunol.* 139: 1621–1628.
46. Kelleher, M. M., A. Dunn-Galvin, C. Gray, D. M. Murray, M. Kiely, L. Kenny, W. H. I. McLean, A. D. Irvine, and J. O. Hourihane. 2016. Skin barrier impairment at birth predicts food allergy at 2 years of age. *J. Allergy Clin. Immunol.* 137: 1111–1116.e8.
47. Rosen, M. J., R. Karns, J. E. Vallance, R. Bezold, A. Waddell, M. H. Collins, Y. Haberman, P. Minar, R. N. Baldassano, J. S. Hyams, et al. 2017. Mucosal expression of type 2 and type 17 immune response genes distinguishes ulcerative colitis from colon-only Crohn's disease in treatment-naive pediatric patients. *Gastroenterology* 152: 1345–1357. e7.
48. He, J., X. Zhang, Y. Wei, X. Sun, Y. Chen, J. Deng, Y. Jin, Y. Gan, X. Hu, R. Jia, et al. 2016. Low-dose interleukin-2 treatment selectively modulates CD4(+) T cell subsets in patients with systemic lupus erythematosus. *Nat. Med.* 22: 991–993.
49. Saadoun, D., M. Rosenzwajg, F. Joly, A. Six, F. Carrat, V. Thibault, D. Sene, P. Cacoub, and D. Klatzmann. 2011. Regulatory T-cell responses to low-dose interleukin-2 in HCV-induced vasculitis. *N. Engl. J. Med.* 365: 2067–2077.
50. Goettel, J., D. Kotlarz, D. Illig, J. Canavan, J. Allegretti, M. Hamilton, R. Kelly, A. Griffith, M. Carellas, A. Nelina, et al. 2017. O-011 low-dose IL-2 administration expands human regulatory T cells in patients with UC and humanized mice and protects against experimental colitis. *Inflamm. Bowel Dis.* 23(Suppl. 1): S4.

Variants in TRIM22 that affect NOD2 signalling are associated with Very-early-onset inflammatory bowel disease.

Gastroenterology 2016;150:1196–1207

Variants in *TRIM22* That Affect NOD2 Signaling Are Associated With Very-Early-Onset Inflammatory Bowel Disease

Qi Li,[1,2,*] **Cheng Hiang Lee**,[3,4,*] **Lauren A. Peters**,[5,6,*] Lucas A. Mastropaolo,[2] Cornelia Thoeni,[1,2] Abdul Elkadri,[1,2,7] Tobias Schwerd,[8] Jun Zhu,[6] Bin Zhang,[6] Yongzhong Zhao,[6] Ke Hao,[6] Antonio Dinarzo,[6] Gabriel Hoffman,[6] Brian A. Kidd,[6] Ryan Murchie,[1,2] Ziad Al Adham,[1,2,7] Conghui Guo,[2] Daniel Kotlarz,[9] Ernest Cutz,[10] Thomas D. Walters,[1,2] Dror S. Shouval,[11] Mark Curran,[12] Radu Dobrin,[12] Carrie Brodmerkel,[12] Scott B. Snapper,[11,13] Christoph Klein,[9] John H. Brumell,[1,7,14] Mingjing Hu,[3,4] Ralph Nanan,[3,4] Brigitte Snanter-Nanan,[3,4] Melanie Wong,[15] Francoise Le Deist,[16] Elie Haddad,[17] Chaim M. Roifman,[18] Colette Deslandres,[19] Anne M. Griffiths,[1,2] Kevin J. Gaskin,[3,4] Holm H. Uhlig,[8] Eric E. Schadt,[6,§] and Aleixo M. Muise[1,2,7,§]

[1]SickKids Inflammatory Bowel Disease Center and Cell Biology Program, Research Institute, Hospital for Sick Children, Toronto, Ontario, Canada; [2]Division of Gastroenterology, Hepatology, and Nutrition, Department of Pediatrics, University of Toronto, Hospital for Sick Children, Toronto, Ontario, Canada; [3]Gastroenterology Department, The Children's Hospital at Westmead, Westmead, New South Wales, Australia; [4]The James Fairfax Institute of Paediatric Nutrition, University of Sydney, New South Wales, Australia; [5]Graduate School of Biomedical Sciences, Icahn School of Medicine at Mount Sinai, New York, New York; [6]Department of Genetics and Genomic Sciences, Icahn School of Medicine at Mount Sinai and the Icahn Institute for Genomics and Multiscale Biology, New York, New York; [7]Institute of Medical Science, University of Toronto, Toronto, Ontario, Canada; [8]Translational Gastroenterology Unit, Nuffield Department of Clinical Medicine, Experimental Medicine Division, University of Oxford and Department of Pediatrics, John Radcliffe Hospital, Oxford, UK; [9]Department of Pediatrics, Dr. von Hauner Children's Hospital, Ludwig-Maximilians-University, Munich, Germany; [10]Division of Pathology, The Hospital for Sick Children, Toronto, Ontario, Canada; [11]Division of Pediatric Gastroenterology, Hepatology, and Nutrition, Department of Pediatrics, Boston Children's Hospital, Harvard Medical School, Boston, Massachusetts; [12]Janssen R&D, LLC, Spring House, Pennsylvania; [13]Division of Gastroenterology and Hepatology, Brigham & Women's Hospital, Department of Medicine, Boston, Massachusetts; [14]Molecular Genetics, University of Toronto, Toronto, Ontario, Canada; [15]Immunology Department, The Children's Hospital at Westmead, Westmead, New South Wales, Australia; [16]Department of Microbiology and Immunology, CHU Sainte Justine and Department of Microbiology, Infectiology and Immunology, University of Montreal, Quebec, Canada; [17]Department of Pediatrics, CHU Sainte-Justine, Department of Microbiology, Infectiology and Immunology, University of Montreal, Quebec, Canada; [18]Division of Immunology, Department of Pediatrics, University of Toronto, The Hospital for Sick Children, Toronto, Canada; and [19]Division of Gastroenterology, Hepatology and Nutrition, Department of Pediatrics, CHU Sainte-Justine, Montreal, Quebec, Canada

See Covering the Cover synopsis on page 1050.

BACKGROUND & AIMS: Severe forms of inflammatory bowel disease (IBD) that develop in very young children can be caused by variants in a single gene. We performed whole-exome sequence (WES) analysis to identify genetic factors that might cause granulomatous colitis and severe perianal disease, with recurrent bacterial and viral infections, in an infant of consanguineous parents. **METHODS:** We performed targeted WES analysis of DNA collected from the patient and her parents. We validated our findings by a similar analysis of DNA from 150 patients with very-early-onset IBD not associated with known genetic factors analyzed in Toronto, Oxford, and Munich. We compared gene expression signatures in inflamed vs noninflamed intestinal and rectal tissues collected from patients with treatment-resistant Crohn's disease who participated in a trial of ustekinumab. We performed functional studies of identified variants in primary cells from patients and cell culture. **RESULTS:** We identified a homozygous variant in the tripartite motif containing 22 gene (*TRIM22*) of the patient, as well as in 2 patients with a disease similar phenotype. Functional studies showed that the variant disrupted the ability of TRIM22 to regulate nucleotide binding oligomerization domain containing 2 (NOD2)–dependent activation of interferon-beta signaling and nuclear factor–κB. Computational studies demonstrated a correlation between the TRIM22–NOD2 network and signaling pathways and genetic factors associated very early onset and adult-onset IBD. TRIM22 is also associated with antiviral and mycobacterial

***Authors share co-first authorship; §Authors share co-senior authorship.**

Abbreviations used in this paper: **eQTL, expression quantitative trait loci; GWAS, genome-wide association study; MDP, muramyl dipeptide; NF-κB, nuclear factor–κB; NOD2, nucleotide binding oligomerization domain containing 2; RSV, to respiratory syncytial virus; TNF, tumor necrosis factor; TRIM22, tripartite motif containing 22 gene; VEOIBD, Very-early-onset inflammatory bowel diseases; WES, whole exome sequencing.**

Most current article

0016-5085

http://dx.doi.org/10.1053/j.gastro.2016.01.031

effectors and markers of inflammation, such as fecal calprotectin, C-reactive protein, and Crohn's disease activity index scores. **CONCLUSIONS:** In WES and targeted exome sequence analyses of an infant with severe IBD characterized by granulomatous colitis and severe perianal disease, we identified a homozygous variant of *TRIM22* that affects the ability of its product to regulate NOD2. Combined computational and functional studies showed that the *TRIM22-NOD2* network regulates antiviral and antibacterial signaling pathways that contribute to inflammation. Further study of this network could lead to new disease markers and therapeutic targets for patients with very early and adult-onset IBD.

Keywords: VEOIBD; NF-kB; Antiviral and Antibacterial Networks.

Very-early-onset inflammatory bowel diseases (VEOIBD) often present with severe multisystemic disease that is difficult to treat with conventional therapies. These young patients frequently have novel causal[1–3] and risk variants[4–8] and common networks are now being established (reviewed in Uhlig et al[9]). For example, mutations in *IL10RA/B* genes cause a Mendelian form of VEOIBD with severe colitis and perianal disease[10] and mutations in *TTC7A* cause a severe form of apoptotic enterocolitis.[1]

Tripartite motif-containing 22 (TRIM22; also known as STAF50*)* is a RING finger E3 ubiquitin ligase[11] that is expressed in the intestine[12] and in macrophages,[13] and has a role in lineage-specific differentiation of lymphocytes.[14] TRIM22 was originally identified as an interferon inducible protein that possesses antiviral activity[15–17] and activates nuclear factor−κB (NF-κB) signaling.[13] Here we identify *TRIM22* functional variants associated with a distinct VEOIBD phenotype characterized by granulomatous colitis and severe perianal disease and show the *TRIM22-NOD2* network as a key antiviral and mycobacterial regulator.

Materials and Methods

See Supplementary Material for full methods information.

Subjects

All experiments were carried out with the approval of the Research Ethics Board at the Hospital for Sick Children. Informed consent to participate in research was obtained. A copy of the consent is available on the NEOPICS (International Early Onset Pediatric IBD Cohort Study) website (http://www.neopics.org/NEOPICS_Documents.html).

Whole Exome Sequencing

For patient 1 and her parents (trio), whole exome sequencing (WES) was performed using the Agilent SureSelect Human All Exon 50-Mb kit with high-throughput sequencing conducted using the SOLiD 4 System at The Center for Applied Genomics through the Hospital for Sick Children (Toronto). Sanger sequencing was used to verify variant genotypes in family 1 and infantile patients from the collaborating institutions were screened for *TRIM22* variants.

Validation

In order to validate these findings, we examined WES results from 150 infantile international VEOIBD patients without a genetic diagnosis who were previously sequenced in Toronto (NEOPICS), Oxford, and Munich (Care for Rare) and targeted exome sequencing of the *TRIM22* gene in 10 *IL10RA/B,* and *IL10*-negative patients without previous WES.

Computational Analysis

Datasets. Biopsy data were collected at baseline from anti−tumor necrosis factor (TNF)-resistant Crohn's patients enrolled in the ustekinumab trial described previously.[18] The ustekinumab trial expression data were used for construction of the adult IBD network. RNA-seq from the RISK cohort, as described previously,[19] was used for generation of the pediatric IBD Bayesian network.

Differential expression. To ascertain tissue-specific signatures, we examined inflamed vs noninflamed tissue from various anatomic regions of the small intestine, colon, and rectum. To identify differential expression signatures, we used an unbiased univariate filter to select top-varying genes and then applied Significance Analysis of Microarrays[20] (SAM) to whole-genome expression data collected from biopsy tissue samples and whole blood of individuals in the ustekinumab trial. To control for multiple hypothesis testing, we used the Benjamini & Hochberg adjustment on the raw P values to control the family-wise error rate and set a false discovery rate threshold of 1% or 5%. All analyses were performed using the R statistical package, version 2.15.24.1

Bayesian network. We employed Monte Carlo Markov Chain[21] simulation to identify potentially thousands of different plausible networks that are then combined to obtain a consensus network. eSNP data were used as priors as follows: genes with cis-eSNP[22] are allowed to be parent nodes of genes without cis-eSNPs, but genes without cis-eSNPs are not allowed to be parents of genes with cis-eSNPs.

Key driver analysis. Key driver analysis takes as input a set of genes (G) and a directed gene network (N) (eg, Bayesian network).[19,23–26] The objective is to identify the key regulators for the gene sets with respect to the given network. Key driver analysis first generates a subnetwork N_G, defined as the set of nodes in N that are no more than h-layers away from the nodes in G, and then searches the h-layer neighborhood (h = 1,..,H) for each gene in N_G ($HLN_{g,h}$) for the optimal h*, such that

$$ES\,h* \;=\; \max\,(\,ES_{\,h,\,g}\,)\,\forall\; g \in N_{\,g},\; h \in \{1\,..\,H\,\}$$

where $ES_{h,g}$ is the computed enrichment statistic for $HLN_{g,h}$. A node becomes a candidate driver if its HLN is significantly enriched for the nodes in G. Candidate drivers without any parent node (ie, root nodes in directed networks) are designated as global drivers, while the remaining are designated as local drivers.

Pathway enrichment. Expression quantitative trait loci (eQTL) analysis was performed on IBD, ulcerative colitis, and Crohn's disease genome-wide association study (GWAS) hits from the National Human Genome Research Institute catalog, plus all Wellcome Trust Case Control Consortium IBD GWAS single nucleotide polymorphisms with $P \leq .001$. Ten percent false discovery rate eGenes were thus extracted, and tested for enrichment of pathways from the Metacore database.

Clinical variable correlation. We used Spearman correlation to examine the relationship between the messenger RNA expression of *TRIM22* in intestine and blood and several key IBD traits. The correlation test was performed with the R function "corr.test." We applied a simple Bonferroni correction to a .01 significance level across all gene-trait correlation tests performed.

Transfection and luciferase reporter assays. NF-κB luciferase reporter plasmids (Promega, Madison, WI) and interferon-stimulated response element promoter and interferon-beta promoter luciferase reporter plasmids were obtained from Dr Hong-bing Shu (Wuhan University). A total of HEK 293 cells (1×10^5) were seeded on 24-well dishes and transfected the following day using Lipofectamine 2000 method. Empty control plasmid was added to ensure that each transfection received the same amount of total DNA. To normalize for transfection efficiency, 0.01 μg pRL-TK (Renilla luciferase) reporter plasmid was added to each transfection. Approximately 24 hours after transfection, luciferase assays were performed using a dual-specific luciferase assay kit (Promega). Firefly luciferase activities were normalized on the basis of Renilla luciferase activities. Cells were treated with recombinant TNFα, respiratory syncytial virus (RSV), or L18-muramyl dipeptide (MDP) (InvivoGen, San Diego, CA). Statistical analysis of luciferase assay data consisted of 2-way analysis of variance followed by Bonferroni post-hoc testing to compare across conditions. Statistical significance was assigned to tests with $P < .05$ after Bonferroni correction.

Coimmunoprecipitation and immunoblot analysis. For transient transfection and coimmunoprecipitation experiments, HEK 293 cells (1×10^6) were seeded for 24 hours then transiently transfected for 18 to 24 hours using Lipofectamine 2000 according to the manufacturer's protocols. Transfected cells were lysed in 1 mL lysis buffer (150 mM NaCl, 50 mM HEPES, 1% Triton X-100, 10% glycerol, 1.5 mM $MgCl_2$, 1.0 mM ethylene glycol-bis[β-aminoethyl ether]-*N,N,N′,N′*-tetraacetic acid) supplemented with protease and phosphatase inhibitors (aprotinin, 1:1000; leupeptin, 1:1000; pepsin, 1:1000; and phenylmethylsulfonyl fluoride, 1:100). For each immunoprecipitation, a 0.9-mL aliquot of the lysate was incubated with 0.5 μL of the indicated antibody and 40 μL of a 1:1 slurry of Protein G Sepharose (Bioshop, Burlington, ON, Canada) for 1 hour. Sepharose beads were washed 3× with 1 mL high salt lysis buffer containing 0.5 M NaCl. The precipitates were analyzed by standard immunoblot procedures using the following antibodies: mouse monoclonal anti-FLAG (Sigma, St Louis, MA), anti-HA (Origene, Rockville, MD), anti-NOD2 (Novus), anti−green fluorescent protein (Invitrogen, Carlsbad, CA), rabbit polyclonal anti-TRIM22 (Abnova, Taipei City, Tawain), and goat polyclonal anti-NOD2 (Ingenix). For endogenous coimmunoprecipitation experiments, HT29 cells (5×10^7) were stimulated with MDP (10 μg/mL) for the indicated times or left untreated. The coimmunoprecipitation and immunoblot experiments were performed as described here.

Results

Case History

Patient 1 was born in Australia to consanguineous parents. She initially presented on day 8 of life with fever, oral ulcers, diarrhea, and failure to thrive and later developed severe fistulizing perianal disease (Figure 1*A*) and granulomatous colitis (Figure 1*B*). She deteriorated despite treatment with corticosteroid and biologic therapy. Symptomatic control was only achieved by fecal stream diversion with combined ileostomy and subtotal colectomy. Patients 2 and 3 had a very similar clinical course, with granulomatous colitis and severe perianal disease (Figure 1*C* and *D*) requiring ileostomy followed by total proctocolectomy. Both patients 2 and 3 presented with severe anemia and severe hypoalbuminemia secondary to colitis. Patients 1 and 2 had numerous bacterial and viral infections. The 3 patients did not have mutations in the *IL10RA/B, IL10, XIAP,* or *NOD2* genes, and were all very difficult to treat medically and surgically, with their disease nonresponsive to anti-TNFα biologic therapy (Supplementary Table 1*A*; see Supplementary Material for full clinical description).

Whole Exome Sequencing

WES of patient 1 (and parents) resulted in >100× the mean exome coverage and identified 152,020 variants, including 16,097 rare variants (minor allelic frequency <0.01) predicted to be damaging (Supplementary Figure 1). From this list, we identified 12 nonsynonymous homozygous variants (Supplementary Table 2) that were inherited in an autosomal recessive manner. Based on known protein function, expression profiles, animal models, mutation conservation, and network analysis. This list was narrowed down to a single candidate gene—*TRIM22*. Patient 1 had a homozygous nonsynonymous variant in exon 7 of the *TRIM22* gene inherited from both parents (Figure 1*E*). This missense variant resulted in an arginine to cysteine substitution (c.1324C>T; p.Arg442Cys) predicted to be highly deleterious (Figure 1*F* and Supplementary Table 1*B*). It is highly conserved in a functionally significant region of the exposed beta sheet around the variable loop 3 (V3) in the B30.2 (SPRY) domain thought to be responsible for subcellular localization[27,28] and the 3-dimensional structure suggest it results in an elongated or additional beta strand, which in the wild type, forms a relaxed loop segment.

To validate, we examined WES from 150 VEOIBD patients, but did not identify damaging variants in *TRIM22*. Therefore, we performed targeted exome sequencing in 10 patients with a similar severe phenotype and identified 2 additional patients with *TRIM22* variants (patients 2 and 3). Patient 2 had compound heterozygous *TRIM22* variants (Figure 1*E*), including a novel arginine to threonine substitution (c.449G>C, p.Arg150Thr) inherited paternally; and a serine to leucine substitution (c.731C>T; p.Ser244Leu) inherited maternally. Both variants were predicted to be damaging and to disrupt the highly conserved coiled-coil region of TRIM22 that facilitates homodimer/heterodimer multimers (Figures 1*F*, Supplementary Figure 2, and Supplementary Table 1*B*). R150T is in an exposed region and S244L is buried and resides in the spacer-2 region that contains a bipartite nuclear localization sequence, and was previously predicted to be a serine phosphorylation site.[27]

Patient 3 had a homozygous *TRIM22* variant inherited from both parents (Figure 1*E*). This nonsynonymous variant

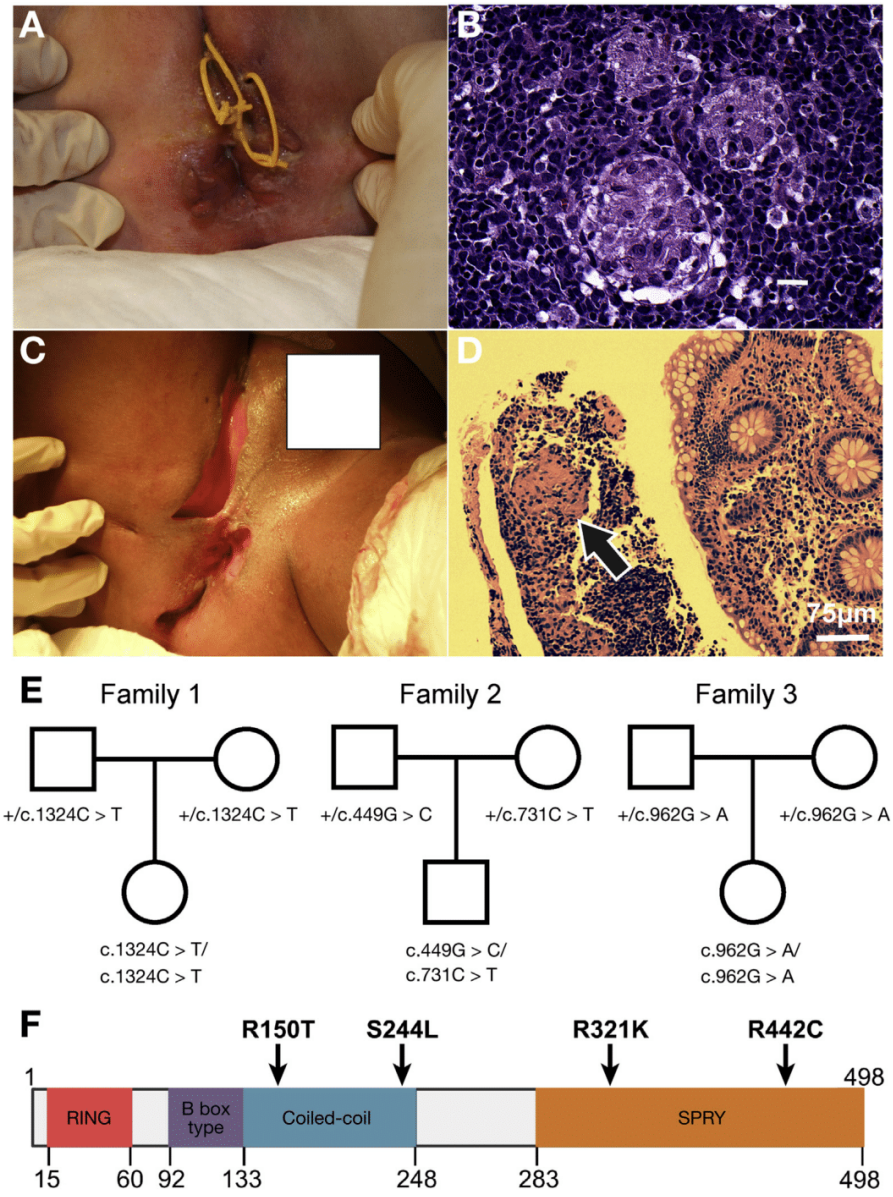

Figure 1. Clinical features and pedigrees of patients with *TRIM22* variants. (*A*, *B*) Clinical presentation and histopathologic findings in colonic biopsy from patient 1. (*A*) Severe perianal fistulization with seton placement. Rectovaginal fistulae were also present. (*B*) Non-caseating granulomas on a background of chronic inflammatory cell infiltrates (H&E stain). (*C*, *D*) Clinical presentation and histopathologic findings in colonic biopsy from patient 2. (*C*) Multiple, severe cavitating perianal fistulae. (*D*) Colonic biopsy showing chronic inflammation with non-caseating granuloma (*black arrow*) (*H&E stain*, scale bar = 75 μm). (*E*) Pedigree analysis of the genetic inheritance pattern for each family trio. (*F*) Schematic view of the protein domain architecture of TRIM22 with the relative position of each identified variant depicted. Number indicates amino acid position.

resulted in an arginine to lysine substitution (p.Arg321Lys; c.962G>A). The R321K variant was predicted to be deleterious and located in the highly conserved SPRY domain on an exposed residue of a beta sheet that has a functional role in the antiviral activity patch of the SPRY domain[27] (Figure 1*F*, Supplementary Table 1*B*).

Integrative Analysis Supports TRIM22 as a Key Regulator in Inflammatory Bowel Disease–Associated Networks

To gain insight into the role of *TRIM22* in the pathogenesis of IBD, we constructed a probabilistic causal network model by integrating 7,568 RNA-sequence–derived gene expression traits from ileal biopsies from 322 treatment-naïve pediatric Crohn's patients in the RISK cohort[19] and eQTL. To identify the VEOIBD component of this molecular network, we projected all genes known to be causally associated with VEOIBD[9] (Supplementary Table 3) onto this network, and then identified the most connected subnetwork containing these VEOIBD genes within the full RISK network, resulting in the VEOIBD network composed of 665 genes, which included *TRIM22* (Figure 2*A*).

To understand the regulation of this VEOIBD network, we employed a previously established procedure[26] to identify key regulator genes that are predicted to modulate the state of the

network (Supplementary Table 4). Interestingly, the most significant key regulators identified in the VEOIBD network included *SNX10*, *STX11*, *CYBB*, and *DRAM1*, which directly connect *TRIM22* to the IBD gene *NOD2* via 2 equidistant paths. The first pathway, *TRIM22*→*SNX10*→*STX11*→*DRAM1*→*NOD2*, is linked to the known VEOIBD gene *STAT1*

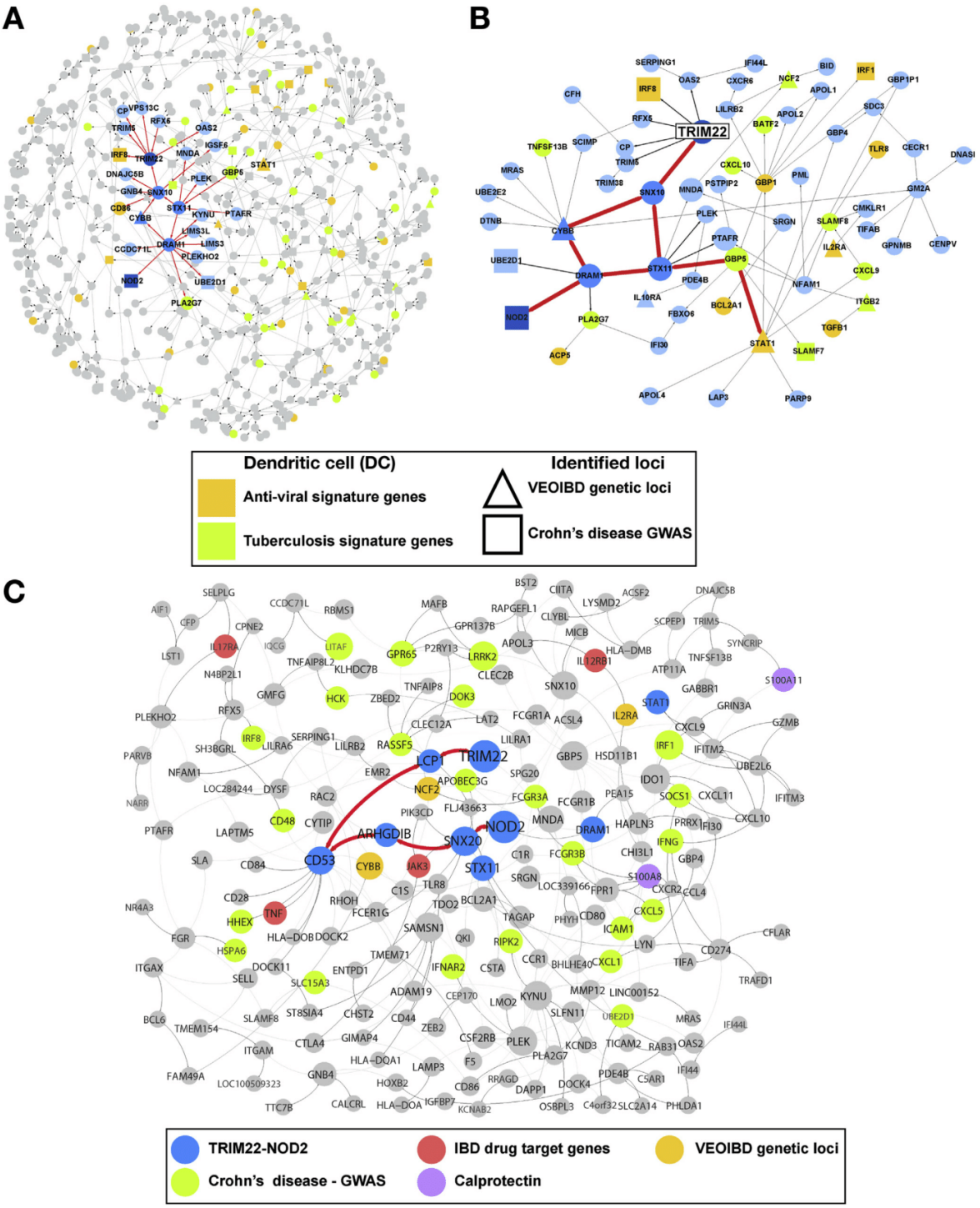

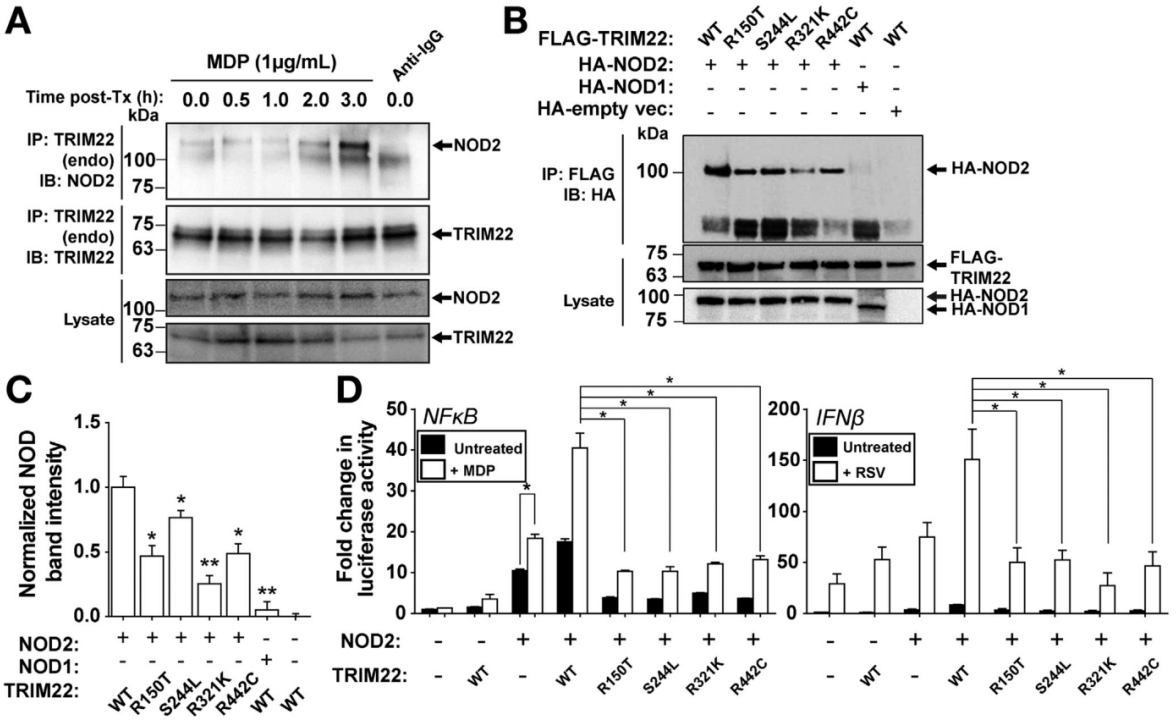

Figure 3. TRIM22 interacts with and activates NOD2 signaling. (A) Endogenous NOD2 and TRIM22 co-immunoprecipitate after MDP stimulation. HT29 cells were stimulated with MDP (1 μg/mL) for various time periods. After treatment, cells were lysed and endogenous TRIM22 was immunoprecipitated using anti-TRIM22 antibody conjugated to Protein G-Sepharose. Bound levels of endogenous NOD2 were evaluated using Western blotting. As stimulation time with MDP increased, the binding of endogenous NOD2 to TRIM22 increased. Immunoprecipitation with IgG bound to Protein G-Sepharose was used as a negative immunoprecipiation control. (*B*) TRIM22 interacts with NOD2. HEK293T cells were transiently cotransfected with HA-NOD2 and either wild-type (WT) or variant (R150T, S244L, R321K, and R442C) FLAG-epitope tagged TRIM22. Twenty-four hours post transfection, cells were lysed followed by immunoprecipitation of the FLAG-TRIM22 by anti-FLAG-agarose. Reduced binding of NOD2 to TRIM22 was observed in varying degrees for each variant compared to the WT protein. HA-NOD1 and an empty vector construct were used as negative controls. (*C*) Quantification of NOD2 co-immunoprecipitation with WT or mutant TRIM22. Densitometry analysis was performed on Western blots performed in (*B*). Each TRIM22 point mutation significantly reduced NOD2 co-immunoprecipitation (Student's *t* test, $^{*}P < .05$; $^{**}P < .01$, n = 3). (*D*) TRIM22 mutants fail to activate NF-κB and interferon-beta downstream of NOD2. HCT116 cells were transiently co-transfected with (or without) NOD2, TRIM22-WT, or TRIM22 point mutants (R150T, S244L, R321K, R442C). Twenty-four hours post transfection, cells were stimulated with either MDP (10 μg/mL) or RSV (0.1 μg) for 18 hours before NF-κB or interferon-beta promoter activation was evaluated by luciferase assay. Cells transfected with TRIM22 mutants showed significantly reduced NF-κB and interferon-beta promoter activation after stimulation compared with WT TRIM22 transfected controls ($^{*}P < .001$ after Bonferroni post-hoc testing, n = 3).

via *STX11* and *GBP5*, while the second pathway, *TRIM22*→*SNX10*→*CYBB*→*DRAM1*→*NOD2*, contains the known VEOIBD gene *CYBB* (Figure 2*B*). Both *STAT1* and *CYBB*, in addition to *IRF8*, which is directly connected to *TRIM22*, are associated with Mendelian susceptibility to mycobacteria deficiency.[29] As expected, we did not identify any common DNA variants from the International Inflammatory Bowel Disease Genetics Consortium GWAS[30] within the *TRIM22* locus

Figure 2. *TRIM22-NOD2* network. (*A*) VEOIBD loci-focused subnetwork within RISK Pediatric Crohn's ileum network. To define the context of VEOIBD in the ileum network, genes known to be causally associated with VEOIBD (not including *TRIM22*) were projected onto the RISK network and extended out a path length of 2. The resulting VEOIBD focused subnetwork is composed of 665 genes and contains *TRIM22* and *NOD2*. The *TRIM22-NOD2* paths are highlighted in *bold* and are connected to the known VEOIBD loci *CYBB* and *STAT1*, as well as the GWAS locus *IRF8*. (*B*) Local network structure surrounding the *NOD2*/*TRIM22* paths in the 665-node VEOIBD focused subnetwork. Representative nodes from the 179-gene TRIM22 network within the 665 node VEOIBD loci focused RISK subnetwork. (*C*) *TRIM22-NOD2* interaction is conserved in the adult IBD intestine. This network provides the context of the *TRIM22-NOD2* interaction in the adult IBD intestine. The 179-gene *TRIM22* network was projected and extended out an additional path length on the adult IBD pan intestine Bayesian network. IBD GWAS (*green*), VEOIBD loci (*orange*), IBD drug targets approved or in clinical development (*red*), and calprotectin (S100A8) (*purple*) are all represented in this conserved subnetwork.

(Supplementary Tables 5 and 6), however, the VEOIBD subnetwork is well represented in genes involved in TRIM22-relevant pathways, including p53, ubiquitin response, and antiviral signaling, which were among the top pathways enriched for genes associated with intestine and blood eQTL that were also associated with adult IBD loci identified in the International Inflammatory Bowel Disease Genetics Consortium cohort (Supplementary Figure 3, Supplementary Table 7). In addition, we found that the VEOIBD network was 2.1-fold enriched ($P = 2.3$ e-5) for Crohn's genes annotated from adult IBD genetic studies that also give rise to blood eQTLs[31] (Supplementary Table 8).

Adult-Onset Inflammatory Bowel Disease Informed by a TRIM22-Centered Network

Given preliminary support for adult IBD in the VEOIBD network, we explored whether the TRIM22 component of the VEOIBD network was associated with adult IBD. We constructed an adult IBD causal gene network from gene expression and genotype data generated on 203 intestinal biopsies, which included inflamed and noninflamed tissues from ileum, ascending colon, descending colon, transverse colon, sigmoid, and rectum. All of these tissues, in addition to blood, were collected at baseline from 54 anti-TNFα–resistant Crohn's patients enrolled in the

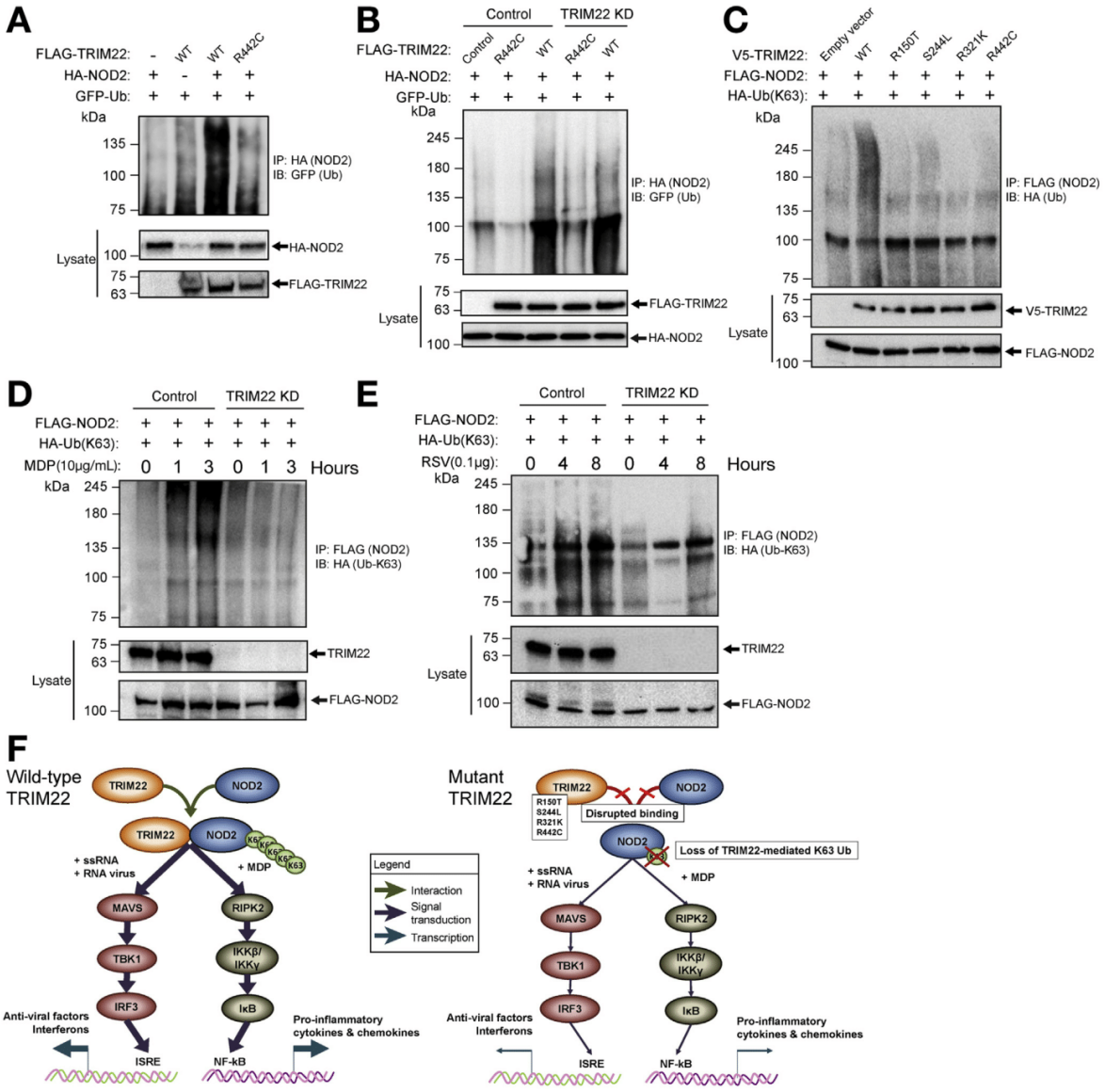

ustekinumab (IL12/IL23 p40 monoclonal antibody) clinical trial[18] (Supplementary Figure 4). We found that TRIM22 was not only a key driver gene in the sigmoid (key driver $p = 4.0e-06$) and rectum (key driver $P = 1.0e-4$) networks, but it was significantly upregulated in inflamed sigmoid (fold change = 2.47, SAM-based $p = 6.31e-05$) and inflamed rectum (fold change = 2.39, SAM-based $P = 5.03$ e-06), compared with non-inflamed samples of these same tissues.

We identified the homologous *TRIM22* component of the adult IBD network by first identifying all genes within a path length of 5 to *TRIM22* in the VEOIBD network, which included NOD2, leaving a network composed of 179 genes (referred to here as the *TRIM22* network; Supplementary Table 9). This *TRIM22* network contained many macrophage/monocyte-expressed genes associated with mycobacterial and antiviral responses (including genes involved in autophagy, NF-κB pathway, and apoptosis; Supplementary Figure 5; Supplementary Table 10). Strikingly, of the 480 key driver genes we identified in the adult IBD network, 62, including *STX11*, *CYBB*, and *DRAM1*, were represented in the pediatric *TRIM22* network, 7.2-fold enrichment over what is expected by chance ($P = 6.5$ e-38) (Supplementary Table 11). Further, the *TRIM22* containing co-expression module from the blood of ustekinumab patients, which was 12.7-fold enriched for response to virus ($P = 6.3e-14$), was 9-fold enriched in the pediatric *TRIM22* network ($P < 1e-16$). Further supporting the pediatric *TRIM22* network's association to viral response was a 3.2-fold enrichment ($P = 2.5e-5$) of eQTLs associated with dendritic cell response to stimulation with flu or interferon beta[32] and an 8.3-fold enrichment ($P = 1.1e-16$) of genes in a tuberculosis infection signature in dendritic cells.[30]

The homologous *TRIM22* network in the adult IBD network was then identified by projecting nodes from the *TRIM22* network onto the adult IBD network, identifying those nodes that were either in the *TRIM22* network or directly connected to such nodes (Figure 2*C*). In this *TRIM22* pediatric-oriented adult IBD network, *TRIM22* is in close proximity to several drug targets that are either approved or in clinical development for IBD, including TNFα, the target of adalimumab (Humira), certolizumab (Cimzia), infliximab (Remicade), and colimumab (Simponi); IL12Rβ, a chain shared between the receptors that bind IL12/23, the molecular target of ustekinumab; JAK3, the target of tofacitinib; and IL17RA, the target of brodalumab.

Because S100A8 (calprotectin), a stool biomarker for inflammation, is also co-localized with TRIM22 in this network[33–35] (Figure 2*C*), we decided to further investigate the role of *TRIM22* in treatment-refractory patients, exploring associations between *TRIM22* and IBD-associated clinical traits in the ustekinumab clinical trial (Supplementary Table 12). We found that expression levels of *TRIM22* in the colon were positively correlated with fecal calprotectin regardless of biopsy inflammation status. Overall, both inflamed and noninflamed baseline intestine levels of *TRIM22* revealed a correlation to blood C-reactive protein, of which consistently high levels are associated with subsequent development of perianal fistulae in Crohn's patients[36] and response to anti-TNFα.[37] *TRIM22* expression levels in blood were positively correlated with Crohn's Disease Activity Index (Supplementary Table 13).

Taken together, the intestinal network models provide causal support for the *TRIM22* regulation of *NOD2* and the correlation of the *TRIM22-NOD2* pathway with predicted disease regulators, functionally relevant VEO and adult-onset IBD genetic loci, effectors of antiviral and mycobacterial function, correlation with inflammatory clinical variables and validated IBD drug targets.

Figure 4. TRIM22 mediates K63-linked NOD2 polyubiquitination. (*A*) TRIM22 enhances NOD2 polyubiquitination in HEK293 cells. HEK293T cells were transiently co-transfected with HA-NOD2, green fluorescent protein (GFP) ubiquitin, and either wild-type (WT) or variant (R442C) FLAG-TRIM22. Twenty-four hours post transfection, cells were lysed followed by immunoprecipitation of HA-NOD2. Ubiquitination of NOD2 was evaluated by immunoblotting for GFP (ubiquitin). Co-transfection with WT TRIM22 enhanced ubiquitination of NOD2, which was abrogated with the R442C variant TRIM22. All experiments were carried out in triplicate, independent experiments. (*B*) Transgenic TRIM22 rescues NOD2 polyubiquitination in TRIM22-shRNA-HT29 cells. HT29 cells stably transduced with control (scramble) or TRIM22 short-hairpin RNA (shRNA) were transiently co-transfected with HA-NOD2 and either WT or variant (R442C) FLAG-TRIM22. Twenty-four hours post transfection, cells were lysed followed by immunoprecipitation of the HA-NOD2. Evaluation of NOD2 poly-ubiquitination by GFP immunoblotting demonstrated rescued ubiquitination after transfection of WT-TRIM22 in the TRIM22 shRNA cell line that was not observed after transfection of the variant R442C. All experiments were carried out in triplicate, independent experiments. (*C*) Variants in TRIM22 abrogates K63-linked NOD2 polyubiquitination. HEK293T cells were transiently cotransfected with FLAG-NOD2, HA-(K63-specific) ubiquitin, and either WT or variant (R150T, S244L, R321K, or R442C) V5-TRIM22. Twenty-four hours post transfection, cells were lysed followed by immunoprecipitation of the FLAG-NOD2. Evaluation of NOD2 K63 specific-ubiquitination by HA immunoblotting demonstrated significantly reduced ubiquitination in cells cotransfected with TRIM22 variants compared to WT. All experiments were carried out in triplicate, independent experiments. (*D*, *E*) TRIM22-shRNA reduces MDP- and RSV-induced K63-linked NOD2 polyubiquitination. HEK293T cells stably transduced with control (scramble) or TRIM22 shRNA were transfected with HA-tagged K63-specific ubiquitin and FLAG-NOD2. Forty-eight hours after transfection, cell lysates were stimulated by MDP (*D*) or RSV (*E*) for indicated the time points, followed by lysis and immunoprecipitation using anti-FLAG-agarose. K63-poly-ubiquination of NOD2 was evaluated by immunoblotting using anti-HA antibody. After stimulation by either MDP or RSV, NOD2 K63-specific ubiquitination increased over treatment time. However, in TRIM22 knockdown cells, this ubiquitination was significantly reduced or absent. All experiments were carried out in triplicate independent experiments and blots are representative. (*F*) Schematic overview of the proposed impact of TRIM22 and its identified variants on the NOD2 signaling axis. WT TRIM22 binds and mediates the K63-specific polyubiquitination of NOD2, potentiating downstream signaling through the MAVS and RIPK2 signaling axes depending on antigen. TRIM22 variants disrupt binding to NOD2, abrogating this polyubiquination thus attenuating downstream pro-inflammatory signaling.

Identification of TRIM22 as a NOD2 Interacting Protein

As NOD2 signaling plays a critical role in Crohn's disease susceptibility[38,39]; we further investigated this *in silico* TRIM22−NOD2 interaction. Immunofluorescence showed that NOD2 and TRIM22 colocalized in colonic biopsies and in the cytoplasm of transient transfected HEK293 cells (Supplementary Figure 6*A*–*C*). This NOD2 immunostaining was blocked by a NOD2-specific peptide and TRIM22 did not colocalize with NOD1 (Supplementary Figure 6*D*–*F*), another member of the NOD family, confirming the specificity of this TRIM22−NOD2 interaction. Immunostaining of colonic biopsy samples from patients 1−3 with TRIM22 variants showed altered expression and localization of NOD2 and TRIM22 (Supplementary Figure 6*A* and *B*).

TRIM22 Influences NOD2 Signaling Pathways

NOD2 senses MDP, a conserved structure in peptidoglycan present in most Gram-negative and Gram-positive bacteria. We found that TRIM22 was weakly associated with endogenous NOD2 in coimmunoprecipitation experiments in unstimulated HT29 cells, a human intestinal epithelial cell line, and this association increased after stimulation with MDP (Figure 3*A*). Furthermore, transiently transfected TRIM22 and NOD2 were found to reciprocally coimmunoprecipitate and these interactions were reduced with the TRIM22 variants (Figure 3*B* and *C* and Supplementary Figure 7*A*).

Because TRIM22 colocalized and coimmunoprecipitated with NOD2, we next determined whether TRIM22 influenced MDP-induced NF-κB signaling via NOD2. In reporter assays, coexpression of TRIM22 and NOD2 enhanced MDP-induced activation of the NF-κB (Figure 3*D*) in HEK293 cells. As TRIM22 regulates viral activity[15–17] and NOD2 functions as cytoplasmic viral pathogen recognition receptor by triggering interferon-beta activation in response to RSV,[40,41] we next determined whether TRIM22 also regulated NOD2-dependent RSV-induced interferon-beta signaling. As shown in Figure 3*D*, overexpression of TRIM22 and NOD2 both enhanced RSV-induced activation of the interferon-beta promoter and the interferon-stimulated response element. Neither wild-type TRIM22 nor the TRIM22-R442C variant enhanced TNFα gene expression in response to TNFα (Supplementary Figure 7*B*). As TNFα activates NF-κB target genes independent of NOD2 signaling,[42] this suggested that TRIM22 regulation of MDP-induced NF-κB activation is NOD2-dependent.

TRIM22 Variants Influence NOD2 Signaling

We next examined the role of TRIM22 to regulate NOD2-dependent NF-κB and interferon-beta signaling. Luciferase assays using HEK293 cells and real-time polymerase chain reaction experiments using HCT116 showed that expression of wild-type TRIM22 potentiated NOD2 signaling in response to both MDP-induced NF-κB and RSV-induced interferon-beta activation (Figures 3*D* and Supplementary Figures 7*C*–*F*). However, the *TRIM22* variants (Figures 3*D* and Supplementary Figures 7*C*–*E*) and *TRIM22* knockdown using short-hairpin RNA (Supplementary Figure 8*A*) showed impaired NOD2-dependent NF-κB and interferon-beta signaling (Supplementary Figure 8*B*). MDP-mediated NOD2-dependent signaling was also significantly reduced in patient 2 only, with the heterozygous *TRIM22* variants in the coiled-coil domain (Supplementary Figure 9 and Supplementary Material). Together, these data suggest that TRIM22 is a positive regulator of antiviral and antibacterial NOD2-dependent signaling pathways.

TRIM22 Mediates K63-Linked Polyubiquitination of NOD2

As TRIM22 is a RING finger E3 ubiquitin ligase[11] and NOD2 has high confidence predicted ubiquitination sites at K436 and K445 (CKSAAP_UbSITE[43]), we next determined whether TRIM22 mediated ubiquitination of NOD2. Immunoprecipitation experiments using a HEK293 cell line co-expressing HA-NOD2 and Flag-TRIM22 showed that overexpression of TRIM22 enhanced NOD2 polyubiquitination (Figure 4*A*). The TRIM22 variants (Figure 4*A* and Supplementary Figure 10*A*) were unable to mediate this NOD2 polyubiquitination. TRIM22 did not increase polyubiquitination of other components (MAVS or RIPK2) of the NOD2 signaling pathways known to be ubiquitinated[44,45] (Supplementary Figure 10*B*). Using the *TRIM22* short-hairpin RNA HT29 stable cell line, we found that only wild-type TRIM22 rescued NOD2 polyubiquitination and not the TRIM22-R442C variant (Figure 4*B*). Taken together, this suggested that TRIM22 specifically mediates NOD2 polyubiquitination.

K63-linked polyubiquitination regulates the localization and signaling activity, whereas K48-linked polyubiquitination often mediates degradation.[46] NOD2 has been previously shown to be K48-linked ubiquitinated by TRIM27 and results in NOD2 degradation.[47] Using ubiquitin mutants, we showed that overexpression of TRIM22 mediated K63-linked but not K48-linked polyubiquitination of NOD2, while the TRIM22 variants were unable to mediate K63- or K48-linked NOD2 polyubiquitination (Figure 4*C* and Supplementary Figure 11*A*). We next determined that TRIM22 is required for MDP- and RSV-induced K63-linked NOD2 polyubiquitination and knockdown of TRIM22 reduced this MDP- and RSV-induced K63-linked (Figure 4*D* and *E*), but not K48-linked NOD2 polyubiquitination (Supplementary Figures 11*B* and *C*).

Discussion

TRIM proteins are involved in a number of biologic processes, including cell proliferation, apoptosis, innate immunity, autoimmunity, and inflammatory response.[48,49] Variants in *TRIM* genes result in monogenic diseases, including familial Mediterranean fever and Opitz syndrome type 1, and are implicated in a number of cancers and autoimmune diseases, including multiple sclerosis, rheumatoid arthritis, and systemic lupus erythematosus.[48,49] TRIM22 belongs to a subfamily of TRIM proteins that contain a SPRY domain and are thought to have evolved to

limit innate immune responses to viruses.[20] Mutations in the SPRY domain of TRIM20 (pyrin) result in autoimmune diseases, including familial Mediterranean fever.[50] Overexpression of TRIM22 is known to activate NF-κB in a dose-dependent manner and both the N-terminal RING domain and C-terminal SPRY domain are crucial for TRIM22-mediated NF-κB activation[13] and antiviral activity,[15–17] and are implicated in the pathogenesis of autoimmune diseases.[51] Patients 1 and 3 both had homozygous variants in the SPRY domain and patient 2 had compound heterozygous variants both predicted to disrupt the coiled-coil domain and had loss of NOD2-dependent MDP signaling. The characterized *TRIM22* variants resulted in impaired NOD2 binding and K63-linked NOD2 polyubiquitination. The predicted NOD2 polyubiquitination sites described earlier are in the NACHT domain, a conserved domain required for NOD2 conformational change in response to MDP sensing through the LRR domain or interaction with binding adaptor proteins for NOD2.[52] Therefore, as all identified *TRIM22* variants disrupt both NOD2-dependent NF-κB and interferon-beta signaling, this suggests that K63-linked polyubiquitination of NOD2 meditated by TRIM22 is critical for NOD2 function (Figure 4*F*).

NOD2 has long been recognized as a critical player in Crohn's disease pathogenesis,[38,39] where it is proposed to regulate innate immunity through NF-κB–induced pro-inflammatory responses triggered by peptidoglycan (reviewed in Shaw et al[53]). Numerous studies have shown that the loss of function variants in NOD2 associated with Crohn's disease result in the loss of NF-κB– induced pro-inflammatory cytokine response to MDP (reviewed in Strober et al[54] and Philpott et al[55]) and, therefore, mirror the defect we observe in patient 2 with TRIM22 mutations in the coiled-coil domain. Similarly, mutations in XIAP (also an E3 ubiquitin ligase) are associated with IBD with granulomatous colitis and perianal disease[56,57] and are associated with loss of NOD2-dependent mediated NF-κB signaling[58–60] and XIAP is also regulated by TRIM proteins.[61] XIAP deficiency usually presents in early childhood, but there are cases of patients presenting with IBD at older than 40 years of age[9] with and without hemophagocytic lymphohistiocytosis (reviewed in Latour and Aguilar[62]). Furthermore, XIAP not only regulates NOD2-dependent innate immunity responses, but also is proposed to regulate inflammasome and adaptive immunity.[62] Loss-of-function NOD2 variants associated with IBD have low penetrance and do not cause the severe early-onset disease observed in this group with either TRIM22 or XIAP deficiency. Therefore, it is most likely that, in patients 1 and 3 with TRIM22 SPRY domain variants, defects in other pathways regulated by TRIM22 result in the early onset and severity of disease. Alternatively, hypomorphic TRIM22 variants act in an oligogenic manner with mutations in other genes similar to what has been observed with hypomorphic XIAP mutations[63] and as observed in patient 3, who is also a carrier of a XIAP mutation. Together, this suggests that loss of NOD2-dependent–mediated signaling in response to MDP contributes to a severe form of IBD and that other yet defined pathways must also be involved in disease pathogenesis. With regard to TRIM22 specifically, we anticipate that other pathways not identified in these studies play a role in disease pathogenesis.

Our computational studies further support our functional studies demonstrating that TRIM22 influences both NOD2-dependent interferon-beta and NF-κB signaling pathways. Although the loss-of-function *TRIM22* variants in our VEOIBD patients can manifest as an immunodeficiency, the inflammation and tissue damage that ensues from a dysregulated response to microbial burden might resemble the profile of adult-onset IBD. The functional outcome of pro-inflammatory NF-κB activation may differ, depending on the cell population in which TRIM22 is expressed, with circulating plasmacytoid dendritic cells and monocytes predominating in the blood and resident intestinal dendritic cells, macrophages, and enterocytes in the intestine. We see from the intestine network that the regulation of causal TRIM22 results in modulation of a mycobacterial and viral response subnetwork that can also result in feedback to TRIM22 expression. Either due to immunodeficiency arising from the *TRIM22* variants or excessive inflammation in non-*TRIM22* variants carried by anti-TNFα refractory patients, TRIM22-driven NOD2 activation in response to MDP or viral stimuli, contributes to dysregulation of NF-κB– and interferon-beta–driven pathways as reflected in the networks. Together, this demonstrates that the *TRIM22-NOD2* network plays a critical role in the development of IBD.

Investigation of VEO and adult-onset IBD in treatment refractory disease will elucidate new treatment opportunities by revealing complexity of disease network dysregulation. Causal- and correlative-based network analysis allows for consideration of the synergistic effects between genes in disease, which can be a greater determinant than evaluation of single target genes to inform disease drivers and opportunities for combinatorial therapy. Network analysis can be focused by novel variants, as seen with *TRIM22* identified through WES in VEOIBD patients to generate hypothesis and potentially identify biomarkers and guide drug discovery and repositioning in both VEO and adult-onset IBD patient subsets.

Supplementary Material

Note: To access the supplementary material accompanying this article, visit the online version of *Gastroenterology* at www.gastrojournal.org, and at http://dx.doi.org/10.1053/j.gastro.2016.01.031.

References

1. **Avitzur Y, Guo C**, Mastropaolo LA, et al. Mutations in tetratricopeptide repeat domain 7A result in a severe form of very early onset inflammatory bowel disease. Gastroenterology 2014;146:1028–1039.
2. **Elkadri A, Thoeni C**, Deharvengt SJ, et al. Mutations in plasmalemma vesicle associated protein result in sieving protein-losing enteropathy characterized by hypoproteinemia, hypoalbuminemia, and hypertriglyceridemia. Cell Mol Gastroenterol Hepatol 2015;1:381–394 e7.

3. Janecke AR, Heinz-Erian P, Yin J, et al. Reduced sodium/proton exchanger NHE3 activity causes congenital sodium diarrhea. Hum Mol Genet 2015;24:6614–6623.
4. Dhillon SS, Fattouh R, Elkadri A, et al. Variants in nicotinamide adenine dinucleotide phosphate oxidase complex components determine susceptibility to very early onset inflammatory bowel disease. Gastroenterology 2014;147:680–689 e2.
5. Dhillon SS, Mastropaolo LA, Murchie R, et al. Higher activity of the inducible nitric oxide synthase contributes to very early onset inflammatory bowel disease. Clin Transl Gastroenterol 2014;5:e46.
6. Moran CJ, Walters TD, Guo CH, et al. IL-10R polymorphisms are associated with very-early-onset ulcerative colitis. Inflamm Bowel Dis 2013;19:115–123.
7. Muise AM, Walters T, Xu W, et al. Single nucleotide polymorphisms that increase expression of the guanosine triphosphatase RAC1 are associated with ulcerative colitis. Gastroenterology 2011;141:633–641.
8. Muise AM, Xu W, Guo CH, et al. NADPH oxidase complex and IBD candidate gene studies: identification of a rare variant in NCF2 that results in reduced binding to RAC2. Gut 2012;61:1028–1035.
9. Uhlig HH, Schwerd T, Koletzko S, et al. The diagnostic approach to monogenic very early onset inflammatory bowel disease. Gastroenterology 2014;147:990–1007.e3.
10. **Glocker EO, Kotlarz D, Boztug K**, et al. Inflammatory bowel disease and mutations affecting the interleukin-10 receptor. N Engl J Med 2009;361:2033–2045.
11. **Duan Z, Gao B**, Xu W, et al. Identification of TRIM22 as a RING finger E3 ubiquitin ligase. Biochem Biophys Res Commun 2008;374:502–506.
12. Sawyer SL, Emerman M, Malik HS. Discordant evolution of the adjacent antiretroviral genes TRIM22 and TRIM5 in mammals. PLoS Pathog 2007;3:e197.
13. **Yu S, Gao B**, Duan Z, et al. Identification of tripartite motif-containing 22 (TRIM22) as a novel NF-kappaB activator. Biochem Biophys Res Commun 2011;410:247–251.
14. Obad S, Olofsson T, Mechti N, et al. Expression of the IFN-inducible p53-target gene TRIM22 is downregulated during erythroid differentiation of human bone marrow. Leuk Res 2007;31:995–1001.
15. Barr SD, Smiley JR, Bushman FD. The interferon response inhibits HIV particle production by induction of TRIM22. PLoS Pathog 2008;4:e1000007.
16. Eldin P, Papon L, Oteiza A, et al. TRIM22 E3 ubiquitin ligase activity is required to mediate antiviral activity against encephalomyocarditis virus. J Gen Virol 2009;90:536–545.
17. **Di Pietro A, Kajaste-Rudnitski A**, Oteiza A, et al. TRIM22 inhibits influenza A virus infection by targeting the viral nucleoprotein for degradation. J Virol 2013;87:4523–4533.
18. Sandborn WJ, Gasink C, Gao LL, et al. Ustekinumab induction and maintenance therapy in refractory Crohn's disease. N Engl J Med 2012;367:1519–1528.
19. Haberman Y, Tickle TL, Dexheimer PJ, et al. Pediatric Crohn disease patients exhibit specific ileal transcriptome and microbiome signature. J Clin Invest 2014;124:3617–3633.
20. Tusher VG, Tibshirani R, Chu G. Significance analysis of microarrays applied to the ionizing radiation response. Proc Natl Acad Sci U S A 2001;98:5116–5121.
21. Madigan D, York J. Bayesian graphical models for discrete data. International Statistical Review 1995;63:215–232.
22. **Schadt EE, Molony C, Chudin E**, et al. Mapping the genetic architecture of gene expression in human liver. PLoS Biol 2008;6:e107.
23. Tran LM, Zhang B, Zhang Z, et al. Inferring causal genomic alterations in breast cancer using gene expression data. BMC Syst Biol 2011;5:121.
24. **Wang IM, Zhang B, Yang X**, et al. Systems analysis of eleven rodent disease models reveals an inflammatome signature and key drivers. Mol Syst Biol 2012;8:594.
25. Yang X, Zhang B, Molony C, et al. Systematic genetic and genomic analysis of cytochrome P450 enzyme activities in human liver. Genome Res 2010;20:1020–1036.
26. Zhang B, Gaiteri C, Bodea LG, et al. Integrated systems approach identifies genetic nodes and networks in late-onset Alzheimer's disease. Cell 2013;153:707–720.
27. Kelly JN, Barr SD. In silico analysis of functional single nucleotide polymorphisms in the human TRIM22 gene. PLoS One 2014;9:e101436.
28. Herr AM, Dressel R, Walter L. Different subcellular localisations of TRIM22 suggest species-specific function. Immunogenetics 2009;61:271–280.
29. Bustamante J, Boisson-Dupuis S, Abel L, et al. Mendelian susceptibility to mycobacterial disease: genetic, immunological, and clinical features of inborn errors of IFN-gamma immunity. Semin Immunol 2014;26:454–470.
30. Jostins L, Ripke S, Weersma RK, et al. Host-microbe interactions have shaped the genetic architecture of inflammatory bowel disease. Nature 2012;491:119–124.
31. **Westra HJ, Peters MJ**, Esko T, et al. Systematic identification of trans eQTLs as putative drivers of known disease associations. Nat Genet 2013;45:1238–1243.
32. **Lee MN, Ye C**, Villani AC, et al. Common genetic variants modulate pathogen-sensing responses in human dendritic cells. Science 2014;343:1246980.
33. Sandborn WJ, Ghosh S, Panes J, et al. Tofacitinib, an oral Janus kinase inhibitor, in active ulcerative colitis. N Engl J Med 2012;367:616–624.
34. Ho GT, Lee HM, Brydon G, et al. Fecal calprotectin predicts the clinical course of acute severe ulcerative colitis. Am J Gastroenterol 2009;104:673–678.
35. Leach ST, Yang Z, Messina I, et al. Serum and mucosal S100 proteins, calprotectin (S100A8/S100A9) and S100A12, are elevated at diagnosis in children with inflammatory bowel disease. Scand J Gastroenterol 2007;42:1321–1331.
36. Radford Smith G, Ferguson E, Hanigan K, et al. P226. Consistently high C reactive protein is associated with subsequent development of perianal fistulae in patients with Crohn's disease. J Crohns Colitis 2015;9(Suppl 1):S188.
37. **Murdoch T, O'Donnell S**, Silverberg MS, et al. Biomarkers as potential treatment targets in inflammatory

bowel disease: a systematic review. Can J Gastroenterol Hepatol 2015;29:203–208.
38. Hugot JP, Chamaillard M, Zouali H, et al. Association of NOD2 leucine-rich repeat variants with susceptibility to Crohn's disease. Nature 2001;411:599–603.
39. Ogura Y, Bonen DK, Inohara N, et al. A frameshift mutation in NOD2 associated with susceptibility to Crohn's disease. Nature 2001;411:603–606.
40. Kim YG, Park JH, Reimer T, et al. Viral infection augments Nod1/2 signaling to potentiate lethality associated with secondary bacterial infections. Cell Host Microbe 2011;9:496–507.
41. Sabbah A, Chang TH, Harnack R, et al. Activation of innate immune antiviral responses by Nod2. Nat Immunol 2009;10:1073–1080.
42. Li Q, Verma IM. NF-kappaB regulation in the immune system. Nat Rev Immunol 2002;2:725–734.
43. Chen Z, Chen YZ, Wang XF, et al. Prediction of ubiquitination sites by using the composition of k-spaced amino acid pairs. PLoS One 2011;6:e22930.
44. Castanier C, Zemirli N, Portier A, et al. MAVS ubiquitination by the E3 ligase TRIM25 and degradation by the proteasome is involved in type I interferon production after activation of the antiviral RIG-I-like receptors. BMC Biol 2012;10:44.
45. Yang S, Wang B, Humphries F, et al. Pellino3 ubiquitinates RIP2 and mediates Nod2-induced signaling and protective effects in colitis. Nat Immunol 2013;14:927–936.
46. **Walczak H, Iwai K, Dikic I**. Generation and physiological roles of linear ubiquitin chains. BMC Biol 2012;10:23.
47. Zurek B, Schoultz I, Neerincx A, et al. TRIM27 negatively regulates NOD2 by ubiquitination and proteasomal degradation. PLoS One 2012;7:e41255.
48. Jefferies C, Wynne C, Higgs R. Antiviral TRIMs: friend or foe in autoimmune and autoinflammatory disease? Nat Rev Immunol 2011;11:617–625.
49. **Kawai T, Akira S**. Regulation of innate immune signalling pathways by the tripartite motif (TRIM) family proteins. EMBO Mol Med 2011;3:513–527.
50. Chae JJ, Wood G, Masters SL, et al. The B30.2 domain of pyrin, the familial Mediterranean fever protein, interacts directly with caspase-1 to modulate IL-1beta production. Proc Natl Acad Sci U S A 2006;103:9982–9987.
51. Hattlmann CJ, Kelly JN, Barr SD. TRIM22: a diverse and dynamic antiviral protein. Mol Biol Int 2012;2012:153415.
52. Zurek B, Proell M, Wagner RN, et al. Mutational analysis of human NOD1 and NOD2 NACHT domains reveals different modes of activation. Innate Immun 2012;18:100–111.
53. Shaw MH, Kamada N, Warner N, et al. The ever-expanding function of NOD2: autophagy, viral recognition, and T cell activation. Trends Immunol 2011;32:73–79.
54. Strober W, Watanabe T. NOD2, an intracellular innate immune sensor involved in host defense and Crohn's disease. Mucosal Immunol 2011;4:484495.
55. Philpott DJ, Sorbara MT, Robertson SJ, et al. NOD proteins: regulators of inflammation in health and disease. Nat Rev Immunol 2014;14:9–23.
56. Marsh RA, Rao K, Satwani P, et al. Allogeneic hematopoietic cell transplantation for XIAP deficiency: an international survey reveals poor outcomes. Blood 2013;121:877–883.
57. Zeissig Y, Petersen BS, Milutinovic S, et al. XIAP variants in male Crohn's disease. Gut 2015;64:66–76.
58. Abbott DW, Yang Y, Hutti JE, et al. Coordinated regulation of Toll-like receptor and NOD2 signaling by K63-linked polyubiquitin chains. Mol Cell Biol 2007;27:6012–6025.
59. **Damgaard RB, Fiil BK**, Speckmann C, et al. Disease-causing mutations in the XIAP BIR2 domain impair NOD2-dependent immune signalling. EMBO Mol Med 2013;5:1278–1295.
60. Krieg A, Correa RG, Garrison JB, et al. XIAP mediates NOD signaling via interaction with RIP2. Proc Natl Acad Sci U S A 2009;106:14524–14529.
61. **Ryu YS, Lee Y**, Lee KW, et al. TRIM32 protein sensitizes cells to tumor necrosis factor (TNFalpha)-induced apoptosis via its RING domain-dependent E3 ligase activity against X-linked inhibitor of apoptosis (XIAP). J Biol Chem 2011;286:25729–25738.
62. Latour S, Aguilar C. XIAP deficiency syndrome in humans. Semin Cell Dev Biol 2015;39:115–123.
63. Rigaud S, Lopez-Granados E, Siberil S, et al. Human X-linked variable immunodeficiency caused by a hypomorphic mutation in XIAP in association with a rare polymorphism in CD40LG. Blood 2011;118:252–261.

Author names in bold designate shared co-first authorship.

Received September 25, 2015. Accepted January 22, 2016.

Reprint requests
Address requests for reprints to: Aleixo Muise, MD, PhD, The Hospital for Sick Children, 555 University Avenue, Toronto, Ontario M5G 1X8, Canada. e-mail: aleixo.muise@utoronto.ca; fax: (416) 813-6531.

Acknowledgments
The authors thank the patients and their families described here from Canada and Australia. The authors thank Karoline Fielder and Dr. Amanda Charlton for assistance with patient-related materials. Thanks to Neil Warner for critical reading of the manuscript.

Lucas A. Mastropaolo, Cornelia Thoeni, Abdul Elkadri, and Tobias Schwerd contributed equally. Eric E. Schadt and Aleixo M. Muise contributed equally.

The current affiliation for Ralph Nanan, Brigitte Snanter-Nanan and Mingjing Hu is Charles Perkins Centre Nepean, The University of Sydney, Sydney Australia.

Conflicts of interest
The authors disclose no conflicts.

Funding
Christoph Klein and Daniel Kotlarz were supported by the Deutsche Forschungsgemeinschaft (SFB1054) and BioSysNe. Holm H. Uhlig is supported by the Crohn's & Colitis Foundation of America (CCFA). Tobias Schwerd is supported by the Deutsche Forschungsgemeinschaft (SCHW1730/1-1). Qi Li and Abdul Elkadri are supported by a Crohn's and Colitis Canada (CCC), Canadian Association of Gastroenterology (CAG), and Canadian Institute of Health Research (CIHR) Fellowship. Aleixo M. Muise is funded by a CIHR-operating grant (MOP119457) and Aleixo M. Muise, Christoph Klein, Scott B. Snapper, Eric E. Schadt, and Holm H. Uhlig are funded by the Leona M. and Harry B. Helmsley Charitable Trust to study VEOIBD.

REFERENCES

1. Hsu P, Santner-Nanan B, Hu M, Skarratt K, Lee CH, Stormon M, et al. IL-10 Potentiates Differentiation of Human Induced Regulatory T Cells via STAT3 and Foxo1. Journal of immunology. 2015;195(8):3665-74.

2. Hsu PS, Lai CL, Hu M, Santner-Nanan B, Dahlstrom JE, Lee CH, et al. IL-2 Enhances Gut Homing Potential of Human Naive Regulatory T Cells Early in Life. Journal of immunology. 2018.

3. Janeway CA, Jr., Medzhitov R. Innate immune recognition. Annual review of immunology. 2002;20:197-216.

4. Monie TP. Section 5 - Connecting the Innate and Adaptive Immune Responses. The Innate Immune System: Academic Press; 2017. p. 171-87.

5. Ljunggren HG, Karre K. In search of the 'missing self': MHC molecules and NK cell recognition. Immunology today. 1990;11(7):237-44.

6. Garrido F, Ruiz-Cabello F, Cabrera T, Perez-Villar JJ, Lopez-Botet M, Duggan-Keen M, et al. Implications for immunosurveillance of altered HLA class I phenotypes in human tumours. Immunology today. 1997;18(2):89-95.

7. Weiss G, Schaible UE. Macrophage defense mechanisms against intracellular bacteria. Immunological reviews. 2015;264(1):182-203.

8. Banchereau J, Steinman RM. Dendritic cells and the control of immunity. Nature. 1998;392(6673):245-52.

9. Steinman RM, Hawiger D, Nussenzweig MC. Tolerogenic dendritic cells. Annual review of immunology. 2003;21:685-711.

10. York IA, Rock KL. Antigen processing and presentation by the class I major histocompatibility complex. Annual review of immunology. 1996;14:369-96.

11. Braciale TJ, Morrison LA, Sweetser MT, Sambrook J, Gething MJ, Braciale VL. Antigen presentation pathways to class I and class II MHC-restricted T lymphocytes. Immunological reviews. 1987;98:95-114.

12. Neefjes JJ, Stollorz V, Peters PJ, Geuze HJ, Ploegh HL. The biosynthetic pathway of MHC class II but not class I molecules intersects the endocytic route. Cell. 1990;61(1):171-83.

13. Miller JFAP. The golden anniversary of the thymus. Nature Reviews Immunology. 2011;11(7):489-95.

14. Wu L, Antica M, Johnson GR, Scollay R, Shortman K. Developmental potential of the earliest precursor cells from the adult mouse thymus. The Journal of experimental medicine. 1991;174(6):1617-27.

15. von Boehmer H, Aifantis I, Gounari F, Azogui O, Haughn L, Apostolou I, et al. Thymic selection revisited: how essential is it? Immunological reviews. 2003;191:62-78.

16. Jameson SC, Hogquist KA, Bevan MJ. Positive selection of thymocytes. Annual review of immunology. 1995;13:93-126.

17. Palmer E. Negative selection--clearing out the bad apples from the T-cell repertoire. Nature Reviews Immunology. 2003;3(5):383-91.

18. Fontenot JD, Gavin MA, Rudensky AY. Foxp3 programs the development and function of CD4+CD25+ regulatory T cells. Nature immunology. 2003;4(4):330-6.

19. Ohkura N, Kitagawa Y, Sakaguchi S. Development and maintenance of regulatory T cells. Immunity. 2013;38(3):414-23.

20. Jiang H, Chess L. Chapter 2 How the Immune System Achieves Self–Nonself Discrimination During Adaptive Immunity. Advances in Immunology. 102: Academic Press; 2009. p. 95-133.

21. Burnet FM. A modification of Jerne's theory of antibody production using the concept of clonal selection. CA: a cancer journal for clinicians. 1976;26(2):119-21.

22. Burnet FMS. The clonal selection theory of acquired immunity. Nashville: Vanderbilt University Press; 1959.

23. Anderson MS, Venanzi ES, Klein L, Chen Z, Berzins SP, Turley SJ, et al. Projection of an Immunological Self Shadow Within the Thymus by the Aire Protein. Science. 2002;298(5597):1395-401.

24. Kont V, Laan M, Kisand K, Merits A, Scott HS, Peterson P. Modulation of Aire regulates the expression of tissue-restricted antigens. Molecular immunology. 2008;45(1):25-33.

25. Liston A, Lesage S, Wilson J, Peltonen L, Goodnow CC. Aire regulates negative selection of organ-specific T cells. Nature immunology. 2003;4(4):350-4.

26. Kyewski B, Klein L. A CENTRAL ROLE FOR CENTRAL TOLERANCE. Annual review of immunology. 2006;24(1):571-606.

27. Bouneaud C, Kourilsky P, Bousso P. Impact of negative selection on the T cell repertoire reactive to a self-peptide: a large fraction of T cell clones escapes clonal deletion. Immunity. 2000;13(6):829-40.

28. Arnold B. Levels of peripheral T cell tolerance. Transplant Immunology. 2002;10(2):109-14.

29. Heath WR, Kurts C, Miller JFAP, Carbone FR. Cross-tolerance: A Pathway for Inducing Tolerance to Peripheral Tissue Antigens. The Journal of experimental medicine. 1998;187(10):1549-53.

30. Jiang H. The Qa-1 dependent CD8+ T cell mediated regulatory pathway. Cellular & molecular immunology. 2005;2(3):161-7.

31. Rosser EC, Mauri C. Regulatory B cells: origin, phenotype, and function. Immunity. 2015;42(4):607-12.

32. Mauri C, Bosma A. Immune Regulatory Function of B Cells. Annual review of immunology. 2012;30(1):221-41.

33. Eberl G, Colonna M, Di Santo JP, McKenzie AN. Innate lymphoid cells. Innate lymphoid cells: a new paradigm in immunology. Science. 2015;348(6237):aaa6566.

34. Artis D, Spits H. The biology of innate lymphoid cells. Nature. 2015;517(7534):293-301.

35. Sakaguchi S. Naturally arising Foxp3-expressing CD25+CD4+ regulatory T cells in immunological tolerance to self and non-self. Nature immunology. 2005;6(4):345-52.

36. Gershon RK, Kondo K. Cell interactions in the induction of tolerance: the role of thymic lymphocytes. Immunology. 1970;18(5):723-37.

37. Ohki H, Martin C, Corbel C, Coltey M, Le Douarin NM. Tolerance induced by thymic epithelial grafts in birds. Science. 1987;237(4818):1032-5.

38. Sakaguchi S, Takahashi T, Nishizuka Y. Study on cellular events in postthymectomy autoimmune oophoritis in mice. I. Requirement of Lyt-1 effector cells for oocytes damage after adoptive transfer. The Journal of experimental medicine. 1982;156(6):1565-76.

39. Sakaguchi S, Fukuma K, Kuribayashi K, Masuda T. Organ-specific autoimmune diseases induced in mice by elimination of T cell subset. I. Evidence for the active participation of T cells in natural self-tolerance; deficit of a T cell subset as a possible cause of autoimmune disease. The Journal of experimental medicine. 1985;161(1):72-87.

40. Fowell D, Mason D. Evidence that the T cell repertoire of normal rats contains cells with the potential to cause diabetes. Characterization of the CD4+ T cell subset that inhibits this autoimmune potential. The Journal of experimental medicine. 1993;177(3):627-36.

41. Hori S, Nomura T, Sakaguchi S. Control of regulatory T cell development by the transcription factor Foxp3. Science. 2003;299(5609):1057-61.

42. Churlaud G, Pitoiset F, Jebbawi F, Lorenzon R, Bellier B, Rosenzwajg M, et al. Human and Mouse CD8(+)CD25(+)FOXP3(+) Regulatory T Cells at Steady State and during Interleukin-2 Therapy. Frontiers in immunology. 2015;6:171.

43. Abbas AK, Benoist C, Bluestone JA, Campbell DJ, Ghosh S, Hori S, et al. Regulatory T cells: recommendations to simplify the nomenclature. Nature immunology. 2013;14(4):307-8.

44. Sakaguchi S, Sakaguchi N, Asano M, Itoh M, Toda M. Immunologic self-tolerance maintained by activated T cells expressing IL-2 receptor alpha-chains (CD25). Breakdown of a single mechanism of self-tolerance causes various autoimmune diseases. Journal of immunology. 1995;155(3):1151-64.

45. Baecher-Allan C, Brown JA, Freeman GJ, Hafler DA. CD4+CD25high regulatory cells in human peripheral blood. Journal of immunology. 2001;167(3):1245-53.

46. Russell WL, Russell LB, Gower JS. EXCEPTIONAL INHERITANCE OF A SEX-LINKED GENE IN THE MOUSE EXPLAINED ON THE BASIS THAT THE X/O SEX-CHROMOSOME CONSTITUTION IS FEMALE. Proceedings of the National Academy of Sciences of the United States of America. 1959;45(4):554-60.

47. Lyon MF, Peters J, Glenister PH, Ball S, Wright E. The scurfy mouse mutant has previously unrecognized hematological abnormalities and resembles Wiskott-Aldrich syndrome. Proceedings of the National Academy of Sciences of the United States of America. 1990;87(7):2433-7.

48. Godfrey VL, Wilkinson JE, Russell LB. X-linked lymphoreticular disease in the scurfy (sf) mutant mouse. The American journal of pathology. 1991;138(6):1379-87.

49. Godfrey VL, Wilkinson JE, Rinchik EM, Russell LB. Fatal lymphoreticular disease in the scurfy (sf) mouse requires T cells that mature in a sf thymic environment:

potential model for thymic education. Proceedings of the National Academy of Sciences of the United States of America. 1991;88(13):5528-32.

50. Godfrey VL, Rouse BT, Wilkinson JE. Transplantation of T cell-mediated, lymphoreticular disease from the scurfy (sf) mouse. The American journal of pathology. 1994;145(2):281-6.

51. Wildin RS, Ramsdell F, Peake J, Faravelli F, Casanova JL, Buist N, et al. X-linked neonatal diabetes mellitus, enteropathy and endocrinopathy syndrome is the human equivalent of mouse scurfy. Nature genetics. 2001;27(1):18-20.

52. Bennett CL, Christie J, Ramsdell F, Brunkow ME, Ferguson PJ, Whitesell L, et al. The immune dysregulation, polyendocrinopathy, enteropathy, X-linked syndrome (IPEX) is caused by mutations of FOXP3. Nature genetics. 2001;27(1):20-1.

53. Lal G, Bromberg JS. Epigenetic mechanisms of regulation of Foxp3 expression. Blood. 2009;114(18):3727-35.

54. Huehn J, Beyer M. Epigenetic and transcriptional control of Foxp3 regulatory T cells. Seminars in immunology. 2015.

55. Mantel PY, Ouaked N, Ruckert B, Karagiannidis C, Welz R, Blaser K, et al. Molecular mechanisms underlying FOXP3 induction in human T cells. Journal of immunology. 2006;176(6):3593-602.

56. Janson PC, Winerdal ME, Marits P, Thorn M, Ohlsson R, Winqvist O. FOXP3 promoter demethylation reveals the committed Treg population in humans. PloS one. 2008;3(2):e1612.

57. Zheng Y, Josefowicz S, Chaudhry A, Peng XP, Forbush K, Rudensky AY. Role of conserved non-coding DNA elements in the Foxp3 gene in regulatory T-cell fate. Nature. 2010;463(7282):808-12.

58. Josefowicz SZ, Lu LF, Rudensky AY. Regulatory T cells: mechanisms of differentiation and function. Annual review of immunology. 2012;30:531-64.

59. Li X, Liang Y, LeBlanc M, Benner C, Zheng Y. Function of a Foxp3 cis-element in protecting regulatory T cell identity. Cell. 2014;158(4):734-48.

60. Allan SE, Crome SQ, Crellin NK, Passerini L, Steiner TS, Bacchetta R, et al. Activation-induced FOXP3 in human T effector cells does not suppress proliferation or cytokine production. International immunology. 2007;19(4):345-54.

61. Gavin MA, Torgerson TR, Houston E, DeRoos P, Ho WY, Stray-Pedersen A, et al. Single-cell analysis of normal and FOXP3-mutant human T cells: FOXP3 expression without regulatory T cell development. Proceedings of the National Academy of Sciences of the United States of America. 2006;103(17):6659-64.

62. Lin W, Haribhai D, Relland LM, Truong N, Carlson MR, Williams CB, et al. Regulatory T cell development in the absence of functional Foxp3. Nature immunology. 2007;8(4):359-68.

63. Delgoffe Greg M, Bettini Matthew L, Vignali Dario AA. Identity Crisis: It's Not Just Foxp3 Anymore. Immunity. 2012;37(5):759-61.

64. Ohkura N, Hamaguchi M, Morikawa H, Sugimura K, Tanaka A, Ito Y, et al. T cell receptor stimulation-induced epigenetic changes and Foxp3 expression are

independent and complementary events required for Treg cell development. Immunity. 2012;37(5):785-99.

65. Curotto de Lafaille MA, Lafaille JJ. Natural and adaptive foxp3+ regulatory T cells: more of the same or a division of labor? Immunity. 2009;30(5):626-35.

66. Weinhold B. Epigenetics: The Science of Change. Environmental Health Perspectives. 2006;114(3):A160-A7.

67. Bird A. Perceptions of epigenetics. Nature. 2007;447:396.

68. Kim JK, Samaranayake M, Pradhan S. Epigenetic mechanisms in mammals. Cellular and molecular life sciences : CMLS. 2009;66(4):596-612.

69. Zaidi SK, Young DW, Montecino M, van Wijnen AJ, Stein JL, Lian JB, et al. Bookmarking the genome: maintenance of epigenetic information. The Journal of biological chemistry. 2011;286(21):18355-61.

70. Floess S, Freyer J, Siewert C, Baron U, Olek S, Polansky J, et al. Epigenetic control of the foxp3 locus in regulatory T cells. PLoS biology. 2007;5(2):e38.

71. Itoh M, Takahashi T, Sakaguchi N, Kuniyasu Y, Shimizu J, Otsuka F, et al. Thymus and autoimmunity: production of CD25+CD4+ naturally anergic and suppressive T cells as a key function of the thymus in maintaining immunologic self-tolerance. Journal of immunology. 1999;162(9):5317-26.

72. Ohkura N, Sakaguchi S. Regulatory T cells: roles of T cell receptor for their development and function. Seminars in immunopathology. 2010;32(2):95-106.

73. Kawahata K, Misaki Y, Yamauchi M, Tsunekawa S, Setoguchi K, Miyazaki J, et al. Generation of CD4(+)CD25(+) regulatory T cells from autoreactive T cells simultaneously with their negative selection in the thymus and from nonautoreactive T cells by endogenous TCR expression. Journal of immunology. 2002;168(9):4399-405.

74. Josefowicz SZ, Rudensky A. Control of regulatory T cell lineage commitment and maintenance. Immunity. 2009;30(5):616-25.

75. Pacholczyk R, Kern J. The T-cell receptor repertoire of regulatory T cells. Immunology. 2008;125(4):450-8.

76. Wolf KJ, Emerson RO, Pingel J, Buller RM, DiPaolo RJ. Conventional and Regulatory CD4+ T Cells That Share Identical TCRs Are Derived from Common Clones. PloS one. 2016;11(4):e0153705.

77. Beyersdorf N, Kerkau T, Hünig T. CD28 co-stimulation in T-cell homeostasis: a recent perspective. Immunotargets and Therapy. 2015;4:111-22.

78. Salomon B, Lenschow DJ, Rhee L, Ashourian N, Singh B, Sharpe A, et al. B7/CD28 costimulation is essential for the homeostasis of the CD4+CD25+ immunoregulatory T cells that control autoimmune diabetes. Immunity. 2000;12(4):431-40.

79. Tang Q, Henriksen KJ, Boden EK, Tooley AJ, Ye J, Subudhi SK, et al. Cutting edge: CD28 controls peripheral homeostasis of CD4+CD25+ regulatory T cells. Journal of immunology. 2003;171(7):3348-52.

80. Tai X, Cowan M, Feigenbaum L, Singer A. CD28 costimulation of developing thymocytes induces Foxp3 expression and regulatory T cell differentiation independently of interleukin 2. Nature immunology. 2005;6(2):152-62.

81. Krummel MF, Allison JP. CD28 and CTLA-4 have opposing effects on the response of T cells to stimulation. The Journal of experimental medicine. 1995;182(2):459.

82. Zheng SG, Wang JH, Stohl W, Kim KS, Gray JD, Horwitz DA. TGF-β Requires CTLA-4 Early after T Cell Activation to Induce FoxP3 and Generate Adaptive CD4⁺CD25⁺ Regulatory Cells. The Journal of Immunology. 2006;176(6):3321-9.

83. Wing K, Onishi Y, Prieto-Martin P, Yamaguchi T, Miyara M, Fehervari Z, et al. CTLA-4 control over Foxp3+ regulatory T cell function. Science. 2008;322(5899):271-5.

84. Chen W, Jin W, Hardegen N, Lei KJ, Li L, Marinos N, et al. Conversion of peripheral CD4+CD25- naive T cells to CD4+CD25+ regulatory T cells by TGF-beta induction of transcription factor Foxp3. The Journal of experimental medicine. 2003;198(12):1875-86.

85. Fantini MC, Becker C, Monteleone G, Pallone F, Galle PR, Neurath MF. Cutting Edge: TGF-β Induces a Regulatory Phenotype in CD4⁺CD25[−] T Cells through Foxp3 Induction and Down-Regulation of Smad7. The Journal of Immunology. 2004;172(9):5149-53.

86. Tran DQ, Ramsey H, Shevach EM. Induction of FOXP3 expression in naive human CD4+FOXP3 T cells by T-cell receptor stimulation is transforming growth factor-beta dependent but does not confer a regulatory phenotype. Blood. 2007;110(8):2983-90.

87. Apostolou I, Verginis P, Kretschmer K, Polansky J, Huhn J, von Boehmer H. Peripherally induced Treg: mode, stability, and role in specific tolerance. Journal of clinical immunology. 2008;28(6):619-24.

88. Liu Y, Zhang P, Li J, Kulkarni AB, Perruche S, Chen W. A critical function for TGF-beta signaling in the development of natural CD4+CD25+Foxp3+ regulatory T cells. Nature immunology. 2008;9(6):632-40.

89. Chen W, Konkel JE. Development of thymic Foxp3(+) regulatory T cells: TGF-beta matters. European journal of immunology. 2015;45(4):958-65.

90. Bird L. Regulatory T cells: Nurtured by TGF[beta]. Nature reviews Immunology. 2010;10(7):466-.

91. Antony PA, Paulos CM, Ahmadzadeh M, Akpinarli A, Palmer DC, Sato N, et al. Interleukin-2-dependent mechanisms of tolerance and immunity in vivo. Journal of immunology. 2006;176(9):5255-66.

92. Malek TR, Bayer AL. Tolerance, not immunity, crucially depends on IL-2. Nature reviews Immunology. 2004;4(9):665-74.

93. Zheng SG, Wang J, Wang P, Gray JD, Horwitz DA. IL-2 is essential for TGF-beta to convert naive CD4+CD25- cells to CD25+Foxp3+ regulatory T cells and for expansion of these cells. Journal of immunology. 2007;178(4):2018-27.

94. Horwitz DA, Zheng SG, Gray JD. Natural and TGF-beta-induced Foxp3(+)CD4(+) CD25(+) regulatory T cells are not mirror images of each other. Trends in immunology. 2008;29(9):429-35.

95. Polansky JK, Kretschmer K, Freyer J, Floess S, Garbe A, Baron U, et al. DNA methylation controls Foxp3 gene expression. European journal of immunology. 2008;38(6):1654-63.

96. Pacholczyk R, Ignatowicz H, Kraj P, Ignatowicz L. Origin and T Cell Receptor Diversity of Foxp3+CD4+CD25+ T Cells. Immunity. 2006;25(2):249-59.

97. Chen Q, Kim YC, Laurence A, Punkosdy GA, Shevach EM. IL-2 controls the stability of Foxp3 expression in TGF-beta-induced Foxp3+ T cells in vivo. Journal of immunology. 2011;186(11):6329-37.

98. Selvaraj RK, Geiger TL. Mitigation of experimental allergic encephalomyelitis by TGF-beta induced Foxp3+ regulatory T lymphocytes through the induction of anergy and infectious tolerance. Journal of immunology. 2008;180(5):2830-8.

99. Selvaraj RK, Geiger TL. A Kinetic and Dynamic Analysis of Foxp3 Induced in T Cells by TGF-β. The Journal of Immunology. 2007;178(12):7667-77.

100. Bluestone JA, Abbas AK. Natural versus adaptive regulatory T cells. Nature reviews Immunology. 2003;3(3):253-7.

101. Huter EN, Punkosdy GA, Glass DD, Cheng LI, Ward JM, Shevach EM. TGF-beta-induced Foxp3+ regulatory T cells rescue scurfy mice. European journal of immunology. 2008;38(7):1814-21.

102. Aricha R, Feferman T, Fuchs S, Souroujon MC. Ex Vivo Generated Regulatory T Cells Modulate Experimental Autoimmune Myasthenia Gravis. The Journal of Immunology. 2008;180(4):2132-9.

103. Weber SE, Harbertson J, Godebu E, Mros GA, Padrick RC, Carson BD, et al. Adaptive Islet-Specific Regulatory CD4 T Cells Control Autoimmune Diabetes and Mediate the Disappearance of Pathogenic Th1 Cells In Vivo. The Journal of Immunology. 2006;176(8):4730-9.

104. DiPaolo RJ, Brinster C, Davidson TS, Andersson J, Glass D, Shevach EM. Autoantigen-Specific TGFβ-Induced Foxp3⁺ Regulatory T Cells Prevent Autoimmunity by Inhibiting Dendritic Cells from Activating Autoreactive T Cells. The Journal of Immunology. 2007;179(7):4685-93.

105. Trzonkowski P, Bieniaszewska M, Juscinska J, Dobyszuk A, Krzystyniak A, Marek N, et al. First-in-man clinical results of the treatment of patients with graft versus host disease with human ex vivo expanded CD4+CD25+CD127- T regulatory cells. Clinical immunology (Orlando, Fla). 2009;133(1):22-6.

106. Singer BD, King LS, D'Alessio FR. Regulatory T cells as immunotherapy. Frontiers in immunology. 2014;5:46.

107. Rossetti M, Spreafico R, Saidin S, Chua C, Moshref M, Leong JY, et al. Ex vivo-expanded but not in vitro-induced human regulatory T cells are candidates for cell therapy in autoimmune diseases thanks to stable demethylation of the FOXP3 regulatory T cell-specific demethylated region. Journal of immunology. 2015;194(1):113-24.

108. Wang J, Ioan-Facsinay A, van der Voort EI, Huizinga TW, Toes RE. Transient expression of FOXP3 in human activated nonregulatory CD4+ T cells. European journal of immunology. 2007;37(1):129-38.

109. Sakaguchi S, Yamaguchi T, Nomura T, Ono M. Regulatory T cells and immune tolerance. Cell. 2008;133(5):775-87.

110. Larche M. Regulatory T cells in allergy and asthma. Chest. 2007;132(3):1007-14.

111. Singh B, Read S, Asseman C, Malmstrom V, Mottet C, Stephens LA, et al. Control of intestinal inflammation by regulatory T cells. Immunological reviews. 2001;182:190-200.

112. Beres AJ, Drobyski WR. The role of regulatory T cells in the biology of graft versus host disease. Frontiers in immunology. 2013;4:163.

113. Littman DR, Rudensky AY. Th17 and regulatory T cells in mediating and restraining inflammation. Cell. 2010;140(6):845-58.

114. Sakaguchi S. Regulatory T cells: key controllers of immunologic self-tolerance. Cell. 2000;101(5):455-8.

115. Miyara M, Sakaguchi S. Natural regulatory T cells: mechanisms of suppression. Trends in molecular medicine. 2007;13(3):108-16.

116. Shevach EM. Mechanisms of Foxp3+ T Regulatory Cell-Mediated Suppression. Immunity. 2009;30(5):636-45.

117. Sakaguchi S, Wing K, Onishi Y, Prieto-Martin P, Yamaguchi T. Regulatory T cells: how do they suppress immune responses? International immunology. 2009;21(10):1105-11.

118. Shevach EM. Mechanisms of foxp3+ T regulatory cell-mediated suppression. Immunity. 2009;30(5):636-45.

119. Takahashi T, Kuniyasu Y, Toda M, Sakaguchi N, Itoh M, Iwata M, et al. Immunologic self-tolerance maintained by CD25+CD4+ naturally anergic and suppressive T cells: induction of autoimmune disease by breaking their anergic/suppressive state. International immunology. 1998;10(12):1969-80.

120. Thornton AM, Shevach EM. CD4+CD25+ immunoregulatory T cells suppress polyclonal T cell activation in vitro by inhibiting interleukin 2 production. The Journal of experimental medicine. 1998;188(2):287-96.

121. Gondek DC, Lu LF, Quezada SA, Sakaguchi S, Noelle RJ. Cutting edge: contact-mediated suppression by CD4+CD25+ regulatory cells involves a granzyme B-dependent, perforin-independent mechanism. Journal of immunology. 2005;174(4):1783-6.

122. Cao X, Cai SF, Fehniger TA, Song J, Collins LI, Piwnica-Worms DR, et al. Granzyme B and perforin are important for regulatory T cell-mediated suppression of tumor clearance. Immunity. 2007;27(4):635-46.

123. Grossman WJ, Verbsky JW, Barchet W, Colonna M, Atkinson JP, Ley TJ. Human T Regulatory Cells Can Use the Perforin Pathway to Cause Autologous Target Cell Death. Immunity. 2004;21(4):589-601.

124. Garin MI, Chu CC, Golshayan D, Cernuda-Morollon E, Wait R, Lechler RI. Galectin-1: a key effector of regulation mediated by CD4+CD25+ T cells. Blood. 2007;109(5):2058-65.

125. Pandiyan P, Zheng L, Ishihara S, Reed J, Lenardo MJ. CD4+CD25+Foxp3+ regulatory T cells induce cytokine deprivation-mediated apoptosis of effector CD4+ T cells. Nature immunology. 2007;8(12):1353-62.

126. Sakaguchi S, Wing K, Onishi Y, Prieto-Martin P, Yamaguchi T. Regulatory T cells: how do they suppress immune responses? International immunology. 2009;21(10):1105-11.

127. Suri-Payer E, Cantor H. Differential Cytokine Requirements for Regulation of Autoimmune Gastritis and Colitis by CD4+CD25+T Cells. Journal of autoimmunity. 2001;16(2):115-23.

128. Piccirillo CA, Letterio JJ, Thornton AM, McHugh RS, Mamura M, Mizuhara H, et al. CD4⁺CD25⁺ Regulatory T Cells Can Mediate Suppressor Function in the Absence of Transforming Growth Factor β1 Production and Responsiveness. The Journal of experimental medicine. 2002;196(2):237-46.

129. Zorn E, Nelson EA, Mohseni M, Porcheray F, Kim H, Litsa D, et al. IL-2 regulates FOXP3 expression in human CD4+CD25+ regulatory T cells through a STAT-dependent mechanism and induces the expansion of these cells in vivo. Blood. 2006;108(5):1571-9.

130. Collison LW, Workman CJ, Kuo TT, Boyd K, Wang Y, Vignali KM, et al. The inhibitory cytokine IL-35 contributes to regulatory T-cell function. Nature. 2007;450(7169):566-9.

131. Bardel E, Larousserie F, Charlot-Rabiega P, Coulomb-L'Herminé A, Devergne O. Human CD4⁺CD25⁺Foxp3⁺ Regulatory T Cells Do Not Constitutively Express IL-35. The Journal of Immunology. 2008;181(10):6898-905.

132. Oderup C, Cederbom L, Makowska A, Cilio CM, Ivars F. Cytotoxic T lymphocyte antigen-4-dependent down-modulation of costimulatory molecules on dendritic cells in CD4+ CD25+ regulatory T-cell-mediated suppression. Immunology. 2006;118(2):240-9.

133. Grohmann U, Orabona C, Fallarino F, Vacca C, Calcinaro F, Falorni A, et al. CTLA-4-Ig regulates tryptophan catabolism in vivo. Nature immunology. 2002;3(11):1097-101.

134. Huang CT, Workman CJ, Flies D, Pan X, Marson AL, Zhou G, et al. Role of LAG-3 in regulatory T cells. Immunity. 2004;21(4):503-13.

135. Liang B, Workman C, Lee J, Chew C, Dale BM, Colonna L, et al. Regulatory T cells inhibit dendritic cells by lymphocyte activation gene-3 engagement of MHC class II. Journal of immunology. 2008;180(9):5916-26.

136. Petrillo MG, Ronchetti S, Ricci E, Alunno A, Gerli R, Nocentini G, et al. GITR+ regulatory T cells in the treatment of autoimmune diseases. Autoimmunity Reviews. 2015;14(2):117-26.

137. McHugh RS, Whitters MJ, Piccirillo CA, Young DA, Shevach EM, Collins M, et al. CD4+CD25+ Immunoregulatory T Cells: Gene Expression Analysis Reveals a

Functional Role for the Glucocorticoid-Induced TNF Receptor. Immunity. 2002;16(2):311-23.

138. Shimizu J, Yamazaki S, Takahashi T, Ishida Y, Sakaguchi S. Stimulation of CD25(+)CD4(+) regulatory T cells through GITR breaks immunological self-tolerance. Nature immunology. 2002;3(2):135-42.

139. Borsellino G, Kleinewietfeld M, Di Mitri D, Sternjak A, Diamantini A, Giometto R, et al. Expression of ectonucleotidase CD39 by Foxp3⁺ Treg cells: hydrolysis of extracellular ATP and immune suppression. Blood. 2007;110(4):1225-32.

140. Herrath J, Chemin K, Albrecht I, Catrina AI, Malmstrom V. Surface expression of CD39 identifies an enriched Treg-cell subset in the rheumatic joint, which does not suppress IL-17A secretion. European journal of immunology. 2014;44(10):2979-89.

141. Deaglio S, Dwyer KM, Gao W, Friedman D, Usheva A, Erat A, et al. Adenosine generation catalyzed by CD39 and CD73 expressed on regulatory T cells mediates immune suppression. The Journal of experimental medicine. 2007;204(6):1257-65.

142. Hutloff A, Dittrich AM, Beier KC, Eljaschewitsch B, Kraft R, Anagnostopoulos I, et al. ICOS is an inducible T-cell co-stimulator structurally and functionally related to CD28. Nature. 1999;397(6716):263-6.

143. McAdam AJ, Chang TT, Lumelsky AE, Greenfield EA, Boussiotis VA, Duke-Cohan JS, et al. Mouse inducible costimulatory molecule (ICOS) expression is enhanced by CD28 costimulation and regulates differentiation of CD4+ T cells. Journal of immunology. 2000;165(9):5035-40.

144. Redpath SA, van der Werf N, Cervera AM, MacDonald AS, Gray D, Maizels RM, et al. ICOS controls Foxp3(+) regulatory T-cell expansion, maintenance and IL-10 production during helminth infection. European journal of immunology. 2013;43(3):705-15.

145. Zheng J, Chan PL, Liu Y, Qin G, Xiang Z, Lam KT, et al. ICOS regulates the generation and function of human CD4+ Treg in a CTLA-4 dependent manner. PloS one. 2013;8(12):e82203.

146. Lohning M, Hutloff A, Kallinich T, Mages HW, Bonhagen K, Radbruch A, et al. Expression of ICOS in vivo defines CD4+ effector T cells with high inflammatory potential and a strong bias for secretion of interleukin 10. The Journal of experimental medicine. 2003;197(2):181-93.

147. Takahashi N, Matsumoto K, Saito H, Nanki T, Miyasaka N, Kobata T, et al. Impaired CD4 and CD8 effector function and decreased memory T cell populations in ICOS-deficient patients. Journal of immunology. 2009;182(9):5515-27.

148. Keir ME, Butte MJ, Freeman GJ, Sharpe AH. PD-1 and its ligands in tolerance and immunity. Annual review of immunology. 2008;26:677-704.

149. Nishimura H, Agata Y, Kawasaki A, Sato M, Imamura S, Minato N, et al. Developmentally regulated expression of the PD-1 protein on the surface of double-negative(CD4–CD8–) thymocytes. International immunology. 1996;8(5):773-80.

150. Dong Y, Sun Q, Zhang X. PD-1 and its ligands are important immune checkpoints in cancer. Oncotarget. 2017;8(2):2171-86.

151. Butte MJ, Keir ME, Phamduy TB, Sharpe AH, Freeman GJ. Programmed death-1 ligand 1 interacts specifically with the B7-1 costimulatory molecule to inhibit T cell responses. Immunity. 2007;27(1):111-22.

152. Sharpe AH, Wherry EJ, Ahmed R, Freeman GJ. The function of programmed cell death 1 and its ligands in regulating autoimmunity and infection. Nature immunology. 2007;8(3):239-45.

153. Keir ME, Butte MJ, Freeman GJ, Sharpe AH. PD-1 and Its Ligands in Tolerance and Immunity. Annual review of immunology. 2008;26(1):677-704.

154. Ansari MJ, Salama AD, Chitnis T, Smith RN, Yagita H, Akiba H, et al. The programmed death-1 (PD-1) pathway regulates autoimmune diabetes in nonobese diabetic (NOD) mice. The Journal of experimental medicine. 2003;198(1):63-9.

155. Salama AD, Chitnis T, Imitola J, Ansari MJ, Akiba H, Tushima F, et al. Critical role of the programmed death-1 (PD-1) pathway in regulation of experimental autoimmune encephalomyelitis. The Journal of experimental medicine. 2003;198(1):71-8.

156. Krupnick AS, Gelman AE, Barchet W, Richardson S, Kreisel FH, Turka LA, et al. Cutting Edge: Murine Vascular Endothelium Activates and Induces the Generation of Allogeneic CD4⁺25⁺Foxp3⁺ Regulatory T Cells. The Journal of Immunology. 2005;175(10):6265-70.

157. Francisco LM, Salinas VH, Brown KE, Vanguri VK, Freeman GJ, Kuchroo VK, et al. PD-L1 regulates the development, maintenance, and function of induced regulatory T cells. The Journal of experimental medicine. 2009;206(13):3015-29.

158. Lee J-J, Yeh C-Y, Jung C-J, Chen C-W, Du M-K, Yu H-M, et al. Skewed Distribution of IL-7 Receptor-α-Expressing Effector Memory CD8+ T Cells with Distinct Functional Characteristics in Oral Squamous Cell Carcinoma. PloS one. 2014;9(1):e85521.

159. Li J, Huston G, Swain SL. IL-7 Promotes the Transition of CD4 Effectors to Persistent Memory Cells. The Journal of experimental medicine. 2003;198(12):1807-15.

160. Liu W, Putnam AL, Xu-Yu Z, Szot GL, Lee MR, Zhu S, et al. CD127 expression inversely correlates with FoxP3 and suppressive function of human CD4+ T reg cells. The Journal of experimental medicine. 2006;203(7):1701-11.

161. Klein J, Sato A. The HLA system. First of two parts. The New England journal of medicine. 2000;343(10):702-9.

162. Chang CH, Hong SC, Hughes CC, Janeway CA, Jr., Flavell RA. CIITA activates the expression of MHC class II genes in mouse T cells. International immunology. 1995;7(9):1515-8.

163. Baecher-Allan C, Wolf E, Hafler DA. MHC Class II Expression Identifies Functionally Distinct Human Regulatory T Cells. The Journal of Immunology. 2006;176(8):4622-31.

164. Curtsinger JM, Schmidt CS, Mondino A, Lins DC, Kedl RM, Jenkins MK, et al. Inflammatory Cytokines Provide a Third Signal for Activation of Naive CD4⁺and CD8⁺T Cells. The Journal of Immunology. 1999;162(6):3256-62.

165. Steinman RM, Cohn ZA. IDENTIFICATION OF A NOVEL CELL TYPE IN PERIPHERAL LYMPHOID ORGANS OF MICE. I MORPHOLOGY, QUANTITATION, TISSUE DISTRIBUTION. 1973;137(5):1142-62.

166. Schraml BU, Reis e Sousa C. Defining dendritic cells. Current opinion in immunology. 2015;32(Supplement C):13-20.

167. Karsunky H, Merad M, Cozzio A, Weissman IL, Manz MG. Flt3 ligand regulates dendritic cell development from Flt3+ lymphoid and myeloid-committed progenitors to Flt3+ dendritic cells in vivo. The Journal of experimental medicine. 2003;198(2):305-13.

168. Liu K, Victora GD, Schwickert TA, Guermonprez P, Meredith MM, Yao K, et al. In vivo analysis of dendritic cell development and homeostasis. Science. 2009;324(5925):392-7.

169. Fogg DK, Sibon C, Miled C, Jung S, Aucouturier P, Littman DR, et al. A clonogenic bone marrow progenitor specific for macrophages and dendritic cells. Science. 2006;311(5757):83-7.

170. Liu K, Nussenzweig MC. Origin and development of dendritic cells. Immunological reviews. 2010;234(1):45-54.

171. Chicha L, Jarrossay D, Manz MG. Clonal Type I Interferon–producing and Dendritic Cell Precursors Are Contained in Both Human Lymphoid and Myeloid Progenitor Populations. The Journal of experimental medicine. 2004;200(11):1519-24.

172. Kalantari T, Kamali-Sarvestani E, Ciric B, Karimi MH, Kalantari M, Faridar A, et al. Generation of immunogenic and tolerogenic Clinical-grade dendritic cells. Immunologic research. 2011;51(2-3):153-60.

173. Dzionek A, Fuchs A, Schmidt P, Cremer S, Zysk M, Miltenyi S, et al. BDCA-2, BDCA-3, and BDCA-4: Three Markers for Distinct Subsets of Dendritic Cells in Human Peripheral Blood. The Journal of Immunology. 2000;165(11):6037-46.

174. Metlay JP, Witmer-Pack MD, Agger R, Crowley MT, Lawless D, Steinman RM. The distinct leukocyte integrins of mouse spleen dendritic cells as identified with new hamster monoclonal antibodies. The Journal of experimental medicine. 1990;171(5):1753-71.

175. Merad M, Sathe P, Helft J, Miller J, Mortha A. The Dendritic Cell Lineage: Ontogeny and Function of Dendritic Cells and Their Subsets in the Steady State and the Inflamed Setting. Annual review of immunology. 2013;31:10.1146/annurev-immunol-020711-74950.

176. Hunger RE, Sieling PA, Ochoa MT, Sugaya M, Burdick AE, Rea TH, et al. Langerhans cells utilize CD1a and langerin to efficiently present nonpeptide antigens to T cells. The Journal of clinical investigation. 2004;113(5):701-8.

177. Zhou LJ, Tedder TF. Human blood dendritic cells selectively express CD83, a member of the immunoglobulin superfamily. Journal of immunology. 1995;154(8):3821-35.

178. Robinson SP, Patterson S, English N, Davies D, Knight SC, Reid CD. Human peripheral blood contains two distinct lineages of dendritic cells. European journal of immunology. 1999;29(9):2769-78.

179. Reizis B, Bunin A, Ghosh HS, Lewis KL, Sisirak V. Plasmacytoid dendritic cells: recent progress and open questions. Annual review of immunology. 2011;29:163-83.

180. Hubo M, Trinschek B, Kryczanowsky F, Tuettenberg A, Steinbrink K, Jonuleit H. Costimulatory molecules on immunogenic versus tolerogenic human dendritic cells. Frontiers in immunology. 2013;4:82.

181. Tisch R. Immunogenic versus tolerogenic dendritic cells: a matter of maturation. International reviews of immunology. 2010;29(2):111-8.

182. Castiello L, Sabatino M, Jin P, Clayberger C, Marincola FM, Krensky AM, et al. Monocyte-derived DC maturation strategies and related pathways: a transcriptional view. Cancer immunology, immunotherapy : CII. 2011;60(4):457-66.

183. Katz SI, Parker D, Turk JL. B-cell suppression of delayed hypersensitivity reactions. Nature. 1974;251(5475):550-1.

184. Wolf SD, Dittel BN, Hardardottir F, Janeway CA. Experimental Autoimmune Encephalomyelitis Induction in Genetically B Cell–deficient Mice. The Journal of experimental medicine. 1996;184(6):2271-8.

185. Mizoguchi A, Mizoguchi E, Takedatsu H, Blumberg RS, Bhan AK. Chronic Intestinal Inflammatory Condition Generates IL-10-Producing Regulatory B Cell Subset Characterized by CD1d Upregulation. Immunity. 2002;16(2):219-30.

186. Duddy M, Niino M, Adatia F, Hebert S, Freedman M, Atkins H, et al. Distinct effector cytokine profiles of memory and naive human B cell subsets and implication in multiple sclerosis. Journal of immunology. 2007;178(10):6092-9.

187. Vivier E, Spits H, Cupedo T. Interleukin-22-producing innate immune cells: new players in mucosal immunity and tissue repair? Nature reviews Immunology. 2009;9(4):229-34.

188. Spits H, Cupedo T. Innate Lymphoid Cells: Emerging Insights in Development, Lineage Relationships, and Function. Annual review of immunology. 2012;30(1):647-75.

189. Spits H, Artis D, Colonna M, Diefenbach A, Di Santo JP, Eberl G, et al. Innate lymphoid cells [mdash] a proposal for uniform nomenclature. Nature reviews Immunology. 2013;13(2):145-9.

190. Wolk K, Kunz S, Witte E, Friedrich M, Asadullah K, Sabat R. IL-22 Increases the Innate Immunity of Tissues. Immunity. 2004;21(2):241-54.

191. Williams Z. Inducing tolerance to pregnancy. The New England journal of medicine. 2012;367(12):1159-61.

192. Tafuri A, Alferink J, Moller P, Hammerling GJ, Arnold B. T cell awareness of paternal alloantigens during pregnancy. Science. 1995;270(5236):630-3.

193. PB M. Some immunological and endocrine problems raised by evolution of viviparity in vertebrates. Symp Soc Exp Biol. 1953;7:320-37.

194. Apps R, Murphy SP, Fernando R, Gardner L, Ahad T, Moffett A. Human leucocyte antigen (HLA) expression of primary trophoblast cells and placental cell lines,

determined using single antigen beads to characterize allotype specificities of anti-HLA antibodies. Immunology. 2009;127(1):26-39.

195. Nelson JL. Microchimerism: incidental byproduct of pregnancy or active participant in human health? Trends in molecular medicine. 2002;8(3):109-13.

196. Lee J, Romero R, Xu Y, Miranda J, Yoo W, Chaemsaithong P, et al. Detection of anti-HLA antibodies in maternal blood in the second trimester to identify patients at risk of antibody-mediated maternal anti-fetal rejection and spontaneous preterm delivery. American journal of reproductive immunology (New York, NY : 1989). 2013;70(2):162-75.

197. Lee J, Romero R, Chaiworapongsa T, Dong Z, Tarca AL, Xu Y, et al. Characterization of the fetal blood transcriptome and proteome in maternal anti-fetal rejection: evidence of a distinct and novel type of human fetal systemic inflammatory response. American journal of reproductive immunology (New York, NY : 1989). 2013;70(4):265-84.

198. Oreshkova T, Dimitrov R, Mourdjeva M. A cross-talk of decidual stromal cells, trophoblast, and immune cells: a prerequisite for the success of pregnancy. American journal of reproductive immunology (New York, NY : 1989). 2012;68(5):366-73.

199. Lee JY, Lee M, Lee SK. Role of endometrial immune cells in implantation. Clinical and experimental reproductive medicine. 2011;38(3):119-25.

200. Burton GJ, Jauniaux E, Charnock-Jones DS. The influence of the intrauterine environment on human placental development. The International journal of developmental biology. 2010;54(2-3):303-12.

201. Geiselhart A, Dietl J, Marzusch K, Ruck P, Ruck M, Horny HP, et al. Comparative analysis of the immunophenotypes of decidual and peripheral blood large granular lymphocytes and T cells during early human pregnancy. American journal of reproductive immunology (New York, NY : 1989). 1995;33(4):315-22.

202. Loubiere LS, Lambert NC, Flinn LJ, Erickson TD, Yan Z, Guthrie KA, et al. Maternal microchimerism in healthy adults in lymphocytes, monocyte/macrophages and NK cells. Laboratory investigation; a journal of technical methods and pathology. 2006;86(11):1185-92.

203. Adams Waldorf KM, Gammill HS, Lucas J, Aydelotte TM, Leisenring WM, Lambert NC, et al. Dynamic changes in fetal microchimerism in maternal peripheral blood mononuclear cells, CD4+ and CD8+ cells in normal pregnancy. Placenta. 2010;31(7):589-94.

204. Verneris M. Fetal microchimerism—what our children leave behind. Blood. 2003;102(10):3465-6.

205. Somerset DA, Zheng Y, Kilby MD, Sansom DM, Drayson MT. Normal human pregnancy is associated with an elevation in the immune suppressive CD25+ CD4+ regulatory T-cell subset. Immunology. 2004;112(1):38-43.

206. Santner-Nanan B, Peek MJ, Khanam R, Richarts L, Zhu E, Fazekas de St Groth B, et al. Systemic increase in the ratio between Foxp3+ and IL-17-producing CD4+ T cells in healthy pregnancy but not in preeclampsia. Journal of immunology. 2009;183(11):7023-30.

207. Jasper MJ, Tremellen KP, Robertson SA. Primary unexplained infertility is associated with reduced expression of the T-regulatory cell transcription factor Foxp3 in endometrial tissue. Molecular human reproduction. 2006;12(5):301-8.

208. Winger EE, Reed JL. Low circulating CD4(+) CD25(+) Foxp3(+) T regulatory cell levels predict miscarriage risk in newly pregnant women with a history of failure. American journal of reproductive immunology (New York, NY : 1989). 2011;66(4):320-8.

209. Santner-Nanan B, Straubinger K, Hsu P, Parnell G, Tang B, Xu B, et al. Fetal-maternal alignment of regulatory T cells correlates with IL-10 and Bcl-2 upregulation in pregnancy. Journal of immunology. 2013;191(1):145-53.

210. Mold JE, Venkatasubrahmanyam S, Burt TD, Michaëlsson J, Rivera JM, Galkina SA, et al. Fetal and Adult Hematopoietic Stem Cells Give Rise to Distinct T Cell Lineages in Humans. Science. 2010;330(6011):1695-9.

211. Firan M, Bawdon R, Radu C, Ober RJ, Eaken D, Antohe F, et al. The MHC class I-related receptor, FcRn, plays an essential role in the maternofetal transfer of gamma-globulin in humans. International immunology. 2001;13(8):993-1002.

212. McKenzie JM, Zakarija M. Fetal and neonatal hyperthyroidism and hypothyroidism due to maternal TSH receptor antibodies. Thyroid : official journal of the American Thyroid Association. 1992;2(2):155-9.

213. Barker DJ, Osmond C. Infant mortality, childhood nutrition, and ischaemic heart disease in England and Wales. Lancet (London, England). 1986;1(8489):1077-81.

214. Fowden AL, Giussani DA, Forhead AJ. Intrauterine Programming of Physiological Systems: Causes and Consequences. Physiology. 2006;21(1):29-37.

215. Ege MJ, Bieli C, Frei R, van Strien RT, Riedler J, Ublagger E, et al. Prenatal farm exposure is related to the expression of receptors of the innate immunity and to atopic sensitization in school-age children. The Journal of allergy and clinical immunology. 2006;117(4):817-23.

216. Schaub B, Liu J, Hoppler S, Schleich I, Huehn J, Olek S, et al. Maternal farm exposure modulates neonatal immune mechanisms through regulatory T cells. The Journal of allergy and clinical immunology. 2009;123(4):774-82.e5.

217. Douwes J, Cheng S, Travier N, Cohet C, Niesink A, McKenzie J, et al. Farm exposure in utero may protect against asthma, hay fever and eczema. The European respiratory journal. 2008;32(3):603-11.

218. Polte T, Hennig C, Hansen G. Allergy prevention starts before conception: Maternofetal transfer of tolerance protects against the development of asthma. Journal of Allergy and Clinical Immunology.122(5):1022-30.e5.

219. Roduit C, Wohlgensinger J, Frei R, Bitter S, Bieli C, Loeliger S, et al. Prenatal animal contact and gene expression of innate immunity receptors at birth are associated with atopic dermatitis. The Journal of allergy and clinical immunology. 2011;127(1):179-85, 85.e1.

220. Prescott SL. Allergy Takes Its Toll: The Role of Toll-like Receptors in Allergy Pathogenesis. The World Allergy Organization journal. 2008;1(1):4-8.

221. Thorburn AN, McKenzie CI, Shen S, Stanley D, Macia L, Mason LJ, et al. Evidence that asthma is a developmental origin disease influenced by maternal diet and bacterial metabolites. Nature communications. 2015;6:7320.

222. Gomez de Agüero M, Ganal-Vonarburg SC, Fuhrer T, Rupp S, Uchimura Y, Li H, et al. The maternal microbiota drives early postnatal innate immune development. Science. 2016;351(6279):1296-302.

223. Haynes BF, Heinly CS. Early human T cell development: analysis of the human thymus at the time of initial entry of hematopoietic stem cells into the fetal thymic microenvironment. The Journal of experimental medicine. 1995;181(4):1445-58.

224. Cupedo T, Nagasawa M, Weijer K, Blom B, Spits H. Development and activation of regulatory T cells in the human fetus. European journal of immunology. 2005;35(2):383-90.

225. Takahata Y, Nomura A, Takada H, Ohga S, Furuno K, Hikino S, et al. CD25+CD4+ T cells in human cord blood: an immunoregulatory subset with naive phenotype and specific expression of forkhead box p3 (Foxp3) gene. Experimental hematology. 2004;32(7):622-9.

226. Mold JE, Michaëlsson J, Burt TD, Muench MO, Beckerman KP, Busch MP, et al. Maternal Alloantigens Promote the Development of Tolerogenic Fetal Regulatory T Cells in Utero. Science. 2008;322(5907):1562-5.

227. Burlingham WJ, Grailer AP, Heisey DM, Claas FH, Norman D, Mohanakumar T, et al. The effect of tolerance to noninherited maternal HLA antigens on the survival of

renal transplants from sibling donors. The New England journal of medicine. 1998;339(23):1657-64.

228. Straubinger K, Paul S, Prazeres da Costa O, Ritter M, Buch T, Busch DH, et al. Maternal immune response to helminth infection during pregnancy determines offspring susceptibility to allergic airway inflammation. Journal of Allergy and Clinical Immunology. 2014;134(6):1271-9.e10.

229. von Mutius E, Radon K. Living on a Farm: Impact on Asthma Induction and Clinical Course. Immunology and Allergy Clinics of North America. 2008;28(3):631-47.

230. Holt PG, Strickland DH. Soothing signals: transplacental transmission of resistance to asthma and allergy. The Journal of experimental medicine. 2009;206(13):2861-4.

231. Gray LE, O'Hely M, Ranganathan S, Sly PD, Vuillermin P. The Maternal Diet, Gut Bacteria, and Bacterial Metabolites during Pregnancy Influence Offspring Asthma. Frontiers in immunology. 2017;8:365.

232. Maukonen J, Saarela M. Human gut microbiota: does diet matter? Proceedings of the Nutrition Society. 2014;74(1):23-36.

233. Conlon MA, Bird AR. The Impact of Diet and Lifestyle on Gut Microbiota and Human Health. Nutrients. 2015;7(1):17-44.

234. Palmer C, Bik EM, DiGiulio DB, Relman DA, Brown PO. Development of the Human Infant Intestinal Microbiota. PLoS biology. 2007;5(7):e177.

235. Bäckhed F, Roswall J, Peng Y, Feng Q, Jia H, Kovatcheva-Datchary P, et al. Dynamics and Stabilization of the Human Gut Microbiome during the First Year of Life. Cell Host & Microbe. 2015;17(5):690-703.

236. Salazar N, Arboleya S, Valdés L, Stanton C, Ross P, Ruiz L, et al. The human intestinal microbiome at extreme ages of life. Dietary intervention as a way to counteract alterations. Frontiers in Genetics. 2014;5(406).

237. Langdon A, Crook N, Dantas G. The effects of antibiotics on the microbiome throughout development and alternative approaches for therapeutic modulation. Genome medicine. 2016;8(1):39.

238. Tanaka M, Nakayama J. Development of the gut microbiota in infancy and its impact on health in later life. Allergology International. 2017;66(4):515-22.

239. Eckburg PB, Bik EM, Bernstein CN, Purdom E, Dethlefsen L, Sargent M, et al. Diversity of the Human Intestinal Microbial Flora. Science (New York, NY). 2005;308(5728):1635-8.

240. Simpson HL, Campbell BJ. Review article: dietary fibre–microbiota interactions. Alimentary pharmacology & therapeutics. 2015;42(2):158-79.

241. Muegge BD, Kuczynski J, Knights D, Clemente JC, Gonzalez A, Fontana L, et al. Diet drives convergence in gut microbiome functions across mammalian phylogeny and within humans. Science. 2011;332(6032):970-4.

242. Wu GD, Chen J, Hoffmann C, Bittinger K, Chen YY, Keilbaugh SA, et al. Linking long-term dietary patterns with gut microbial enterotypes. Science. 2011;334(6052):105-8.

243. Faith JJ, McNulty NP, Rey FE, Gordon JI. Predicting a human gut microbiota's response to diet in gnotobiotic mice. Science. 2011;333(6038):101-4.

244. David LA, Maurice CF, Carmody RN, Gootenberg DB, Button JE, Wolfe BE, et al. Diet rapidly and reproducibly alters the human gut microbiome. Nature. 2014;505(7484):559-63.

245. Tidjani Alou M, Lagier J-C, Raoult D. Diet influence on the gut microbiota and dysbiosis related to nutritional disorders. Human Microbiome Journal. 2016;1(Supplement C):3-11.

246. Maslowski KM, Mackay CR. Diet, gut microbiota and immune responses. Nature immunology. 2010;12:5.

247. Hong YH, Nishimura Y, Hishikawa D, Tsuzuki H, Miyahara H, Gotoh C, et al. Acetate and propionate short chain fatty acids stimulate adipogenesis via GPCR43. Endocrinology. 2005;146(12):5092-9.

248. Kamada N, Seo S-U, Chen GY, Nunez G. Role of the gut microbiota in immunity and inflammatory disease. Nature reviews Immunology. 2013;13(5):321-35.

249. Thaiss CA, Zmora N, Levy M, Elinav E. The microbiome and innate immunity. Nature. 2016;535(7610):65-74.

250. Thaiss CA, Levy M, Itav S, Elinav E. Integration of Innate Immune Signaling. Trends in immunology. 2016;37(2):84-101.

251. Kawai T, Akira S. The roles of TLRs, RLRs and NLRs in pathogen recognition. International immunology. 2009;21(4):317-37.

252. Haverson K, Rehakova Z, Sinkora J, Sver L, Bailey M. Immune development in jejunal mucosa after colonization with selected commensal gut bacteria: A study in germ-free pigs. Veterinary immunology and immunopathology. 2007;119(3):243-53.

253. Mikkelsen HB, Garbarsch C, Tranum-Jensen J, Thuneberg L. Macrophages in the small intestinal muscularis externa of embryos, newborn and adult germ-free mice. Journal of molecular histology. 2004;35(4):377-87.

254. Iwasaki A, Kelsall BL. Freshly isolated Peyer's patch, but not spleen, dendritic cells produce interleukin 10 and induce the differentiation of T helper type 2 cells. The Journal of experimental medicine. 1999;190(2):229-39.

255. Smythies LE, Sellers M, Clements RH, Mosteller-Barnum M, Meng G, Benjamin WH, et al. Human intestinal macrophages display profound inflammatory anergy despite avid phagocytic and bacteriocidal activity. The Journal of clinical investigation. 2005;115(1):66-75.

256. Smythies LE, Shen R, Bimczok D, Novak L, Clements RH, Eckhoff DE, et al. Inflammation anergy in human intestinal macrophages is due to Smad-induced IkappaBalpha expression and NF-kappaB inactivation. The Journal of biological chemistry. 2010;285(25):19593-604.

257. Smythies LE, Sellers M, Clements RH, Mosteller-Barnum M, Meng G, Benjamin WH, et al. Human intestinal macrophages display profound inflammatory anergy despite avid phagocytic and bacteriocidal activity. The Journal of clinical investigation. 2005;115(1):66-75.

258. Sawa S, Cherrier M, Lochner M, Satoh-Takayama N, Fehling HJ, Langa F, et al. Lineage relationship analysis of RORgammat+ innate lymphoid cells. Science. 2010;330(6004):665-9.

259. Sanos SL, Bui VL, Mortha A, Oberle K, Heners C, Johner C, et al. ROR[gamma]t and commensal microflora are required for the differentiation of mucosal interleukin 22-producing NKp46+ cells. Nature immunology. 2009;10(1):83-91.

260. Sawa S, Lochner M, Satoh-Takayama N, Dulauroy S, Berard M, Kleinschek M, et al. ROR[gamma]t+ innate lymphoid cells regulate intestinal homeostasis by integrating negative signals from the symbiotic microbiota. Nature immunology. 2011;12(4):320-6.

261. Sonnenberg GF, Monticelli LA, Alenghat T, Fung TC, Hutnick NA, Kunisawa J, et al. Innate lymphoid cells promote anatomical containment of lymphoid-resident commensal bacteria. Science. 2012;336(6086):1321-5.

262. Hepworth MR, Monticelli LA, Fung TC, Ziegler CG, Grunberg S, Sinha R, et al. Innate lymphoid cells regulate CD4+ T-cell responses to intestinal commensal bacteria. Nature. 2013;498(7452):113-7.

263. Hepworth MR, Fung TC, Masur SH, Kelsen JR, McConnell FM, Dubrot J, et al. Immune tolerance. Group 3 innate lymphoid cells mediate intestinal selection of commensal bacteria-specific CD4(+) T cells. Science. 2015;348(6238):1031-5.

264. Brandtzaeg P, Halstensen TS, Kett K, Krajci P, Kvale D, Rognum TO, et al. Immunobiology and immunopathology of human gut mucosa: humoral immunity and intraepithelial lymphocytes. Gastroenterology. 1989;97(6):1562-84.

265. Crabbe PA, Bazin H, Eyssen H, Heremans JF. The normal microbial flora as a major stimulus for proliferation of plasma cells synthesizing IgA in the gut. The germ-free intestinal tract. International archives of allergy and applied immunology. 1968;34(4):362-75.

266. Hapfelmeier S, Lawson MA, Slack E, Kirundi JK, Stoel M, Heikenwalder M, et al. Reversible microbial colonization of germ-free mice reveals the dynamics of IgA immune responses. Science. 2010;328(5986):1705-9.

267. Macpherson AJ, Martinic MM, Harris N. The functions of mucosal T cells in containing the indigenous commensal flora of the intestine. Cellular and molecular life sciences : CMLS. 2002;59(12):2088-96.

268. Mazmanian SK, Liu CH, Tzianabos AO, Kasper DL. An immunomodulatory molecule of symbiotic bacteria directs maturation of the host immune system. Cell. 2005;122(1):107-18.

269. Ivanov II, McKenzie BS, Zhou L, Tadokoro CE, Lepelley A, Lafaille JJ, et al. The Orphan Nuclear Receptor RORγt Directs the Differentiation Program of Proinflammatory IL-17+ T Helper Cells. Cell. 2006;126(6):1121-33.

270. Ivanov, II, Frutos Rde L, Manel N, Yoshinaga K, Rifkin DB, Sartor RB, et al. Specific microbiota direct the differentiation of IL-17-producing T-helper cells in the mucosa of the small intestine. Cell Host Microbe. 2008;4(4):337-49.

271. Hirota K, Turner J-E, Villa M, Duarte JH, Demengeot J, Steinmetz OM, et al. Plasticity of TH17 cells in Peyer's patches is responsible for the induction of T cell-dependent IgA responses. Nature immunology. 2013;14(4):372-9.

272. Honda K, Littman DR. The microbiota in adaptive immune homeostasis and disease. Nature. 2016;535(7610):75-84.

273. Sefik E, Geva-Zatorsky N, Oh S, Konnikova L, Zemmour D, McGuire AM, et al. MUCOSAL IMMUNOLOGY. Individual intestinal symbionts induce a distinct population of RORgamma(+) regulatory T cells. Science. 2015;349(6251):993-7.

274. Yang BH, Hagemann S, Mamareli P, Lauer U, Hoffmann U, Beckstette M, et al. Foxp3(+) T cells expressing RORgammat represent a stable regulatory T-cell effector lineage with enhanced suppressive capacity during intestinal inflammation. Mucosal Immunology. 2016;9(2):444-57.

275. Kim KS, Hong SW, Han D, Yi J, Jung J, Yang BG, et al. Dietary antigens limit mucosal immunity by inducing regulatory T cells in the small intestine. Science. 2016;351(6275):858-63.

276. Arpaia N, Campbell C, Fan X, Dikiy S, van der Veeken J, deRoos P, et al. Metabolites produced by commensal bacteria promote peripheral regulatory T-cell generation. Nature. 2013;504(7480):451-5.

277. Smith PM, Howitt MR, Panikov N, Michaud M, Gallini CA, Bohlooly YM, et al. The microbial metabolites, short-chain fatty acids, regulate colonic Treg cell homeostasis. Science. 2013;341(6145):569-73.

278. Furusawa Y, Obata Y, Fukuda S, Endo TA, Nakato G, Takahashi D, et al. Commensal microbe-derived butyrate induces the differentiation of colonic regulatory T cells. Nature. 2013;504(7480):446-50.

279. Cummings JH, Pomare EW, Branch WJ, Naylor CP, Macfarlane GT. Short chain fatty acids in human large intestine, portal, hepatic and venous blood. Gut. 1987;28(10):1221-7.

280. Macfarlane S, Macfarlane GT. Regulation of short-chain fatty acid production. The Proceedings of the Nutrition Society. 2003;62(1):67-72.

281. G. Macfarlane GG. Microbiological aspects of SCFA production in the large bowel. In: John H. Cummings JLR, Takashi Sakata, editor. Physiological and Clinical Aspects of Short-Chain Fatty Acids. London: CAMBRIDGE UNIVERSITY PRESS; 1995. p. 87-106.

282. Kim CH, Park J, Kim M. Gut microbiota-derived short-chain Fatty acids, T cells, and inflammation. Immune network. 2014;14(6):277-88.

283. Fleming SE, Choi SY, Fitch MD. Absorption of short-chain fatty acids from the rat cecum in vivo. The Journal of nutrition. 1991;121(11):1787-97.

284. Cook SI, Sellin JH. Review article: short chain fatty acids in health and disease. Alimentary pharmacology & therapeutics. 1998;12(6):499-507.

285. Wolever TM, Josse RG, Leiter LA, Chiasson JL. Time of day and glucose tolerance status affect serum short-chain fatty acid concentrations in humans. Metabolism: clinical and experimental. 1997;46(7):805-11.

286. Muir JG, Lu ZX, Young GP, Cameron-Smith D, Collier GR, O'Dea K. Resistant starch in the diet increases breath hydrogen and serum acetate in human subjects. The American journal of clinical nutrition. 1995;61(4):792-9.

287. Ganapathy V, Thangaraju M, Prasad PD, Martin PM, Singh N. Transporters and receptors for short-chain fatty acids as the molecular link between colonic bacteria and the host. Current opinion in pharmacology. 2013;13(6):869-74.

288. Brown AJ, Goldsworthy SM, Barnes AA, Eilert MM, Tcheang L, Daniels D, et al. The Orphan G protein-coupled receptors GPR41 and GPR43 are activated by propionate and other short chain carboxylic acids. The Journal of biological chemistry. 2003;278(13):11312-9.

289. Le Poul E, Loison C, Struyf S, Springael JY, Lannoy V, Decobecq ME, et al. Functional characterization of human receptors for short chain fatty acids and their role in polymorphonuclear cell activation. The Journal of biological chemistry. 2003;278(28):25481-9.

290. Park J, Kim M, Kang SG, Jannasch AH, Cooper B, Patterson J, et al. Short-chain fatty acids induce both effector and regulatory T cells by suppression of histone deacetylases and regulation of the mTOR-S6K pathway. Mucosal Immunology. 2015;8(1):80-93.

291. Kim MH, Kang SG, Park JH, Yanagisawa M, Kim CH. Short-chain fatty acids activate GPR41 and GPR43 on intestinal epithelial cells to promote inflammatory responses in mice. Gastroenterology. 2013;145(2):396-406 e1-10.

292. Tunaru S, Kero J, Schaub A, Wufka C, Blaukat A, Pfeffer K, et al. PUMA-G and HM74 are receptors for nicotinic acid and mediate its anti-lipolytic effect. Nature medicine. 2003;9(3):352-5.

293. Thangaraju M, Cresci GA, Liu K, Ananth S, Gnanaprakasam JP, Browning DD, et al. GPR109A is a G-protein-coupled receptor for the bacterial fermentation product butyrate and functions as a tumor suppressor in colon. Cancer research. 2009;69(7):2826-32.

294. Blad CC, Tang C, Offermanns S. G protein-coupled receptors for energy metabolites as new therapeutic targets. Nature reviews Drug discovery. 2012;11(8):603-19.

295. Singh N, Gurav A, Sivaprakasam S, Brady E, Padia R, Shi H, et al. Activation of Gpr109a, receptor for niacin and the commensal metabolite butyrate, suppresses colonic inflammation and carcinogenesis. Immunity. 2014;40(1):128-39.

296. Miyauchi S, Gopal E, Fei YJ, Ganapathy V. Functional identification of SLC5A8, a tumor suppressor down-regulated in colon cancer, as a Na(+)-coupled transporter for short-chain fatty acids. The Journal of biological chemistry. 2004;279(14):13293-6.

297. Gopal E, Miyauchi S, Martin PM, Ananth S, Roon P, Smith SB, et al. Transport of nicotinate and structurally related compounds by human SMCT1 (SLC5A8) and its relevance to drug transport in the mammalian intestinal tract. Pharmaceutical research. 2007;24(3):575-84.

298. Zimmerman MA, Singh N, Martin PM, Thangaraju M, Ganapathy V, Waller JL, et al. Butyrate suppresses colonic inflammation through HDAC1-dependent Fas

upregulation and Fas-mediated apoptosis of T cells. American journal of physiology Gastrointestinal and liver physiology. 2012;302(12):G1405-15.

299. Li H, Myeroff L, Smiraglia D, Romero MF, Pretlow TP, Kasturi L, et al. SLC5A8, a sodium transporter, is a tumor suppressor gene silenced by methylation in human colon aberrant crypt foci and cancers. Proceedings of the National Academy of Sciences of the United States of America. 2003;100(14):8412-7.

300. Gurav A, Sivaprakasam S, Bhutia YD, Boettger T, Singh N, Ganapathy V. Slc5a8, a Na+-coupled high-affinity transporter for short-chain fatty acids, is a conditional tumour suppressor in colon that protects against colitis and colon cancer under low-fibre dietary conditions. The Biochemical journal. 2015;469(2):267-78.

301. Singh N, Thangaraju M, Prasad PD, Martin PM, Lambert NA, Boettger T, et al. Blockade of dendritic cell development by bacterial fermentation products butyrate and propionate through a transporter (Slc5a8)-dependent inhibition of histone deacetylases. The Journal of biological chemistry. 2010;285(36):27601-8.

302. Luger K, Mader AW, Richmond RK, Sargent DF, Richmond TJ. Crystal structure of the nucleosome core particle at 2.8 A resolution. Nature. 1997;389(6648):251-60.

303. Allfrey VG, Faulkner R, Mirsky AE. ACETYLATION AND METHYLATION OF HISTONES AND THEIR POSSIBLE ROLE IN THE REGULATION OF RNA SYNTHESIS. Proceedings of the National Academy of Sciences of the United States of America. 1964;51:786-94.

304. Choudhary C, Kumar C, Gnad F, Nielsen ML, Rehman M, Walther TC, et al. Lysine acetylation targets protein complexes and co-regulates major cellular functions. Science. 2009;325(5942):834-40.

305. Yang XJ, Seto E. The Rpd3/Hda1 family of lysine deacetylases: from bacteria and yeast to mice and men. Nature reviews Molecular cell biology. 2008;9(3):206-18.

306. Blander G, Guarente L. The Sir2 family of protein deacetylases. Annual review of biochemistry. 2004;73:417-35.

307. Candido EP, Reeves R, Davie JR. Sodium butyrate inhibits histone deacetylation in cultured cells. Cell. 1978;14(1):105-13.

308. Sealy L, Chalkley R. The effect of sodium butyrate on histone modification. Cell. 1978;14(1):115-21.

309. Cousens LS, Gallwitz D, Alberts BM. Different accessibilities in chromatin to histone acetylase. The Journal of biological chemistry. 1979;254(5):1716-23.

310. Davie JR. Inhibition of histone deacetylase activity by butyrate. The Journal of nutrition. 2003;133(7 Suppl):2485s-93s.

311. Yu X, Shahir AM, Sha J, Feng Z, Eapen B, Nithianantham S, et al. Short-chain fatty acids from periodontal pathogens suppress histone deacetylases, EZH2, and SUV39H1 to promote Kaposi's sarcoma-associated herpesvirus replication. Journal of virology. 2014;88(8):4466-79.

312. Lau E, Ronai ZeA. ATF2 – at the crossroad of nuclear and cytosolic functions. Journal of Cell Science. 2012;125(12):2815-24.

313. Cani PD, Everard A, Duparc T. Gut microbiota, enteroendocrine functions and metabolism. Current opinion in pharmacology. 2013;13(6):935-40.

314. Vinolo MA, Ferguson GJ, Kulkarni S, Damoulakis G, Anderson K, Bohlooly YM, et al. SCFAs induce mouse neutrophil chemotaxis through the GPR43 receptor. PloS one. 2011;6(6):e21205.

315. Carretta MD, Conejeros I, Hidalgo MA, Burgos RA. Propionate induces the release of granules from bovine neutrophils. Journal of dairy science. 2013;96(4):2507-20.

316. Takaki Y, Shimamura S, Nakagawa S, Fukuhara Y, Horikawa H, Ankai A, et al. Bacterial lifestyle in a deep-sea hydrothermal vent chimney revealed by the genome sequence of the thermophilic bacterium Deferribacter desulfuricans SSM1. DNA research : an international journal for rapid publication of reports on genes and genomes. 2010;17(3):123-37.

317. Bergman EN. Energy contributions of volatile fatty acids from the gastrointestinal tract in various species. Physiological reviews. 1990;70(2):567-90.

318. Delgoffe GM, Kole TP, Zheng Y, Zarek PE, Matthews KL, Xiao B, et al. The mTOR kinase differentially regulates effector and regulatory T cell lineage commitment. Immunity. 2009;30(6):832-44.

319. Dennis PB, Jaeschke A, Saitoh M, Fowler B, Kozma SC, Thomas G. Mammalian TOR: a homeostatic ATP sensor. Science. 2001;294(5544):1102-5.

320. Kim M, Qie Y, Park J, Kim CH. Gut Microbial Metabolites Fuel Host Antibody Responses. Cell host & microbe. 2016;20(2):202-14.

321. Kramer OH, Zhu P, Ostendorff HP, Golebiewski M, Tiefenbach J, Peters MA, et al. The histone deacetylase inhibitor valproic acid selectively induces proteasomal degradation of HDAC2. The EMBO journal. 2003;22(13):3411-20.

322. Aoyama M, Kotani J, Usami M. Butyrate and propionate induced activated or non-activated neutrophil apoptosis via HDAC inhibitor activity but without activating GPR-41/GPR-43 pathways. Nutrition (Burbank, Los Angeles County, Calif). 2010;26(6):653-61.

323. Rogler G, Brand K, Vogl D, Page S, Hofmeister R, Andus T, et al. Nuclear factor kappaB is activated in macrophages and epithelial cells of inflamed intestinal mucosa. Gastroenterology. 1998;115(2):357-69.

324. Luhrs H, Gerke T, Muller JG, Melcher R, Schauber J, Boxberge F, et al. Butyrate inhibits NF-kappaB activation in lamina propria macrophages of patients with ulcerative colitis. Scandinavian journal of gastroenterology. 2002;37(4):458-66.

325. Säemann MD, Parolini O, Böhmig GA, Kelemen P, Krieger P-M, Neumüller J, et al. Bacterial metabolite interference with maturation of human monocyte-derived dendritic cells. Journal of leukocyte biology. 2002;71(2):238-46.

326. Waldecker M, Kautenburger T, Daumann H, Busch C, Schrenk D. Inhibition of histone-deacetylase activity by short-chain fatty acids and some polyphenol metabolites formed in the colon. The Journal of nutritional biochemistry. 2008;19(9):587-93.

327. Dangond F, Gullans SR. Differential expression of human histone deacetylase mRNAs in response to immune cell apoptosis induction by trichostatin A and butyrate. Biochemical and biophysical research communications. 1998;247(3):833-7.

328. Parish CR. Fluorescent dyes for lymphocyte migration and proliferation studies. Immunology and cell biology. 1999;77(6):499-508.

329. Harb H, Amarasekera M, Ashley S, Tulic MK, Pfefferle PI, Potaczek DP, et al. Epigenetic Regulation in Early Childhood: A Miniaturized and Validated Method to Assess Histone Acetylation. International archives of allergy and immunology. 2015;168(3):173-81.

330. Hsu P, Santner-Nanan B, Dahlstrom JE, Fadia M, Chandra A, Peek M, et al. Altered Decidual DC-SIGN+ Antigen-Presenting Cells and Impaired Regulatory T-Cell Induction in Preeclampsia. The American journal of pathology. 2012;181(6):2149-60.

331. Hsu P, Nanan R. Foetal immune programming: hormones, cytokines, microbes and regulatory T cells. Journal of reproductive immunology. 2014;104(Supplement C):2-7.

332. Nakajima A, Kaga N, Nakanishi Y, Ohno H, Miyamoto J, Kimura I, et al. Maternal High Fiber Diet during Pregnancy and Lactation Influences Regulatory T Cell Differentiation in Offspring in Mice. The Journal of Immunology. 2017;199(10):3516-24.

333. Jenmalm MC. Childhood immune maturation and allergy development: regulation by maternal immunity and microbial exposure. American journal of reproductive immunology (New York, NY : 1989). 2011;66 Suppl 1:75-80.

334. Prescott SL. Early-life environmental determinants of allergic diseases and the wider pandemic of inflammatory noncommunicable diseases. The Journal of allergy and clinical immunology. 2013;131(1):23-30.

335. Molodecky NA, Soon IS, Rabi DM, Ghali WA, Ferris M, Chernoff G, et al. Increasing incidence and prevalence of the inflammatory bowel diseases with time, based on systematic review. Gastroenterology. 2012;142(1):46-54 e42; quiz e30.

336. Abegunde AT, Muhammad BH, Bhatti O, Ali T. Environmental risk factors for inflammatory bowel diseases: Evidence based literature review. World J Gastroenterol. 2016;22(27):6296-317.

337. Hirahara K, Liu L, Clark RA, Yamanaka K, Fuhlbrigge RC, Kupper TS. The majority of human peripheral blood CD4+CD25highFoxp3+ regulatory T cells bear functional skin-homing receptors. J Immunol. 2006;177(7):4488-94.

338. Grindebacke H, Stenstad H, Quiding-Jarbrink M, Waldenstrom J, Adlerberth I, Wold AE, et al. Dynamic development of homing receptor expression and memory cell differentiation of infant CD4+CD25high regulatory T cells. J Immunol. 2009;183(7):4360-70.

339. Tan J, McKenzie C, Vuillermin PJ, Goverse G, Vinuesa CG, Mebius RE, et al. Dietary Fiber and Bacterial SCFA Enhance Oral Tolerance and Protect against Food Allergy through Diverse Cellular Pathways. Cell reports. 2016;15(12):2809-24.

340. Cosmi L, Annunziato F, Galli MIG, Maggi RME, Nagata K, Romagnani S. CRTH2 is the most reliable marker for the detection of circulating human type 2 Th and type 2 T cytotoxic cells in health and disease. Eur J Immunol. 2000;30(10):2972-9.

341. Kimmig S, Przybylski GK, Schmidt CA, Laurisch K, Mowes B, Radbruch A, et al. Two subsets of naive T helper cells with distinct T cell receptor excision circle content in human adult peripheral blood. J Exp Med. 2002;195(6):789-94.

342. Correa-Oliveira R, Fachi JL, Vieira A, Sato FT, Vinolo MA. Regulation of immune cell function by short-chain fatty acids. Clinical & translational immunology. 2016;5(4):e73.

343. Ding L, Shevach EM. IL-10 inhibits mitogen-induced T cell proliferation by selectively inhibiting macrophage costimulatory function. J Immunol. 1992;148(10):3133-9.

344. de Waal Malefyt R, Abrams J, Bennett B, Figdor CG, de Vries JE. Interleukin 10(IL-10) inhibits cytokine synthesis by human monocytes: an autoregulatory role of IL-10 produced by monocytes. J Exp Med. 1991;174(5):1209-20.

345. de Waal Malefyt R, Yssel H, de Vries JE. Direct effects of IL-10 on subsets of human CD4+ T cell clones and resting T cells. Specific inhibition of IL-2 production and proliferation. J Immunol. 1993;150(11):4754-65.

346. Taga K, Mostowski H, Tosato G. Human interleukin-10 can directly inhibit T-cell growth. Blood. 1993;81(11):2964-71.

347. Chaudhry A, Samstein RM, Treuting P, Liang Y, Pils MC, Heinrich J-M, et al. Interleukin-10 signaling in regulatory T cells is required for suppression of Th17 cell-mediated inflammation. Immunity. 2011;34(4):566-78.

348. Murai M, Turovskaya O, Kim G, Madan R, Karp CL, Cheroutre H, et al. Interleukin 10 acts on regulatory T cells to maintain expression of the transcription factor Foxp3 and suppressive function in mice with colitis. Nat Immunol. 2009;10(11):1178-84.

349. Cose S. T-cell migration: a naive paradigm? Immunology. 2007;120(1):1-7.

350. Guy-Grand D, Vassalli P, Eberl G, Pereira P, Burlen-Defranoux O, Lemaitre F, et al. Origin, trafficking, and intraepithelial fate of gut-tropic T cells. J Exp Med. 2013;210(9):1839-54.

351. Houston EG, Jr., Nechanitzky R, Fink PJ. Cutting edge: Contact with secondary lymphoid organs drives postthymic T cell maturation. J Immunol. 2008;181(8):5213-7.

352. Marino E, Richards JL, McLeod KH, Stanley D, Yap YA, Knight J, et al. Gut microbial metabolites limit the frequency of autoimmune T cells and protect against type 1 diabetes. Nature immunology. 2017;18(5):552-62.

353. Schmidt A, Eriksson M, Shang MM, Weyd H, Tegner J. Comparative Analysis of Protocols to Induce Human CD4+Foxp3+ Regulatory T Cells by Combinations of IL-2, TGF-beta, Retinoic Acid, Rapamycin and Butyrate. PloS one. 2016;11(2):e0148474.

354. Miyara M, Yoshioka Y, Kitoh A, Shima T, Wing K, Niwa A, et al. Functional delineation and differentiation dynamics of human CD4+ T cells expressing the FoxP3 transcription factor. Immunity. 2009;30(6):899-911.

355. Shevach EM, Thornton AM. tTregs, pTregs, and iTregs: similarities and differences. Immunological reviews. 2014;259(1):88-102.

356. Fantini MC, Dominitzki S, Rizzo A, Neurath MF, Becker C. In vitro generation of CD4+ CD25+ regulatory cells from murine naive T cells. Nature protocols. 2007;2(7):1789-94.

357. Wang J, Huizinga TW, Toes RE. De novo generation and enhanced suppression of human CD4+CD25+ regulatory T cells by retinoic acid. Journal of immunology. 2009;183(6):4119-26.

358. Candia E, Reyes P, Covian C, Rodriguez F, Wainstein N, Morales J, et al. Single and combined effect of retinoic acid and rapamycin modulate the generation, activity and homing potential of induced human regulatory T cells. PloS one. 2017;12(7):e0182009.

359. Long SA, Buckner JH. Combination of rapamycin and IL-2 increases de novo induction of human CD4(+)CD25(+)FOXP3(+) T cells. Journal of autoimmunity. 2008;30(4):293-302.

360. Jeffery LE, Burke F, Mura M, Zheng Y, Qureshi OS, Hewison M, et al. 1,25-Dihydroxyvitamin D3 and IL-2 combine to inhibit T cell production of inflammatory cytokines and promote development of regulatory T cells expressing CTLA-4 and FoxP3. Journal of immunology. 2009;183(9):5458-67.

361. Chang CC, Satwani P, Oberfield N, Vlad G, Simpson LL, Cairo MS. Increased induction of allogeneic-specific cord blood CD4+CD25+ regulatory T (Treg) cells: a comparative study of naive and antigenic-specific cord blood Treg cells. Experimental hematology. 2005;33(12):1508-20.

362. den Braber I, Mugwagwa T, Vrisekoop N, Westera L, Mogling R, de Boer AB, et al. Maintenance of peripheral naive T cells is sustained by thymus output in mice but not humans. Immunity. 2012;36(2):288-97.

363. Silva SL, Sousa AE. Establishment and Maintenance of the Human Naive CD4+ T-Cell Compartment. Frontiers in pediatrics. 2016;4:119.

364. Qi Q, Liu Y, Cheng Y, Glanville J, Zhang D, Lee J-Y, et al. Diversity and clonal selection in the human T-cell repertoire. Proceedings of the National Academy of Sciences. 2014;111(36):13139-44.

365. Goronzy JJ, Fang F, Cavanagh MM, Qi Q, Weyand CM. Naive T cell maintenance and function in human aging. Journal of immunology. 2015;194(9):4073-80.

366. Teteloshvili N, Kluiver J, van der Geest KSM, van der Lei RJ, Jellema P, Pawelec G, et al. Age-Associated Differences in MiRNA Signatures Are Restricted to CD45RO Negative T Cells and Are Associated with Changes in the Cellular Composition, Activation and Cellular Ageing. PloS one. 2015;10(9):e0137556.

367. Millard AL, Mertes PM, Ittelet D, Villard F, Jeannesson P, Bernard J. Butyrate affects differentiation, maturation and function of human monocyte-derived dendritic cells and macrophages. Clinical and experimental immunology. 2002;130(2):245-55.

368. Wang B, Morinobu A, Horiuchi M, Liu J, Kumagai S. Butyrate inhibits functional differentiation of human monocyte-derived dendritic cells. Cellular immunology. 2008;253(1-2):54-8.

369. Nastasi C, Candela M, Bonefeld CM, Geisler C, Hansen M, Krejsgaard T, et al. The effect of short-chain fatty acids on human monocyte-derived dendritic cells. Scientific reports. 2015;5:16148.

370. Nencioni A, Beck J, Werth D, Grünebach F, Patrone F, Ballestrero A, et al. Histone Deacetylase Inhibitors Affect Dendritic Cell Differentiation and Immunogenicity. Clinical Cancer Research. 2007;13(13):3933-41.

371. Porcelli SA, Modlin RL. The CD1 system: antigen-presenting molecules for T cell recognition of lipids and glycolipids. Annual review of immunology. 1999;17:297-329.

372. Kaisar MMM, Pelgrom LR, van der Ham AJ, Yazdanbakhsh M, Everts B. Butyrate Conditions Human Dendritic Cells to Prime Type 1 Regulatory T Cells via both Histone Deacetylase Inhibition and G Protein-Coupled Receptor 109A Signaling. Frontiers in immunology. 2017;8(1429).

373. Asarat M, Apostolopoulos V, Vasiljevic T, Donkor O. Short-Chain Fatty Acids Regulate Cytokines and Th17/Treg Cells in Human Peripheral Blood Mononuclear Cells in vitro. Immunological investigations. 2016;45(3):205-22.

374. Asarat M, Apostolopoulos V, Vasiljevic T, Donkor O. Short-chain fatty acids produced by synbiotic mixtures in skim milk differentially regulate proliferation and cytokine production in peripheral blood mononuclear cells. International Journal of Food Sciences and Nutrition. 2015;66(7):755-65.

375. Vosters O, Lombard C, Andre F, Sana G, Sokal EM, Smets F. The interferon-alpha and interleukin-10 responses in neonates differ from adults, and their production

remains partial throughout the first 18 months of life. Clinical and experimental immunology. 2010;162(3):494-9.

376. Trompette A, Gollwitzer ES, Yadava K, Sichelstiel AK, Sprenger N, Ngom-Bru C, et al. Gut microbiota metabolism of dietary fiber influences allergic airway disease and hematopoiesis. Nature medicine. 2014;20(2):159-66.

377. Needell JC, Ir D, Robertson CE, Kroehl ME, Frank DN, Zipris D. Maternal treatment with short-chain fatty acids modulates the intestinal microbiota and immunity and ameliorates type 1 diabetes in the offspring. PloS one. 2017;12(9):e0183786.

378. Zhou J, Gao S, Chen J, Zhao R, Yang X. Maternal sodium butyrate supplement elevates the lipolysis in adipose tissue and leads to lipid accumulation in offspring liver of weaning-age rats. Lipids in health and disease. 2016;15(1):119.

379. Huang Y, Gao S, Chen J, Albrecht E, Zhao R, Yang X. Maternal butyrate supplementation induces insulin resistance associated with enhanced intramuscular fat deposition in the offspring. Oncotarget. 2017;8(8):13073-84.

380. Huang Y, Gao S, Jun G, Zhao R, Yang X. Supplementing the maternal diet of rats with butyrate enhances mitochondrial biogenesis in the skeletal muscles of weaned offspring. The British journal of nutrition. 2017;117(1):12-20.

381. Qiu C, Coughlin KB, Frederick IO, Sorensen TK, Williams MA. Dietary Fiber Intake in Early Pregnancy and Risk of Subsequent Preeclampsia. American Journal of Hypertension. 2008;21(8):903-9.

382. Shin D, Lee KW, Song WO. Dietary Patterns during Pregnancy Are Associated with Risk of Gestational Diabetes Mellitus. Nutrients. 2015;7(11):9369-82.

383. Tan J, McKenzie C, Potamitis M, Thorburn AN, Mackay CR, Macia L. Chapter Three - The Role of Short-Chain Fatty Acids in Health and Disease. In: Alt FW, editor. Advances in Immunology. 121: Academic Press; 2014. p. 91-119.

384. Tan J, McKenzie C, Vuillermin Peter J, Goverse G, Vinuesa Carola G, Mebius Reina E, et al. Dietary Fiber and Bacterial SCFA Enhance Oral Tolerance and Protect against Food Allergy through Diverse Cellular Pathways. Cell Reports. 2016;15(12):2809-24.

385. Marques FZ, Nelson E, Chu P-Y, Horlock D, Fiedler A, Ziemann M, et al. High-Fiber Diet and Acetate Supplementation Change the Gut Microbiota and Prevent the Development of Hypertension and Heart Failure in Hypertensive MiceClinical Perspective. Circulation. 2017;135(10):964-77.

386. James SL, Christophersen CT, Bird AR, Conlon MA, Rosella O, Gibson PR, et al. Abnormal fibre usage in UC in remission. Gut. 2015;64(4):562-70.

387. Halmos EP, Christophersen CT, Bird AR, Shepherd SJ, Gibson PR, Muir JG. Diets that differ in their FODMAP content alter the colonic luminal microenvironment. Gut. 2015;64(1):93-100.

388. Ríos-Covián D, Ruas-Madiedo P, Margolles A, Gueimonde M, de los Reyes-Gavilán CG, Salazar N. Intestinal Short Chain Fatty Acids and their Link with Diet and Human Health. Frontiers in microbiology. 2016;7:185.

389. Raqib R, Sarker P, Mily A, Alam NH, Arifuzzaman ASM, Rekha RS, et al. Efficacy of sodium butyrate adjunct therapy in shigellosis: a randomized, double-blind, placebo-controlled clinical trial. BMC Infectious Diseases. 2012;12(1):111.